

# **Influencia de los microorganismos y parámetros físicoquímicos (radiación, temperatura) en la integridad de las barreras de contenedor de cobre y bentonita de los almacenamientos geológicos profundos**

**TESIS DOCTORAL**

Granada, 2024

**Mar Morales Hidalgo**



**Influencia de los microorganismos y parámetros  
fisicoquímicos (radiación, temperatura) en la  
integridad de las barreras de contenedor de cobre y  
bentonita de los almacenamientos geológicos  
profundos**



UNIVERSIDAD  
DE GRANADA

Universidad de Granada

Facultad de Ciencias

Departamento de Microbiología

*The influence of microorganisms and physicochemical  
parameters (radiation, temperature) on the integrity of the  
copper canister and bentonite in deep geological  
repositories*

TESIS DOCTORAL

**Mar Morales Hidalgo**

Granada, 2024

Programa de Doctorado en Biología Fundamental y de Sistemas

Influencia de los microorganismos y parámetros físicoquímicos (radiación, temperatura) en la integridad de las barreras de contenedor de cobre y bentonita de los almacenamientos geológicos profundos

**TESIS DOCTORAL**

Programa de Doctorado en Biología Fundamental y de Sistemas

Departamento de Microbiología, Facultad de Ciencias

Universidad de Granada

Granada, 2024

Memoria presentada por Dña. Mar Morales Hidalgo para aspirar al Grado de Doctor por la Universidad de Granada con Mención Internacional. Esta Tesis Doctoral ha sido dirigida por D. Mohamed Larbi Merroun, Catedrático de la Universidad de Granada, y Dña. Fadwa Jroundi Mesbahi, Profesora Titular de la misma universidad

**Vº Bº del Director**

**Vº Bº del Director**

**Mohamed Larbi Merroun**  
Catedrático de Universidad  
Universidad de Granada

**La doctoranda**

**Fadwa Jroundi Mesbahi**  
Profesora Titular  
Universidad de Granada

**Mar Morales Hidalgo**

Editor: Universidad de Granada. Tesis Doctorales  
Autor: Mar Morales Hidalgo  
ISBN: 978-84-1195-660-4  
URI: <https://hdl.handle.net/10481/102025>

El doctorando / The *doctoral candidate* **Mar Morales Hidalgo** y los directores de la tesis / and the thesis supervisor/s: **Mohamed Larbi Merroun y Fadwa Jroundi Mesbahi**

Garantizamos, al firmar esta tesis doctoral, que el trabajo ha sido realizado por el doctorando bajo la dirección de los directores de la tesis y hasta donde nuestro conocimiento alcanza, en la realización del trabajo, se han respetado los derechos de otros autores a ser citados, cuando se han utilizado sus resultados o publicaciones.

/

*Guarantee, by signing this doctoral thesis, that the work has been done by the doctoral candidate under the direction of the thesis supervisor/s and, as far as our knowledge reaches, in the performance of the work, the rights of other authors to be cited (when their results or publications have been used) have been respected.*

Lugar y fecha / Place and date:

Director/es de la Tesis/  
*Thesis supervisor/s:*

Doctorando/  
*Doctoral candidate:*

Firma / Signed

Firma / Signed



Esta Tesis Doctoral ha sido realizada en el Departamento de Microbiología (Facultad de Ciencias) de la Universidad de Granada durante los años 2021-2024 dentro del Grupo de Investigación Geomicrobiología y Biogeoquímica (BIO103).

Para la realización de este trabajo, la doctoranda disfrutó de dos contratos: i) contrato con cargo al Proyecto del Plan Nacional “*Impacto de los procesos microbianos en la interfaz contenedor de cobre-bentonita compactada y sus efectos sobre la movilización del selenio*” (ref. RTI2018-101548-B-I00) financiado por el Ministerio de Ciencia, Innovación y Universidades, ii) contrato FPU (Formación de Profesorado Universitario) con referencia FPU20/00583 del Ministerio de Ciencia, Innovación y Universidades.

Además, esta Tesis Doctoral también ha sido financiada a través del proyecto europeo “*EURAD - European Joint Programme on Radioactive Waste Management*” (ref. 847593, EURATOM - NFRP-2018) financiado a su vez por la Comisión Europea con el Dr. Mohamed L. Merroun como investigador principal de dicho proyecto en la Universidad de Granada.

La doctoranda también ha disfrutado de tres Ayudas de Movilidad con el fin de realizar estancias de investigación en centros de investigación extranjeros:

- Estancia breve de tres meses en el Institute for Nanomaterials, Advanced Technology and Innovation (Technical University of Liberec, República Checa) bajo la supervisión de la Dra. Kateřina Černá. Fechas estancia: 20/09/2023 – 19/12/2023. Financiación: beca de movilidad del programa Erasmus Prácticas (Erasmus+) del Vicerrectorado de Estudiantes de la Universidad de Granada y ayuda “EURAD Mobility Programme” del proyecto europeo *EURAD - European Joint Programme on Radioactive Waste Management*” (ref. 847593, EURATOM - NFRP-2018).

- Estancia breve de dos semanas en el Institute for Nanomaterials, Advanced Technology and Innovation (Technical University of Liberec, República Checa) bajo la supervisión de la Dra. Kateřina Černá. Fechas estancia: 06/05/2024 – 17/05/2024. Financiación: ayuda de movilidad “EURAD Mobility Programme” del proyecto europeo *EURAD - European Joint Programme on Radioactive Waste Management*” (ref. 847593, EURATOM - NFRP-2018).



UNIVERSIDAD  
DE GRANADA



Durante el desarrollo de esta Tesis Doctoral, parte de los resultados han sido publicados en revistas científicas de alto impacto, así como en congresos a nivel nacional e internacional:

### 1) Publicaciones científicas relacionadas con esta tesis doctoral:

**Morales-Hidalgo, M\***, Povedano-Priego, C., Martinez-Moreno, M. F., Ojeda, J. J., Jroundi, F., & Merroun, M. L. (2024). Long-term tracking of the microbiology of uranium-amended water-saturated bentonite microcosms: a mechanistic characterization of U speciation. *Journal of Hazardous Materials*, 476, 135044. <https://doi.org/10.1016/j.jhazmat.2024.135044> **IF: 12.2 – Q1 (D1)**

**Morales-Hidalgo, M\***, Povedano-Priego, C., Martinez-Moreno, M. F., Ruiz-Fresneda, M. A., Lopez-Fernandez, M., Jroundi, F\*, & Merroun, M. L. (2024). Insights into the Impact of Physicochemical and Microbiological Parameters on the Safety Performance of Deep Geological Repositories. *Microorganisms*, 12(5), 1025. <https://doi.org/10.3390/microorganisms12051025> **IF: 4.1 – Q2**

### 2) Artículos científicos afines publicados durante el periodo doctoral:

Martinez-Moreno, M. F., Povedano-Priego, C., **Morales-Hidalgo, M.**, Mumford, A. D., Aranda, E., Vilchez-Vargas, R., ... & Merroun, M. L. (2024). Microbial influence in Spanish bentonite slurry microcosms: unveiling a-year long geochemical evolution and early-stage copper corrosion related to nuclear waste repositories. *Environmental Pollution*, 124491. <https://doi.org/10.1016/j.envpol.2024.124491> **IF: 7.6 – Q1 (D1)**

Ruiz-Fresneda, M. A., **Morales-Hidalgo, M.**, Povedano-Priego, C., Jroundi, F., Hidalgo-Iruela, J., Cano-Cano, M., ... & Martín-Sánchez, I. (2024). Unlocking the key role of bentonite fungal isolates in tellurium and selenium bioremediation and biorecovery: Implications in the safety of radioactive waste disposal. *Science of the Total Environment*, 912, 169242. <https://doi.org/10.1016/j.scitotenv.2023.169242> **IF: 8.2 – Q1 (D1)**

Martinez-Moreno, M.F., Povedano-Priego, C., Mumford, A.D., **Morales-Hidalgo, M.**, Mijndonckx, K., Jroundi, F., Ojeda, J.J., Merroun, M.L., (2024). Microbial responses to elevated temperature: Evaluating bentonite mineralogy and copper

canister corrosion within the long-term stability of deep geological repositories of nuclear waste. *Science of The Total Environment*, 915, 170149. <https://doi.org/10.1016/j.scitotenv.2024.170149> **IF: 8.2 – Q1 (D1)**

Povedano-Priego, C., Jroundi, F., **Morales-Hidalgo, M.**, Pinel-Cabello, M., Peula-Ruiz, E., Merroun, M. L., & Martin-Sánchez, I. (2024). Unveiling fungal diversity in uranium and glycerol-2-phosphate-amended bentonite microcosms: Implications for radionuclide immobilization within the Deep Geological Repository system. *Science of the Total Environment*, 908, 168284. <https://doi.org/10.1016/j.scitotenv.2023.168284> **IF: 8.2 – Q1 (D1)**

Ruiz-Fresneda, M. A\*, Martinez-Moreno, M. F., Povedano-Priego, C., **Morales-Hidalgo, M.**, Jroundi, F., & Merroun, M. L. (2023). Impact of microbial processes on the safety of deep geological repositories for radioactive waste. *Frontiers in Microbiology*, 14, 1134078. <https://doi.org/10.3389/fmicb.2023.1134078> **IF: 5.2 – Q2**

Martinez-Moreno, M. F., Povedano-Priego, C., **Morales-Hidalgo, M.**, Mumford, A. D., Ojeda, J. J., Jroundi, F., & Merroun, M. L. (2023). Impact of compacted bentonite microbial community on the clay mineralogy and copper canister corrosion: a multidisciplinary approach in view of a safe Deep Geological Repository of nuclear wastes. *Journal of Hazardous Materials*, 458, 131940. <https://doi.org/10.1016/j.jhazmat.2023.131940> **IF: 12.2 – Q1 (D1)**

Povedano-Priego, C., Jroundi, F., Lopez-Fernandez, M., **Morales-Hidalgo, M.**, Martin-Sánchez, I., Huertas, F. J., ... & Merroun, M. L. (2022). Impact of anoxic conditions, uranium(VI) and organic phosphate substrate on the biogeochemical potential of the indigenous bacterial community of bentonite. *Applied clay science*, 216, 106331. <https://doi.org/10.1016/j.clay.2021.106331> **IF: 5.6 – Q2**

### **3) Congresos nacionales e internacionales dónde se han presentado resultados de esta Tesis Doctoral:**

**Morales-Hidalgo, Mar\***; Povedano-Priego, Cristina; Martinez-Moreno, Marcos F.; Alonso, Ursula; Fernandez, Ana M.; Jroundi, Fadwa; Merroun, Mohamed L. (9 – 13 julio, 2023). *Responses of the bentonite microbial community to conditions relevant to*

*nuclear waste repository: radiation and high compaction. [Póster]. FEMS2023. Hamburgo (Alemania).*

Alonso, Ursula\*; García-Gutiérrez, Miguel; Fernández, Ana María; Valdivieso, Pedro; Soto-Ruiz, Carla; Morejón, Jesús; Mingarro, Manuel; **Morales-Hidalgo, Mar**; Povedano-Priego, Cristina; Jroundi, Fadwa; Merroun, Mohamed L.; Missana, Tiziana. (24 – 27 julio, 2023). *Canister corrosion accelerated by 14 kGy gamma-radiation: impact on bentonite properties. [Comunicación oral]. EUROCLAY 2023. Bari (Italia).*

**Morales-Hidalgo, Mar\***; Povedano-Priego, Cristina; Huertas, F. Javier; Guerra-Tschuschke, Isabel; de la Prada Sánchez, Cecilia; Jroundi, Fadwa; Merroun, Mohamed L. (28 junio – 1 julio, 2022). *Influencia de la comunidad microbiana de la bentonita en la biotransformación del Se(IV) y la corrosión del cobre a altas temperaturas. [Comunicación oral]. XXXIX Reunión Científica de la Sociedad Española de Mineralogía y XXVI Reunión Científica de la Sociedad Española de Arcillas. Baeza (España). Premio Jóvenes Investigadores 2022 Sociedad Española de Arcillas.*

**Morales-Hidalgo, Mar\***; Povedano-Priego, Cristina; Martínez-Moreno, Marcos F.; Huertas, F. Javier; Jroundi, Fadwa; Merroun, Mohamed L. (22 - 24 junio, 2022). *Efecto de la microbiología de la bentonita sobre la corrosión del cobre y el ciclo biogeoquímico del Se a 60 °C: perspectivas de futuro para el almacenamiento de residuos radiactivos. [Comunicación oral]. III Congreso / V Jornadas: Investigadores en Formación (JIFFI). Fomentando la Interdisciplinariedad. Granada (España).*

**Morales-Hidalgo, Mar\***; Povedano-Priego, Cristina; Vilchez-Vargas, Ramiro; Jroundi, Fadwa; Merroun, Mohamed L. (13 – 16 junio, 2022). *Tracking the biogeochemistry and microbiology of uranium-treated water-saturated bentonite microcosms: Insights into the safety of Deep Geological Repository. [Póster]. Clay Conference 2022: 8th International Conference on clays in Natural and Engineered Barriers for Radioactive Waste Confinement. Nancy (Francia).*

#### **4) Otras comunicaciones y divulgación científica relacionadas con la Tesis Doctoral:**

**Morales-Hidalgo, Mar\***. (27 – 29 mayo, 2024). *Assessing the impact of radiation and high compaction on FEBEX bentonite: microbial and copper corrosion studies*. [Comunicación oral]. Final ConCorD WP project meeting within EU-project EURAD (European Joint Programme on Radiactive Waste Management). Berna (Suiza).

**Mar Morales Hidalgo, et al.** (2024). Integration of the findings on the impact of irradiation, dry density and particle size on the microbial community. Deliverable D15.9 of the HORIZON 2020 project EURAD. EC Grant agreement no: 847593.

**Morales-Hidalgo, Mar\***. (22 – 24 mayo, 2023). *The impact of radiation exposure and high compaction on the microbiology and mineralogy of FEBEX bentonite and the characterization of copper corrosion products*. [Comunicación oral]. 2nd Annual ConCorD WP project meeting within EU-project EURAD (European Joint Programme on Radiactive Waste Management). Madrid (España).

**Morales-Hidalgo, Mar\***; Povedano-Priego, Cristina; Jroundi, Fadwa; Vilchez-Vargas, Ramiro; Guerra-Tschuschke, Isabel; Abad-Ortega, María del Mar; Martín-Sánchez, Inés; Merroun, Mohamed L. (4 – 9 julio, 2021). *Responses of the bentonite microbial community to Se(IV) exposure: insights into selenium biogeochemical cycle*. [Comunicación oral]. Goldschmidt2021 Virtual Conference. Online.

**Morales-Hidalgo, Mar\***; Povedano-Priego, Cristina; Cano-Cano, Mónica; Jroundi, Fadwa; Hidalgo-Iruela, Javier; Martín-Sánchez, Inés; Merroun, Mohamed L. (28 junio – 2 julio, 2021). *El papel de los hongos en la biorremediación de Se, Te y Pb para la detoxificación de ambientes contaminados*. [Comunicación oral]. XXVIII Congreso de la Sociedad Española de Microbiología. Online.

**Morales-Hidalgo, Mar\***; Povedano-Priego, Cristina; Cano-Cano, Mónica; Jroundi, Fadwa; Martín-Sánchez, Inés; Merroun, Mohamed L. (2 – 3 diciembre, 2021). [Póster]. *Life in presence of heavy metals: the role of fungi in lead, tellurium and selenium bioremediation*. New Topics in Mineralogy 2: The mineral-microbe interface through time and space. Online.

## AGRADECIMIENTOS

Quisiera empezar agradeciendo a mis dos directores de tesis Mohamed L. Meroun y Fadwa Jroundi Mesbahi. Gracias, Mohamed, por haber confiado en mí desde el primer momento. Tu confianza me ha hecho superarme día a día tanto a nivel científico como personal y me ha permitido haber podido lograr llegar hasta aquí. Siempre te estaré agradecida por haberme acogido en tu familia científica y no haber parado de ofrecerme oportunidades. De corazón, gracias. Gracias, Fadwa, por haberme acompañado desde que empecé como tu alumna de TFM y no haberme soltado en todos estos años. Por haberme apoyado en este duro camino y siempre haber estado dispuesta a ayudarme en todo lo que he necesitado. Ser tu primera doctoranda siempre me hará sentir especial. En definitiva, muchas gracias a los dos por haberme ayudado a desarrollar mi potencial y acercarme a cumplir unos de mis sueños a nivel profesional. Asimismo, me gustaría agradecer a quién me inició en el mundo de la investigación, a quién se convirtió para mí en mucho más que una profesora. A mi confidente y amiga, Inés. Quiero que sepas que, a día de hoy, estoy donde estoy en muy gran parte gracias a ti. Me inicié en este mundo de tu mano y me transmitiste tanto amor por lo que hacías que vivir la ciencia a través de tu vocación fue lo mejor que me pudo pasar para enamorarme de la microbiología. Nunca hay que olvidarse de quién estuvo en los inicios, y en mi caso contigo no pude tener más suerte. Y también, gracias, Cristina, por guiarme desde el principio en el mundo de la bentonita hasta haberme convertido en un pollito capaz de volar.

*I want to express my deepest gratitude to Dr. Kateřina Černá, my host supervisor at the CXI of the Technical University of Liberec during my 3-month research stay. From the very beginning, you have been incredibly supportive and made me feel like I truly belonged to the team. Over these*

*months, our connection has grown into something truly special, and I hope it will continue for years to come. I also want to say a heartfelt thank you to Nhung. Your warm welcome from day one and your constant, infectious smile made my experience unforgettable. And, of course, to my Czech mum, Klára. Thank you for capturing my heart and giving me so much more than I could ever repay. You've been the best qPCR teacher I could have asked for, and I cherish all our tea-time chats about life. Most of all, thank you for embracing me as part of your family. You will always be one of the main reasons I look forward to coming back to the Czech Republic. Z celého srdce vám všem děkuji.*

Una tesis es trabajo en equipo y no puedo dejar de agradecer a todos los colaboradores que me han ayudado durante estos años. Gracias, Javier Huertas, por descíframe en tantas ocasiones lo que para mí son puros rompecabezas geológicos. Gracias, Jesús Ojeda, por demostrarme que existen profesores por el mundo tan “cool” como tú y por tus clases magistrales sobre XPS. Gracias, Úrsula y Ana María, por haberme acogido siempre con una sonrisa en el CIEMAT y haber compartido juntas momentos alrededor de Europa. Gracias, Isabel Guerra, por tu implicación en todas y cada una de las citas de microscopía que he tenido contigo. Sacas oro de barro y nunca has perdido la paciencia cuando yo ya me daba por rendida. En general, gracias al personal del CIC, Daniel, Conchi, María del Mar, Nieves, Jaime, Isabel, por haberme ayudado a poder sacar adelante este trabajo.

Esta etapa de mi vida ha sido dura, pero también muy bonita ya que me ha permitido cruzarme con personas inolvidables que me han aportado como mínimo algún momento, situación, gesto o conversación que ha calado en mí.

Gracias a todos los compañeros de departamento, estudiantes y alumnos de TFG y TFM. En especial a Lidia (hongos), Esther (team bolitas), Sonia (la

chica de la sonrisa infinita), Tamara, Rauliyo y Nacho (cocinero de galletas y torrijas) por tantos buenos momentos entre pipetas, probetas, guantes y centrífugas. Gracias a Manolo por ser mi suministrador oficial de caramelos y mecheros, por las verdaderas charlas de sabiduría sobre la vida y por enseñarme el verdadero amor hacia los perros. También agradecer a Ana por tener mucha paciencia entre burocracia, dietas y perlicos y aun así nunca perder la sonrisa. Gracias a Conchi por nuestras charlas, tu ayuda durante las prácticas y tu calidad profesional, que es digna de admirar. Gracias, Marga, por haberme animado siempre y haber tenido palabras bonitas hacia mí. Gracias, Guille, por tu ayuda siempre que la he necesitado. *To Adam, for being the most Andalusian Brit there is and for always bringing such positive energy.* Gracias, Migue, por ser la definición de compañerismo, por estar siempre dispuesto a ayudar y sobre todo por tu labia granaína que siempre hace reír. Gracias, Jaime, por volver soleados días grises con tu humor, tus trolleos y tus historias. Siempre admiraré la imaginación de tu mente. Gracias, Chachito, por ser luz en el camino. Literalmente, luz. Nunca la pierdas. Gracias, a Newman, por todo. No puedo especificar. Eres genial. Gracias, a mi italiana favorita, Paquita, porque estar contigo 5 minutos te recarga la vitalidad para los siguientes 5 años. Gracias, Li, por enseñarme que cada día puede ser el mejor día de tu vida. Gracias, Laura, porque tenerte como alumna fue un rayo de luz. Siempre estaremos conectadas. Gracias a mi minion chiquitillo, mi Esther, por todos los momentos vividos (y los que nos quedan), todas las charlas trambólicas de la vida, todas las complicidades y por los infinitos videos que nos mandamos que nos alegran el día. Y agradecer a un largo etcétera por haberme aportado cada uno algo positivo en este camino: Pablo, María, Chemi, Elena, Inés y Claudia.

Infinitas gracias a los mejores amigos del mundo, Álex y Marcos. Álex, conectamos desde el primer segundo y desde entonces no nos hemos

separado. Somos los dramáticos más dramáticos, pero solo entre dramáticos nos entendemos. Eres ejemplo de amistad, constancia, valentía y buen corazón. Me faltan palabras de agradecimiento por todo lo vivido juntos y lo mucho que nos queda. Mi Markillos, mi M de M&M, mi pin del ¿pon? O mi pon del ¿pin? Siempre será la duda... Porque cada día de estos cuatro años ha merecido la pena gracias a tenerte a mi lado. Por ser mi líder, por ir de la mano en todo, por haber sido uno de mis pilares fundamentales que me ha permitido no caer. Os quiero mucho y corto y cambio que nos ponemos tiernicos.

Gracias a mi hermana querida, Clara. Porque juntas empezamos en esto. Porque desde 2015 no has dejado de estar ahí para mí. Y porque sé que siempre lo estarás. Porque, aunque la vida adulta nos separe, siempre estaremos unidas. Gracias a mis niñas, Ne, Ele y Lau. Nos hemos visto crecer y cumplir muchos logros. Nos hemos acompañado en tantas etapas de la vida que espero seguir tendiéndooos a mi lado muchos años más. Gracias a Marta. Qué descubrimiento. Por nuestros cafés de horas que parecen minutos y nuestras charlas de la vida intentando descifrar el mundo. Gracias a Encarni, Pedro y Dani, por ser una familia preciosa que desde el principio me ha acogido, querido y apoyado.

A mi familia. Gracias, mamá y papá. Soy quien soy gracias a vosotros. Si de algo estoy agradecida en esta vida es que me hayáis tocado como padres. Me habéis hecho creer en mí cuando yo no lo hacía, me habéis animado a superar situaciones que yo veía incapaz de superar, me habéis hecho ser más fuerte cuando yo pensaba que era débil. Vuestra confianza ciega me ha permitido ser la mejor versión de mí misma y que, con apoyo, amor y constancia, todo se logra mejor. Gracias a mi yayo, mi referente de vida. La persona más fuerte que he conocido. Ojalá algún día llegue a parecerme simplemente un

poco a ti. Porque nada te ha frenado nunca y has podido con todo. Qué mejor ejemplo que ese. A mi bebo, por ser la estrella que me guía y nunca me deja sola. A mis tíos y mis primas, por siempre darme palabras de apoyo y cariño. Y a mis tres niños, G, T y M, por aportarme amor infinito y sólo y únicamente, felicidad.

Y por último y no menos importante a ti, Migue. Vale, sí, lo digo. Tenías razón. Una vez más. Te lo reconozco aquí delante de todo el que lo lea. Gracias por nunca haber dejado de creer en mí. Por no haber dejado que me rinda en las tantas veces que me he quedado sin fuerzas. Gracias por acompañarme incondicionalmente en cada situación que se ha topado en nuestro camino. Gracias por ser el mejor compañero de vida. Gracias por el efecto Migue. Estoy impaciente por saber qué nos deparará esta nueva etapa. También juntos. Y gracias por hacerme saber que siempre seré capaz de cruzar cualquier “Paladin Strait” porque estarás tú en la otra orilla, esperando...

*“I would swim the Paladin Strait*

*Without any flotation*

*Just a glimpse of visual aid*

*Of you on the other shoreline*

*Waiting, expectations*

*That I'm gonna make it”*



*It is a rough road that leads to the heights of greatness*

Séneca



## LIST OF ABBREVIATIONS

**AGP:** Almacenamiento Geológico Profundo

**ANDRA:** Agence Nationale pour la gestion des Déchets Radioactifs

***a*-Se:** amorphous selenium

**ATCC:** American Type Culture Collection

**BLAST:** Basic Local Alignment Search Tool

**BSE:** Backscattered Electrons

**CEC:** Cation Exchange Capacity

**CIC:** Centro de Instrumentación Científica

**CMIC:** Chemical Microbially Induced Corrosion

**DGR:** Deep Geological Repository

**DNA:** Deoxyribonucleic Acid

**DRX:** Difracción de Rayos-X

**DSMZ:** Deutsche Sammlung Von Mikroorganismen Und Zellkulturen

**EDX:** Energy Dispersive X-ray

**EG:** Ethylene Glycol

**EMIC:** Electrical Microbially Influenced Corrosion

**ENRESA:** Empresa Nacional de Residuos Radiactivos, S.A.

**EPS:** Extracellular Polymeric Substance

**EsB:** Energy selective Backscattered

**ESEM:** Environmental Scanning Electron Microscopy

**FESEX:** Full-scale Engineered Barriers Experiment

**FFT:** Fast Fourier Transform

**G2P:** Glycerol-2-Phosphate

**Gy:** Gray

**HAADF-STEM:** High-Angle Annular Dark Field Scanning Electron Microscopy

**HLW:** High-Level Waste

**HRTEM:** High Resolution Transmission Electron Microscopy

**IAEA:** International Atomic Energy Agency

**ICP-MS:** Inductively Coupled Plasm-Mass Spectrometry

**IRB:** Iron-Reducing Bacteria

**LB:** Lysogeny Broth

**LOI:** Loss On Ignition

**MIC:** Microbially Influenced Corrosion

**MPN:** Most Probable Number

***m*-Se:** monoclinic selenium

**NCBI:** National Centre for Biotechnology Information

**NCIMB:** National Collection of Industrial Food and Marine Bacteria

**NGS:** Next Generation Sequencing

**NTC:** Non-Template Control

**NWMO:** Nuclear Waste Management Organization

**OA:** Oriented Aggregates

**OTU:** Operational Taxonomical Unit

**PCoA:** Principal Coordinate Analysis

**PCR:** Polymerase Chain Reaction

**qPCR:** quantitative Polymerase Chain Reaction

**ROS:** Reactive Oxygen Species

**RQ:** Relative Quantification

**rRNA:** ribosomal Ribonucleic Acid

**SAED:** Selected-Area Electron Diffraction

**Se(0):** elemental selenium

**Se(IV):** selenite

**SE:** Secondary Electrons

**SEM:** Scanning Electron Microscopy

**SeNP:** Selenium Nanoparticle

**SF:** Spent Fuel

**SRB:** Sulfate-Reducing Bacteria

***t*-Se:** trigonal selenium

**VP-FESEM:** Variable Pressure Field Emission Scanning Electron Microscopy

**WNA:** World Nuclear Association

**XPS:** X-Ray Photoelectron Spectroscopy

**XRD:** X-Ray Diffraction

**XRF:** X-Ray Fluorescence

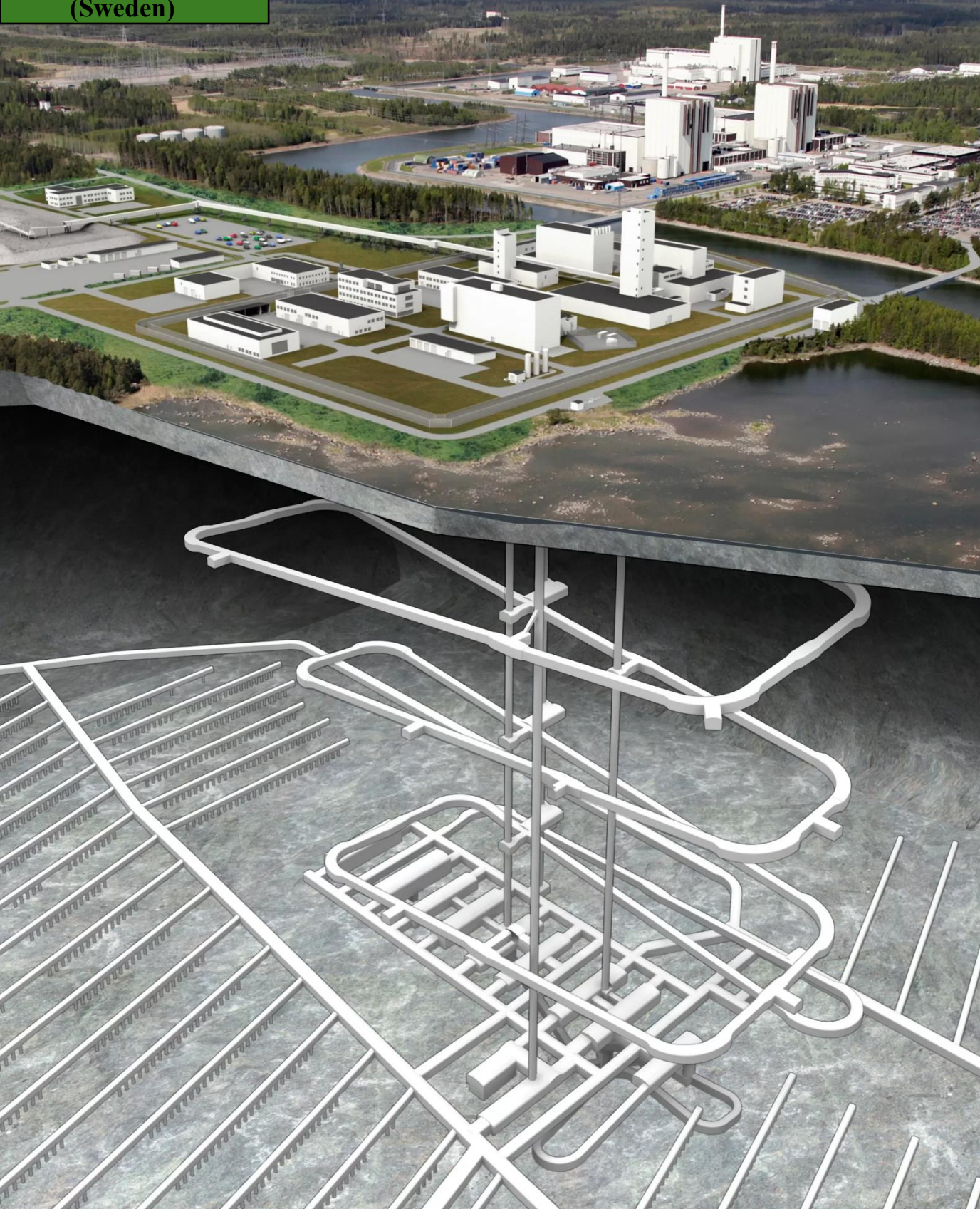
## ÍNDICE DE CONTENIDOS

<b>RESUMEN</b> .....	1
<b>SUMMARY</b> .....	9
<b>INTRODUCTION: Insights into the impact of physicochemical and microbiological parameters on the safety performance of deep geological repositories</b> .....	15
Introduction.....	19
Effect of radiation.....	22
Effect of bentonite dry density and microbial activity on bentonite performance as an engineered barrier in DGRs.....	27
Effect of radionuclides on the diversity and viability of bentonite microbial communities.....	33
Copper corrosion under repository conditions.....	40
Effect of oxygen, gasses, and nutrients on the microorganisms.....	44
Effect of temperature.....	47
Limitations, challenges, and opportunities.....	52
Conclusions.....	53
<b>OBJECTIVES</b> .....	73
<b>MATERIALS AND METHODS</b> .....	77
Bentonite sample collection and storage.....	79
Copper material for corrosion studies.....	80
Characterization of bentonite microbial communities.....	81
Molecular identification of bacterial isolates and culture-media enrichments.....	83
Microscopic and spectroscopic analysis.....	84

Mineralogical and chemical characterization of bentonite.....	87
Irradiation conditions.....	90
<b>CHAPTER 1:</b> Assessing the impact of radiation and high compaction on FEBEX bentonite: microbial, mineralogical, and copper corrosion studies.....	93
<i>Supplementary material for Chapter 1</i> .....	157
<b>CHAPTER 2:</b> High temperature impact on bentonite microbial communities: A study of Se(IV) biogeochemical cycle.....	171
<i>Supplementary material for Chapter 2</i> .....	227
<b>CHAPTER 3:</b> High-temperature microbial corrosion of copper by sulfate-reducing bacteria in water-saturated bentonite microcosms and its relevance to nuclear waste deep geological repositories.....	239
<i>Supplementary material for Chapter 3</i> .....	287
<b>CHAPTER 4:</b> Long-term tracking of the microbiology of uranium- amended water-saturated bentonite microcosms: a mechanistic characterization of U speciation.....	295
<i>Supplementary material for Chapter 4</i> .....	345
<b>GENERAL DISCUSSION</b> .....	359
<b>CONCLUSIONS</b> .....	381
<b>CONCLUSIONES</b> .....	387



Image from SKB  
(Sweden)





# *Resumen*



# *Summary*



## RESUMEN / SUMMARY

**RESUMEN**

Los residuos radiactivos de alta actividad (RRAA, por sus siglas en español) pueden emitir radiación durante cientos de miles de años. Para gestionar este riesgo y proteger la biosfera los RRAA se confinarán en almacenamientos geológicos profundos (AGP). Este método de almacenamiento consiste en un sistema de múltiples barreras que incluye un contenedor metálico resistente a la corrosión (fabricado con acero al carbono, cobre, etc.), rodeado de materiales de relleno y sellado, como arcilla bentonita o cemento, todo ello colocado a profundidades de hasta 1.000 metros en una roca madre hospedadora geológicamente estable. Supone un desafío significativo el tener que garantizar la seguridad de este sistema durante largos periodos de hasta 100.000 años. Por este motivo, se han estudiado extensamente las propiedades químicas, físicas y geológicas de estas barreras, sin embargo, el impacto de los microorganismos sobre ellas y bajo condiciones relevantes para el almacenamiento, sigue siendo aún un área relativamente inexplorada. Investigaciones recientes se han centrado en comprender la influencia de microorganismos, tanto autóctonos como accidentalmente incorporados durante la construcción, en la seguridad del almacenamiento. Estos microorganismos podrían afectar la integridad y estabilidad de este sistema de almacenamiento a través de diferentes procesos, entre los que se incluyen la corrosión del contenedor metálico, la alteración de la mineralogía de la bentonita/roca hospedante, la transformación de la especiación química de los radionúclidos, y la generación de gases que aumentarían la presión interna.

ENRESA (Empresa Nacional de Residuos Radiactivos S.A.) es la organización responsable de la gestión de residuos radiactivos en España y quien está liderando la planificación y desarrollo del futuro almacenamiento geológico profundo español. El programa español aún se encuentra en sus primeras

## RESUMEN / SUMMARY

etapas, pero ya se han definido algunos detalles, como la selección inicial de materiales de referencia, entre los que destaca la bentonita de "El Cortijo de Archidona", conocida como FEBEX (*Full-scale Engineered Barriers Experiment*). Esta bentonita ha sido sometida a extensos ensayos geoquímicos y mineralógicos para evaluar su idoneidad como barrera artificial, mientras que la investigación sobre su microbiología apenas ha comenzado a lo largo de la última década.

De acuerdo con lo mencionado anteriormente, el principal objetivo de esta tesis doctoral es evaluar los efectos de diversos factores fisicoquímicos, como la radiación, las altas temperaturas, la compactación de la bentonita y la actividad del agua, así como factores bióticos, entre ellos la actividad de las bacterias reductoras de sulfato (SRB por sus siglas en inglés), sobre la estabilidad de las barreras artificiales del AGP. En particular, el estudio se ha centrado en la bentonita española y contenedores metálicos basados en cobre bajo condiciones relevantes para el almacenamiento. Otro objetivo importante ha sido investigar la respuesta de los microorganismos autóctonos de la bentonita en caso de fallo del sistema, incluyendo situaciones donde radionúclidos como el selenio o el uranio pudieran liberarse y filtrarse al ambiente circundante.

En una primera fase se investigó un escenario más realista que consideraba los efectos combinados de alta densidad de compactación ( $1,6 \text{ g/cm}^3$ ) y radiación gamma (14 kGy o 28 kGy), así como condiciones de saturación de agua, presencia de bacterias reductoras de sulfato y una atmósfera anóxica en bloques de bentonita FEBEX. Además, los bloques de bentonita contenían un disco de cobre puro (Cu) para estudiar la corrosión bajo estas condiciones. Los análisis microbiológicos mediante métodos moleculares (*Next-generation sequencing*) y dependientes de cultivo revelaron que las condiciones de compactación, el entorno anóxico y la baja disponibilidad de nutrientes

favorecían la proliferación de microorganismos formadores de esporas. Más específicamente, tras un año de incubación, se identificaron géneros resistentes a condiciones adversas, como *Saccharopolyspora*, *Streptomyces*, *Massilia* y *Acinetobacter*. Por otra parte, la radiación gamma parecía tener un efecto negativo sobre la viabilidad de los microorganismos heterótrofos aeróbicos y las SRB. No obstante, se observó que un periodo de incubación de los bloques de bentonita previo a la exposición de radiación mejoraba la supervivencia microbiana a este agente. Los estudios de corrosión del cobre revelaron que los óxidos de este metal, especialmente CuO, eran los productos de corrosión predominantes en todas las muestras. Además, la radiación gamma ralentizó la corrosión biótica al impactar negativamente en la microbiota y promover la precipitación de sales, incluidos posibles sulfatos de cobre. Las SRB fueron responsables de la formación de sulfuros de cobre biogénicos, los cuales se hallaron exclusivamente en la bentonita. A pesar de estos efectos, tanto la radiación como las demás condiciones experimentales no alteraron negativamente las propiedades mineralógicas de la bentonita FEBEX que se mantuvieron estables tras un año de incubación.

Una vez sellado, el almacenamiento pasará por varias fases durante los próximos miles de años. Inicialmente, la interfaz metal-bentonita estará expuesta a condiciones secas, óxicas y a temperaturas de alrededor de 100 °C debido a los residuos radiactivos almacenados. Con el tiempo estas temperaturas disminuirán gradualmente, estabilizándose por encima de los 60 °C durante unos cientos de años. En este contexto, la presente tesis doctoral también investiga los efectos de las altas temperaturas sobre la microbiología de la bentonita, la corrosión del cobre y la estabilidad mineralógica y química de la bentonita. En concreto, estos estudios simulan un posible fallo del sistema que incluye la fuga de residuos (selenio), la infiltración de aguas subterráneas que provoca la pérdida de compactación de la bentonita (bentonita

## RESUMEN / SUMMARY

hipersaturada de agua), la disponibilidad de donadores y aceptores de electrones (acetato, lactato, sulfato) y una alta actividad bacteriana (un consorcio bacteriano compuesto por especies identificadas de forma natural en la bentonita española). Para llevar a cabo estos estudios, se añadió selenito de sodio (2 mM) como análogo inactivo del isótopo radiactivo crítico  $^{79}\text{Se}$ . Tras dos meses de incubación, tanto la alta temperatura (60 °C) como el tratamiento térmico (tindalización a 110 °C) promovieron el crecimiento de géneros termófilos nativos de la bentonita tales como *Clostridium*, *Pseudomonas*, *Caloribacterium* y *Thermaerobacter*. Además, el consorcio bacteriano inoculado influyó significativamente en las comunidades microbianas, resultando en la predominancia de *Stenotrophomonas* y *Pseudomonas*. Por otro lado, este consorcio tuvo un notable impacto en la reducción de Se(IV) como se evidenció por el cambio de color a naranja tras solo 4 días de incubación, indicando la presencia de Se(0). Este hallazgo se confirmó mediante análisis con espectrometría de masas, que mostró una reducción del Se(IV) soluble de casi el 100 % en los tratamientos con consorcio bacteriano tras 2 meses de incubación. Además, mediante técnicas microscópicas y espectroscópicas se corroboró esta reducción de Se(IV) que ocurrió en forma de nanopartículas de Se(0) con diversas morfologías, así como nanoagregados de Se+Fe que probablemente correspondían al mineral ferroselita ( $\text{FeSe}_2$ ). En ausencia del consorcio bacteriano el porcentaje de reducción fue mucho menor, aunque aún se observó, posiblemente facilitado por la presencia de donadores y aceptores de electrones. Debido a la naturaleza insoluble y estable de Se(0) y las fases minerales como  $\text{FeSe}_2$ , la reducción de Se(IV) soluble promovería eficazmente la bioinmovilización de este metaloide. Así pues, las comunidades microbianas en la bentonita tendrían un impacto positivo en el ciclo biogeoquímico del selenio, inmovilizando este radionúclido crítico y reduciendo su movilidad dentro de las barreras del DGR. Curiosamente, la presencia de selenio redujo

el impacto de la actividad microbiana sobre la corrosión del cobre. Este efecto probablemente se debió a la competencia entre Se(IV) y Cu por el sulfuro de hidrógeno ( $\text{HS}^-$ ), producido por las SRB. La interacción entre Se(IV) y  $\text{HS}^-$  reduciría la disponibilidad de sulfuro libre, disminuyendo así las posibilidades de que reaccione con el cobre. Aunque el selenito afectó negativamente la viabilidad de las SRB, según se puso de manifiesto por el método del número más probable (NMP), todos los tratamientos con selenio mostraron resultados positivos de viabilidad para este grupo bacteriano.

Por último, también se llevó a cabo un estudio a largo plazo para investigar más a fondo el impacto de los microorganismos en la especiación química del uranio (U). Esta investigación se realizó bajo condiciones simuladas de fallo del sistema, considerando alta actividad bacteriana (consorcio bacteriano inoculado), disponibilidad de agua, presencia de donadores de electrones (acetato y glicerol-2-fosfato) y una simulación de fuga de  $^{235}\text{U}$  (utilizando una solución de 1,26 mM de acetato de uranio). Los microcosmos tratados fueron incubados durante tres años en condiciones anóxicas a 28 °C. Tras este período de incubación, los resultados de la secuenciación Illumina revelaron una diversidad bacteriana en la bentonita dominada por microorganismos anaerobios y formadores de esporas, principalmente del filo Firmicutes. Además, la incubación en presencia de uranio enriqueció aislados bacterianos viables y tolerantes a este metal, pertenecientes a los géneros *Peribacillus*, *Bacillus* y algunas SRB como *Desulfovibrio* y *Desulfosporosinus*. Los análisis espectroscópicos revelaron la presencia de U(VI), identificado como fosfatos biogénicos de  $\text{U(VI)[(U(VO}_2)(\text{PO}_4)_2)]$  ubicados en las superficies internas de membranas celulares bacterianas, así como U(VI) adsorbido en montmorillonita, mineral mayoritario de la bentonita. Además, se detectaron especies de U(IV), como la uraninita, probablemente formadas mediante la reducción enzimática bacteriana de U(VI). Estos resultados son consistentes

## RESUMEN / SUMMARY

con los hallazgos de la investigación sobre selenio, indicando que, cuando se exponen a condiciones óptimas de crecimiento, las bacterias nativas de la bentonita española influyen activamente en la especiación química del uranio, facilitando su estabilización en formas menos solubles.

En términos generales, los hallazgos de esta tesis doctoral ofrecen nuevas perspectivas sobre el impacto de los procesos microbianos en la estabilidad de las barreras de bentonita y contenedor metálico de cobre en un sistema AGP. Los resultados obtenidos simulando tanto condiciones relevantes del almacenamiento (radiación, compactación, anoxia, temperatura) como escenarios en los que el sistema falla, han destacado el papel crucial de los microorganismos como una barrera adicional en caso de fuga de residuos nucleares.

**SUMMARY**

High-level radioactive waste (HLW) can emit radiation for up to hundreds of thousands of years. To manage this risk and protect the biosphere, HLW would be confined in deep geological repositories (DGRs). This disposal approach consists of a multi-barrier system that includes a corrosion-resistant metal canister (made of carbon steel, copper, etc.), surrounded by backfilling and sealing materials such as bentonite clay or cement, all placed at depths of up to 1,000 meters in a geologically stable host rock. Ensuring the safety of this system over long timescales, up to 100,000 years, presents a significant challenge. While the chemical, physical, and geological properties of these barriers have been extensively studied, the impact of microorganisms on their integrity under repository relevant conditions remains relatively unexplored. Recent research has focused on understanding the influence of both indigenous and accidentally introduced microorganisms on the repository safety. These microorganisms could affect the integrity and stability of this disposal system through different processes including, among others, metal canister corrosion, bentonite/host rock mineralogy alteration, radionuclide chemical speciation transformation, and generation of gases that increase internal pressure. ENRESA (Empresa Nacional de Residuos Radiactivos S.A.), the organization responsible for radioactive waste management in Spain, is leading the planning and development of future Spanish deep geological repository. Although the program is still in its early stages, initial reference material selection has already been specified, including bentonite from “El Cortijo de Archidona”, known as FEBEX (Full-scale Engineered Barriers Experiment). This bentonite has undergone extensive geochemical and mineralogical characterizations to assess its suitability as an engineered barrier, while research on its microbiology has only recently begun, within the last decade.

## RESUMEN / SUMMARY

Therefore, the main objective of this Ph.D. thesis is to assess the effects of various physicochemical factors, such as radiation, high temperatures, bentonite compaction, and water activity, along with biotic factors, including the activity of sulfate-reducing bacteria (SRB), on the stability of the artificial DGR barriers. Specifically, the study focused on bentonite and copper metal canisters under relevant repository conditions. Another key objective was to investigate the behavior of the indigenous bentonite microorganisms in the event of a system failure, where radionuclides such as selenium or uranium might leak into the surrounding environment.

At first, a more realistic scenario was investigated taken in account the combined effects of high compaction density ( $1.6 \text{ g/cm}^3$ ) and gamma radiation (14 kGy or 28 kGy), as well as conditions of water saturation, the presence of SRB, and an anoxic atmosphere in FEBEX bentonite blocks. In addition, the bentonite blocks contained pure copper (Cu) disks, in order to study the corrosion induced under such conditions. Next-generation sequencing and culture-dependent microbiological analyses revealed that spore-forming microorganisms were promoted by the conditions of compaction, anoxic environment, and low nutrient availability. More specifically, after one year of incubation, harsh condition-resistant genera such as *Saccharopolyspora*, *Streptomyces*, *Massilia* and *Acinetobacter* were identified. Moreover, gamma radiation seemed to adversely affect the viability of aerobic heterotrophs and SRB. However, a pre-exposure incubation period of the bentonite blocks was found to enhance microbial survival to such radiation. Copper corrosion studies revealed the presence of oxides of this metal, mainly CuO, as the predominant corrosion products in all samples. Furthermore, gamma radiation delayed biotic corrosion by negatively impacting the microbiology and promoting salt precipitation, including potential copper sulfates. The SRBs were responsible for producing biogenic copper sulfides, which were found

exclusively within the bentonite. Despite these effects, the radiation and the other experimental conditions did not adversely affect the mineralogical properties of FEBEX bentonite, which remained stable after one year.

Once sealed, the repository will undergo various phases over the next thousand years. Initially, the interface metal canister/bentonite will be exposed to dry, oxic conditions and temperatures around 100 °C due to the stored HLW. These temperatures will gradually decrease over the time, stabilizing above 60 °C for a few hundred years. Therefore, this Ph.D. thesis also investigates the effects of high temperatures on bentonite microbiology, copper corrosion, and the mineralogical and chemical stability of bentonite. Specifically, these studies mimic a possible system failure that includes waste leakage (selenium), groundwater seepage causing loss of bentonite compaction (bentonite slurry), availability of electron donors and acceptors (acetate, lactate, sulfate), and high bacterial activity (a bacterial consortium composed of bacteria naturally identified in Spanish bentonite). To carry out this studies, sodium selenite (2 mM) was added as the inactive analogue of the critical radioactive isotope <sup>79</sup>Se. After two months of incubation, the high-temperature (60 °C) and heat-shocked bentonite treatment (tyndallization at 110 °C) promoted the growth of thermophilic genera, indigenous to bentonite, including *Clostridium*, *Pseudomonas*, *Caloribacterium*, and *Thermaerobacter*. Additionally, the amended bacterial consortium significantly influenced the microbial communities, resulting in the predominance of *Stenotrophomonas* and *Pseudomonas*. On the other hand, this consortium highly impacted the reduction of Se(IV), as demonstrated by the color change to orange within just 4 days of incubation, indicative of the resulting Se(0). Inductively coupled plasma mass spectrometry (ICP-MS) analysis confirmed this finding, revealing a nearly 100% reduction of soluble Se(IV) after two months in consortium treatments. Results from scanning transmission electron

## RESUMEN / SUMMARY

microscopy (STEM) combined with energy dispersive X-ray (EDX) spectroscopy further confirmed the reduction of Se(IV) to Se(0) nanoparticles with different morphologies, as well as Se+Fe nanoaggregates that likely corresponded to the mineral ferroselite (FeSe<sub>2</sub>). In the absence of the bacterial consortium, the percentage reduction was much lower but still occurred, possibly facilitated by the presence of the electron donors and acceptors. Due to the insoluble and stable nature of Se(0) and mineral phases such as FeSe<sub>2</sub>, the reduction of soluble Se(IV) would effectively promote the bioimmobilization of this metalloid. Thus, the microbial communities in bentonite would positively impact the biogeochemical cycling of selenium by immobilizing this critical radionuclide, thereby reducing its mobility within DGR barriers. Interestingly, the presence of Se reduced the impact of microbial activity on copper corrosion. This effect probably occurred due to the competition between Se(IV) and Cu for hydrogen sulfide (HS<sup>-</sup>), which is produced by SRB. The interaction between Se(IV) and HS<sup>-</sup> would hinder the availability of free sulfide, thereby reducing the chances of it reacting with copper. Selenite negatively affected the viability of SRB as determined by the most probable number (MPN) method; however, all selenium treatments still indicated positive viability results for this bacterial group.

Additionally, a long-term study was conducted to further investigate the impact of microorganisms on the chemical speciation of uranium (U). This research was also performed under simulated system failure conditions, considering high bacterial activity (inoculated bacterial consortium), water availability, electron donor loading (acetate and glycerol-2-phosphate), and a simulated leakage of <sup>235</sup>U (using 1.26 mM solution of uranyl acetate). Three years of incubation was carried out for the treated microcosms under anoxic conditions at 28 °C. After such incubation time, Illumina sequencing results revealed a bentonite bacterial diversity dominated by anaerobic and spore-forming

microorganisms, mainly belonging to the phylum Firmicutes. Highly U-tolerant and viable bacterial isolates belonging to the genera *Peribacillus*, *Bacillus*, and some SRB such as *Desulfovibrio* and *Desulfosporosinus* were enriched from the U-treated bentonite. Spectroscopic analyses by X-ray photoelectron spectroscopy (XPS) and X-ray diffraction (XRD) revealed the presence of U(VI), identified as biogenic U(VI) phosphates ( $U(VO_2)(PO_4)_2$ ) located on the inner surfaces of bacterial cell membranes, as well as U(VI) adsorbed onto montmorillonite, the major mineral of bentonite. Additionally, U(IV) species, such as uraninite, were also detected, being probably formed through the bacterial enzymatic reduction of U(VI). These results demonstrated to be consistent with the selenium research findings, indicating that when exposed to optimal growth conditions, the bacteria native to Spanish bentonite actively influence the chemical speciation of uranium, thereby facilitating its stabilization in less soluble forms.

In broad terms, the findings of this Ph.D. thesis provide novel insights into the impact of microbial processes on the performance of the bentonite and copper canister barriers in the DGR system. Novel outcomes are reported under both realistic repository conditions (radiation, compaction, anoxia, temperature) and system failure scenarios, demonstrating the role of microorganisms as an additional barrier in the event of nuclear waste leakage.

Image from iStock

**RADIOACTIVE  
WASTE**



CAUTION: HIGHLY CORROSIVE MATERIALS CAN CAUSE RAPID DAMAGE.  
KEEP OFFICE, INDOORS AND OUTDOORS. STORE AND USE IN  
APPROPRIATE VENTILATION. DO NOT BREATHE VAPOR OR USE AND  
WASH GLOVES. USE WITH EQUIPMENT SALES FOR PROTECTIVE  
EQUIPMENT. ALWAYS SECURE CLOSURE. CONTACT 1-800-451-7888  
FOR MORE INFO.

**FOR INDUSTRIAL USE ONLY**

**RADIOACTIVE  
WASTE**



CAUTION: HIGHLY CORROSIVE MATERIALS CAN CAUSE RAPID DAMAGE.  
KEEP OFFICE, INDOORS AND OUTDOORS. STORE AND USE IN  
APPROPRIATE VENTILATION. DO NOT BREATHE VAPOR OR USE AND  
WASH GLOVES. USE WITH EQUIPMENT SALES FOR PROTECTIVE  
EQUIPMENT. ALWAYS SECURE CLOSURE. CONTACT 1-800-451-7888  
FOR MORE INFO.

**FOR INDUSTRIAL USE ONLY**



## *Introduction*

Insights into the impact of physicochemical and microbiological parameters on the safety performance of deep geological repositories

### *Authors*

**Mar Morales-Hidalgo\***, Cristina Povedano-Priego, Marcos F. Martinez-Moreno, Miguel A. Ruiz-Fresneda, Margarita Lopez-Fernandez, Fadwa Jroundi\* and Mohamed L. Merroun

---

*Faculty of Sciences, Department of Microbiology, University of Granada, Granada, Spain*

This introduction section has been published as review article in *Microorganisms*: <https://doi.org/10.3390/microorganisms12051025>

**IF: 4.1 / Q2**

## INTRODUCTION

### **Abstract**

Currently, the production of radioactive waste from nuclear industries is increasing, leading to the development of reliable containment strategies. The deep geological repository (DGR) concept has emerged as a suitable storage solution, involving the underground emplacement of nuclear waste within stable geological formations. Bentonite clay, known for its exceptional properties, serves as a critical artificial barrier in the DGR system. Recent studies have suggested the stability of bentonite within DGR relevant conditions, indicating its potential to enhance the long-term safety performance of the repository. On the other hand, due to its high resistance to corrosion, copper is one of the most studied reference materials for canisters. This review provides a comprehensive perspective on the influence of nuclear waste conditions on the characteristics and properties of DGR engineered barriers. This paper outlines how evolving physico-chemical parameters (e.g., temperature, radiation) in a nuclear repository may impact these barriers over the lifespan of a repository and emphasizes the significance of understanding the impact of microbial processes, especially in the event of radionuclide leakage (e.g., U, Se) or canister corrosion. Therefore, this review aims to address the long-term safety of future DGRs, which is critical given the complexity of such future systems.

**Keywords:** *Nuclear waste; Radiation; Bentonite; Corrosion; Microorganism; Compaction; Temperature; Deep Geological Repository.*

## INTRODUCTION

## 1. Introduction

The increasing production of radioactive waste due to the extensive use of nuclear power has underscored the urgency for developing reliable strategies for the long-term containment of these hazardous materials. In response to this emerging challenge, the deep geological repository (DGR) model has been proposed for the secure confinement of radioactive waste (IAEA 2022). This system entails depositing nuclear waste in metallic canisters underground at a depth of approximately 500 m within stable geological formations. Depending on the country, the materials used in the various barriers, as well as other physico-chemical characteristics related to the design of the repository, may vary. **Table 1** presents the main information concerning the materials and their properties to be expected in future repositories of the principal national companies involved in the development of DGRs. In many countries including Spain, Switzerland, Belgium, Finland, France, and Canada, the canisters will be surrounded by compacted clay materials selected for their ability to provide mechanical, hydraulic, and thermal protection (Xu et al., 2019; Bajestani et al., 2023). Specifically, bentonite clay has been recognized as a suitable material to use as both artificial and natural barriers within the DGR systems due to its exceptional properties. The utilization of bentonite from various locations has been extensively investigated as a buffer material. Notable examples include MX80 from the United States, FEBEX from Spain, FoCa from France, and GMZ from China. These formations particularly exhibit low permeability (resulting in a decrease in groundwater filtrations), mechanical support (ensuring stability), swelling capacity (facilitating the self-sealing of cracks), thermal conductivity (preventing overheating), and ion exchange capacity (enabling radionuclide retention) (García-Romero et al., 2019). In addition, bentonite presents optimal compaction properties, which not only significantly contribute to improving the mechanical support, thermal conductivity, and

## INTRODUCTION

sealing properties mentioned previously, but may also influence the viability of the bentonite microbial communities.

Highly compacted bentonite blocks are thought to prevent microbial growth (Stroes-Gascoyne et al., 2010). Despite this, recent studies have demonstrated microbial stability in compacted bentonite under conditions that mimic a DGR (Engel et al., 2023). Thus, these microorganisms are expected to maintain their viability and metabolic activity within such a harsh system.

Microorganisms have the potential to affect their surrounding environment and, consequently, the safety of DGRs through various processes. These include the generation of gases, corrosion of metal canisters (Dou et al., 2020), alteration of redox conditions (Hall et al., 2021), transformation of mineral clays (Mills et al., 2022), and interaction with radionuclides (Ruiz-Fresneda et al., 2023; 2024). A wide variety of physical (temperature, radiation, groundwater filtration, bentonite compaction, etc.), chemical (gaseous compounds, corrosion, presence/absence of oxygen, etc.), and biological factors (microbial activity) may compromise the performance of both bentonite barriers and their microbial communities. Given all these considerations, evaluating how these factors may compromise the safety of these storage facilities is of crucial importance to ensure the secure disposal of these highly polluting and hazardous waste materials, which threaten the health of living organisms.

This review provides a comprehensive analysis of the most recent advances in studies predicting and evaluating environmental conditions that would affect the performance and safety of future deep geological repository systems. A special focus is given to the effect of radiation, temperature, bentonite compaction and various biotic and abiotic factors on the microbial behavior in bentonite barriers.

**Table 1.** Information on DGR models to be followed by each company representing the main countries involved in the management of high-level nuclear waste.

COUNTRY	COMPANY	CANISTER	BUFFER	BUFFER DENSITY (g/cm <sup>3</sup> )	HOST ROCK	ABSORBED DOSE AT THE SURFACE (Gy/h)	TEMPERATURE AT THE SURFACE (°C)	REFERENCES
Spain	ENRESA	Carbon steel	Bentonite	1.65	Clay / Granite	Not determined	< 100	Villar et al., 2006; 7° Plan General 2023
Finland	POSIVA	Copper + cast iron	Bentonite	1.55	Crystalline	0.33	~ 90	Werme et al., 1998; Bennett et al., 2008; Jonsson et al., 2018
Sweden	SKB	Copper + cast iron	Bentonite	1.6	Crystalline	0.2	~ 90	Bennett et al., 2008; Abdelouas et al., 2022
Switzerland	NAGRA	Carbon steel	Bentonite	> 1.45	Opalinus clay	< 0.035	< 150	Bennett et al., 2008; Johnson et al., 2002; Landolt et al., 2009
France	ANDRA	Carbon steel	none	-	Granite	< 10	~ 90	Bennet et al., 2008; Abdelouas et al., 2022
Czech Republic	SÚRAO	Carbon steel	Bentonite	1.4	Crystalline	0.3	< 95	Abdelouas et al., 2022; Pospiskova et al., 2017; Prachař et al., 2017
Belgium	ONDRAF-NIRAS	Carbon steel	Cement / Concrete	-	Boom clay	25	~ 95	Bennett et al., 2008; Abdelouas et al., 2022
Canada	NWMO	Carbon steel coated with copper	Bentonite	1.6	Crystalline / sedimentary	2	< 100	McMurry et al., 2004; Guo et al., 2020; Binns et al., 2023

## INTRODUCTION

### 2. Effect of radiation

The DGR concept is designed almost exclusively for the management of so-called high-level waste (HLW). HLW includes radioactive waste with substantial amounts of long-lived alpha and beta–gamma emitters, making this waste highly radioactive and capable of generating high temperatures. Most of this type of waste includes spent nuclear fuel (SF) generated by nuclear power plants. The other minority contains waste resulting from the reprocessing of SF, as well as residues from research, industry, and mining (ENRESA, Cátedra Enresa). One of the main concerns regarding HLW is the presence of elements with very long half-lives, spanning hundreds of thousands of years (Chapman, 2006). Hence, examining the impact of radiation, particularly gamma radiation due to its high penetrative ability, on different barriers of future repositories has been of paramount importance from the outset to guarantee long-term safety. The measurement of radiation energy absorbed by a material is quantified as the absorbed dose, which is expressed in the international system of units (SI) as Gray (Gy). Ionizing radiation can interact with matter through various mechanisms and thus alter its properties (Jonsson, 2012). This section will only focus on the effects of gamma radiation on copper (Cu) corrosion, bentonite stability, and microbial presence and survival. In general, the absorbed doses at the surface level of the canister are expected to be relatively low, though this will vary depending on the DGR model (**Table 1**). Furthermore, as the distance from the radiation source increases, the received radiation doses decrease progressively. Consequently, the radiation levels experienced within the canister will be higher than those within the engineered bentonite barrier, and the radiation within the latter will be higher than that received by the host rock. Despite the relatively low radiation doses experienced in the various barriers, some studies have been conducted on the

impact of gamma radiation on canister corrosion and the bentonite barrier to prevent potential leaks.

## **2.1. Copper corrosion**

Gamma radiation primarily arises from the decay of the fission product Cs-137, which possesses a relatively short half-life of 30 years. Consequently, the intensity of this radiation is expected to decrease relatively quickly following the closure of the repository (Soroka et al., 2021). Its impact on copper corrosion would be mainly indirect, occurring through its reaction with water and the subsequent decomposition into oxidizing ( $\text{HO}\cdot$  and  $\text{H}_2\text{O}_2$ ) and reducing agents ( $\text{H}\cdot$  and  $\text{H}_2$ ), which is known as the radiolysis process (Spinks et al., 1990). Of all the species generated, the most concerning are hydrogen peroxide ( $\text{H}_2\text{O}_2$ ) and the hydroxyl radical ( $\text{HO}\cdot$ ), as they are the most thermodynamically stable and have higher standard reduction potential than copper (Björkbacka et al., 2015). In addition, radiolysis of humid air can also generate other reactive species such as  $\text{NO}_x$  and  $\text{HNO}_3$  (Reed and Konynenburg, 1987). Björkbacka et al. (2013) reported that absorbed doses of gamma radiation caused corrosion in copper under conditions of anoxic aqueous solutions, both uniformly and locally. The main corrosion products were copper(I) oxide ( $\text{Cu}_2\text{O}$ ) along with a small fraction of copper(II) oxide ( $\text{CuO}$ ). In recent years, several studies have been focused on examining the corrosion products on the surface of copper canisters following exposure to gamma radiation doses. However, a challenge persists as most of these studies have been conducted at doses significantly higher than those expected in the repository. This discrepancy arises from the challenge of conducting experiments under realistic repository conditions, where radiation exposure rates will be very low but extended over time. Consequently, the corrosion magnitude observed in these studies surpasses that predicted by simulation

## INTRODUCTION

models (Björkbacka et al., 2016; 2017; Norrfors et al., 2018). The research by King et al. (2010) demonstrated that to induce significant corrosion concerns, a threshold of 100 Gy/h would need to be surpassed. Additionally, they suggested that dose values below this threshold could marginally decrease corrosion, possibly due to the formation of a passive protective oxide layer that many metals develop to resist corrosion.

### **2.2. Bentonite stability**

Due to the dispersal capability of gamma radiation, potential effects could occur on the buffer barrier as well (Galamboš et al., 2012; Allard et al., 2009). This review will specifically focus on its impact on the chemical and mineralogical composition of bentonite clay, as well as its cation exchange capacity (Allard et al., 2009). Therefore, one of the essential requirements for its utilization as a buffer and sealing material would be the rheological and chemical stability when exposed to ionizing radiation and even in the presence of radionuclides in the worst-case scenario of a waste leak (Striček et al., 2008; 2010; Plötze et al., 2003). Radiation can impact the clay structure and, consequently, its properties, through processes such as inducing amorphization and affecting the sorption capacity of elements. This would compromise the long-term stability of this material and, thus, the safety and integrity of the repository (Allard et al., 2012). However, most experiments clearly indicate that the amorphization of bentonite can be ruled out under radiation levels anticipated in future DGRs, as this phenomenon only occurs at significantly higher levels. For instance, Sorieul et al. (2008) reported that a radiation dose of at least 1011 Gy is required for clay to become amorphous. Additionally, Galamboš et al. (2012) concluded that bentonite from Slovakia exhibited no changes or very insignificant ones in their structural properties after exposure to gamma radiation. Nevertheless, in a study conducted in 2011 by Holmboe

et al., the effects of  $\gamma$  radiation on the ability of MX80 bentonite to retain radionuclides were tested. They observed a notable decrease in  $\text{Co}_2^+$  sorption in irradiated samples but not in  $\text{Cs}^+$  which may suggest that this form of irradiation could have altered the surface characteristics relevant to the sorption of this radionuclide. Additionally, bentonite is notable for its high content of accessory minerals. It has been observed that the distribution of these minerals could also impact the behavior of this clay, as they may dissolve and alter the properties under radiation conditions. On the other hand, other studies have demonstrated that the stability of bentonite against radiation depends on the water content, attributed to the radiolysis effect occurring within its pores. Gu et al. (2001) noted that the stability of bentonite increases when the water content is lower, as it results in a lower number of products from the radiolysis of water. More recent studies, such as that of Chikkamath et al. (2021), have corroborated this effect by finding that doses of up to 12 kGy/h had no effect on Fe(II)-clay powder samples. This outcome was probably due to the fact that the irradiated samples were dry, resulting in a lower impact of water radiolysis. Indeed, it has already been highlighted the contradictory results concerning the alterations in the surface reactivity of bentonite when subjected to radiation (Allard et al., 2009). Whilst some authors have reported an increase in the ion exchange capacity, others have observed the opposite effect. Accordingly, current knowledge continues to advance in this field to establish the impact of this radiation on buffer clay materials.

### **2.3. Microbial viability**

Radiation would also affect the microbial communities present in the future repositories by altering their structure, viability, and activity. To compare radiation sensitivity of microorganisms, the term decimal reduction dose (D10)

## INTRODUCTION

is used, which is defined as the radiation dose (in kGy) necessary to reduce a microbial population by 90% of its total number (Van Gerwen et al., 1999). As previously mentioned, the effect of radiation depends on the perceived dose, which will vary depending on various factors including the distance from the radiation source, the barrier model, the type of radionuclide contained, and its lifetime (Černá et al., 2019). Not only does radiation itself cause changes and damage at the cellular level, but the reactive oxygen species (ROS) resulting from the radiolysis process will also affect most biomolecules. One of the most prominent forms of damage is to DNA, causing DNA strand breaks, base changes, mutations, etc. (Wouters et al., 2009). In general, microorganisms respond to such damage with different defense mechanisms to repair as much as possible. These mechanisms include DNA repair systems, production of antioxidant enzymes to cope with reactive oxygen species, and antioxidant processes involving increased intracellular concentrations of inorganic solutes and pigments (Jung et al., 2017). The response of microorganisms to radiation varies amongst strains, as sensitivity depends on factors such as cellular water content, DNA size and structure, antioxidant, and DNA repair systems, as well as the ability to develop resistant cell forms, amongst others. The latter is particularly important, as several studies have shown that the tolerance of bacterial spores to radiation is significantly higher than that of vegetative cells (Van Gerwen et al., 1999). Furthermore, this sensitivity also depends on environmental conditions: water activity, level of desiccation, presence or absence of oxygen, etc. For instance, many studies reported that conditions such as a dry environment, lack of oxygen, and low temperatures enhance radiation resistance (Mattimore et al., 1996; Alper et al., 1956; Musilova et al., 2015). The literature on bacterial species highly resistant to radiation is quite limited; however, two strains are referenced and have been well studied for their high resistance to radiation, namely *Deinococcus radiodurans*, with a

tolerance of up to 17 kGy (Daly et al., 2009), and *Kineococcus radiotolerans* (Phillips et al., 2002; Bagwell et al., 2008). In general, the majority of strains capable of resisting certain doses tend to be extremophiles, exhibiting tolerance to other extreme conditions of temperature, desiccation, or high concentration of salts (Černá et al., 2019). On the other hand, regarding the bentonite bacterial community, some studies have reported *Bacillus*, *Acinetobacter*, *Desulfosporosinus*, and *Clostridium* to also be resistant to radiation doses (Stroes-Gascoyne et al., 1994; Haynes et al., 2018).

Nevertheless, in the future repositories, microorganisms will not only face radiation as a stress factor. Therefore, more research is needed to understand the evolution of microbial communities under the combination of various repository conditions.

### **3. Effect of bentonite dry density and microbial activity on bentonite performance as an engineered barrier in DGRs**

HLW will be contained within canisters crafted from corrosion-resistant materials such as copper, stainless steel, or “novel materials”, which are typically subjected to very low corrosion rates. Regarding novel metal canisters, the advanced coatings and alloys (e.g., Ni or Ti alloy and ceramic coated metals) are expected to delay corrosion, but their degradation is not ruled out when subjected to hydration, irradiation, and temperature. The different metallic canisters will be encased in a protective buffer of compacted bentonite securely stored deep underground, at depths of several hundred meters, thus ensuring a robust containment system for the safe disposal of the nuclear waste (Ojovan et al., 2022).

Bentonite is rich in a swelling mineral, typically montmorillonite, which is a key component with a notable swelling ability (Marsh et al., 2021; Sellin et al., 2013). Montmorillonite, belonging to the smectite mineral group, acts as an

## INTRODUCTION

ion exchanger. It features a stable negatively charged silicate layer with an interlayer hosting mobile counter cations and water molecules. The predominant counter ions are often  $\text{Na}^+$  and  $\text{Ca}^{2+}$ , resulting in Na- and Ca-bentonite, respectively, although other ions may also be present (Svensson et al., 2011). High quality commercial bentonite typically consists of over 80% montmorillonite. However, this content varies significantly amongst different commercial bentonites, ranging from 60% to more than 80% (Porrás et al., 2021). During the canister deposition process, the bentonite buffer is composed of low-water-content (10–17%) bentonite blocks. Strategic slots will be positioned between the bentonite, the canister, and the rock, enabling a smooth lowering of canisters and blocks into deposition holes. Upon contact with the groundwater, bentonite will expand and undergo mechanical pressure until it attains the intended full compaction density of  $2 \text{ kg/m}^3$  and a relatively low water content of approximately 26%, leading to the sealing of the repository (Engel et al., 2023). In this way, the buffer materials will allow an effective sealing of any potential radiation leakage pathways and maintain the mechanical integrity of the canister, thereby enhancing the safety of the DGR (Marsh et al., 2021; Chen et al., 2023). Consequently, bentonite has emerged as the preferred choice for the final setup of the disposal due to its advantageous mechanical support, ensuring stability for canisters. Additionally, its low permeability mitigates groundwater infiltration, whilst its high ion exchange capacity aids in the retention and retardation of radionuclides in case of a system breach (Marsh et al., 2021; Pedersen et al., 2000; Rättö et al., 2012). Furthermore, its high plasticity and swelling capacity facilitate the self-sealing of canister cracks, whilst its good thermal conductivity and optimal properties for compaction enhance its suitability for repository applications (García-Romero et al., 2019; Martínez-Moreno et al., 2023; 2024). Across different waste disposal concepts, the target swelling

pressure is set at a minimum of 5 MPa, requiring a dry clay density of  $> 1.6 \text{ g/cm}^3$  (Posiva, 2017). A primary concern associated with the bentonite buffer involves the potential interaction of microorganisms with minerals, leading to weathering, dissolution, and the formation of secondary minerals (Beaver et al., 2024). A high bentonite density is thought to exert an inhibiting effect on the activity of the natural bacterial populations within bentonite clay (Engel et al., 2023; Man et al., 2024). The inhibition of bacterial growth and the spore germination is likely due to limited pore space, low water activity, and high swelling pressure. These findings that are supported by many previous studies (Beaver et al., 2024), indicating the restricted microbial activities under  $1.6 \text{ g/cm}^3$  or higher, were further corroborated by the low extractability of solid-phase bentonite natural organic matter (Man et al., 2024). Although these studies were conducted for a duration of up to 18 months, the authors extrapolate their results to the expected time frame required for a DGR to reach full saturation, which ranges from 50 to 5000 years (Beaver et al., 2024). These outputs suggest that bentonite compacted to densities higher than this threshold may exhibit a long-term greater stability and has significant practical implications for the safety assessment of the DGRs.

Nevertheless, there are many prokaryotes adapted to survive in high pressure environments, as well as the endospore of any spore-forming bacteria, which have been reported to not completely disappear after 15 months under the repository conditions (Burzan et al., 2022). Therefore, a continuous evaluation of microbial activity and diversity in such a challenging environment is essential for the safety assessments of the DGR concept. In recent years, numerous studies have investigated the behavior of allochthonous bacteria in highly compacted bentonite (**Figure 1**), as well as the cultivation of microbes derived from the bentonite itself (Engel et al., 2023; Porrás et al., 2021; Maanoja et al., 2021; Povedano-Priego et al., 2021). For instance, Jaliq et al.

## INTRODUCTION

(2016) identified Gram-positive spore-forming bacteria in highly compacted bentonite and inferred that the formation of spores might enhance bacterial survival in the challenging conditions of this environment.

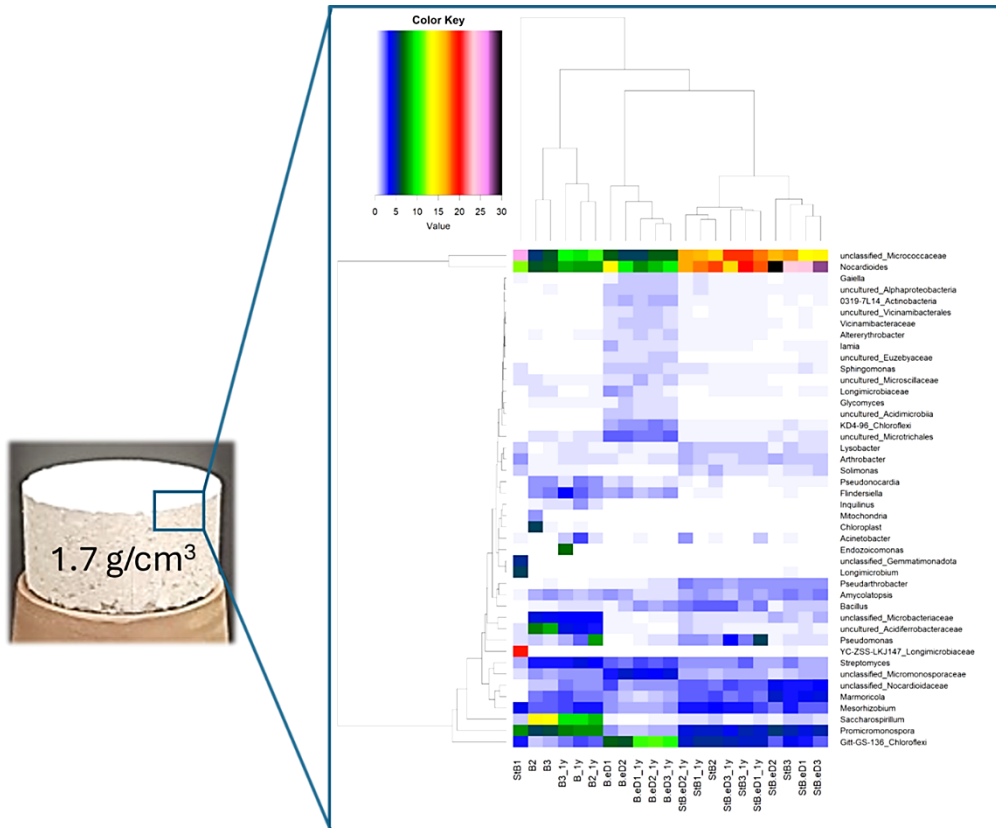


**Figure 1.** A Spanish bentonite block compacted at a dry density of  $1.7 \text{ g cm}^{-3}$ . Heatmap of the relative abundance of the samples at genus level in triplicate (duplicates in StB.eD, B, and B.eD). Cut off: 0.5% of r.a. Different colors show the relative abundance of each genus (the warmer the color, the greater relative abundance). Data from Martinez-Moreno et al. (2023).

In addition, according to Bengtsson and Pedersen (2017), a high density of bentonite buffers in future DGRs will significantly reduce the risk for sulfide production in the buffer and the concomitant corrosion of copper canisters by limiting microbial activity. However, even under these harsh conditions, certain anaerobic bacterial groups, notably sulfate-reducing bacteria (SRB) and iron-reducing bacteria (IRB), have been reported with the potential to be

active within the harsh conditions of highly compacted bentonite (Engel et al., 2023; Burzan et al., 2022). The adverse effects of their activity encompass the initiation of microbiologically influenced corrosion (MIC) processes, the conversion of Fe(III) to Fe(II) in smectite (the primary mineral in bentonite), and the dissimilatory reduction in sulfate, thiosulfate, and sulfur to sulfide by sulfide-producing bacteria (SPB) as a main concern for the safety of a geological disposal, since sulfide is a corrosive agent for metal waste canisters, and, in particular, for copper canisters (Johansson et al., 2017). In line with this, Povedano-Priego et al. (2021) reported that high bacterial diversity was detected in the acetate-treated Spanish bentonite compacted at 1.5 and 1.7 g/cm<sup>3</sup> densities after 24 months of anoxic incubation. Amongst the identified microorganisms in the highly compacted bentonite, there were bacteria involved in the sulfur (e.g., *Desulfuromonas* and *Desulfosporosinus*) and iron (e.g., *Thiobacillus* and *Rhodobacter*, *Geobacillus*) biogeochemical cycles, as well as those (e.g., *Delftia* and *Stenotrophomonas*) enriched by the presence of acetate, as the electron donor. In addition, in their study, Martinez-Moreno et al. (2023) reported on the survival of SRB in compacted Spanish bentonite (1.7 g/cm<sup>3</sup>) with a copper disc placed in the core, after one-year anoxic incubation at 30 °C, although their growth was stimulated by the presence of electron donors (lactate and acetate) and sulfate (electron acceptor). However, in a more realistic scenario, simulating a post-closure DGR phase, highly compacted bentonite blocks (1.7 g cm<sup>-3</sup>) with high-purity copper disks in the core, and incubation at a high temperature (60 °C), the number of SRB was drastically reduced, even when electron donors/acceptor were added to the system, and only *Pseudomonas* as well as some bacterial groups adapted to extreme conditions were able to survive (Martinez-Moreno et al., 2024). A step forward to the improved understanding of the influence of higher temperatures on the bentonite bacterial communities and radionuclide migration through the

## INTRODUCTION

engineered barriers is crucial to determine the validity of bentonite buffer safety functions.

Of particular concern is the biotransformation of smectite into illite through Fe(III) bioreduction, which stands out as one of the most alarming processes (Gilmour et al., 2022). An attack of iron-reducing bacteria to the ferric iron component within bentonite buffers is expected to diminish the swelling capacity of the clay (Chen et al., 2023). This, in turn, may create conditions that stimulate the microbial activity within the buffer, enhancing the diffusion of sulfide and potentially leading to the release of radionuclides (Liu et al., 2012; Zhang et al., 2012). Nevertheless, many studies have demonstrated that no illitization process was detected in highly compacted bentonite under different conditions relevant to DGRs, and different temperature incubation (both at 30 °C and 60 °C) for one year at anoxic conditions, thus confirming the mineralogical stability of the bentonite and its crucial role as effective barrier for future DGRs (Martinez-Moreno et al., 2023; 2024; Povedano-Priego et al., 2021).

Additional research involving extended incubation periods (e.g., spanning at least 10 years), providing suitable electron donors (e.g., lactate and acetate) alongside terminal electron acceptors such as sulfate and Fe(III) are imperative to resolve remaining key issues about the roles of SRB and IRB and whether they can accelerate the degradation of bentonite-based buffers and thus threaten, the safety of the whole repository system. In general, conducting both short- and long-term experiments, along with modeling efforts, is essential to showcase the resilience of the DGR waste management concept. These endeavors are crucial for enhancing comprehension and predictability regarding the influence of fundamental processes and their interconnections.

Such attempts pave the way for advancing our understanding throughout the long-term management of radioactive waste.

#### **4. Effect of radionuclides on the diversity and viability of bentonite microbial communities**

HLW is primarily composed of spent fuel from nuclear power plants, which is the most hazardous residue due to its radioactivity, which may persist for up to 1,000 years. This waste contains a high number of radionuclides including uranium (in the form of enriched  $\text{UO}_2$  pellets with  $^{235}\text{U}$ ), transuranic elements (plutonium and minor actinides), fission products (e.g., Be, Ce, and Se), and activation products (e.g., Ni, Mo, and Sr) (Darda et al., 2021). Hence, the radionuclides present in HLW can pose challenges to the environment and public health due to their emission of radioactivity, in the form of beta particles.

The mobility of uranium in the environment depends on its speciation and redox state. In natural environments, U(VI) under aerobic conditions exists as  $\text{UO}_2^{2+}$ , hydroxyl complexes, and uranyl carbonate at pH below 2.5, 6.5, and 7, respectively (Acharya, 2015). The oxidized forms of U carry a higher number of positive charges, leading to increased solubility and mobility, thereby increasing its toxicity towards microbial cells. Conversely, U(IV) remains insoluble and exhibits lower toxicity in anaerobic environments (Ruiz-Fresneda et al., 2023). The toxicity of selenium also correlates with its oxidation state, with oxyanions (selenate [Se(VI)] and selenite [Se(IV)]) representing the most toxic forms of Se due to their high solubility and mobility, causing harmful effects in the environment. On the other hand, metallic selenium [Se(0)] and selenides [Se(-II)] in terrestrial and aquatic ecosystems exhibit low solubility and mobility, thus presenting lower toxicity levels (Avendaño et al., 2016; Povedano-Priego et al., 2023).

## INTRODUCTION

All the scenarios contemplated for the DGRs suggest that the release of radionuclides, during the long-term repository period, may be inevitable due to natural evolutionary processes and water contacting the source term. The consequence is that the radionuclides could migrate through the repository barriers and ultimately reach the biosphere (Flamíková et al., 2020). The leakage of radionuclides from the canisters to the bentonite (the engineered barrier) could impact the diversity and viability of the microorganisms naturally inhabiting this material. As such, these microorganisms may influence the speciation and mobility of the radionuclides, thus limiting their migration into the biosphere.

### **4.1. Uranium**

Most of the toxicity associated with uranium is due more to its chemistry as a heavy metal rather than its radiotoxicity. The toxic effects vary among plants, animals, and microorganisms, consequently leading to differing mechanisms of action (Gao et al., 2019). In microorganisms, uranium toxicity results in reduced cell viability and metabolic activity, along with increased DNA damage. Additionally, such toxicity has been associated with elevated membrane permeability, oxidative stress, and temporary RNA degradation (Banala et al., 2021). However, microorganisms inhabiting metal-contaminated environments may possess an increased tolerance to heavy metals and radionuclides and develop diverse mechanisms for their immobilization such as biosorption, biomineralization, bioreduction, and bioaccumulation (Lopez-Fernandez et al., 2021).

Povedano-Priego et al. (2019) demonstrated the effect of uranium on the microbial diversity of various bentonite microcosms treated with uranyl nitrate and glycerol-2-phosphate (G2P). In those microcosms incubated under aerobic conditions, significant U effects were observed, leading to the enrichment of

microorganisms with ability to immobilize U through U phosphate biomineralization process, given the aerobic condition of the environment. Phosphatases play a key role in the precipitation of uranium. Production of inorganic phosphates by intracellular phosphatase, stimulated by U(VI), enhances the immobilization of uranium and its precipitation as uranium phosphates, thereby reducing the toxicity of U(VI) to cells (Povedano-Priego et al., 2019; Yu et al., 2023). Interestingly, *Amycolatopsis* was identified in high abundance in G2P-uranium-treated bentonite microcosms. This bacterium has been proven to efficiently immobilize U as uranium phosphates through phosphatase activity induced by the presence of G2P (**Figure 2**; Yu et al., 2023). Additionally, these actinobacteria can remove uranium through its biosorption by carboxyl, amide, and hydroxyl groups (Celik et al., 2018). Similarly, *Bacillus*, a bacterial genus renowned for its biomineralization and uranium biosorption capabilities, has been identified in the uranium-treated bentonites (Lopez-Fernandez et al., 2018). For instance, Merroun et al. (2005) reported that the S-layer, a protein envelope encasing *Bacillus sphaericus* JG-A12, exhibited the capacity to sequester uranium and other heavy metals owing to the presence of carboxyl and phosphate groups (Merroun et al., 2005). Additionally, in *Bacillus* sp. dw-2, the presence of uranium precipitates in the form of small needles has been observed (Zhao et al., 2016). The denitrifying *Pseudomonas* genus has been distributed with high relative abundance in different bentonite samples (Engel et al., 2023; Povedano-Priego et al., 2022; 2023), which is well-known for their capacity to interact with uranium through the different mechanisms that contribute to U immobilization. The study of Povedano-Priego et al. (2022) discovered the presence of *Desulfovibrio* within the bacterial community of G2P-uranium-treated bentonite under anoxic conditions. The capacity of members of this genus to use glycerol as electron donors had earlier been reported (Ben Ali Gam et al., 2018). In this case, the

## INTRODUCTION

oxidation of glycerol, acetate, or lactate to CO<sub>2</sub> is coupled to the reduction in U(VI) to U(IV), producing the immobilization of uranium as uraninite (Zhou et al., 2014). This capacity allows *Desulfovibrio* to survive in uranium-contaminated sediments (Newsome et al., 2014), and waters (Jroundi et al., 2020).

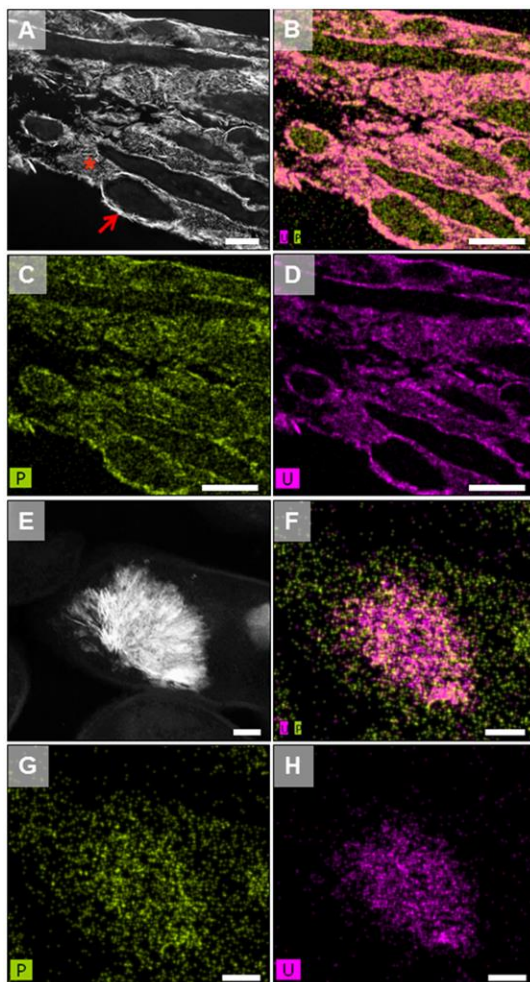


**Figure 2.** High-angle annular dark-field scanning transmission electron microscopy (STEM-HAADF) images of thin sections of *Amycolatopsis ruanii* cells treated with uranium and glycerol-2-phosphate (G2P) showing U-P deposits at cell wall level (arrow), extra- (asterisk) and intracellular (dashed arrow) uranium phosphates (A,E), and their corresponding EDX maps with the distribution of P (C,G), U (D,H), and P + U (B,F). Bar scale: 500 nm (A); 800 nm (B–D); 100 nm (E–H). Figure from Povedano-Priego et al. (2019).

As in bacteria, the fungal community in bentonite is also affected by the presence of uranium in the environment. This group of microorganisms has not been extensively studied, and there is still a lack of understanding regarding its behavior within the framework of DGRs. In fact, Povedano-Priego et al. (2024) found that the fungal diversity in bentonites treated with uranyl nitrate was completely different from U unamended samples, with *Penicillium* and *Fusarium* exhibiting the highest relative abundances in the presence of this radionuclide. High-angle annular dark-field (HAADF) analyses revealed the ability of *F. oxysporum* B1, isolated from uranium-treated microcosms, to generate U-phosphate phases, thereby aiding in the immobilization and detoxification of uranium (Povedano-Priego et al., 2024). In **Table 2** is shown the different microorganisms found in bentonite samples with the capacity to interact with this heavy metal.

**Table 2.** Microorganisms found in bentonite samples with the capacity to interact with heavy metals and metalloids.

Microorganism	Taxonomic affiliation	Interaction mechanism	Metal	Reference
<i>Amycolatopsis ruanii</i>	Actinomycetota (Bacteria)	Biom mineralization	U	Yu et al., 2023
<i>Bacillus sphaericus</i>	Bacillota (Bacteria)	Biosorption	U	Povedano-Priego et al., 2022
<i>Bacillus</i> sp.	Bacillota (Bacteria)	Biosorption Bioaccumulation	U	Ben Ali Gam et al., 2018
<i>Desulfovibrio vulgaris</i>	Pseudomonadota (Bacteria)	Bioreduction	U	Jroundi et al., 2020
<i>Fusarium oxysporum</i>	Ascomycota (Fungi)	Biom mineralization	U	Wells et al., 2019
<i>Bacillus selenitireducens</i>	Bacillota (Bacteria)	Bioreduction	Se	Ruiz-Fresneda et al., 2018
<i>Shewanella oneidensis</i>	Pseudomonadota (Bacteria)	Bioreduction	Se	Hunter et al., 2014
<i>Stenotrophomonas bentonitica</i>	Pseudomonadota (Bacteria)	Bioreduction	Se	Pinel-Cabello et al., 2021
<i>Pseudomonas seleniipraecipitans</i>	Pseudomonadota (Bacteria)	Bioreduction	Se	Ruiz-Fresneda et al., 2019

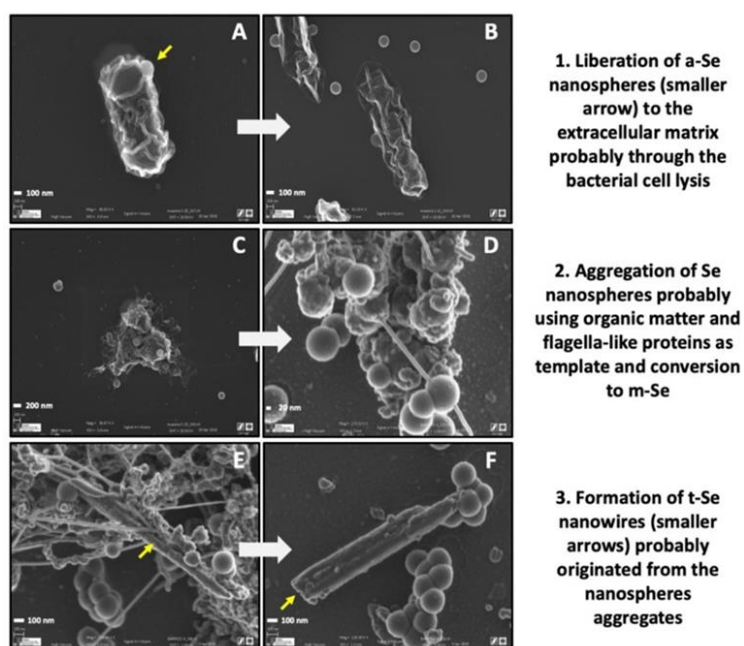
## INTRODUCTION

### 4.2. Selenium

Selenium plays a crucial role as a micronutrient essential for various biological systems, including antioxidant pathways. Nevertheless, whilst beneficial at low concentrations, Se contamination and subsequent bioaccumulation can lead to environmental and human health risks. Se is toxic for bacteria due to its incorporation into sulfur-containing proteins (Kushwaha et al., 2022). The presence of Se(IV) impacts the microbial diversity of bentonite, as described by Povedano-Priego et al. (2023). They observed that the relative abundance of the archaea *Methanosarcina* decreased significantly in the selenite-treated bentonite microcosms induced by the toxic effect of Se(IV) (Povedano-Priego et al., 2023). However, *Methanosarcina* recovered when the selenite was reduced in the bentonite by members of a bacterial consortium added in the microcosms.

The presence of selenium in bentonite may also influence the bacterial communities, leading to an increase in the abundance of bacteria capable of tolerating the metalloid, developing diverse detoxification mechanisms, such as *Pseudomonas*, *Stenotrophomonas*, and *Desulfosporosinus*, amongst others (Povedano-Priego et al., 2023). Several studies have described the reduction in oxidized and soluble forms of Se (selenite and selenate) to insoluble Se(0) in bacteria, such as *Bacillus* (Wells et al., 2019), *Shewanella* (Li et al., 2014), *Stenotrophomonas* (Ruiz-Fresneda et al., 2018), and *Pseudomonas* (Hunter et al., 2014). The reduction process could be carried out through different enzymatic pathways mediated by different reductase activities such as nitrite, sulfite, fumarate, and selenite reductases (Ruiz-Fresneda et al., 2023). In addition, the Se(IV) reduction could be mediated by molecules containing reduced thiol groups (-SH) such as glutathione (GSH). Pinel-Cabello et al. (2021) detected an increase in the presence of glutathione reductase,

glutathione-disulfide reductase, and thioredoxin-disulfide reductase in *Stenotrophomonas bentonitica* BII-R7 culture treated with Se(IV), demonstrating that the mechanism for Se(IV) reduction is activated in presence of this toxic element. The produced Se(0) by bacteria is accumulated in the extracellular space and form Se nanoparticles (SeNPs) with different allotropy; amorphous, monoclinic, and trigonal selenium (**Figure 3**; Ruiz-Fresneda et al., 2019). The transformation of amorphous to monoclinic and trigonal Se may be mediated by proteins excreted by bacteria, although the specific process is still unknown (Ruiz-Fresneda et al., 2020). This process has also been observed in bentonite microcosms treated with selenite and spiked with a bacterial consortium after 6-month anoxic incubation (Povedano-Priego et al., 2023). It was demonstrated for the first time that Se transformation generating Se nanostructures composed by the trigonal phase, the most stable form, was detected in a ternary system (bentonite, microorganisms, and Se). **Table 2** summarizes some of the autochthonous bentonite microorganisms that have been reported with the ability to interact with this metalloid selenium.



## INTRODUCTION

**Figure 3.** VP-FESEM images illustrating the Se transformation from *a*-Se nanospheres to *t*-Se nanowires, with an intermediate step of *m*-Se aggregates by using proteins as a template. The images correspond to samples prepared by growing *Stenotrophomonas bentonitica* anaerobically. Scale bars: 100 nm (A,B,E,F), 200 nm (C), and 20 nm (D). Yellow arrow in (A): *a*-Se nanospheres; yellow arrow in (E,F): *t*-Se nanowires. Figure from Ruiz-Fresneda et al. (2019).

### 5. Copper corrosion under repository conditions

Extensive research has been conducted on the corrosion of canister materials under controlled experimental conditions. Therefore, it is necessary to extrapolate the experimental data to take into account the fluctuating evolution of chemical, mechanical, and redox conditions that will occur during the repository post-closure period. Based on the report of Landolt et al. (2009) regarding the NAGRA design concept, four phases have been identified to occur on the canister surface from the time of repository closure up to millions of years: (1) in the first tens of years, an initial phase will develop characterized by dry and oxic conditions, with high temperatures; (2) second oxic and unsaturated phase would last the first few hundreds of years; (3) third phase of more advanced hundreds of years, wherein oxygen would have already been consumed and an anaerobic phase with unsaturated conditions would be established; and (4) the cold, anoxic, and long-lasting final phase with fully saturated conditions would be established. The evolution and fluctuations in temperature and oxygen concentration projected over the years after the closure of future nuclear repositories are illustrated in **Figure 4** (King, 2017).

According to the various phases anticipated after repository closure, the primary factors expected to play a significant role in the corrosion of copper canisters would include: the presence/absence of oxygen, radiation (Section 2), and microbiologically influenced corrosion (MIC) (Hall et al., 2021). With regard to oxygen, its presence will be limited to the first years of the repository, as it will be consumed by bacterial activity and by the oxidation of minerals

present in the different barriers (Hall et al., 2017; King et al., 2017). The most plausible reaction expected to occur is the one that results in copper oxide(I) according to the following equation:  $4\text{Cu} + \text{O}_2 \rightarrow 2\text{Cu}_2\text{O}$  (Hall et al., 2021). However, when these oxidic phases come to an end after the total consumption of  $\text{O}_2$ , the environment becomes completely anaerobic. In the context of this reducing environment, copper corrosion processes are primarily expected to result from water reduction, wherein copper would react with water molecules, leading to the formation of copper(I) oxides ( $\text{Cu}_2\text{O}$ ) alongside  $\text{H}_2$  (Hall et al., 2021; Hultquist et al., 1986).

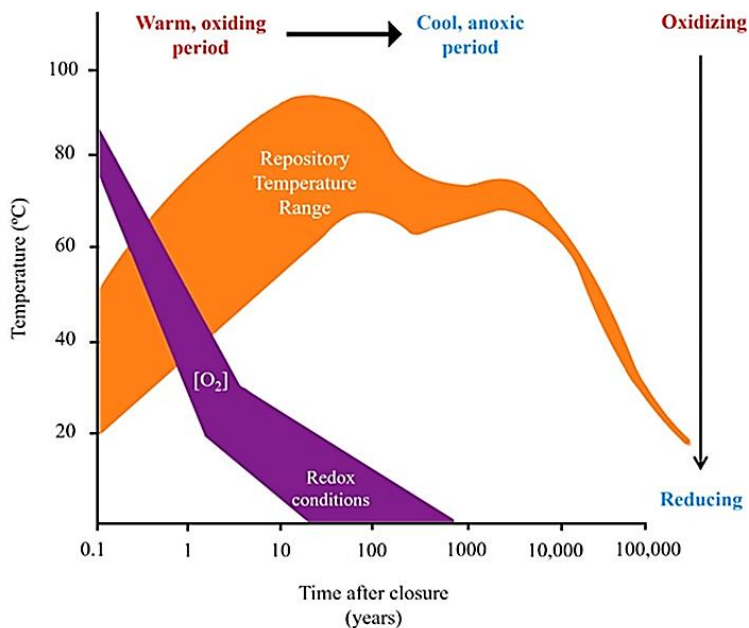


**Figure 4.** Diagrammatic representation of the evolution of the near-field environment for a repository. Modified from King, (2017).

## INTRODUCTION

Nevertheless, one of the most critical sources of corrosion would be due to microbial activity. Sulfate-reducing bacteria are frequently responsible for MIC damage, primarily due to the abundance of sulfate in anaerobic environments. This corrosion process can occur through two different routes: an indirect route known as chemical MIC (CMIC), where corrosion is caused by the products resulting from microbial metabolism; and/or a direct route, known as electrical MIC (EMIC), where the transfer of electrons from the metal directly interfaces with the bacteria and it requires biofilm formation (Little et al., 2020; Enning et al., 2014). The formation of biofilms on the surface of the canister is highly improbable in a repository concept that includes the direct contact of bentonite backfill with the canister (Abdelouas et al., 2022). Additionally, copper lacks the energetic potential for SRB to utilize it as a source of electrons for generating energy through dissimilatory sulfate reduction (DSR). Therefore, between the two pathways, CMIC would predominantly engage SRB since this bacterial group utilizes sulfate, not copper, as final electron acceptor in the respiratory process (dissimilatory sulfate reduction). This allows them to obtain energy by releasing  $\text{HS}^-$  (bisulfide) or  $\text{H}_2\text{S}$  (sulfide), depending on the pH value (Dou et al., 2020; Thauer et al., 2007). The copper would corrode due to these biogenic sulfides resulting in the formation of copper sulfides as described by the following equation:  $2\text{Cu} + \text{HS}^- + \text{H}^+ \rightarrow \text{Cu}_2\text{S} (\text{s}) + \text{H}_2 (\text{g})$  (Huttunen-Saarivirta et al., 2016) (**Figure 5**). Deep underground water sources might contain elevated levels of dissolved sulfate ions, which could support the sustenance of these SRB. Additionally, nutrients could be sourced from natural organic materials within the clay, fracture fluids, or neighboring minerals (Hall et al., 2021; Marshall et al., 2014).

To date, there is robust evidence indicating that the requisite conditions for facilitating localized corrosion phenomena, such as pitting, are unlikely to take

place in a post-closure nuclear repository using copper as a corrosion barrier (King et al., 2019; Martino et al., 2019; SKB 2019; Qin et al., 2017). Furthermore, it should be noted that this sulfur flow would occur during the later stages of the DGR, once water saturation has taken place. By this time, it is anticipated that O<sub>2</sub> consumption will have been completed, thus bringing an end to the oxic corrosion mentioned earlier.

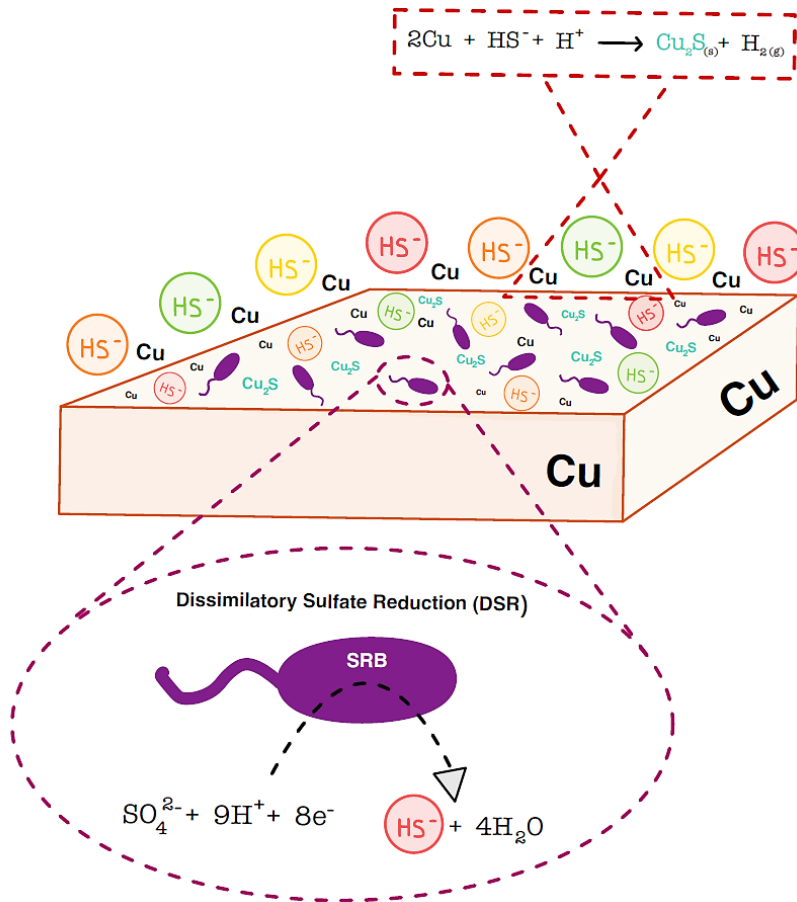


**Figure 5.** Schematic representation of chemical microbially induced corrosion (CMIC) of copper by sulfate-reducing bacteria (SRB).

## INTRODUCTION

Consequently, when sulfide becomes available, the copper would probably encounter a layer composed of copper oxides or hydroxides already formed, rather than pure copper. Smith et al. (2007) documented the conversion of  $\text{Cu}_2\text{O}$  to  $\text{Cu}_2\text{S}$  under aqueous sulfide conditions ( $\text{HS}^-$ ), and similar reactions involving other copper species such as  $\text{Cu}^+$  or  $\text{CuCl}_2$  have been reported in other studies. Therefore, the significance of these transformations lies in the fact that under repository conditions, the incoming sulfide will interact with corrosion products such as copper oxides or dissolved copper that have already formed. However, this corrosion product layer prior to sulfide exposure can serve as a barrier, redirecting sulfide to react with the pre-existing corroded material rather than with new canister sections (Hall et al, 2021).

### **6. Effect of oxygen, gasses, and nutrients on the microorganisms**

With the final closure of the repository, the initial oxic conditions would lead to a complete anoxic environment with time. Initially, oxygen can be consumed by different processes including corrosion of the canister (Landolt et al., 2009), reduced components of the rocks and backfill (West et al., 2002), oxidation of bentonite Fe containing minerals (Giroud et al., 2018), and microbial activity in bentonite (Giroud et al., 2018). The necessary time to re-establish the anoxic conditions depends on the above-mentioned processes, ranging from months to thousands of years (Abdelouas et al., 2022). For example, Giroud et al. (2018) considered gas exchange with bentonite pore water and adsorption on mineral surfaces as the most important processes controlling  $\text{O}_2$ , with it being fully consumed after only a few months. However, according to Wersin et al. (2007), anoxic conditions would be re-established in the buffer after a period ranging between 7 and 290 years, whilst Grandia et al. (2006) predicted that aerobic conditions may prevail for more than 5000 years in the absence of  $\text{O}_2$  consumption in the buffer. As far as the microbial

involvement in the process is concerned, several authors have confirmed the short term of O<sub>2</sub> consumption (Abdelouas et al., 2022). Apart from the oxygen trapped in the pore spaces, the radiolysis of humid air or water also produces oxidizing species that will increase the general metal corrosion rates, as previously mentioned (Crusset et al., 2017). The effect of the radiolysis of water on corrosion, however, can be significantly attenuated in the absence of oxygen (Lapuerta et al., 2008). Moreover, a significant volume of other gasses would be generated with time in the DGR which may affect the long-term safety of the system by shifting the containment functions of engineered and natural barriers through over-pressurization of the repository. In addition, the hydraulic and mechanical properties of engineered barriers and host rock might be altered (Wendling et al., 2019; Liu et al., 2018). Gas would be generated through several abiotic processes such as anaerobic corrosion of metal canister and ferrous components in the engineered barrier system, biotic degradation of organic materials and radiolysis of water (Wendling et al., 2019). Hydrogen is expected to be the dominant gas generated in a deep geological repository (Croisé et al., 2011; Perko et al., 2011) and could also potentially act as a carrier for radioactive gaseous species (e.g., H-3, C-14, Rn-222, etc. (Enssle et al., 2014; O'Brien et al., 2014)). The formation of H<sub>2</sub> by anaerobic corrosion of metals may further contribute to gas generation (such as CH<sub>4</sub>, H<sub>2</sub>S or CO<sub>2</sub>), as H<sub>2</sub> can be used as an electron donor in microbial processes (Libert et al., 2011). Soluble organic degradation products (e.g., formic acid, acetic acid or methanol, among others) also have the potential to enhance corrosion and form aqueous complexes with radionuclides, which may affect their mobility and release from the repository (Vikman et al., 2019). Methane and carbon dioxide are generated as a result of microbiological degradation of organic materials, which could lead to overpressure in the repository and migration of water-borne radionuclides in fractures of crystalline bedrock and may drive the

## INTRODUCTION

transport of radionuclide contaminated groundwater to the biosphere (Vikman et al., 2019). In addition, irradiated metals and waste materials may contain radionuclides, which can be volatilized to the biosphere in the form of gas (Peitzsch et al., 2010). Although it is assumed that gas-generating materials are not altered prior to the operational and post-closure repository phase, the environmental conditions which control the gas production (e.g., temperature, concentration of reactants, availability of catalysts, salinity, pH, redox potential) may increase or decrease it. Generally, production, transport and consumption of gas and water in a closed deep geological repository are coupled processes. Gas and water transport affect the production/consumption of water and gas, e.g., by controlling the gas pressure and the availability of water for corrosion and degradation reactions, whilst water and gas production/consumption will influence the movement of water and gas (Poller et al., 2016).

Another important factor to consider is the extreme oligotrophic conditions deep underground in the repository. Life in the continental deep biosphere is broadly constrained by energy and nutrient availability (Lopez-Fernandez et al., 2019). However, it has been demonstrated that deep biosphere microorganisms are active, and able to influence the environmental conditions and material integrity in deep geological repositories (Lopez-Fernandez et al., 2018; Rajala et al., 2023). These extreme and deep ecosystems foster diverse, yet cooperative, communities adapted to this setting (Mehrshad et al., 2021). Metabolic cooperation, via syntrophy between sub-surface microbial groups, is critical for the survival of the whole community under the oligotrophic conditions that dominate in the sub-surface, where microbial ecosystems are typically supported by H<sub>2</sub>. Methanogens such as *Methanosarcina*, *Methanoculleus*, and *Methanocella*, and sulfate reducers like *Desulfosporosinus*, *Desulfovibrio*, and *Desulfotomaculum*, and the respective

energy processes, are thought to be the dominant players (Lau et al., 2016). Furthermore, the main source of microorganisms in the bentonite appears to be the bentonite itself rather than the host rock or its pore water. The number of microorganisms is predicted to increase until full saturation of bentonite is reached and would remain at stable numbers for decades (Rajala et al., 2023). Interestingly, Burzan et al. (2022) observed the growth of aerobic heterotrophs instead of anaerobes in the bentonite despite the nominally anoxic conditions. The microbial activity of anaerobic microorganisms (most commonly sulfate-reducing bacteria) can lead to corrosion of the metallic waste canister materials (Burzan et al., 2022), and the production of gasses such as methane, hydrogen sulfide, and nitrogen (Nazina et al., 2006), affecting the long-term safety of the repository. Therefore, taxonomically and metabolically diverse microorganisms developed syntrophic partnerships to actively overcome all the difficulties imposed by the environmental conditions in the deep subsurface, and thus, affect the safety of the DGRs for nuclear waste.

## **7. Effect of temperature**

### **7.1. Impact of temperature evolution on nuclear repository barriers**

The waste disposal temperature will be shaped by the layout, design, and decay of radionuclides within the spent nuclear fuel bundles in the DGR (King et al., 2017). Then, the subsequent evolution of the temperature over the storage time would be predominantly determined by the thermal behavior of the canisters due to the heat generated by the decay of the radionuclides. Different models based on the DGR designs of each country predict a gradual increase in the temperature in the canister's surface, reaching a maximum peak of  $\approx 100$  °C within the first decades (**Table 1**). Additionally, this generated heat would dissipate into the nearby engineering barriers and the host rock. The temperature evolution is a key factor that may alter the properties and stability

## INTRODUCTION

of engineered barriers such as the bentonite sealing material or the metal canisters. Since the DGR environment would not be sterile, the temperature evolution could affect the microbial communities within the repository.

Elevated temperatures can compromise the mineralogical, mechanical, and index characteristics of bentonite. Kale and Ravi (2021) reported that, with an increase in the temperature, the liquid limit (the water content where the soil starts to behave as a liquid) of the bentonite decreases. This is also affected by the clay content, since the higher the clay content, the higher percentage reduction in the liquid limit. This decrease in the liquid limit, with a temperature rise, would affect the plasticity (ability to undergo deformation without cracking) index in the same way. Moreover, the specific gravity (density of a substance in comparison to the density of water) of smectite soil was found to be reduced by the increase in the temperature. Based on the results of Tan et al. (2004), if the temperature reaches  $> 100\text{ }^{\circ}\text{C}$ , the specific gravity will decrease gradually up to  $400\text{ }^{\circ}\text{C}$  followed by a slow decrease up to  $800\text{ }^{\circ}\text{C}$ . Additionally, the maximum dry density increases with an increase in the temperature (Kale et al., 2021). Exposure to high temperatures results in several physical and chemical transformations in clay, such as mineral composition/decomposition, reduction in moisture layers, and alterations in mass and density, contributing to the degradation of its structural integrity (Sun et al., 2016). The water content is influenced by the temperature since water layers begin to reduce their size when the clay is in contact with heat (Lingnau et al., 1996). The moisture layers can be removed when the temperature is between  $100\text{ }^{\circ}\text{C}$  and  $110\text{ }^{\circ}\text{C}$  (absorbed moisture) leading to the collapse of the interlayer pore space. The optimum moisture content is less affected at  $100\text{ }^{\circ}\text{C}$ , whilst up to  $400\text{ }^{\circ}\text{C}$ , a drastic decrease can be observed. Subsequently, this loss of water affects the macro and microporosity of the clay minerals and their plasticity. The physicochemical properties of bentonite can be also affected by

an increase in temperature. Estabragh et al. (2016) showed a gradual decrease in  $\text{Na}^+$  concentration, linked with an increase in temperature, affecting the cation exchange capacity (CEC) of the bentonite, whilst a pH decrease was evidenced when the temperature was  $> 150\text{ }^\circ\text{C}$ . When clay is heated, the bonds at the edges of the interlayer units, especially in montmorillonite, will be broken due to the presence of weak Van der Waals forces. At a mineralogical level, one of the main concerns related to elevated temperatures is the irreversible smectite-to-illite transformation that affects the swelling capacity of the bentonite (Kaufhold et al., 2010). This process, known as illitization, involves the chemical alteration of expandable smectite into non-expandable illite. This change is typically prompted by elevated temperature exposure ( $100\text{--}200\text{ }^\circ\text{C}$ ) over a long period of time (Ohazuruike et al., 2023). The process of illitization may be initiated by potassium ions, potentially originating from the clay K-feldspars, which integrate into the smectite layers and form covalent bonds with oxygen (Kaufhold et al., 2010).

Moreover, in this context, published studies show that shifts in temperature have a negative effect on metal canister corrosion affecting the corrosion kinetics and the solubility of mineral phases in contact with the canisters (Abdelouas et al., 2022). The corrosion rates of passive metals are remarkably low (around  $0.01\text{ }\mu\text{m/year}$ ). However, the integrity of passive self-forming surface films faces threats from localized corrosion, including pitting and crevice corrosion, with temperature playing an important role in initiating corrosion (Payer et al., 2019). A suitable material for canisters must preserve its structural integrity, corrosion resistance, and radiation shielding capabilities at temperatures  $> 100\text{ }^\circ\text{C}$ , potentially up to an upper threshold of  $300\text{ }^\circ\text{C}$  (**Table 1**). Hence, the concern that sensitized microstructures susceptible to localized corrosion may be produced, compromising the mechanical integrity of the canisters, does not appear to be an important issue under the temperatures

## INTRODUCTION

expected in a DGR. Due to the heat on the surface of the canisters, the initial humidity in the bentonite would be distributed to cooler areas. This would result in dry and uniform oxidation on the surface of the canisters. Studies conducted by Stoulil et al. (2019) have shown that high temperatures compact the corrosion layers on the surface of the canisters, which slightly reduces the corrosion rate. Schlegel et al. (2018) showed that under fluctuating temperature conditions (85 °C with a drop to 25 °C, and then 85 °C again), steel corrosion presented areas of extensive corrosion with depressions filled with corrosive products. This fluctuating temperature produced a high rate of corrosion compared to when the temperature was static at 85 °C. Moreover, in conditions where the temperature varies, the formation of carbonates, chlorides, sulfides, Fe-silicates, and magnetite as corrosive products are common. Schlegel et al. (2018) determined that significant effects of low-temperature fluctuations include accelerated metal oxidation compared to the formation of corrosive products (Nešić, 2007), growth of microbial colonies leading to biofilms or Fe-sulfide generation, and a decrease in air tightness. However, with a rise in temperature, corrosive product deposition intensifies, which in turn decelerates the corrosion process. In the case of copper, the main corrosive agent under anaerobic conditions is hydrogen sulfide produced by SRB (Bengtsson et al., 2017). Martinez-Moreno et al. (2024) showed that these bacteria do not exhibit viability at high temperatures (60 °C). Therefore, no precipitates related to copper anaerobic corrosion ( $\text{Cu}_x\text{S}$ ) were observed, with copper oxide being the main corrosive product detected.

### **7.2. Impact of temperature evolution on microorganisms**

One of the aspects to consider when ensuring the stability of a DGR is the effect that microorganisms will have on the different containment barriers under repository-relevant conditions (Ruiz-Fresneda et al., 2023). The elevated

temperature could affect the microbial communities within the DGR, especially those naturally occurring in the bentonite. Martinez-Moreno et al. (2024) proved that high temperature (60 °C) reduces the microbial diversity and the number of SRB in compacted bentonite after a one-year incubation. Moreover, at this temperature, whilst some aerobic bacteria (e.g., *Aeribacillus*) showed growth capacity at 60 °C, certain anaerobic bacteria (IRB and SRB) did not. The activity absence of IRB and SRB at 60 °C, or higher temperatures, is of particular interest related to the MIC of metal canisters previously mentioned, as this fact would retard the MIC on the canister surface. Additionally, Bartak et al. (2024) found a decline in microbial activity as temperature rose, and that thermal treatment significantly impacted the microbial community composition within the bentonite, identifying various thermophilic species (e.g., *Caldinitratiruptor* and *Brockia*) or thermotolerant spore-forming genera (e.g., *Thermincola* and *Bacillus*). Moreover, they determined a threshold temperature of 90 °C to inhibit microbial activity and growth across all the tested bentonite suspensions. Furthermore, previous research has demonstrated that bacteria can withstand extreme environments either through the formation of spores (e.g., *Desulfosporosinus* and *Desulfotomaculum*), or by entering into a dormant state, such as desiccated cells (Grigoryan et al., 2018; Masurat et al., 2010). Since high temperatures turn the bentonite/canister interface into a dry environment, bacteria could face water loss enhanced by the strong affinity of the bentonite, which draws water away from the cells causing cell inactivation and inducing spore formation. Moreover, the formation of biofilms and sporulation are well known tactics used by bacteria to withstand desiccation (Laskowska et al., 2020). Once the temperature starts to be cooler during the anoxic period (**Figure 4**), bacteria can recover their cell viability under favorable conditions (Martinez-Moreno et al., 2024; Masurat et al., 2010).

### **8. Limitations, challenges, and opportunities**

Ensuring the long-term stability of future nuclear waste repositories requires very comprehensive studies based on multidisciplinary approaches, combining engineering, chemistry, physics, mathematics, geology, and microbiology. The effect of mineralogical and biogeochemical parameters (e.g., clay mineralogy and compaction density, pore water chemistry, etc.) on the stability of DGR barriers have been well studied. However, very few studies were conducted to investigate the combined impact of different DGR physico-chemical parameters (e.g., radiation, temperature) on the presence and activity of microbes. Incorporating these microbiological data in the geochemical models is of great importance to achieve an accurate prediction of the long-term stability and safety of the different DGR barriers. Nevertheless, this topic is in its infancy and close collaborations between experimentalists (microbiologists, chemists, mineralogists, physicists, etc.) and modelers should be conducted to fill the gaps. Introducing bacterial activity into long-term mathematical models presents a challenge due to the inherent complexity of biological systems and the interactions between their components (e.g., complexity and diversity of bacterial behaviors, dynamic and nonlinear interactions, variability and heterogeneity within the bacterial community, etc.). Therefore, the principal challenge facing the scientists working in this field is the complexity of these studies as they require taking into consideration the physiochemical and microbiological relevant conditions for future DGR (temperature, radiation, water activity, etc.) and a long-term duration of the research projects. Therefore, in order to simulate a more realistic scenario, this kind of studies should be conducted at the underground laboratories such as Mont Terri Rock (Switzerland), Hades (Belgium), Äspö Hard Rock (Sweden), and Meuse/Haute Marne (France). The access to such laboratories is, however, very limited. Advance in this field of study is crucial and should be based on the

communication between experts in the relevant disciplines. This will enable the collection of comprehensive, realistic data and the development of accurate strategies to guarantee the long-term safety of these systems.

## **9. Conclusions**

The aim of this review is to outline how various conditions evolving over the lifespan of a nuclear waste repository can impact the properties of engineered barriers (metal canister and backfill/seal barrier). Key parameters influencing the safety of these repositories include radiation, temperature fluctuations, bentonite compaction density, and abiotic/biotic factors (e.g., oxic/anoxic atmosphere, nutrient-enriched groundwater seepage, gas production), amongst others. We have also discussed the impact of microbial processes on the safety performance of DGR barriers. Despite the harsh conditions involved within a DGR that may impact the survival and viability of microorganisms, some autochthonous microbes from bentonite and those that will be accidentally introduced due to human activity may be inhabiting there. Hence, understanding the interaction between microorganisms and the barriers is crucial since they are able to completely modify the surrounding environment. For this reason, research on the microbiology of repositories has been increasing in recent years. Moreover, within this review, we have highlighted the behavior of autochthonous bentonite microorganisms in response to radionuclide leaks from the nuclear waste, such as U or Se, underscoring the capacity of certain microbes to retard their mobility and migration through bioimmobilization processes. In this context, understanding the conditions that could impact the different barriers is crucial for ensuring the long-term safety of future DGRs, since these systems will be highly complex.

## **Conflicts of interest**

The authors declare no conflicts of interest.

## INTRODUCTION

### **Author Contributions**

M.M.-H., F.J. and M.L.M. planned the work. M.M.-H. was the main contributor to the manuscript. The other co-authors (M.L.M., F.J., M.F.M.-M., C.P.-P., M.L.-F. and M.A.R.-F.) also assisted in writing certain sections of the manuscript. The final version was edited and revised by all the authors. All the authors contributed to the article and approved the final submitted version. All authors have read and agreed to the published version of the manuscript.

### **Funding**

This work has been supported by the grant PID2022-138402NB-C21 funded by MICIU/AEI/10.13039/501100011033 and by ERDF/EU. In addition, it was supported by the grant FPU20/00583 to the first author from the Spanish Government.

### **Acknowledgments**

The authors acknowledge the assistance of Angela Tate for the revision of the English language.

### **References**

- 7º Plan General de Residuos Radiactivos. (2023). Ministerio para la transición ecológica y el reto demográfico. <https://www.miteco.gob.es/es/energia/nuclear/residuos/plan-general.html>
- Abdelouas A., Alonso U., Bernier-Latmani R., Bosch C., Cherkouk A., Dobrev D., Fernández A.M., Finck N., Gaggiano R., Havlová V., Hesketh J., Idiart A., Mijndonckx K., Montoya V., Muñoz A.G., Padovani, C., Pont A., Rajala P., Riba O., Sarrasin L., Sayenko S., Smart N., Texier-Mandoki N., Wersin P. (2022): Initial State-of-the-Art of WP ConCorD. Final version as of 17.08.2022 of deliverable D15.1 of the HORIZON 2020 project EURAD. EC Grant agreement no: 847593
- Acharya, C., (2015). Microbial bioremediation of Uranium: an overview. BARC Newsletter 27–30.

- Allard, T., and Calas, G. (2009). Radiation effects on clay mineral properties. *Applied Clay Science*, 43(2), 143-149. <https://doi.org/10.1016/j.clay.2008.07.032>
- Allard, T., Balan, E., Calas, G., Fourdrin, C., Morichon, E., and Sorieul, S. (2012). Radiation-induced defects in clay minerals: A review. *Nuclear Instruments and Methods in Physics Research Section B: Beam Interactions with Materials and Atoms*, 277, 112-120. <https://doi.org/10.1016/j.nimb.2011.12.044>
- Alper, T., and Howard-Flanders, P. (1956). Role of oxygen in modifying the radiosensitivity of *E. coli* B. *Nature*, 178(4540), 978-979. <https://doi.org/10.1038/178978a0>
- Avendaño, R., Chaves, N., Fuentes, P., Sánchez, E., Jiménez, J.I., Chavarría, M., (2016). Production of selenium nanoparticles in *Pseudomonas putida* KT2440. *Scientific Reports*, 6, 1–9. <https://doi.org/10.1038/srep37155>
- Bagwell, C. E., Bhat, S., Hawkins, G. M., Smith, B. W., Biswas, T., Hoover, T. R., Saunders, E., Han, C. S., Tsodikov, O. V. and Shimkets, L. J. (2008). Survival in nuclear waste, extreme resistance, and potential applications gleaned from the genome sequence of *Kineococcus radiotolerans* SRS30216. *PloS one*, 3(12), e3878. <https://doi.org/10.1371/journal.pone.0003878>
- Bagjestani, M.S.; Nasir, O.; Oh, W.T. (2023). Properties of Bentonite-Based Sealing Materials during Hydration. *Minerals*, 13, 1412. <https://doi.org/10.3390/min13111412>
- Banala, U.K., Das, N.P.I., Toleti, S.R. (2021). Microbial interactions with uranium: Towards an effective bioremediation approach. *Environmental Technology & Innovation*, 21, 101254. <https://doi.org/10.1016/j.eti.2020.101254>
- Bartak, D., Bedrníková, E., Kašpar, V., Říha, J., Hlaváčková, V., Večerník, P., Šachlová, K. & Černá, K. (2024). Survivability and proliferation of microorganisms in bentonite with implication to radioactive waste geological disposal: strong effect of temperature and negligible effect of pressure. *World Journal of Microbiology and Biotechnology*, 40(1), 41. <https://doi.org/10.1007/s11274-023-03849-0>
- Beaver R.C., Vachon M.A., Tully C.S., Engel K., Spasov E., Binns W.J., Noël J.J., Neufeld J.D (2024). Impact of dry density and incomplete saturation on microbial growth in bentonite clay for nuclear waste storage. *Journal of Applied Microbiology*, 135 (3), 1xae053. <https://doi.org/10.1093/jambio/1xae053>
- Ben Ali Gam, Z., Thioye, A., Cayol, J.-L., Joseph, M., Fauque, G., and Labat, M. (2018). Characterization of *Desulfovibrio salinus* sp. nov., a slightly halophilic sulfate-reducing bacterium isolated from a saline lake in Tunisia. *International Journal of Systematic and Evolutionary Microbiology*, 68, 715–720. <https://doi.org/10.1099/ijsem.0.002567>

## INTRODUCTION

- Bengtsson, A., Pedersen, K., (2017). Microbial sulphide-producing activity in water saturated Wyoming MX-80, Asha and Calcigel bentonites at wet densities from 1500 to 2000 kgm<sup>-3</sup>. *Applied Clay Science*, 137, 203–212. <https://doi.org/10.1016/j.clay.2016.12.024>
- Bennett, D. G., & Gens, R. (2008). Overview of European concepts for high-level waste and spent fuel disposal with special reference waste container corrosion. *Journal of Nuclear Materials*, 379(1-3), 1-8. <https://doi.org/10.1016/j.jnucmat.2008.06.001>
- Binns, W. J., Behazin, M., Briggs, S., & Keech, P. G. (2023). An overview of the Canadian nuclear waste corrosion program. *Materials and Corrosion*, 74, 1580–1586 <https://doi.org/10.1002/maco.202313763>
- Björkbacka, Å., Hosseinpour, S., Johnson, M., Leygraf, C., & Jonsson, M. (2013). Radiation induced corrosion of copper for spent nuclear fuel storage. *Radiation Physics and Chemistry*, 92, 80-86. <https://doi.org/10.1016/j.radphyschem.2013.06.033>
- Björkbacka, Å., Johnson, C. M., Leygraf, C., & Jonsson, M. (2016). Role of the oxide layer in radiation-induced corrosion of copper in anoxic water. *The Journal of Physical Chemistry C*, 120(21), 11450-11455. <https://doi.org/10.1021/acs.jpcc.6b00269>
- Björkbacka, Å., Johnson, C. M., Leygraf, C., & Jonsson, M. (2017). Radiation induced corrosion of copper in humid air and argon atmospheres. *Journal of The Electrochemical Society*, 164(4), C201. <http://dx.doi.org/10.1149/2.1331704jes>
- Björkbacka, Å., Yang, M., Gasparini, C., Leygraf, C., & Jonsson, M. (2015). Kinetics and mechanisms of reactions between H<sub>2</sub>O<sub>2</sub> and copper and copper oxides. *Dalton Transactions*, 44(36), 16045-16051. <https://doi.org/10.1039/C5DT02024G>
- Burzan, N., Murad Lima, R., Frutschi, M., Janowczyk, A., Reddy, B., Rance, A., Nikitas, D. & Bernier-Latmani, R. (2022). Growth and persistence of an aerobic microbial Community in Wyoming Bentonite MX-80 despite anoxic in situ conditions. *Frontiers in Microbiology*, 13, 858324. <https://doi.org/10.3389/fmicb.2022.858324>
- Cátedra ENRESA; <http://www.catedraenresauc.com/>
- Celik, F., Camas, M., Kyeremeh, K., Sazak Camas, A. (2018). Microbial Sorption of Uranium Using *Amycolatopsis* sp. K47 Isolated from Uranium Deposits. *Water, Air, & Soil Pollution*, 229, 112. <https://doi.org/10.1007/s11270-018-3766-5>
- Černá, K., Bartak, D. S. (2019). State of art – attachment I to the Work report 2019, Project Limiting Factors for survivability and proliferation of microorganisms significant for

## INTRODUCTION

- corrosion of deep geological repository barrier systems (BioBen) Project number: TAČR TK02010169
- Chapman, N. (2006). Geological disposal of radioactive wastes—concept, status and trends. *Journal of Iberian Geology*, 32(1), 7-14.
- Chen, B., Peng, F., Zhang, L., Sun, D., (2023). Investigation on swelling characteristics of GMZ bentonite with different initial water contents. *Annals of Nuclear Energy*, 181, 109565. <https://doi.org/10.1016/j.anucene.2022.109565>
- Chikkamath, S., Manjanna, J., Kabadagi, A., Patil, D., Tripathi, V. S., Kar, A. S., & Tomar, B. S. (2021). Gamma ( $^{60}\text{Co}$ ) irradiation and thermal effect on redox behavior of interlayer iron in montmorillonite. *Applied Clay Science*, 200, 105893. <https://doi.org/10.1016/j.clay.2020.105893>
- Croisé J, Mayer G, Talandier J, Wendling J (2011) Impact of water consumption and saturation-dependent corrosion rate on hydrogen generation and migration from an intermediate-level radioactive waste repository. *Transport in Porous Media*, 90(1), 59–75 <https://doi.org/10.1007/s11242-011-9803-0>
- Crusset, D. et al. (2017). Corrosion of carbon steel components in the French high-level waste program: evolution of disposal concept and selection of materials. *Corrosion Engineering, Science and Technology*, 52, 17-24. <https://doi.org/10.1080/1478422X.2017.1344416>
- Daly, M. J. (2009). A new perspective on radiation resistance based on *Deinococcus radiodurans*. *Nature Reviews Microbiology*, 7(3), 237-245. <https://doi.org/10.1038/nrmicro2073>
- Darda, S.A., Gabbar, H.A., Damideh, V., Aboughaly, M., Hassen, I., (2021). A comprehensive review on radioactive waste cycle from generation to disposal. *Journal of Radioanalytical and Nuclear Chemistry*, 329, 15–31. <https://doi.org/10.1007/s10967-021-07764-2>
- Dou, W., Pu, Y., Han, X., Song, Y., Chen, S., & Gu, T. (2020). Corrosion of Cu by a sulfate reducing bacterium in anaerobic vials with different headspace volumes. *Bioelectrochemistry*, 133, 107478. <https://doi.org/10.1016/j.bioelechem.2020.107478>
- Engel, K., Ford, S. E., Binns, W. J., Diomidis, N., Slater, G. F., & Neufeld, J. D. (2023). Stable microbial community in compacted bentonite after 5 years of exposure to natural granitic groundwater. *MSphere*, 8(5), e00048-23. <https://doi.org/10.1128/msphere.00048-23>

## INTRODUCTION

Enning, D., & Garrelfs, J. (2014). Corrosion of iron by sulfate-reducing bacteria: new views of an old problem. *Applied and environmental microbiology*, 80(4), 1226-1236. <https://doi.org/10.1128/AEM.02848-13>

ENRESA. <https://www.enresa.es/>

Enssle CP, Brommundt J, Kaempfer ThU, Mayer G, Wendling J. (2014). Full-scale 3D modelling of a nuclear waste repository in the Callovo-Oxfordian clay. Part 2: thermo-hydraulic two-phase transport of water, hydrogen, <sup>14</sup>C and <sup>129</sup>I. In: Norris et al (eds) Clays in natural and engineered barriers for radioactive waste confinement, special publications, 400. *Geological Society, London*, pp 469–481

Estabragh, A. R., Khosravi, F., & Javadi, A. A. (2016). Effect of thermal history on the properties of bentonite. *Environmental Earth Sciences*, 75, 1-10. <https://doi.org/10.1007/s12665-016-5416-9>

Flamíková, D., Nečas, V. (2020). Assessment of the impact of selected changes in the deep geological repository model on its long-term safety. *EPJ Web Conf*, 225, 06012. <https://doi.org/10.1051/epjconf/202022506012>

Galamboš, M., Daňo, M., Rosskopfová, O., Šeršeň, F., Kufčáková, J., Adamcová, R., & Rajec, P. (2012). Effect of gamma-irradiation on adsorption properties of Slovak bentonites. *Journal of Radioanalytical and Nuclear Chemistry*, 292(2), 481-492. <https://doi.org/10.1007/s10967-012-1638-9>

Gao, N., Huang, Z., Liu, H., Hou, J., Liu, X. (2019). Advances on the toxicity of uranium to different organisms. *Chemosphere*, 237, 124548. <https://doi.org/10.1016/j.chemosphere.2019.124548>

García-Romero, E., María Manchado, E., Suárez, M., García-Rivas, J., (2019). Spanish Bentonites: A Review and New Data on Their Geology, Mineralogy, and Crystal Chemistry. *Minerals*, 9, 696. <https://doi.org/10.3390/min9110696>

Gilmour, K.A., Davie, C.T., Gray, N., (2022). Survival and activity of an indigenous iron-reducing microbial community from MX80 bentonite in high temperature / low water environments with relevance to a proposed method of nuclear waste disposal. *Science of The Total Environment*, 814, 152660. <https://doi.org/10.1016/j.scitotenv.2021.152660>

Giroud, N., Tomonaga, Y., Wersin, P., Briggs, S., King, F., Vogt, T., & Diomidis, N. (2018). On the fate of oxygen in a spent fuel emplacement drift in Opalinus Clay. *Applied geochemistry*, 97, 270-278. <https://doi.org/10.1016/j.apgeochem.2018.08.011>

- Grandia, F., Domènech, C., Arcos, D., & Duro, L. (2006). Assessment of the oxygen consumption in the backfill. Geochemical modelling in a saturated backfill (No. SKB-R--06-106). Swedish Nuclear Fuel and Waste Management Co.
- Grigoryan, A. A., Jalique, D. R., Medihala, P., Stroes-Gascoyne, S., Wolfaardt, G. M., McKelvie, J., & Korber, D. R. (2018). Bacterial diversity and production of sulfide in microcosms containing uncompacted bentonites. *Heliyon*, 4, e00722. <https://doi.org/10.1016/j.heliyon.2018.e00722>
- Gu, B. X., Wang, L. M., Minc, L. D., Ewing, R. C. (2001). Temperature Effects on the Radiation Stability and Ion Exchange Capacity of Smectites. *Journal of Nuclear Materials*, 297, 345–54. [https://doi.org/10.1016/S0022-3115\(01\)00631-6](https://doi.org/10.1016/S0022-3115(01)00631-6)
- Guo, M. (2020). The electrochemical and corrosion study of copper for nuclear waste containers under deep geological disposal conditions (Doctoral dissertation, The University of Western Ontario (Canada)).
- Hall, D. S. and Keech, P. G. (2017). An overview of the Canadian corrosion program for the long-term management of nuclear waste. *Corrosion Engineering, Science and Technology*, 52(sup1), 2–5. <https://doi.org/10.1080/1478422X.2016.1275419>
- Hall, D. S., Behazin, M., Binns, W. J., & Keech, P. G. (2021). An evaluation of corrosion processes affecting copper-coated nuclear waste containers in a deep geological repository. *Progress in Materials Science*, 118, 100766. <https://doi.org/10.1016/j.pmatsci.2020.100766>
- Haynes, H. M., Pearce, C. I., Boothman, C., and Lloyd, J. R. (2018). Response of bentonite microbial communities to stresses relevant to geodisposal of radioactive waste. *Chemical Geology*, 501, 58-67. <https://doi.org/10.1016/j.chemgeo.2018.10.004>
- Holmboe, M., Norrfors, K. K., Jonsson, M., and Wold, S. (2011). Effect of  $\gamma$ -radiation on radionuclide retention in compacted bentonite. *Radiation Physics and Chemistry*, 80(12), 1371-1377. <https://doi.org/10.1016/j.radphyschem.2011.08.004>
- Hultquist, G. (1986). Hydrogen evolution in corrosion of copper in pure water. *Corrosion Science*, 26(2), 173-177. [https://doi.org/10.1016/0010-938X\(86\)90044-2](https://doi.org/10.1016/0010-938X(86)90044-2)
- Hunter, W.J. (2014). *Pseudomonas seleniipraecipitans* Proteins Potentially Involved in Selenite Reduction. *Current Microbiology*, 69, 69–74. <https://doi.org/10.1007/s00284-014-0555-2>
- Huttunen-Saarivirta, E., Rajala, P., & Carpén, L. (2016). Corrosion behaviour of copper under biotic and abiotic conditions in anoxic groundwater: Electrochemical study. *Electrochimica Acta*, 203, 350-365. <https://doi.org/10.1016/j.electacta.2016.01.098>

## INTRODUCTION

- IAEA. (2018). Status and trends in spent fuel and radioactive waste management. Vienna, International Atomic Energy Agency. Nuclear Energy Series No. NW-T-1.14, 74. Available at: [https://www-pub.iaea.org/MTCD/Publications/PDF/PUB1963\\_web.pdf](https://www-pub.iaea.org/MTCD/Publications/PDF/PUB1963_web.pdf)
- Jalique, D.R., Stroes-Gascoyne, S., Hamon, C.J., Priyanto, D.G., Kohle, C., Evenden, W.G., Wolfaardt, G.M., Grigoryan, A.A., McKelvie, J., Korber, D.R., (2016). Culturability and diversity of microorganisms recovered from an eight-year old highly-compacted, saturated MX-80 Wyoming bentonite plug. *Applied Clay Science*, 126, 245–250. <https://doi.org/10.1016/j.clay.2016.03.022>
- Johansson, A.J., Lilja, C., Sjögren, L., Gordon, A., Hallbeck, L., Johansson, L., (2017). Insights from post-test examination of three packages from the MiniCan test series of copper-cast iron canisters for geological disposal of spent nuclear fuel: impact of the presence and density of bentonite clay. *Corrosion Engineering, Science and Technology*, 52, 54–60. <https://doi.org/10.1080/1478422X.2017.1296224>
- Johnson, L. H., Niemeyer, M., Klubertanz, G., Siegel, P., & Gribi, P. (2002). Calculations of the temperature evolution of a repository for spent fuel, vitrified high-level waste and intermediate level waste in Opalinus Clay (No. NTB--01-04). *National Cooperative for the Disposal of Radioactive Waste (NAGRA)*, 80, 1015-2636
- Jonsson, M. (2012). Radiation Effects on Materials Used in Geological Repositories for Spent Nuclear Fuel. *International Scholarly Research Notices*, 1-13. <https://doi.org/10.5402/2012/639520>
- Jonsson, M., Emilsson, G., & Emilsson, L. (2018). Mechanical design analysis for the canister. Posiva SKB Report, 4, 147.
- Jroundi, F., Descostes, M., Povedano-Priego, C., Sánchez-Castro, I., Suvannagan, V., Grizard, P., et al. (2020). Profiling native aquifer bacteria in a uranium roll-front deposit and their role in biogeochemical cycle dynamics: insights regarding in situ recovery mining. *Science of The Total Environment*, 721, 137758. <https://doi.org/10.1016/j.scitotenv.2020.137758>
- Jung, K. W., Lim, S., & Bahn, Y. S. (2017). Microbial radiation-resistance mechanisms. *Journal of Microbiology*, 55, 499-507. <https://doi.org/10.1007/s12275-017-7242-5>
- Kale, R. C., & Ravi, K. (2021). A review on the impact of thermal history on compacted bentonite in the context of nuclear waste management. *Environmental Technology & Innovation*, 23, 101728. <https://doi.org/10.1016/j.eti.2021.101728>

- Kaufhold, S., & Dohrmann, R. (2010). Stability of bentonites in salt solutions: II. Potassium chloride solution—Initial step of illitization. *Applied Clay Science*, 49(3), 98-107. <https://doi.org/10.1016/j.clay.2010.04.009>
- King, F. (2017). Nuclear waste canister materials: Corrosion behavior and long-term performance in geological repository systems. In *Geological repository systems for safe disposal of spent nuclear fuels and radioactive waste* (pp. 365-408). Woodhead Publishing. <https://doi.org/10.1016/B978-0-08-100642-9.00013-X>
- King, F., & Kolář, M. (2019). Lifetime predictions for nuclear waste disposal containers. *Corrosion*, 75(3), 309-323. <https://doi.org/10.5006/2994>
- King, F., Hall, D. S., & Keech, P. G. (2017). Nature of the near-field environment in a deep geological repository and the implications for the corrosion behaviour of the container. *Corrosion Engineering, Science and Technology*, 52(sup1), 25-30. <https://doi.org/10.1080/1478422X.2017.1330736>
- King, F., Lilja, C., Pedersen, K., Pitkänen, P., and Vähänen, M. (2010). An update of the state-of-the-art report on the corrosion of copper under expected conditions in a deep geologic repository (No. SKB-TR--10-67). Swedish Nuclear Fuel and Waste Management Co.
- Kushwaha, A., Goswami, L., Lee, J., Sonne, C., Brown, R.J.C., Kim, K.-H. (2022). Selenium in soil-microbe-plant systems: Sources, distribution, toxicity, tolerance, and detoxification. *Critical Reviews in Environmental Science and Technology*, 52, 2383–2420. <https://doi.org/10.1080/10643389.2021.1883187>
- Landolt, D., Davenport A., Payer A., Shoesmith D. (2009). A review of materials and corrosion issues regarding canisters for disposal of spent fuel and high-level waste in Opalinus clay. NAGRA Technical Report 09-02.
- Lapuerta, S., Béreard, N., Moncoffre, N., Millard-Pinard, N., Jaffrézic, H., Crusset, D., Féron, D. (2008). The Influence of Relative Humidity on Iron Corrosion under Proton Irradiation. *Journal of Nuclear Materials*, 375, 80–85. <https://doi.org/10.1016/j.jnucmat.2007.10.011>
- Laskowska, E., & Kuczyńska-Wiśnik, D. (2020). New insight into the mechanisms protecting bacteria during desiccation. *Current genetics*, 66(2), 313-318. <https://doi.org/10.1007/s00294-019-01036-z>
- Lau, M. C., Kieft, T. L., Kuloyo, O., Linage-Alvarez, B., Van Heerden, E., Lindsay, M. R., ... & Onstott, T. C. (2016). An oligotrophic deep-subsurface community dependent on syntrophy is dominated by sulfur-driven autotrophic denitrifiers. *Proceedings of the*

## INTRODUCTION

- National Academy of Sciences*, 113(49), E7927-E7936.  
<https://doi.org/10.1073/pnas.1612244113>
- Li, D.-B., Cheng, Y.-Y., Wu, C., Li, W.-W., Li, N., Yang, Z.-C., Tong, Z.-H., Yu, H.-Q. (2014). Selenite reduction by *Shewanella oneidensis* MR-1 is mediated by fumarate reductase in periplasm. *Scientific Reports*, 4, 1–7. <https://doi.org/10.1038/srep03735>
- Libert, M., Bildstein, O., Esnault, L., Jullien, M., & Sellier, R. (2011). Molecular hydrogen: an abundant energy source for bacterial activity in nuclear waste repositories. *Physics and Chemistry of the Earth, Parts A/B/C*, 36(17-18), 1616-1623.
- Lingnau, B. E., Graham, J., Yarechewski, D., Tanaka, N., & Gray, M. N. (1996). Effects of temperature on strength and compressibility of sand-bentonite buffer. *Engineering Geology*, 41(1-4), 103-115. [https://doi.org/10.1016/0013-7952\(95\)00028-3](https://doi.org/10.1016/0013-7952(95)00028-3)
- Little, B. J., Hinks, J., & Blackwood, D. J. (2020). Microbially influenced corrosion: Towards an interdisciplinary perspective on mechanisms. *International Biodeterioration & Biodegradation*, 154, 105062. <https://doi.org/10.1016/j.ibiod.2020.105062>
- Liu, D., Dong, H., Bishop, M.E., Zhang, J., Wang, H., Xie, S., Wang, S., Huang, L., Eberl, D.D., (2012). Microbial reduction of structural iron in interstratified illite-smectite minerals by a sulfate-reducing bacterium. *Geobiology*, 10, 150–162. <https://doi.org/10.1111/j.1472-4669.2011.00307.x>
- Liu, J. F., Wu, Y., Cai, C. Z., Ni, H. Y., Cao, X. L., Pu, H., Shuai-bing, S., Sheng-yan, P. & Skoczylas, F. (2018). Investigation into water retention and gas permeability of Opalinus clay. *Environmental earth sciences*, 77, 1-13. <https://doi.org/10.1007/s12665-018-7397-3>
- Lopez-Fernandez, M., Jroundi, F., Ruiz-Fresneda, M.A., Merroun, M.L. (2021). Microbial interaction with and tolerance of radionuclides: underlying mechanisms and biotechnological applications. *Microbial Biotechnology*, 14, 810–828. <https://doi.org/10.1111/1751-7915.13718>
- Lopez-Fernandez, M., Broman, E., Simone, D., Bertilsson, S., & Dopson, M. (2019). Statistical analysis of community RNA transcripts between organic carbon and geogas-fed continental deep biosphere groundwaters. *MBio*, 10(4), 10-1128. <https://doi.org/10.1128/mbio.01470-19>
- Lopez-Fernandez, M., Vilchez-Vargas, R., Jroundi, F., Boon, N., Pieper, D., Merroun, M.L. (2018). Microbial community changes induced by uranyl nitrate in bentonite clay microcosms. *Applied Clay Science, ACS - SI ICC 2017 XVI International Clay Conference – Clays, from the oceans to space*, 160, 206–216. <https://doi.org/10.1016/j.clay.2017.12.034>

- Maanoja, S., Palmroth, M., Salminen, L., Lehtinen, L., Kokko, M., Lakaniemi, A.-M., Auvinen, H., Kiczka, M., Muuri, E., Rintala, J., (2021). The effect of compaction and microbial activity on the quantity and release rate of water-soluble organic matter from bentonites. *Applied Clay Science* 211, 106192. <https://doi.org/10.1016/j.clay.2021.106192>
- Man M., Tong H., Srikanthan N., Usman M.O., Tully C.S., Noël J.J., Behazin M., Binns W. J., Keech P.G., Simpson M.J. (2024). Analysis of natural organic matter chemistry in bentonite clay under compaction using different dry densities and duration. *Applied Geochemistry*, 166, 105985. <https://doi.org/10.1016/j.apgeochem.2024.105985>
- Marsh, A.I., Williams, L.G., Lawrence, J.A., (2021). The important role and performance of engineered barriers in a UK geological disposal facility for higher activity radioactive waste. *Progress in Nuclear Energy*, 137. <https://doi.org/10.1016/j.pnucene.2021.103736>
- Marshall, M. H., & Simpson, M. J. (2014). State of science review: natural organic matter in clays and groundwater. NWMO TR-2014-05
- Martinez-Moreno, M.F., Povedano-Priego, C., Mumford, A.D., Morales-Hidalgo, M., Mijndonckx, K., Jroundi, F., Ojeda, J.J., Merroun, M.L., (2024). Microbial responses to elevated temperature: Evaluating bentonite mineralogy and copper canister corrosion within the long-term stability of deep geological repositories of nuclear waste. *Science of The Total Environment*, 915, 170149. <https://doi.org/10.1016/j.scitotenv.2024.170149>
- Martinez-Moreno, Marcos F., Povedano-Priego, C., Morales-Hidalgo, M., Mumford, A.D., Ojeda, J.J., Jroundi, F., Merroun, M.L., (2023). Impact of compacted bentonite microbial community on the clay mineralogy and copper canister corrosion: a multidisciplinary approach in view of a safe Deep Geological Repository of nuclear wastes. *Journal of Hazardous Materials*, 458, 131940. <https://doi.org/10.1016/j.jhazmat.2023.131940>
- Martino, T., Chen, J., Guo, M., Ramamurthy, S., Shoesmith, D. W., & Noël, J. J. (2019). Comments on E. Huttunen-Saarivirta et al., “Kinetic Properties of the Passive Film on Copper in the Presence of Sulfate-Reducing Bacteria”[J. Electrochem. Soc., 165, C450 (2018)]. *Journal of the Electrochemical Society*, 166(10), Y13. <http://dx.doi.org/10.1149/2.0761910jes>
- Masurat, P., Eriksson, S., & Pedersen, K. (2010). Evidence of indigenous sulphate-reducing bacteria in commercial Wyoming bentonite MX-80. *Applied Clay Science*, 47(1-2), 51-57. <https://doi.org/10.1016/j.clay.2008.07.002>

## INTRODUCTION

- Mattimore, V., and Battista, J. R. (1996). Radioresistance of *Deinococcus radiodurans*: functions necessary to survive ionizing radiation are also necessary to survive prolonged desiccation. *Journal of bacteriology*, 178(3), 633-637. <https://doi.org/10.1128/jb.178.3.633-637.1996>
- McMurry, J., Dixon, D. A., Garroni, J. D., Ikeda, B. M., Stroes-Gascoyne, S., Baumgartner, P., & Melnyk, T. W. (2004). Evolution of a Canadian deep geologic repository (No. 06819-REP, pp. 01200-100092). Ontario Power Generation Report.
- Mehrshad, M., Lopez-Fernandez, M., Sundh, J., Bell, E., Simone, D., Buck, M., Bernier-Latmani, R., Bertilsson, E. & Dopson, M. (2021). Energy efficiency and biological interactions define the core microbiome of deep oligotrophic groundwater. *Nature Communications*, 12(1), 4253. <https://doi.org/10.1038/s41467-021-24549-z>
- Merroun, M.L., Raff, J., Rossberg, A., Hennig, C., Reich, T., Selenska-Pobell, S. (2005). Complexation of Uranium by Cells and S-Layer Sheets of *Bacillus sphaericus* JG-A12. *Applied and Environmental Microbiology*, 71, 5532–5543. <https://doi.org/10.1128/AEM.71.9.5532-5543.2005>
- Mills, M. M., Sanchez, A. C., Boisvert, L., Payne, C. B., Ho, T. A., and Wang, Y. (2022). Understanding smectite to illite transformation at elevated (> 100 °C) temperature: effects of liquid/solid ratio, interlayer cation, solution chemistry and reaction time. *Chemical Geology*, 615, 121214. <https://doi.org/10.1016/j.chemgeo.2022.121214>
- Musilova, M., Wright, G., Ward, J. M., & Dartnell, L. R. (2015). Isolation of radiation-resistant bacteria from Mars analog Antarctic Dry Valleys by preselection, and the correlation between radiation and desiccation resistance. *Astrobiology*, 15(12), 1076-1090. <https://doi.org/10.1089/ast.2014.1278>
- Nazina, T. N., Luk'yanova, E. A., Zakharova, E. V., Ivoilov, V. S., Poltarau, A. B., Kalmykov, S. N., Belyaev, S.S. & Zubkov, A. A. (2006). Distribution and activity of microorganisms in the deep repository for liquid radioactive waste at the Siberian chemical combine. *Microbiology*, 75, 727-738. <https://doi.org/10.1134/S0026261706060178>
- Nešić, S. (2007). Key issues related to modelling of internal corrosion of oil and gas pipelines—A review. *Corrosion science*, 49(12), 4308-4338. <https://doi.org/10.1016/j.corsci.2007.06.006>
- Newsome, L., Morris, K., Trivedi, D., Atherton, N., and Lloyd, J. R. (2014). Microbial reduction of uranium VI in sediments of different lithologies collected from Sellafield. *Applied Geochemistry*, 51, 55–64. <https://doi.org/10.1016/j.apgeochem.2014.09.008>

- Norrfors, K. K., Björkbacka, Å., Kessler, A., Wold, S., & Jonsson, M. (2018).  $\gamma$ -radiation induced corrosion of copper in bentonite-water systems under anaerobic conditions. *Radiation Physics and Chemistry*, 144, 8-12. <https://doi.org/10.1016/j.radphyschem.2017.11.004>
- O'Brien KE, Rainham D, O'Beirne-Ryan AM. (2014) Using field analogue soil column experiments to quantify radon-222 gas migration and transport through soils and bedrock of Halifax, Nova Scotia, Canada. *Environmental Earth Sciences*, 72, 2607–2620. <https://doi.org/10.1007/s12665-014-3168-y>
- Ohazuruike, L., & Lee, K. J. (2023). A comprehensive review on clay swelling and illitization of smectite in natural subsurface formations and engineered barrier systems. *Nuclear Engineering and Technology*, 55(4), 1495-1506. <https://doi.org/10.1016/j.net.2023.01.007>
- Ojovan, M.I., Steinmetz, H.J., (2022). Approaches to Disposal of Nuclear Waste. *Energies*, 15, 7804. <https://doi.org/10.3390/en15207804>
- Payer, J. H., Finsterle, S., Apps, J. A., & Muller, R. A. (2019). Corrosion performance of engineered barrier system in deep horizontal drillholes. *Energies*, 12(8), 1491. <https://doi.org/10.3390/en12081491>
- Pedersen, K., Motamedi, M., Karland, O., Sandén, T., (2000). Mixing and sulphate-reducing activity of bacteria in swelling, compacted bentonite clay under high-level radioactive waste repository conditions. *Journal of Applied Microbiology*, 89, 1038–1047. <https://doi.org/10.1046/j.1365-2672.2000.01212.x>
- Peitzsch, M., Kremer, D., & Kersten, M. (2010). Microfungal alkylation and volatilization of selenium adsorbed by goethite. *Environmental science & technology*, 44(1), 129-135. <https://doi.org/10.1021/es9006492>
- Perko J, Weetjens E. (2011) Thermohydraulic analysis of gas generation in a disposal facility for vitrified high-level radioactive waste in boom clay. *Nuclear Technology*, 174(3), 401–410 <https://doi.org/10.13182/NT11-A11748>
- Phillips, R. W., Wiegel, J., Berry, C. J., Fliermans, C., Peacock, A. D., White, D. C., and Shimkets, L. J. (2002). *Kineococcus radiotolerans* sp. nov., a radiation-resistant, gram-positive bacterium. *International journal of systematic and evolutionary microbiology*, 52(3), 933-938. <https://doi.org/10.1099/00207713-52-3-933>
- Pinel-Cabello, M., Chapon, V., Ruiz-Fresneda, M.A., Alpha-Bazin, B., Berthomieu, C., Armengaud, J., Merroun, M.L. (2021). Delineation of cellular stages and identification of key proteins for reduction and biotransformation of Se(IV) by

## INTRODUCTION

- Stenotrophomonas bentonitica* BII-R7. *Journal of Hazardous Materials*, 418, 126150. <https://doi.org/10.1016/j.jhazmat.2021.126150>
- Plötze, M., Kahr, G., and Stengele, R. H. (2003). Alteration of clay minerals — gamma-irradiation effects on physico chemical properties. *Applied Clay Science*, 23, 195–202. [https://doi.org/10.1016/S0169-1317\(03\)00103-0](https://doi.org/10.1016/S0169-1317(03)00103-0)
- Poller, A., Mayer, G., Darcis, M., & Smith, P. (2016). Modelling of gas generation in deep geological repositories after closure (No. NTB--16-04). National Cooperative for the Disposal of Radioactive Waste (NAGRA).
- Porras, D.E.V., Angélica, R.S., Paz, S.P.A.D., (2021). Practical mineralogical quantification of bentonites supported for a PXRD calibrated hkl model. *Braz. The Journal of Geology*, 51, e20200088. <https://doi.org/10.1590/2317-4889202120200088>
- Posiva, (2017). Safety functions, performance targets and technical design requirements for a KBS-3V repository – Conclusions and recommendations from a joint SKB and Posiva working group. Posiva SKB Rep. 01.
- Pospiskova, I., Dobrev, D., Kouril, M., Stouilil, J., Novikova, D., Kotnour, P., & Matal, O. (2017). Czech national programme and disposal canister concept. *Corrosion Engineering, Science and Technology*, 52(sup1), 6-10. <https://doi.org/10.1080/1478422X.2017.1300379>
- Povedano-Priego, C., Jroundi, F., Morales-Hidalgo, M., Pinel-Cabello, M., Peula-Ruiz, E., Merroun, M.L., Martín-Sánchez, I. (2024). Unveiling fungal diversity in uranium and glycerol-2-phosphate-amended bentonite microcosms: Implications for radionuclide immobilization within the Deep Geological Repository system. *Science of The Total Environment*, 908, 168284. <https://doi.org/10.1016/j.scitotenv.2023.168284>
- Povedano-Priego, C., Jroundi, F., Solari, P.L., Guerra-Tschuschke, I., Abad-Ortega, M. del M., Link, A., Vilchez-Vargas, R., Merroun, M.L. (2023). Unlocking the bentonite microbial diversity and its implications in selenium bioreduction and biotransformation: Advances in deep geological repositories. *Journal of Hazardous Materials*, 445, 130557. <https://doi.org/10.1016/j.jhazmat.2022.130557>
- Povedano-Priego, C., Jroundi, F., Lopez-Fernandez, M., Morales-Hidalgo, M., Martín-Sánchez, I., Huertas, F.J., Dopson, M., Merroun, M.L. (2022). Impact of anoxic conditions, uranium(VI) and organic phosphate substrate on the biogeochemical potential of the indigenous bacterial community of bentonite. *Applied Clay Science*, 216, 106331. <https://doi.org/10.1016/j.clay.2021.106331>
- Povedano-Priego, C., Jroundi, F., Lopez-Fernandez, M., Shrestha, R., Spanek, R., Martín-Sánchez, I., Villar, M.V., Ševců, A., Dopson, M., Merroun, M.L., (2021).

- Deciphering indigenous bacteria in compacted bentonite through a novel and efficient DNA extraction method: Insights into biogeochemical processes within the Deep Geological Disposal of nuclear waste concept. *Journal of Hazardous Materials*, 408, 124600. <https://doi.org/10.1016/j.jhazmat.2020.124600>
- Povedano-Priego, C., Jroundi, F., Lopez-Fernandez, M., Sánchez-Castro, I., Martín-Sánchez, I., Huertas, F.J., Merroun, M.L. (2019). Shifts in bentonite bacterial community and mineralogy in response to uranium and glycerol-2-phosphate exposure. *Science of The Total Environment*, 692, 219–232. <https://doi.org/10.1016/j.scitotenv.2019.07.228>
- Prachař, I., Pospíšková, I., Vokal, A., Steinerova, L., & Vondrovic, L. (2017). DGR development in the Czech Republic. Action Plan 2017-2025 (No. SURAO--112-2017). Radioactive Waste Repository Administration.
- Qin, Z., Daljeet, R., Ai, M., Farhangi, N., Noël, J. J., Ramamurthy, S., Shoesmith, D., King, F., & Keech, P. (2017). The active/passive conditions for copper corrosion under nuclear waste repository environment. *Corrosion Engineering, Science and Technology*, 52(sup1), 45-49. <https://doi.org/10.1080/1478422X.2016.1274088>
- Rajala, P., & Bomberg, M. (2023). Geomicrobes: Life in terrestrial deep subsurface, volume II. *Frontiers in Microbiology*, 14, 1169127. <https://doi.org/10.3389/fmicb.2023.1169127>
- Rättö, M., Itävaara, M., (2012). Microbial activity in bentonite buffers: Literature study, VTT Technology. VTT Technical Research Centre of Finland, Espoo.
- Reed D.T and Konynenburg, R. A.V. (1987). Effect of ionizing radiation on moist air systems. *MRS Online Proceedings Library (OPL)*, 112, 393. <https://doi.org/10.1557/PROC-112-393>
- Ruiz-Fresneda, M. A., Morales-Hidalgo, M., Povedano-Priego, C., Jroundi, F., Hidalgo-Iruela, J., Cano-Cano, M., Pérez-Muelas, E., Merroun, M. L., & Martín-Sánchez, I. (2024). Unlocking the key role of bentonite fungal isolates in tellurium and selenium bioremediation and biorecovery: Implications in the safety of radioactive waste disposal. *Science of The Total Environment*, 912, 169242. <https://doi.org/10.1016/J.SCITOTENV.2023.169242>
- Ruiz-Fresneda, M. A., Fernández-Cantos, M. v, Gómez-Bolívar, J., Eswayah, A. S., Gardiner, P. H. E., Pinel-Cabello, M., Solari, P. L., & Merroun, M. L. (2023). Combined bioreduction and volatilization of SeVI by *Stenotrophomonas bentonitica*: Formation of trigonal selenium nanorods and methylated species. *Science of The Total Environment*, 858, 160030. <https://doi.org/10.1016/j.scitotenv.2022.160030>

## INTRODUCTION

- Ruiz-Fresneda, M. A., Martínez-Moreno, M. F., Povedano-Priego, C., Morales-Hidalgo, M., Jroundi, F., & Merroun, M. L. (2023). Impact of microbial processes on the safety of deep geological repositories for radioactive waste. *Frontiers in Microbiology*, 14, 1134078. <https://doi.org/10.3389/fmicb.2023.1134078>
- Ruiz-Fresneda, M. A., Eswayah, A. S., Romero-González, M., Gardiner, P. H. E., Solari, P. L., and Merroun, M. L. (2020). Chemical and structural characterization of SeIV biotransformations by *Stenotrophomonas bentonitica* into Se0 nanostructures and volatile Se species. *Environmental Science: Nano journal*, 7, 2140–2155. <https://doi.org/10.1039/D0EN00507J>
- Ruiz-Fresneda, M.A., Gomez-Bolivar, J., Delgado-Martin, J., Abad-Ortega, M. del M., Guerra-Tschuschke, I., Merroun, M.L. (2019). The Bioreduction of Selenite under Anaerobic and Alkaline Conditions Analogous to Those Expected for a Deep Geological Repository System. *Molecules*, 24, 3868. <https://doi.org/10.3390/molecules24213868>
- Ruiz-Fresneda, M.A., Martín, J.D., Bolívar, J.G., Cantos, M.V.F., Bosch-Estévez, G., Moreno, M.F.M., Merroun, M.L. (2018). Green synthesis and biotransformation of amorphous Se nanospheres to trigonal 1D Se nanostructures: impact on Se mobility within the concept of radioactive waste disposal. *Environmental Science: Nano journal*, 5, 2103–2116. <https://doi.org/10.1039/C8EN00221E>
- Schlegel, M. L., Necib, S., Daumas, S., Labat, M., Blanc, C., Foy, E., & Linard, Y. (2018). Corrosion at the carbon steel-clay borehole water interface under anoxic alkaline and fluctuating temperature conditions. *Corrosion Science*, 136, 70-90. <https://doi.org/10.1016/j.corsci.2018.02.052>
- Sellin, P., Leupin, O.X., (2013). The use of clay as an engineered barrier in radioactive-waste management – A Review. *Clays and Clay Minerals*, 61, 477–498. <https://doi.org/10.1346/CCMN.2013.0610601>
- SKB. (2019). Supplementary information on canister integrity issues; Technical Report SKB TR-19-15; Stockholm, Sweden: SKB; p. 135.
- Smith, J. M., Wren, J. C., Odziemkowski, M., & Shoesmith, D. W. (2007). The electrochemical response of preoxidized copper in aqueous sulfide solutions. *Journal of the Electrochemical Society*, 154(8), C431. <https://doi.org/10.1149/1.2745647>
- Sorieul, S., Allard, T., Wang, L.M., Grambin-Lapeyre, C., Lian, J., Calas, G., Ewing, R.C. (2008). Radiation-Stability of Smectite. *Environmental science & technology*, 42(22), 8407-8411. <https://doi.org/10.1021/es800766b>

- Soroka, I., Chae, N., Jonsson, M. (2021). On the mechanism of  $\gamma$ -radiation-induced corrosion of copper in water. *Corrosion Science*, 182, 109279. <https://doi.org/10.1016/j.corsci.2021.109279>
- Spinks, J.W.T., and Woods, R.J. (1990). An introduction to radiation chemistry. United States: N. p. Web.
- Stoulil, J., Pavlova, L., & Kouřil, M. (2019). Localised corrosion of stainless steels 316L and 2205 in synthetic bentonite pore water and bentonite slurry. *Acta Metallurgica Slovaca*, 25(1), 24-32. 10.36547/ams.25.1.4
- Striček I. (2010). Mineral stability of bentonites in barrier conditions. Dissertation thesis. Comenius University in Bratislava. Faculty of Natural Sciences. Department of Geology of Mineral Deposits.
- Striček I., Šucha V., Uhlík P. (2008). Gamma-irradiation effects on smectite properties. 4. Mid-European clay conference, Zakopane, Poland, Abstracts, Mineralogia—*Special papers*, 33, 157
- Stroes-Gascoyne, S., Hamon, C. J., Maak, P., & Russell, S. (2010). The effects of the physical properties of highly compacted smectitic clay (bentonite) on the culturability of indigenous microorganisms. *Applied Clay Science*, 47(1–2), 155–162. <https://doi.org/10.1016/J.CLAY.2008.06.010>
- Stroes-Gascoyne, S., Lucht, L. M., Borsa, J., Delaney, T. L., Haveman, S. A., and Hamon, C. J. (1994). Radiation resistance of the natural microbial population in buffer materials. *MRS Online Proceedings Library (OPL)*, 353, 345. <https://doi.org/10.1557/PROC-353-345>
- Sun, Q., Zhang, W., & Qian, H. (2016). Effects of high temperature thermal treatment on the physical properties of clay. *Environmental Earth Sciences*, 75, 1-8. 10.1007/s12665-016-5402-2
- Svensson, D., Dueck, A., Nilsson, U., Olsson, S., Sandén, T., Lydmark, S., Jägerwall, S., Pedersen, K., Hansen, S., (2011). Alternative buffer material. Status of the ongoing laboratory investigation of reference materials and test package 1. SKB Report TR-11-06. Swedish Nuclear Fuel and Waste Management Co, Stockholm, Sweden
- Tan, Ö., Yılmaz, L., & Zaimoğlu, A. S. (2004). Variation of some engineering properties of clays with heat treatment. *Materials Letters*, 58(7-8), 1176-1179. <https://doi.org/10.1016/j.matlet.2003.08.030>

## INTRODUCTION

- Thauer, R. K., Stackebrandt, E., & Hamilton, W. A. (2007). Energy metabolism and phylogenetic diversity of sulphate-reducing bacteria. *Sulphate-reducing bacteria*, 1-38.
- Van Gerwen, S. J., Rombouts, F. M., Van't Riet, K., & Zwietering, M. H. (1999). A data analysis of the irradiation parameter D10 for bacteria and spores under various conditions. *Journal of food Protection*, 62(9), 1024-1032. <https://doi.org/10.4315/0362-028X-62.9.1024>
- Vikman, M., Marjamaa, K., Nykyri, M., Small, J. S., Miettinen, H., Heikinheimo, L., Haavisto, T. & Itävaara, M. (2019). The biogeochemistry of gas generation from low-level nuclear waste: Microbiological characterization during 18 years study under in situ conditions. *Applied Geochemistry*, 105, 55-67. <https://doi.org/10.1016/j.apgeochem.2019.04.002>
- Villar, M. V., Pérez del Villar, L., Martín, P. L., Pelayo, M., Fernández, A. M., Garralón, A., Cuevas, J., Leguey, S., Caballero, E., Huertas, F. J., Jiménez de Cisneros, C., Linares, J., Reyes, E., Delgado, A., Fernández-Soler, J. M., & Astudillo, J. (2006). The study of Spanish clays for their use as sealing materials in nuclear waste repositories: 20 years of progress. *Journal of Iberian Geology*, 32, 15–36.
- Wells, M., McGarry, J., Gaye, M.M., Basu, P., Oremland, R.S., Stolz, J.F. (2019). Respiratory Selenite Reductase from *Bacillus selenitireducens* Strain MLS10. *Journal of Bacteriology*, 201. <https://doi.org/10.1128/JB.00614-18>
- Wendling, J., Justinavicius, D., Sentis, M., Amaziane, B., Bond, A., Calder, N. J., & Treille, E. (2019). Gas transport modelling at different spatial scales of a geological repository in clay host rock. *Environmental Earth Sciences*, 78, 1-16. <https://doi.org/10.1007/s12665-019-8230-3>
- Werme, L. (1998). Design premises for canister for spent nuclear fuel. Posiva SKB Technical Report TR-98-08.
- Wersin, P., Johnson, L. H., & McKinley, I. G. (2007). Performance of the bentonite barrier at temperatures beyond 100 °C: A critical review. *Physics and Chemistry of the Earth, Parts A/B/C*, 32(8-14), 780-788. <https://doi.org/10.1016/j.pce.2006.02.051>
- West, J. M., McKinley, I. G., & Stroes-Gascoyne, S. (2002). Microbial effects on waste repository materials. *In Radioactivity in the Environment*, 2, 255-277.
- Wouters, B. G., and Begg, A. C. (2009). Irradiation-induced damage and the DNA damage response. *Basic clinical radiobiology*, 4, 11-26.

- Xu, Y., Zeng, Z., and Lv, H. (2019). Temperature dependence of apparent thermal conductivity of compacted bentonites as buffer material for high-level radioactive waste repository. *Applied Clay Science*, 174, 10–14. <https://doi.org/10.1016/j.clay.2019.03.017>
- Yu, Q., Cui, O., Yu, Q., Cui, O. (2023). Enrichment and remediation of uranium by microorganisms: A review. *Open Journal of Environmental Biology*, 8, 020–038. <https://doi.org/10.17352/ojeb.000037>
- Zhang, J., Dong, H., Liu, D., Fischer, T.B., Wang, S., Huang, L. (2012). Microbial reduction of Fe(III) in illite–smectite minerals by methanogen *Methanosarcina mazei*. *Chemical Geology*, 292–293, 35–44. <https://doi.org/10.1016/j.chemgeo.2011.11.003>.
- Zhao, C., Liu, J., Li, X., Li, F., Tu, H., Sun, Q., Liao, J., Yang, J., Yang, Y., Liu, N. (2016). Biosorption and bioaccumulation behavior of uranium on *Bacillus* sp. dwc-2: Investigation by Box-Behenken design method. *Journal of Molecular Liquids*, 221, 156–165. <https://doi.org/10.1016/j.molliq.2016.05.085>
- Zhou, C., Vannela, R., Hyun, S.P., Hayes, K.F., Rittmann, B.E. (2014). Growth of *Desulfovibrio vulgaris* When Respiring U(VI) and Characterization of Biogenic Uraninite. *Environmental Science & Technology*, 48, 6928–6937. <https://doi.org/10.1021/es501404h>

Image from iStock



A vertical photograph on the left side of the page shows a white microscope in the foreground, with its objective lenses and eyepiece visible. Below the microscope, a white cylindrical container sits on a laboratory bench. The background is a plain, light-colored wall.

*Objectives*

## OBJECTIVES

**OBJECTIVES**

The main objective of this Ph.D. thesis is to evaluate the influence of different physicochemical and microbiological parameters on the stability of different barriers (bentonite and metal canisters) in future deep geological repositories (DGRs) for radioactive waste. Furthermore, understanding the impact of DGR relevant conditions on the microbial activity is particularly important for assessing their effect on both the stability of bentonite and the integrity of the copper-based metal canisters. The present doctoral thesis offers new insights into the microbiology of DGRs, thereby contributing to the evaluation of the long-term safety and performance of these multisystem storage sites.

Therefore, the specific objectives of this Ph.D. thesis are:

- 1) To study the combined effect of gamma radiation and high compaction (dry density of  $1.6 \text{ g/cm}^3$ ) on the diversity and viability of native microorganisms in FEBEX bentonite, on copper corrosion, and on the mineralogical stability of bentonite.
- 2) To assess the influence of high temperature (incubation at  $60 \text{ }^\circ\text{C}$  and a heat-shock treatment) and selenium exposure on the Spanish bentonite microbial communities under water-saturated conditions, along with exploring changes in selenium chemical speciation.
- 3) To evaluate the viability of native sulfate-reducing bacteria of bentonite after exposure to high temperature and simulated selenium leakage, and to investigate their impact on copper corrosion.
- 4) To explore the long-term effects of uranium exposure on bentonite microbiology under conditions of high bacterial activity, and to analyze changes in the chemical speciation of this radionuclide.

Image from personal  
archive





*Materials and methods*

## MATERIALS AND METHODS

## MATERIALS AND METHODS

This section outlines the materials and methodology employed in the main experimental setup of the present Ph.D. thesis. For more detailed information regarding the development of the experiments or the preparation of any of its components, please refer to the specific "Materials and Methods" section of the corresponding chapter (**Chapters 1-4**).

### **1. Bentonite sample collection and storage**

This Ph.D. thesis studied Spanish bentonite from the geological site called "Cortijo de Archidona" in Almería, Spain. **Chapters 2-4** utilized fresh bentonite collected from this geological formation in collaboration with Dr. F. Javier Huertas (Instituto Andaluz de Ciencias de la Tierra, University of Granada). Regarding **Chapter 1**, it was developed using bentonite from the same site, provided by CIEMAT (Centro de Investigaciones Energéticas, Medioambientales y Tecnológicas), and previously sampled for the development of the Full-scale Engineered Barriers Experiment (FEBEX) project (Huertas et al., 2000). This bentonite was named during that project, and thus it will be referred to as FEBEX.

To obtain the freshly collected bentonite, sampling was carried out using a soil auger under aseptic conditions to prevent contamination from exogenous microorganisms. The extraction depth was approximately 90 centimeters (**Fig. 1**). Once in the laboratory, the bentonite was dried in a laminar flow hood for three to four days at room temperature. The grain size was then reduced and homogenized using a carbon steel nonstick roller pin under sterile conditions. Then, the bentonite was kept at 4 °C until it was needed.

## MATERIALS AND METHODS



**Figure 1.** Bentonite sampling at “Cortijo de Archidona” site (Almería, Spain) in February 2021.

### 2. Copper material for corrosion studies

The copper material used as representative of future copper canisters was provided from Goodfellow Cambridge Ltd. (UNS number C10100; <https://www.goodfellow.com>) for **Chapter 1** and from the Centro de Instrumentación Científica de la Universidad de Granada (CIC, UGR) for **Chapter 3 (Fig. 2)**. In both cases, the material corresponded to an oxygen-free copper, with a purity percentage between 99% and 100%.

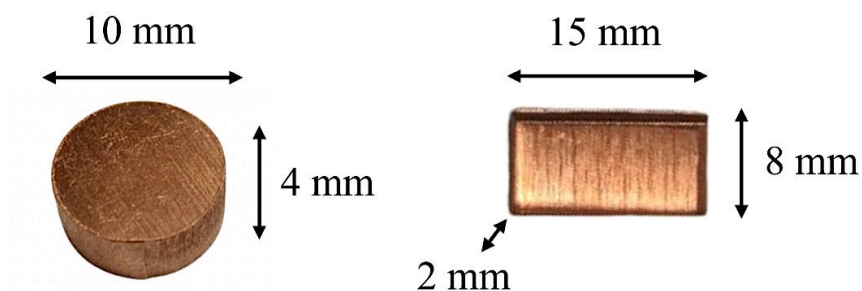


**Figure 2.** Pure copper material used in corrosion analysis: Cu disk (left, Chapter 1) and Cu plate (right, Chapter 3).

**Chapter 1** included copper disks with dimensions of 10 mm in diameter and 4 mm in thickness. For **Chapter 3**, the copper consisted of plates with dimensions of 8 mm in height, 15 mm in width, and 2 mm in thickness. Prior to their use, the Cu plates/disks were subjected to a chemical cleaning and sterilization process following the protocol reported by Guo M. (2020). Details of this cleaning treatment are provided in the materials and methods sections of **Chapters 1** and **3** of this Ph.D. thesis.

### **3. Characterization of bentonite microbial communities**

#### *DNA extraction and sequencing*

DNA extractions from all bentonite samples followed the protocol established by Povedano-Priego et al. (2021), which is based on the traditional phenol-chloroform method. Due to difficulties in extracting DNA from the samples relevant to **Chapter 1**, some modifications to the protocol were implemented and are detailed in that chapter. The concentration of the total extracted DNA was quantified using Qubit 3.0 Fluorometer (Life Technology, Invitrogen™).

Regarding the experiments of water-saturated bentonite (**Chapters 2** and **4**), the amplification, sequencing, and subsequent bioinformatics analyses were conducted at StabVida Company (Caparica, Portugal; <https://www.stabvida.com>). For library construction, V3-V4 variable regions of the bacterial 16S rRNA gene were amplified by PCR using the universal primers 341F (5'-CCTACGGGNGGCWGCAG-3') and 785R (5'-GACTACHVGGGTATCTAATCC-3'). The sequencing was conducted on the Illumina MiSeq platform, employing Next-Generation Sequencing (NGS) technology.

Conversely, the sequencing of compacted bentonite, **Chapter 1**, was performed in collaboration with Dr. Kateřina Černá from the Institute for

## MATERIALS AND METHODS

Nanomaterials, Advanced Technology and Innovation (<https://cxi.tul.cz/en>), at the Technical University of Liberec (Czech Republic), during the Ph.D. research stay. The extracted DNA was sequenced on the Ion Torrent Personal Genome Machine (PGM) using the Ion PGM Hi-Q Sequencing Kit and the Ion 314 Chip v. 2 (Thermo Fisher Scientific®, USA). Two consecutive PCR reactions were performed for each sample to amplify the V4 region of the bacterial 16S rRNA gene. Universal primers 530F (5'-GTGCCAGCMGCNGCGG-3') and 802R (5'-TACNVGGGTATCTAATCC-3') were used for the subsequent amplicon sequencing.

### *Bioinformatic and statistical data processing*

Sequencing data from StabVida Company were processed and analyzed using QIIME2 v2022.2. Raw data were denoised using the DADA2 plugin to remove low-quality regions, dereplicate reads, and filter chimeras. Alpha rarefaction curves were employed to assess sequencing quality. Afterwards, reads were grouped into Operational Taxonomic Units (OTUs) and taxonomically classified using the SILVA database (release 138 in QIIME), applying a clustering threshold of 99% similarity.

Regarding the sequencing performed in the Technical University of Liberec, the raw reads were initially divided into individual samples using Mothur software, followed by processing with the DADA2 R software package. Taxonomic classification was then carried out using the same DADA2 package with the SILVA v. 132 database ([www.arb-silva.de](http://www.arb-silva.de)).

In all cases, relative abundances of taxa and alpha diversity indices were obtained using Explicit 2.10.5. To represent differences between the bentonite treatments, principal coordinate analysis (PCoA) based on the Bray-Curtis algorithm was conducted using Past 4.04 software. Additionally, heatmaps were also generated using the heatmap.2 function in R v.4.2.1 software.

### Quantitative polymerase chain reaction (qPCR)

Quantitative polymerase chain reaction (qPCR) was employed to assess changes in total bacterial content in response to different treatments. Reactions were performed on a LightCycler 480 instrument (Roche, Switzerland). Universal primers, U16SRT-F and U16SRT-R, were utilized for amplifying the V3 region of the 16S rRNA gene. Specific genes for sulfate-reducing bacteria (SRB) were also targeted, including the adenosine 5'-phosphosulfate reductase gene *apsA* and the dissimilatory sulfate reductase gene *dsrA*. The *apsA* gene was amplified using primers RH1-aps-F and RH2-aps-R, while the *dsrA* gene was amplified using primers RH1-dsr-F and RH3-dsr-R. The data was processed using the relative quantitative (RQ) calculation method  $\Delta\Delta Cq$ , which evaluates the magnitude of the difference in quantification cycle values ( $Cq$ ) between samples. This method calculates RQ as  $RQ = \text{efficiency}^{(-\Delta\Delta Cq)}$ .

## **4. Molecular identification of bacterial isolates and culture-media enrichments**

### **4.1. Amplification and identification of bacterial isolates**

Bacterial colonies of interest grown in culture media (Lysogeny broth, R2A) were suspended in MilliQ water and heated to 100 °C for 10 minutes to facilitate the extraction of genomic DNA. The 16S rRNA gene was amplified using universal bacterial primers 27F (5'-AAGAGTTTGATYMTGGCTCAG-3') and 1492R (5'-TACGGYTACCTTGTTACGACTT-3'), followed by bidirectional Sanger sequencing technology. The resulting sequences were compiled, aligned using BioEdit software, and subjected to comparative analysis by aligning them with sequences in the GenBank database using the Basic Local Alignment Search Tool (BLAST).

## MATERIALS AND METHODS

### 4.2. Most probable number of sulfate-reducing bacteria

The estimation of SRB was determined using the most probable number (MPN) method developed by Biotechnology Solutions (Houston, USA, <https://biotechnologysolutions.com>). This method is based on triplicate decimal dilutions in Postgate medium (DSMZ Medium 63, [www.dsmz.de/](http://www.dsmz.de/)). The MPN of SRB per gram of bentonite was then calculated by comparing the number of positive bottles (presence of black precipitates, **Fig. 3**) with the reference table from Biotechnology Solutions. The DNeasy PowerSoil Pro Kit (Qiagen, <https://www.qiagen.com/us>) was employed to extract total DNA from positive Postgate cultures.

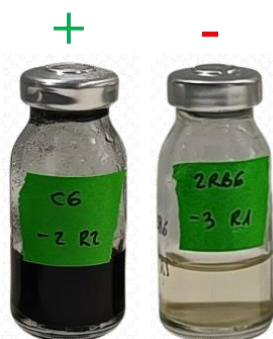


**Figure 3.** Example of a positive (black) and a negative serum bottle of Postgate medium from the MPN experiment after 30 days of anoxic incubation.

## 5. Microscopic and spectroscopic analysis

### High resolution transmission electron microscopy

Scanning transmission electron microscopes coupled with high-angle annular dark-field (STEM/HAADF) imaging (Thermo Fisher Scientific TALOS F200X and FEI TITAN G2) were used to characterize the selenium reduction products (**Fig. 4**). Energy dispersive X-ray spectroscopy (EDX) microanalysis, at an acceleration voltage of 200 kV or 300 kV, depending on the microscope,

was coupled to analyze the elemental composition. The crystallinity of Se nanoparticles was analyzed using selected-area electron diffraction (SAED) and high-resolution transmission electron microscopy (HRTEM) combined with fast fourier transform (FFT).



**Figure 4.** Ultra-high resolution transmission electron microscopes with high-angle annular dark-field (HAADF): FEI TITAN G2 (left) and Thermo Fisher Scientific TALOS F200X (right).

#### High resolution scanning electron microscopy

The surface of Cu disks and plates were analyzed using both variable pressure field emission scanning electron microscopy (VP-FESEM, Zeiss SUPRA40VP) and environmental scanning electron microscopy (ESEM, FEG-ESEM QUEMSCAN 650F) equipped with secondary electrons (SE), SE-inLens, backscattered electrons (BSE), energy selective backscattered (EsB), and STEM detectors (**Fig. 5**). Both microscopes were coupled with EDX microanalysis for analysis of elements with atomic numbers greater than beryllium.



**Figure 5.** Environmental scanning electron microscopy (ESEM, FEG-ESEM QUEMSCAN 650F) (left) and copper disks on the holder of the variable pressure field emission scanning electron microscope (VP-FESEM, Zeiss SUPRA40VP) (right).

### X-ray photoelectron spectroscopy (XPS)

X-ray photoelectron spectroscopy (XPS) is a surface-sensitive quantitative spectroscopic technique that determines the elemental composition, oxidation state, and electronic state of the elements that exist within the material's surface. This spectroscopy technique employs X-ray irradiation of a sample, which enables the measurement of the kinetic energy and number of electrons emitted from the topmost layers of atoms in the sample (**Fig. 6**). These measurements yield information about the chemical bonding environment and elemental composition of the material's surface. In the present Ph.D. thesis, XPS has been utilized to characterize copper surface corrosion products in **Chapter 1** and to determinate uranium species in the case of **Chapter 4**. XPS studies were conducted in collaboration with Prof. Jesus Ojeda from Swansea University, using the Kratos AXIS Supra Photoelectron Spectrometer. The X-ray source was a monochromated Al  $K\alpha$  (1486.6 eV), with a ray emission current set at 20 mA and a high anode voltage of 15 kV. Component speciation was performed for each analysis using both a broad survey scan and a high-

resolution scan. The XPS spectra peaks were analyzed using CasaXPS 2.3.22 software.

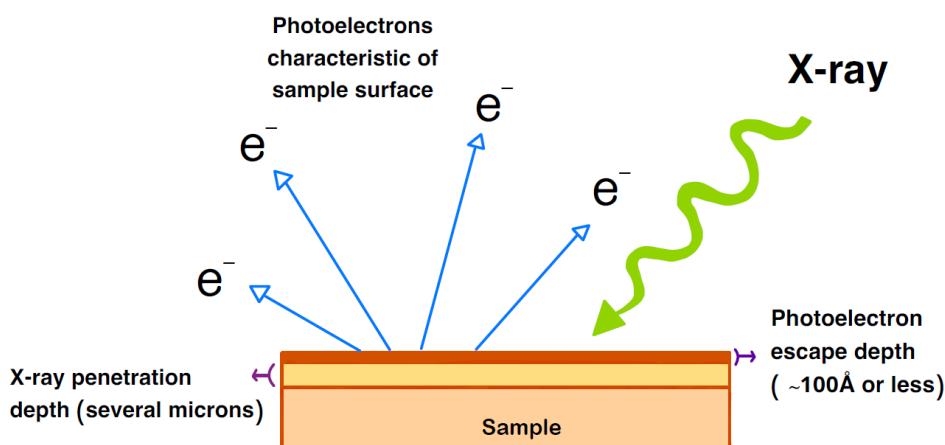


**Figure 6.** Principle of X-ray spectroscopy (XPS) technique. Image modified from <https://www.eag.com/techniques/spectroscopy/x-ray-photoelectron-spectroscopy-xps-esca/>

## 6. Mineralogical and chemical characterization of bentonite

### X-ray diffraction (XRD)

X-ray diffraction (XRD) is an analytical technique used to determine the crystallographic structure and chemical composition of a material. When a material is exposed to X-rays, the atoms within the material scatter the X-ray beams in specific directions. The angles and intensities of the scattered beams are measured, thereby generating a diffraction pattern (**Fig. 7**). This technique has been used to assess the mineralogical stability of bentonite. The bentonite powder samples were analyzed using a Philips X'Pert PRO MPD diffractometer. The analysis employed a Cu-K $\alpha$  anticathode at 45 kV and 40 mA, equipped with a fixed divergence slit (0.1245° size) and a Scientific X'celerator detector. The oriented aggregates (OA) of the bentonite samples, both with and without ethylene glycol treatment, were also analyzed in detail

## MATERIALS AND METHODS

to identify the clay minerals. The diffractograms were analyzed using HighScore software.

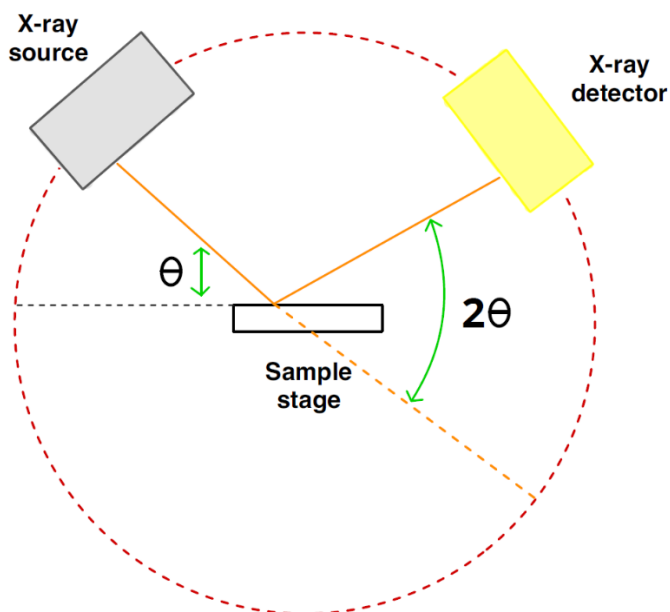


**Figure 7.** Principle of X-ray diffraction (XRD) technique. Image modified from <https://www.tribonet.org/wiki/xrd-x-ray-diffraction/>

### X-ray fluorescence (XRF)

X-ray fluorescence (XRF) is a non-destructive analytical technique used to determine the elemental composition of materials. Exposure of a material to high-energy X-rays induces the excitation of its atoms, resulting in the emission of secondary X-rays, which exhibit fluorescence (**Fig. 8**). These emitted secondary X-rays possess energies characteristic of each element present in the sample. The elemental composition of the different bentonite treatments was studied using XRF analysis with a PANalytical Zetium instrument. This instrument utilizes a rhodium anode ceramic X-ray tube equipped with an ultra-thin, high-transmission beryllium front window.

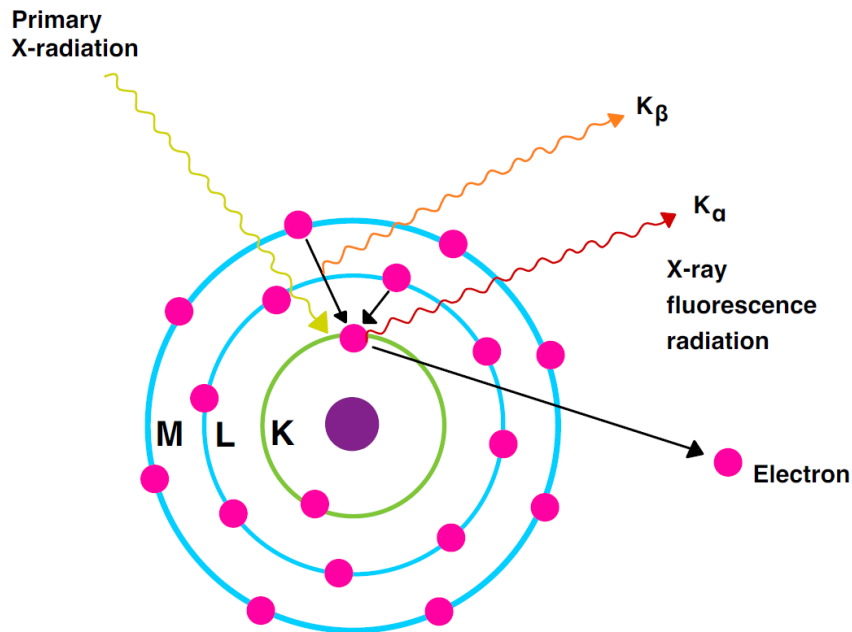


**Figure 8.** Principle of X-ray fluorescence (XRF) technique. Image modified from <https://wpo-altertechnology.com/>

### Inductively coupled plasma-mass spectrometry (ICP-MS)

The trace element composition of the equilibrium water from Spanish bentonite was analyzed using Inductively Coupled Plasma-Mass Spectrometry (ICP-MS) with a NexION 300D spectrometer. The concentration of soluble Se(IV) in the microcosms supernatants of **Chapter 2** was also determined via ICP-MS. All the samples were acidified (4% HNO<sub>3</sub>) before measurements.

### pH measurements

The pH of the bentonite samples was measured in triplicate using a multi-parameter probe, HQd Field Case HACH, which had been calibrated beforehand using commercially available reference solutions (pH 4.00 and 7.00). In **Chapter 1**, pH measurements of compacted bentonite blocks were

## MATERIALS AND METHODS

performed using an ORION 720A pH-meter with a Metrohm 6.0224.100 combined pH micro-electrode.

### 7. Irradiation conditions

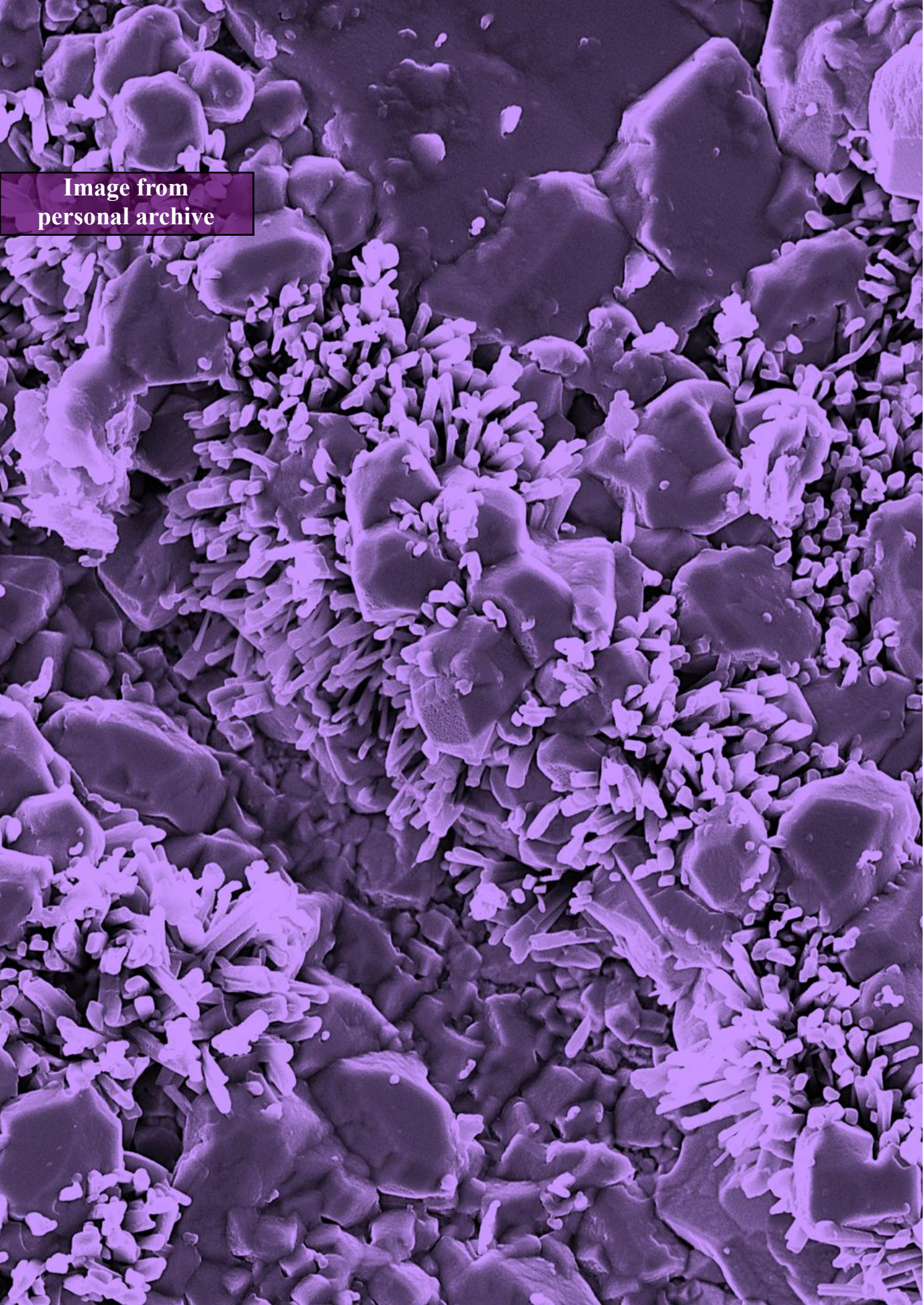
The bentonite blocks in **Chapter 1** were irradiated at the CIEMAT Nayade  $^{60}\text{Co}$  gamma irradiation pool facility (**Fig. 9**). The samples were placed within specific metal container and subsequently submerged in a pool of water with a depth of 4.5 m and a width of 1.2 m. In each instance, the samples were irradiated for 9 days at a dose rate of 66 Gy/h, leading to a total accumulated dose of 14 kGy. Additionally, a total cumulative dose of 28 kGy was also studied. These samples underwent two cumulative dose treatments of 14 kGy each, separated by a 6-month interval.



**Figure 9.** Nayade  $^{60}\text{Co}$  gamma irradiation pool facility at CIEMAT.

## MATERIALS AND METHODS

Image from  
personal archive



A scanning electron microscope (SEM) image showing the surface morphology of bentonite particles. The image displays a complex, porous structure with various sized particles, some appearing as large, rounded aggregates and others as smaller, more crystalline fragments. The overall texture is highly irregular and textured.

## Chapter 1

Assessing the impact of radiation and high compaction on FEBEX bentonite: microbial, mineralogical, and copper corrosion studies

### Authors

**Mar Morales-Hidalgo**<sup>1,\*</sup>, Marcos F. Martinez-Moreno<sup>1</sup>, Cristina Povedano-Priego<sup>1</sup>, Kateřina Černá<sup>2</sup>, Ana Maria Fernandez<sup>3</sup>, Ursula Alonso<sup>3</sup>, Adam D. Mumford<sup>4</sup>, Jesus Ojeda<sup>4</sup>, Fadwa Jroundi<sup>1</sup> and Mohamed L. Merroun<sup>1</sup>

---

<sup>1</sup>*Faculty of Sciences, Department of Microbiology, University of Granada, Granada, Spain*

<sup>2</sup>*Technical University of Liberec, Institute for Nanomaterials, Advanced Technologies and Innovations, Bendlova 1407/7, 461 17 Liberec 1, Czech Republic*

<sup>3</sup>*Departamento de Impacto Ambiental de la Energia, CIEMAT, Avenida Complutense, 22-28040 Madrid, Spain*

<sup>4</sup>*Department of Chemical Engineering, Faculty of Science and Engineering, Swansea University, Swansea, United Kingdom*

## CHAPTER 1

**Abstract**

One of the major challenges facing future Deep Geological Repositories (DGRs) for radioactive waste is ensuring complete safety over very long timescales, up to 100,000 years. This study investigated the combined effect of high compaction density ( $1.6 \text{ g/cm}^3$ ) and gamma radiation (14 kGy or 28 kGy) under pore water saturation conditions, the presence of sulfate-reducing bacteria (SRB), and an anoxic atmosphere on FEBEX bentonite blocks. Small pure-copper disks were included in the core of each bentonite block for corrosion analysis. Culture-dependent microbiological and next-generation sequencing (NGS) analyses showed that compaction at  $1.6 \text{ g/cm}^3$ , anoxic conditions, and low nutrient availability favor spore-forming microorganisms. After 1-year incubation, genera like *Saccharopolyspora* and *Streptomyces* were identified. In addition, gamma radiation negatively impacted the viability of aerobic heterotrophs and SRB. However, an incubation period preceding radiation exposure was found to enhance microbial resistance with respect to this parameter. Copper corrosion studies indicated that the main corrosion products were copper oxides, primarily CuO, present in all samples. Furthermore, gamma radiation delayed biotic corrosion by negatively affecting the microbial community and promoting salt precipitation, including potential copper sulfates. The SRB were implicated in producing biogenic copper sulfides detected only within the bentonite. Mineralogically, neither gamma radiation nor other conditions adversely affected the properties of FEBEX bentonite, which remained stable after one year. This study offers new insights into the combined effects of gamma radiation and other DGR key conditions on bentonite's microbiology, mineralogy, and copper corrosion.

**Keywords:** *Gamma radiation, FEBEX bentonite, Sulfate-reducing bacteria, Copper corrosion, Nuclear waste repository.*

## CHAPTER 1

## 1. Introduction

Ensuring the confinement of radioactive waste over very long periods of time (approximately 100,000 years) is one of the main challenges facing future deep geological repository (DGR) systems (Ewing et al., 2016). While the chemical, physical, or geological properties have been extensively studied, regarding these future multi-systems, the impact of microorganisms on the integrity of different barriers under repository conditions remains relatively underexplored. In recent decades, however, research about the influence of such microorganisms, both indigenous of the DGR barriers and those accidentally introduced during repository construction, on the safety of these systems has progressed (Martinez-Moreno et al., 2024; Povedano-Priego et al., 2023; Ruiz-Fresneda et al., 2023; Shrestha et al., 2021). The barriers that will be part of these future systems will consist of a metallic container (steel, copper, nickel, titanium) surrounded by a backfilling and sealing material (bentonite clay or cement), and the whole located at depths of up to 1000 m within a geologically stable host rock (IAEA, 2018). Microorganisms could affect these barriers through the following processes: (1) interacting with the minerals of the bentonite or host rock, leading to weathering, dissolution, and the formation of secondary minerals (such as smectite biotransformation into illite through Fe(III) bio-reduction) (Meleshyn, 2014); (2) inducing corrosion of metal containers through direct or indirect microbiologically influenced corrosion (MIC) processes (Hall et al., 2021); and (3) immobilizing radionuclides (e.g., Se, U) in case of waste leakage through biomineralization, bioreduction, or biotransformation processes (Ruiz-Fresneda et al, 2024; Morales-Hidalgo et al., 2024b; Povedano-Priego et al, 2023; Lopez-Fernandez et al., 2014).

## CHAPTER 1

In Spain, ENRESA (*Empresa Nacional de Residuos Radiactivos S. A.*) is the current national company responsible for radioactive waste management, including the planning and development of future Spanish DGRs. Although the Spanish repository approach is still in its initial stages, certain decisions have already been made about the materials to be used. Bentonite from El Cortijo de Archidona (known as FEBEX, *Full-scale Engineered Barriers Experiment*) has undergone extensive multidisciplinary studies, including geochemical and mineralogical investigations, to determine its suitability as an artificial barrier (Zheng & Fernández, 2023; García-Siñeriz, 2021; Huertas et al., 2021; Villar et al., 2006). However, research on the microbiology of FEBEX bentonite began only a decade ago. Lopez-Fernández et al. (2014) were the first to describe the microbial communities found in this bentonite. Subsequent research by Povedano-Priego et al. (2021) revealed the high bacterial diversity of FEBEX bentonite after 24 months of anoxic incubation at compaction densities of 1.5 and 1.7 g/cm<sup>3</sup>. Povedano-Priego et al. (2019; 2022) also described the changes exhibited by the autochthonous bentonite communities when exposed to a simulated uranium leak under both oxic and anoxic conditions. Furthermore, recent studies by Martínez-Moreno et al. (2023, 2024) have reported on the combined effect of temperature (30 °C and 60 °C) and compaction at 1.7 g/cm<sup>3</sup> on bentonite's microbial communities, as well as the indirect impact on copper corrosion. The research focused on the effect of these two variables on the survival of sulfate-reducing bacteria (SRB). This group of bacteria is primarily associated with the MIC of copper due to its ability to produce sulfide, which could react with copper in the canister, leading to the formation of copper sulfides (corrosion products). On the other hand, radiation is a primary concern for future repositories, especially its effect during the first few years when high levels are expected to be emitted (Hall, et al. 2021; Morales-Hidalgo et al., 2024a). High-level radioactive waste (HLW)

are the main responsible for these emissions and have extremely long half-life (Chapman, 2006). Therefore, the understanding of the radiation effects on the different repository barriers (e.g., copper corrosion, bentonite mineralogy, microbial survival, etc.) is crucial to guarantee the long-term safety of these complex systems. The literature on radiation and autochthonous microorganisms of bentonites is very scarce. Specifically, only one research, by Haynes et al. (2018), has so far focused on analyzing the impact of this variable on the microorganisms of the FEBEX bentonite. They reported that after 1 kGy radiation dose, only *Desulfosporosinus*, *Bacillus*, and *Clostridium* were detected in the Postgate medium. To the best of our knowledge, the present work is the first multidisciplinary investigation studying the combined effect of radiation and compaction on the microbiology and mineralogy of FEBEX bentonite, as well as on the corrosion of copper canisters. Furthermore, it focused on the SRB group due to its significant impact on copper corrosion, as mentioned above. Therefore, to simulate conditions similar to those of a DGR during the early post-closure years, i.e. bentonite with the highest degree of compaction and radiation doses, FEBEX bentonite was compacted to a density of 1.6 g/cm<sup>3</sup> containing a pure copper disk at its core. Then, these blocks were irradiated at cumulative radiation doses of 14 or 28 kGy and at different incubation times. Additionally, a bacterial consortium mainly composed of SRB was added to some treatments to enhance and accelerate their metabolic activity, thereby enabling a broader-scale analysis of their impact on copper corrosion. Hence, the main objective of this work was to study the combined effect of gamma radiation (14 or 28 kGy) and compaction (1.6 g/cm<sup>3</sup>) on: (1) the diversity and viability of the native microbial communities of FEBEX bentonite, with special emphasis on the SRB group; (2) the corrosion of copper canisters; and (3) the mineralogy and physicochemical stability of the bentonite.

## 2. Materials and methods

### 2.1. FEBEX bentonite

Bentonite from the “Cortijo de Archidona” deposit (Almería), named as FEBEX after the Full-scale Engineered Barriers Experiment project, was selected for the present study (Huertas et al, 2000). The FEBEX bentonite contains over 90% montmorillonite, with accessory minerals including quartz, plagioclase, potassic feldspar, calcite, and tridymite. Illite/smectite interstratifications may be present up to 15%. In this study, 2.5 kg of FEBEX bentonite from the batch referenced as FEBEX 70-IMA-3-4-0 were used, grounded and sieved to a fraction of  $< 0.5$  mm.

### 2.1. Experimental setup

#### 2.1.1. Artificial FEBEX pore water

At first, FEBEX bentonite was saturated at 100% by adding the corresponding volume of artificial FEBEX pore water according to the compaction density of  $1.6 \text{ g/cm}^3$ . The synthetic pore water was prepared following the recipe proposed by Fernandez & Rivas (2005), and with a chemical composition shown in **Table 1**.

**Table 1.** Chemical composition (mg/L) and salt content (M) of synthetic pore water prepared for FEBEX bentonite samples compacted at  $1.6 \text{ g/cm}^3$ . Recipes from Fernandez & Rivas, 2005.

Chemical composition (mg/L)							
Cl	SO <sub>4</sub> <sup>2-</sup>	HCO <sub>3</sub> <sup>2-</sup>	Na	K	Ca	Mg	pH
$3.05 \cdot 10^{-3}$	$4.41 \cdot 10^{-3}$	6.16	$2.63 \cdot 10^{-3}$	4.26	$6.01 \cdot 10^{-2}$	$4.04 \cdot 10^{-2}$	7.55
Salt content (M)							
KCl	CaCl <sub>2</sub> ·2H <sub>2</sub> O	MgCl <sub>2</sub> ·6H <sub>2</sub> O	Na <sub>2</sub> SO <sub>4</sub>	NaCl	NaHCO <sub>3</sub>	pH	
$1.09 \cdot 10^{-3}$	$1.50 \cdot 10^{-2}$	$1.66 \cdot 10^{-2}$	$4.59 \cdot 10^{-2}$	$2.16 \cdot 10^{-2}$	$1.01 \cdot 10^{-3}$	7.55	

The salt content required for the preparation of the pore water at a density of  $1.6 \text{ g/cm}^3$  is also included in **Table 1**. To avoid altering its chemical properties, the pore water was sterilized before its use by filtration through  $0.22 \text{ }\mu\text{m}$  nitrocellulose filters.

### **2.1.2. Bacterial consortium and electron donor**

In order to accelerate the microbial processes, a bacterial consortium composed of five genera, four of which belong to the group of sulfate-reducing bacteria (SRB) and one to the group of iron-reducing bacteria (IRB), was added to some of the blocks. The genera included tend to represent the SRB group previously identified in FEBEX bentonite diversity studies (Morales-Hidalgo et al., 2024b; Martinez-Moreno, et al., 2023; Povedano-Priego et al., 2022). The treatments assigned as “B” included the bacterial consortium. *Desulfosporosinus acidiphilus* DSM 22704, *Desulfotomaculum reducens* DSM 100696, *Desulfuromonas* sp. DSM 101009, *Desulfovibrio desulfuricans* DSM 642 and *Geobacter metallireducens* DSM 7210 were used for the inoculation. All strains were purchased from the Leibniz Institute DSMZ collection (<https://www.dsmz.de/>). The strains were grown under anoxic conditions in their respective culture media following the manufacturer’s conditions. Each strain was added to the bentonite in its corresponding culture medium as detailed below (section 2.1.4). The volumes added from each strain were as follows: 0.5 mL of *D. acidiphilus*, 0.3 mL of *D. reducens*, 0.3 mL of *Desulfuromonas* sp., 0.5 mL of *D. desulfuricans* and 0.2 mL of *G. metallireducens*. To avoid decompensation of the compounds available in the bentonite blocks, the same volumes of culture medium, but filtered through sterile  $0.22 \text{ }\mu\text{m}$  nitrocellulose filters, were added to the non-consortium treatments.

## CHAPTER 1

Additionally, the bentonite was amended with sodium acetate 1.5 mM in a final volume of 5 mL. A 150  $\mu$ L aliquot of a 50 mM stock solution, previously sterilized by 0.22  $\mu$ m nitrocellulose filters, was added to the corresponding grams of bentonite for each block.

### **2.1.3. Copper disks**

Oxygen-free pure copper (Cu) disks (Cu 99.99%) from Goodfellow Cambridge Ltd. Company (UNS number C10100; <https://www.goodfellow.com>) were used as representative of the future metal canisters. The elemental composition was 99.9 – 100% Cu, with small impurities of S (< 0.0015%), Pb (< 0.0005%), Sb (< 0.0004%), P (< 0.0003%), and Zn (< 0.0001%). Each Cu disk was designed with a diameter of  $10 \pm 0.5$  mm and a thickness of  $4 \pm 10\%$  mm. The average weight was 2.8 g/disk. Prior to use, each disk was chemically cleaned to remove impurities and organic traces following the protocol outlined by the Guo, M. (2020). Cu disks were subjected to an initial degreasing process by sonication for 5 minutes in a vial filled with absolute ethanol. Subsequently, they were cleaned with ultrapure MilliQ water and swirled to eliminate any remaining ethanol. Afterwards, the disks were submerged in 10 mM nitric acid and subjected to an additional 5-minute sonication cycle. This sequence was repeated three times. Cu disks were then dried using nitrogen gas and stored in a sealed glass container. All the bentonite blocks contained in their core a pure copper disk to carry out corrosion analysis.

### **2.1.4. Block assembly, treatments, and compaction.**

The assembly and compaction processes of the samples were conducted in the “Unidad de Físicoquímica de Actínidos y Productos de Fisión” (CIEMAT, Madrid, Spain). The samples consisted of bentonite cylindrical blocks (diameter x height: 38 x 25 mm), compacted at a density of 1.6 g/cm<sup>3</sup>, saturated

at 100% with pore water and inoculated with a bacterial consortium or its filtered culture media, amended with sodium acetate (1.5 mM), and containing a pure Cu disk in their core. The amount of bentonite powder needed for each block was measured in a porcelain crucible, along with the cleaned Cu coupon. The volume ( $0.31 \text{ cm}^3$ ) of the Cu disk has been considered (subtracted) in the clay mass calculations to ensure the desired dry density. The average clay mass for each sample at a density of  $1.6 \text{ g/cm}^3$  was 51.28 g. It was also calculated that a final volume of 5 ml was required to achieve 100% saturation. This final volume included 3.2 mL of artificial pore water (**Table 1**), a total of 1.8 mL of the different bacterial consortium strains in their culture media (filtered or not) and 150  $\mu\text{l}$  of sodium acetate (150 mM). Reference pore water and the bacterial consortium were separately prepared and stored in a laminar flow cabinet. A 3.2 mL aliquot of pore water and 150  $\mu\text{L}$  of sodium acetate (150 mM) were added to 51.28 g powdered FEBEX bentonite. At this step, if required, the bacterial consortium (1.8 mL) was inoculated. Non-consortium samples were traced with 1.8 mL of filtered culture media using 0.22  $\mu\text{m}$  nitrocellulose filters.

The moistened clay was gently mixed under sterilized conditions with a spatula until the sample was homogenized. The compaction procedure consisted of pouring 25.64 g of the wet bentonite mixture into an aseptic stainless-steel mold, placing the copper disk in the center, and subsequently adding on the top another 25.64 g of wet bentonite. Finally, the blocks were compacted to the desired density of  $1.6 \text{ g/cm}^3$  using a press. The incubation was performed in an anoxic atmosphere, darkness and 28 °C. To achieve the anoxic conditions, each block was transferred to an individual aseptic polyethylene vessel filled with  $\text{N}_2$ . All vessels were then transferred to an anaerobic jar, for their storage and incubation, until the end of the incubation periods. Throughout the sample's preparation process, all utensils and equipment were continuously disinfected

## CHAPTER 1

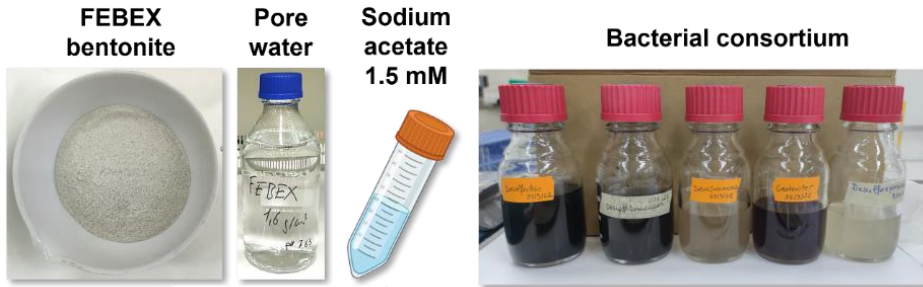
with analytical grade ethanol. All treatments were conducted in triplicate, except for the double-irradiated ones, which were prepared in duplicate.

### **2.1.5. Irradiation conditions**

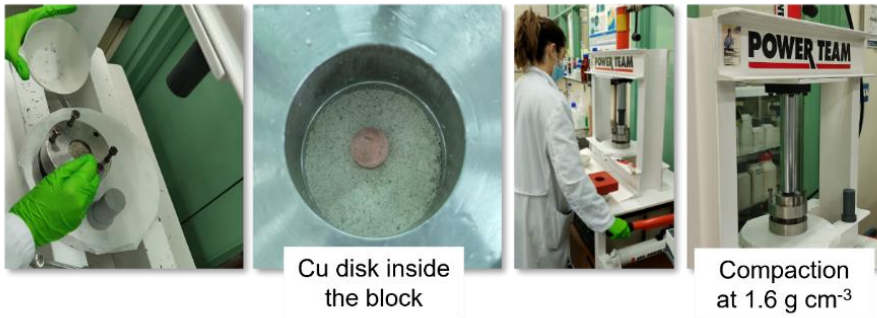
Different irradiation treatments were carried out in this study and classified based on the total cumulative dose received, 14 kGy (R) or 28 kGy (2R), and according to the time in which the radiation was employed: 1) at the beginning of the experiment, prior to incubation as early radiation (e\_R) stage or 2) after 6 months of anoxic incubation as late radiation (l\_R) stage. For their irradiation, the samples were placed inside specific metal containers and then submerged in the CIEMAT Nayade <sup>60</sup>Co gamma irradiation pool facility. In all cases, the samples were irradiated for 9 days at a dose rate of 66 Gy/h, resulting in a total accumulated dose of 14 kGy. Regarding the double-irradiated treatments (2R), two rounds of radiation (14 kGy each) were administered: the first round was carried out before the start of incubation and the second round after 6 months of anoxic incubation. Following the second irradiation, the samples were further incubated for an additional 6 months.

Based on all the aforementioned information, **Table 2** outlines the different treatments tested in this study, while the experimental setup is illustrated in **Figure 1** and **Figure 2**.

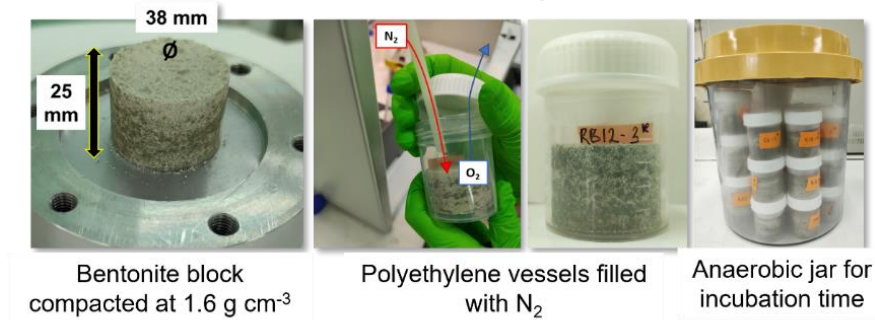
### 1. Compaction setup



100% saturation



### 2. Anoxic atmosphere



### 3. Gamma radiation



**Figure 1.** Experimental setup: compaction procedure, anoxic atmosphere and gamma radiation conditions.

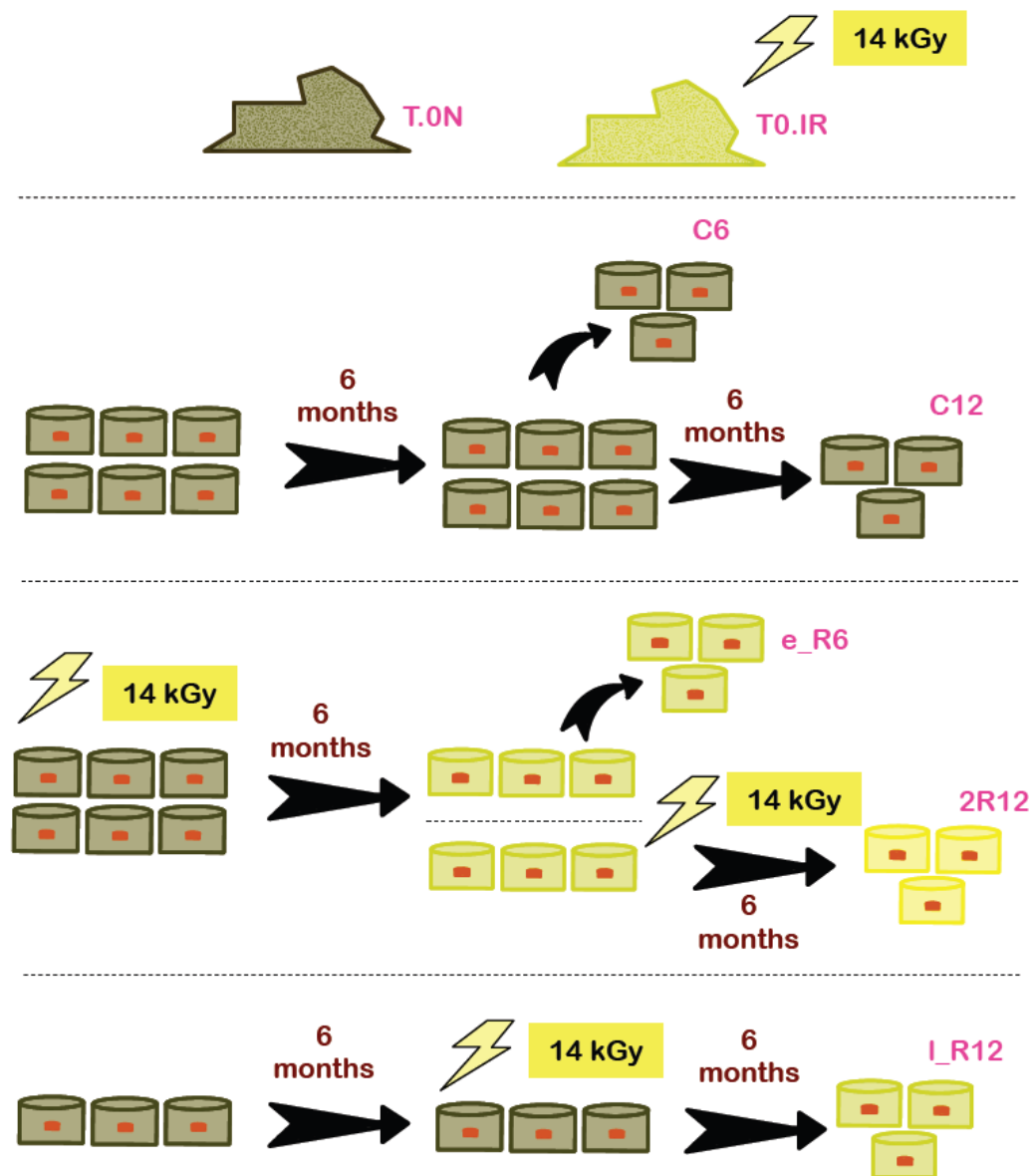


**Figure 2.** Schematic representation of the different FEBEX bentonite treatments. Only treatments without SRB bacterial consortium are shown. The same procedure was performed for samples with SRB consortium (B). Glossary: T.0 N: non-incubated non-irradiated powdered bentonite; T.0 IR: non-incubated irradiated powdered bentonite (14 kGy); C: non-irradiated compacted treatments; e\_R: one-time irradiated treatments prior incubation time as early exposure (14 kGy); I\_R: one-time irradiated treatments in the middle of the incubation time as late exposure (14 kGy); 2R: two-times irradiated treatments (28 kGy); 6: total of six months of anoxic incubation; 12: total of one year of anoxic incubation.

**Table 2.** Summary table of the experimental conditions for each treatment. Glossary: T.0 N: non-incubated non-irradiated powdered bentonite; T.0 IR: non-incubated irradiated powdered bentonite (14 kGy); C: non-irradiated compacted treatments; B: SRB consortium; e\_R: one-time irradiated treatments prior incubation time as early exposure (14 kGy); l\_R: one-time irradiated treatments in the middle of the incubation time as late exposure (14 kGy); 2R: two-times irradiated treatments (28 kGy); 6: six months of anoxic incubation; 12: one year of anoxic incubation.

Label	Bacterial Consortium (B)	Copper Disk	Early radiation (e_R) (dose: 66 Gy/h)	Late radiation (l_R) [at 6 months] (dose: 66 Gy/h)	Double radiation dose (2R)	Total cumulative dose (kGy)	Powdered bentonite weight (g)	Cu disk weight (g)	Block final weight (g)	Pore water volume (mL)	Total volume inoculated culture media / filtered culture media (mL)	Sodium acetate 1.5 mM (μL)	Total volume (mL)	Purpose (Treatment)
T.0 N														Non-incubated natural powdered FEBEX bentonite
T.0 IR			✓			14								Non-incubated irradiated powdered FEBEX bentonite
C6		✓					51.28	2.83	54.11	3.2	1.8	150	5	6-month incubation control
CB6	✓	✓					51.28	2.77	54.05	3.2	1.8	150	5	6-month incubation control + B
C12		✓					51.28	2.77	54.06	3.2	1.8	150	5	12-month incubation control
CB12	✓	✓					51.28	2.79	54.08	3.2	1.8	150	5	12-month incubation control + B
e_R6		✓	✓			14	51.28	2.82	54.10	3.2	1.8	150	5	1 dose R prior incubation + 6-month incubation
e_RB6	✓	✓	✓			14	51.28	2.81	54.09	3.2	1.8	150	5	1 dose R prior incubation + B + 6-month incubation
l_R12		✓		✓		14	51.28	2.81	54.09	3.2	1.8	150	5	1 dose R at 6-month incubation + another 6-month incubation
l_RB12	✓	✓		✓		14	51.28	2.82	54.10	3.2	1.8	150	5	1 dose R at 6-month incubation + B + another 6-month incubation
2R12		✓	✓	✓	✓	28	51.28	2.77	54.05	3.2	1.8	150	5	1 dose R prior incubation + 1 dose at 6-months (total 28 kGy) (total 12-month incubation)
2RB12	✓	✓	✓	✓	✓	28	51.28	2.81	54.09	3.2	1.8	150	5	1 dose R prior incubation + 1 dose at 6-months (total 28 kGy) + B (total 12-month incubation)

### **2.2. Microbiological studies**

The bentonite blocks were stored at 4 °C for culture-dependent viability studies and at -20 °C for the microbial diversity analyses. Before each study, the blocks were powdered under sterile conditions and homogenized to a powder-like consistency using a porcelain mortar sterilized by ethanol (70%).

#### **2.2.1. Molecular microbial analyses**

##### **2.2.1.1. DNA extraction, amplification, and sequencing**

Before DNA extraction, sterile ultrapure MilliQ water was added to the pre-ground bentonite at a ratio of 1:2 (g:mL). The mixture was vigorously stirred for 3-5 minutes and subsequently stored at 4 °C for 3 days. DNA extractions were performed in triplicate for each treatment, except for the double-irradiated treatments (2R12 and 2RB12), which were conducted in duplicate. The extractions followed the phenol-chloroform-based protocol outlined in Povedano-Priego et al. (2021), with some modifications. Briefly, 0.9 g of wet bentonite was transferred to 2 mL screw tubes containing two sizes of sterile glass beads (3 mm diameter and 0.3 mm diameter) for mechanical lysis. A solution including 400 mL of NaH<sub>2</sub>PO<sub>4</sub> (0.12 M, pH 8), 650 mL of lysis buffer, and 28 µL of freshly prepared lysozyme, along with 4 µL of proteinase K, was added to induce chemical lysis. Shaking cycles using FastPrep® FP120 at a speed of 5.5 m s<sup>-1</sup> for 45 s, were extended from 2 to 3 to further induce mechanical disruption of the cells. The thermal incubation times at both 37 °C and 60 °C were also extended to allow for enhanced activity of the previously added enzymes and buffers. Subsequent phenol-chloroform washing steps were performed to separate DNA from cellular debris. After extraction, the concentrations of the total DNA were determined using a Qubit 3.0 Fluorometer (Life Technology, Invitrogen™).

The extracted DNA was amplified by using two sequential PCR reactions for each sample. The V4 region of the bacterial 16S rRNA gene was amplified, employing both standard and barcode fusion primers. Universal primers 530F (5'-GTGCCAGCMGCNGCGG-3') (Dowd et al., 2008) and 802R (5'-TACNVGGGTATCTAATCC - 3') (Claesson et al., 2010) were used. PCR conditions were the same as those described in Cernoušek et al., (2020). The process of the library preparation and the subsequent bioinformatic processing followed the method described in Shrestha et al., (2022, 2021). Briefly, the PCR products were purified using the Agencourt Ampure XP system (Beckman Coulter, Brea, CA, USA) and their concentrations were measured using a Qubit 3.0 Fluorometer. Following this, barcode-tagged amplicons from various samples were combined in equimolar concentrations. Libraries sequencing was performed on the Ion Torrent Personal Genome Machine (PGM) utilizing the Ion PGM Hi-Q Sequencing Kit with the Ion 314 Chip v. 2 (Thermo Fisher Scientific®, USA), in accordance with the manufacturer's instructions. Raw reads were separated into individual samples using Mothur software (Schloss et al., 2009) and then processed using the DADA2 R software package (Callahan et al., 2016). Such process included the removal of low quality, short reads, and chimeric sequences prior to further analysis. Taxonomic classification was performed with the DADA2 package, using the SILVA v. 132 database ([www.arb-silva.de](http://www.arb-silva.de)). The output from DADA2 was converted to a Phyloseq object using R (McMurdie and Holmes, 2013). Rarefaction curves were generated using both the Phyloseq and vegan packages within the R software.

Relative abundances of taxa and alpha diversity indices were calculated using Explicet 2.10.5 (Robertson et al., 2013). A principal coordinate analysis (PCoA) was conducted using Past 4.04 software, based on the Bray-Curtis

algorithm (Hammer, 2021). The PCoA was generated to illustrate differences among the bentonite treatments.

### 2.2.1.2. Quantitative polymerase chain reaction (qPCR)

Quantitative polymerase chain reaction (qPCR) was used to analyze changes in total bacterial content quantification according to incubation time and different treatments. All reactions were conducted on a LightCycler 480 instrument (Roche, Switzerland). The procedure followed for both qPCR conditions and data analysis was as detailed in Shrestha et al. (2022). Briefly, universal primers U16SRT-F and U16SRT-R were used for the V3 region of the 16S rRNA gene (Clifford et al., 2012). For SRB quantification, more specific genes were analyzed including the detection of the adenosine 5'-phosphosulfate reductase gene *apsA* and the dissimilatory sulfate reductase gene *dsrA*. The *apsA* gene was amplified using the primers RH1-aps-F and RH2-aps-R, while the *dsrA* gene was amplified using the primers RH1-dsr-F and RH3-dsr-R (Ben-Dov et al., 2007). The qPCR mix included template DNA, KAPA SYBER FAST qPCR kit (Kapa Biosystems. Inc., MA, USA), forward and reverse primer mixtures (Generi Biotech, Czech Republic; IDT, USA), and ultrapure water (Bioline, UK). A non-template control (NTC) was included for each marker in every qPCR run to confirm the detection limit of the background. Furthermore, each sample was subjected to duplicate runs (difference between duplicates Cq values < 0.5). For the data processing, as described in Shrestha et al. (2022), due to the complexity of the environmental samples, absolute quantification of genes without a standardized calibration curve would yield highly inaccurate results. Consequently, the data was processed by the relative quantitation (RQ) calculation method  $\Delta\Delta Cq$ , which estimates the magnitude of the difference in quantification cycle values (Cq) between samples using the formula  $RQ = \text{effectivity}^{(-\Delta Cq)}$ .

## **2.2.2. Microbial viability analysis**

### **2.2.2.1. Heterotrophic aerobic viability**

The viability of heterotrophic aerobic bacteria was studied at time 0, for both natural and irradiated samples, as well as in the unirradiated and irradiated compacted treatments incubated for either 6 or 12 months. The viable microorganisms were enumerated in triplicate using R2A agar medium and counted as colony-forming units (CFU). For this purpose, 0.5 g of ground bentonite were resuspended in 4.5 mL of phosphate-buffered saline (PBS) and the suspensions were stirred for 24 h at 128 rpm. Subsequently, decimal dilutions were conducted (up to a dilution of  $10^{-5}$ ) and used to inoculate plates containing R2A agar medium in triplicate. These plates were then aerobically incubated for 72 hours at 28 °C.

From the samples of 6 months of incubation, a process of isolation and identification of macroscopically different bacterial colonies was carried out. Individual colonies were suspended in MilliQ water and heated at 100 °C for 10 minutes to extract genomic DNA. The 16S rRNA gene was amplified from the extracted DNA using universal bacterial primers 27F (5'-AAGAGTTTGATYMTGGCTCAG-3') and 1492R (5'-TACGGYTACCTTGTTACGACTT-3'). PCR amplifications were performed with the Recombinant Taq Polymerase kit (M.B.L., Material Blanco de Laboratorio, S.L., Spain). Prior to sequencing, PCR products were purified using the Clean-Easy™ PCR Purification Kit (Canvax Biotech, Spain) and subsequently sequenced using bidirectional Sanger technology. Sequences were compiled, aligned using BioEdit, and subjected to comparative analysis by matching them with sequences in the NCBI GenBank database using the Basic Local Alignment Search Tool (BLAST).

### **2.2.2.2. Most probable number of sulfate-reducing bacteria**

The estimation of sulfate-reducing bacteria present in each treatment was conducted based on the Most Probable Number (MPN) method of Biotechnology Solutions (Houston, USA, <https://biotechnologysolutions.com>). Bentonite from each treatment (mixed from 3 block biological replicates) were collected and ground in a N<sub>2</sub> glove box to maintain anoxic conditions. Specifically, 0.5 g of treated bentonite was mixed with 4.5 mL of N<sub>2</sub>-degassed and sterile PBS. To disaggregate the clay and disperse the cells, the serum bottles were shaken at 180 rpm for 24 hours. Then, 0.5 mL of the suspension was transferred to 10 mL serum bottles previously filled with 4.5 mL of anoxic N<sub>2</sub>-degassed Postgate's medium (DSMZ Medium 63, [www.dsmz.de/](http://www.dsmz.de/)). Decimal dilutions were elaborated in triplicate from 10<sup>-1</sup> to 10<sup>-5</sup>. The whole process was conducted in a glove box to maintain the anoxic atmosphere. The serum bottles were sealed and then incubated static in darkness for 30 days at 28 °C. After the incubation time, the presence of black precipitates indicated the proliferation of bacteria involved in sulfate reduction. The MPN of SRB was estimated by comparing the number of positive bottles with the reference table provided by Biotechnology Solutions (MPN Method, <https://biotechnologysolutions.com>). DNeasy PowerSoil Pro Kit (Qiagen, <https://www.qiagen.com/us>) was used to extract total DNA from some positive Postgate cultures, in order to study the diversity of SRB enriched.

### **2.3. Copper disks corrosion studies**

The Cu disks surfaces and corrosion products of the metal were analyzed using a combination of microscopic and spectroscopic techniques, including Variable Pressure Field Emission Scanning Electron Microscopy (VP-FESEM) and X-ray Photoelectron Spectroscopy (XPS). The preparation of Cu disks for VP-FESEM was carried out as detailed in Martinez-Moreno et al. (2023). Briefly,

each disk was fixed with a 2.5% glutaraldehyde solution prepared with 0.1 M cacodylate buffer (pH = 7.4) for 24 h at 4 °C. Subsequently, the Cu disks were washed in the same buffer, post-fixed in 1% osmium tetroxide, washed again in distilled water, and dehydrated in increasing concentration gradient of ethanol. Lastly, Cu disks were dried using the Critical Point Drying (CPD) method (Anderson, 1951) with carbon dioxide in a Leica EM CPD300 and coated with carbon by evaporation in an EMITECH K975X Carbon Evaporator.

On the other hand, non-fixed Cu disks were analyzed by XPS following Martinez-Moreno et al. (2023) procedure. Surface chemistry XPS analyses were conducted using a Kratos AXIS Supra Photoelectron Spectrometer. A monochromated Al K $\alpha$  source (1486.6 eV) was used, with X-ray emission current set at 20 mA and anode high tension (acceleration voltage) at 15 kV. The take-off angle remained constant at 90° in relation to the sample plane. Data were collected from three randomly chosen points, with each acquisition area being approximately a 110  $\mu\text{m}$  x 110  $\mu\text{m}$  rectangle (FOV2 lens). Each analysis included both a broad survey scan (with a step energy of 160 eV and a step size of 1.0 eV) and a high-resolution scan (with a step energy of 20 eV and a step size of 0.1 eV) for component speciation. The integral Kratos charge neutralizer served as an electron source to mitigate any potential for differential charging. The binding energy scale was calibrated using the Au 4f<sub>5/2</sub> (83.9 eV), Cu 2p<sub>3/2</sub> (932.7 eV), and Ag 3d<sub>5/2</sub> (368.27 eV) lines obtained from cleaned gold, copper, and silver standards provided by the National Physical Laboratory (NPL), UK. CasaXPS 2.3.22 software (Fairley, 2019) was used to analyze the XPS spectra peaks. To counteract any surface charge effects, all binding energies were referenced to the C 1s adventitious carbon peak at 285 eV.

### **2.4. Characterization of mineralogical changes in FEBEX bentonite blocks**

#### **2.4.1. X-ray diffraction and pH measurements**

X-ray diffraction (XRD) patterns were obtained from random powders and oriented aggregates in order to identify the mineralogical species in the samples. The bulk sample powders were obtained by grinding the samples in a RETSCH RM 100 mortar grinder with a pestle of agate to a size of less than 63  $\mu\text{m}$  after drying them at ambient temperature. The powders were analysed with a Philips X'Pert –PRO MPD diffractometer, using an anticathode Cu-K $\alpha$  at 45 kV and 40 mA, equipped with a fixed divergence slit (0.1245° size), Scientific X'celerator detector. The samples were measured from 2° to 70° 2 $\theta$  with a step size 0.017° 2 $\theta$ , and a scan rate of 50 s per step for the powder samples. For mineral identification, the power diffraction file from the International Center for Diffraction Data (ICDD) was used as XRD database, and the HighScore Plus version 5.1 was used as a software for the semiquantification.

The modified Jackson (2005) treatment was used to separate the clay minerals from the rock matrix (Moore and Reynolds, 1989). The fine fraction of less than 2  $\mu\text{m}$  was obtained by suspension and sedimentation in deionised water. In case of necessity and depending on the sample, the clay suspension was successively treated with a 0.5 M sodium acetate (NaOAc) buffer at pH 5 in order to remove carbonates; with a H<sub>2</sub>O<sub>2</sub> (30%)/NaOAc mixture (pH 5) to eliminate organic matter; and with a citrate-bicarbonate-dithionite (CBD) solution to remove Fe and Mn oxy/hydroxides. Each of the preceding treatment was followed by careful washing with deionised water and a mixture solution of ethanol/water at 1:1 ratio. The final clay suspension was ultrasonic dispersed using 1 g in 5 mL of deionized water. Oriented aggregates were prepared by

suction of the dispersion through 3 mm thick ceramic tiles by applying vacuum. These clay films (air dried, ethylene glycol solvated and 550 °C heated) were X-rayed from 2° to 35° 2 $\theta$  using a Bruker D8 Advance diffractometer with an anticathode Cu-K $\alpha$  at 40 kV and 30 mA, equipped with a fixed divergence slit (0.15° size). The samples were analysed with a step size of 0.02° 2 $\theta$ , and a scan rate of 2 s per step.

In addition, the pH was measured by means of an ORION 720A pH-meter equipped with a Metrohm 6.0224.100 combined pH micro-electrode. Merck pH buffer solutions of pH 4.00 and 7.00 were used for pH-meter calibration.

### **3. Results and discussion**

This study focuses on two main factors: bentonite compaction and gamma radiation. FEBEX bentonite was compacted to a dry density of 1.6 g/cm<sup>3</sup> after being saturated to 100% with pore water. The diameter and height of all blocks were measured after 6 months and 1 year of incubation to ensure that the compaction density was maintained. All blocks retained their initial proportions of 38 x 25 mm, thus maintaining a density of 1.6 g/cm<sup>3</sup> throughout the study period.

#### **3.1. Estimation of the viability and survival of bacteria**

Several factors can affect the viability and survival of bacterial cells. According to previous studies, the limits of dry density for microbial activity or survival are reported to vary depending on the type of bentonite. Although there is no established threshold limit for the survival of microorganisms in bentonite, a significant decrease in the survival and diversity of bentonite microbial communities is usually observed above a density of 1.5 g/cm<sup>3</sup> (Gregory et al., 2024). As shown in **Table 3**, after six months of incubation, non-irradiated compacted bentonite blocks (C6 and CB6) exhibited a reduction

## CHAPTER 1

in the viability of aerobic heterotrophs, as evidenced by a decrease in the colony forming units (CFU), when compared to natural bentonite powder (T.0 N). However, the CFU data for the same treatments incubated for a full year (C12 and CB12) were higher. Although high compaction density is expected to inhibit the activity of indigenous bentonite communities, there are microorganisms adapted to thrive in high-pressure environments (Engel et al., 2023). Most of these microorganisms tend to form spores, enabling them to withstand such environmental conditions in a dormant state (Burzan et al., 2022; Pedersen et al., 2000).

**Table 3.** Colony forming units (CFU) per gram of bentonite in the different treatments at 0, 6 months and 1 year of incubation. -: no growth was detected. T.0 N: non-incubated non-irradiated powdered bentonite; T.0 IR: non-incubated irradiated powdered bentonite (14 kGy); C: non-irradiated compacted treatments; B: SRB consortium; e\_R: one-time irradiated treatments prior incubation time as early exposure (14 kGy); l\_R: one-time irradiated treatments in the middle of the incubation time as late exposure (14 kGy); 2R: two-times irradiated treatments (28 kGy); 6: six months of anoxic incubation; 12: one year of anoxic incubation.

Sample	CFU g <sup>-1</sup> bentonite
T.0 N	$(1.05 \pm 0.13) \times 10^6$
T.0 IR	-
C6	$(6.30 \pm 0.49) \times 10^4$
CB6	$(6.50 \pm 0.21) \times 10^4$
e_R6	-
e_RB6	$(5.50 \pm 0.71) \times 10^2$
C12	$(8.40 \pm 1.42) \times 10^6$
CB12	$(9.20 \pm 2.70) \times 10^6$
l_R12	$(4.90 \pm 0.45) \times 10^4$
l_RB12	$(7.20 \pm 6.81) \times 10^2$
2R12	-
2RB12	-

In order to identify the main viable colonies, the strains grown on the CFU count plates of the 6-month incubation treatments were analyzed (**Table 4**). A total of 20 strains were isolated, most of them belonging to the C6 treatment. Only 3 out of the 20 strains were from the CB6 treatment, and one was from e\_RB6. All isolates belonged to the phylum Bacillota, except one isolate from the phylum Actinomycetota. In addition to *Arthrobacter*, the isolates were phylogenetically close to the *Bacillus* genus. These included the genera *Paenibacillus*, *Peribacillus*, *Neobacillus*, *Lysinibacillus*, and *Bacillus* itself. Most of the genera in the family Bacillaceae are known for their ability to survive in extreme environments such as drought or nutrient deficiency. Mandic-Mulec et al., (2016) reported that the most distinguishing characteristic of many Bacillaceae family members is their capacity to produce endospores.

On the other hand, the impact of gamma radiation could be estimated from the CFU data, though it cannot be distinguished from other variables such as bentonite compaction, low nutrient concentration, and anoxic conditions. However, comparing irradiated and non-irradiated treatments showed that the observed differences were mainly due to gamma radiation. Time 0 (non-incubated powdered bentonite) results showed that 14 kGy of gamma irradiation was enough to eradicate all the viable bacterial cells. There was also a lack of growth in the early irradiated treatments after 6 months of anoxic incubation (14 kGy at the beginning of the incubation as early radiation). However, a few colonies were found in the irradiated treatment with the SRB consortium (e\_RB6) in the plates inoculated directly without any dilution. All these colonies were isolated and identified as *Lysinibacillus fusiformis* (**Table 4**). In relation to the 1-year samples, there was a lack of growth in the two times irradiated (total cumulative dose 28 kGy) treatments (2R12, 2RB12). Growth was however detected in the one-time irradiated treatment in the middle of the

## CHAPTER 1

incubation time as late radiation (1\_R12 and 1\_RB12). The incubation period before and after irradiation could have allowed the bacterial community to recover better from the radiation dose. Therefore, these results suggested that gamma irradiation would affect cell viability differently, depending on the stage in which the bacterial community is found since the same dose, 14 kGy, resulted in growth or not according to the moment at which the samples were irradiated. These findings aligned with Pitonzo et al., (1999) who observed that irradiated bacteria (up to a total dose of 9.34 kGy) could potentially be reactivated to a completely cultivable state over time as environmental conditions become more favorable. Furthermore, the ability of these bacteria to form spores is an important feature of radiation resistance, as spores are significantly more tolerant to radiation than vegetative cells (Van Gerwen et al., 1999; Jung et al., 2017).

The establishment of radiation thresholds tolerable by microorganisms is a challenging issue due to the variety of strategies used to assess radiation resistance and the limited availability of experimental data derived from relevant environmental conditions or long-term studies. For example, the effects on microorganisms of short, high-dose radiation exposure differ significantly from that of prolonged, lower-dose exposure. Therefore, the limited information on survival and activity under long-term irradiation at lower dose rates is the major challenge for understanding the microbiology in repository environments (Gregory et al., 2024).

**Table 4.** Affiliation of the 16S rRNA of 6-month treatment microbial isolates. BLAST revealed the closest phylogenetic relative strains, along with the similarity percentage and accession number. C: non-irradiated compacted treatments; B: SRB consortium; e\_R: one-time irradiated treatments prior incubation time as early exposure (14 kGy); 6: six months of anoxic incubation.

Phylum	Isolate	Closest phylogenetic relative	Similarity (%), Accession no.
Bacillota	C6_6	<i>Paenibacillus elgii</i> strain PK2-14.2	100, MN428210.1
Bacillota	C6_13	<i>Bacillus thuringiensis</i> strain NB49	99.85, MT534571.1
Bacillota	C6_7	<i>Peribacillus frigiditolerans</i> strain WS2-1	99.88, MT605504.1
Bacillota	C6_3	<i>Peribacillus frigiditolerans</i> strain GB_5_SAUDI	99.93, PP346331.1
Bacillota	C6_10	<i>Bacillus</i> sp. 2011SOCCUA3	100, KF582893.1
Bacillota	C6_5	<i>Peribacillus frigiditolerans</i> strain BB026	100, PP087454.1
Bacillota	C6_2 / CB6_18	<i>Bacillus</i> sp. (in: Bacteria) strain HBUM207125	100, MT598008.1
Bacillota	C6_26	<i>Bacillus</i> sp. (in: Bacteria) strain FJAT-21373	99.77, KY949517.1
Bacillota	C6_16	<i>Peribacillus frigiditolerans</i> strain S4T2	99.53, MZ544535.1
Actinomycetota	CB6_17	<i>Arthrobacter</i> sp. 210_15	99.79, GQ199717.1
Bacillota	CB6_18	<i>Neobacillus niacini</i> strain V5754	99.93, PP257246.1
Bacillota	e_RB6_11	<i>Lysinibacillus fusiformis</i> strain WS1-3	100, MT605500.1

### **3.1.1. Quantification of the SRB viability by most probable number method**

The presence of viable SRB cells was estimated after different treatments and at different incubation times using quantification by the most probable number (MPN) per gram of bentonite in Postgate medium (**Table 5**). Positive results for the presence of this bacterial group were found in unincubated natural bentonite (T.0 N) as well as in the non-spiked and compacted treatments (C6 and C12), since black precipitates were detected. No color changes were observed throughout the study in the negative control, corresponding to Postgate medium without inoculated bentonite.

These results demonstrated that this bacterial group is naturally present in the FEBEX bentonite, and that it has survived the compaction conditions under extended periods of time (1 year). However, the values after 1 year of incubation C12 ( $2.25 \times 10^1$  MPN g<sup>-1</sup> bentonite) were lower than those at T.0 N and C6 ( $1.5 \times 10^4$  and  $> 1.4 \times 10^5$  MPN g<sup>-1</sup> bentonite, respectively). The decrease in viability of the cells cannot be attributed to a single factor, as mentioned above, since there are several variables such as nutrient concentration, water availability and compaction that could have affected their persistence. At time 0, the natural bentonite had no nutrients added or water availability, but non-compacting conditions were tested. At 6 months, hypothetically the presence of nutrients and water was expected to be higher than at 1 year. This is because, at the beginning of the incubation, 1.5 mM sodium acetate was added, and the blocks were fully saturated with pore water. Therefore, it was expected that the consumption of these nutrients and water would have occurred at a greater rate by 1 year. Hence, by comparing the viability of SRB under conditions of water and nutrient deficiency but with compaction (C12), it was estimated a severe effect on their survival, in contrast to the natural time 0 (T.0 N). Previous studies have also discussed the presence

and viability of this bacterial group in the same bentonite type (e.g.: Martinez-Moreno et al. 2023, 2024). Specifically, Martinez-Moreno et al. (2023) reported on the viability of SRB cells after one year of incubation in anoxic conditions under compaction at a density of 1.7 g/cm<sup>3</sup>. They observed similar behavior, where the viability of SRB, measured by MPN g<sup>-1</sup> bentonite as well, decreased under compaction conditions after one year of incubation compared to the initial bentonite. Moreover, they reported a slight increase in SRB viability in bentonite blocks that were amended with a combination of the electron donors.

**Table 5.** Most probable number (MPN) of SRB per gram of bentonite (MPN g<sup>-1</sup>). All the values were calculated considering the initial suspension for cell's dispersion (1 g of bentonite in 9 mL of PBS). T.0 N: non-incubated non-irradiated powdered bentonite; T.0 IR: non-incubated irradiated powdered bentonite (14 kGy); C: non-irradiated compacted treatments; B: SRB consortium; e\_R: one-time irradiated treatments prior incubation time as early exposure (14 kGy); l\_R: one-time irradiated treatments in the middle of the incubation time as late exposure (14 kGy); 2R: two-times irradiated treatments (28 kGy); 6: six months of anoxic incubation; 12: one year of anoxic incubation.

Sample	XYZ pattern*	MPN value**	3PB dilution***	MPN g <sup>-1</sup> bentonite
T.0 N	321	15	10 <sup>-1</sup>	1.50 x 10 <sup>4</sup>
T.0 IR	000	< 3	-	< 3
C6	333	+140	10 <sup>-2</sup>	> 1.40 x 10 <sup>5</sup>
CB6	333	+140	10 <sup>-2</sup>	> 1.40 x 10 <sup>5</sup>
e_R6	000	< 3	-	< 3
e_RB6	320	9.5	10 <sup>0</sup>	9.50 x 10 <sup>1</sup>
C12	300	2.5	10 <sup>0</sup>	2.25 x 10 <sup>1</sup>
CB12	320	9.5	10 <sup>0</sup>	8.55 x 10 <sup>1</sup>
l_R12	000	< 3	-	< 0.3
l_RB12	000	< 3	-	< 0.3
2R12	000	< 3	-	< 0.3
2RB12	100	0.4	10 <sup>0</sup>	0.4

## CHAPTER 1

\*XYZ pattern: number of positive bottles after 3PB dilution

\*\*MPN value: MPN data from the reference table

\*\*\*3PB dilution: dilution with 3 positive bottles prior to XYZ pattern

Interestingly, no evidence of SRB growth was detected in the irradiated treatments at time 0 (T\_0 IR, 14 kGy), 6 months (e\_R6, early 14 kGy), nor 1 year (l\_R12, l\_RB12, late 14 kGy; or 2R12, 2RB12, 28 kGy). Only a few bottles tested positive in the early irradiated SRB-spiked treatment at 6 months (e\_RB6). The results of 16S rRNA gene sequencing of the e\_RB6 positive bottles revealed the presence of *Desulfosporosinus* and *Bacillus*. Therefore, both strains would have survived such an irradiation dose and remained viable during the whole time of incubation. Sequencing results of such exception agreed with Haynes et al. (2018) who, using FEBEX bentonite subjected to 1 kGy gamma dose, detected *Desulfosporosinus* and *Bacillus* in the MPN enrichments. Nevertheless, since all other irradiated experiments remained negative regarding the viability of this bacterial group, the main finding was that gamma irradiation at either a total cumulative dose of 14 kGy or 28 kGy appeared to have an adverse impact on the survival of such bacterial group.

### **3.2. Response of microbial diversity to incubation conditions**

Following a one-year anoxic incubation at room temperature, DNA was extracted in triplicate from the different bentonite blocks, except for 2R12 and 2RB12, which were performed in duplicate. All samples achieved enough sequencing depth as shown by the rarefaction curves (**Supplementary Fig. S1**). Only one replicate of the C12 treatment failed, although it was repeated until sufficient sequencing depth was reached. As a result of amplification of the V3-V4 variable regions of the 16S rRNA gene, a total of 740 phylotypes were annotated. The sequencing depth was excellent for all replicates, as indicated by the Good's coverage value, which was > 99.99% in all cases.

Community alpha diversity analyses were carried out using the Sobs, ShannonH, SimpsonD and ShannonE indices using a bootstrap of 100 (data shown in **Table 6**). The diversity indices (Shannon H and Simpson D) and Shannon's evenness showed lower values in the non-irradiated treatments (C12, CB12), as well as in the late-irradiated treatments (1\_R12 and 1\_RB12), indicating taxa dominance. However, the same indices were higher in the treatments irradiated twice (2R12, 2RB12), indicating a higher evenness.

**Table 6.** Richness (Sobs), diversity (ShannonH and SimpsonD), and evenness (ShannonE) indices values of the bacterial communities of the different treatments after 1 year of anoxic incubation. C: non-irradiated compacted treatments; B: SRB consortium; 1\_R: one-time irradiated treatments in the middle of the incubation time as late exposure (14 kGy); 2R: two-times irradiated treatments (28 kGy); 12: one year of anoxic incubation.

Sample	Sobs	ShannonH	ShannonE	SimpsonD
C12	122.07	2.40	0.35	0.55
CB12	89.60	2.74	0.42	0.63
1_R12	74.47	1.91	0.30	0.49
1_RB12	82.21	1.91	0.30	0.44
2R12	100.83	4.09	0.61	0.87
2RB12	83.00	4.81	0.75	0.94

The annotated phylotypes were classified and identified into 21 phyla, of which 20 belonged to the Bacteria domain and only one, Halobacterota, belonged to the Archaea domain (**Supplementary Table S1**). The phyla Actinomycetota, Pseudomonadota and Bacillota were the most abundant representing 65.31%, 23.87% and 7.18%, respectively. At the genus level, the phylotypes were further grouped into 295 OTUs (**Supplementary Table S2**).

A principal coordinate analysis (PCoA) analysis using the Bray-Curtis distance revealed the differences between the samples. The dissimilarity between

## CHAPTER 1

double-irradiated samples (2R12, 2RB12) and non-irradiated (C12, CB12) together with late-irradiated samples (1\_R12, 1\_RB12) was demonstrated. Two main clusters differed as shown in **Figure 3**.

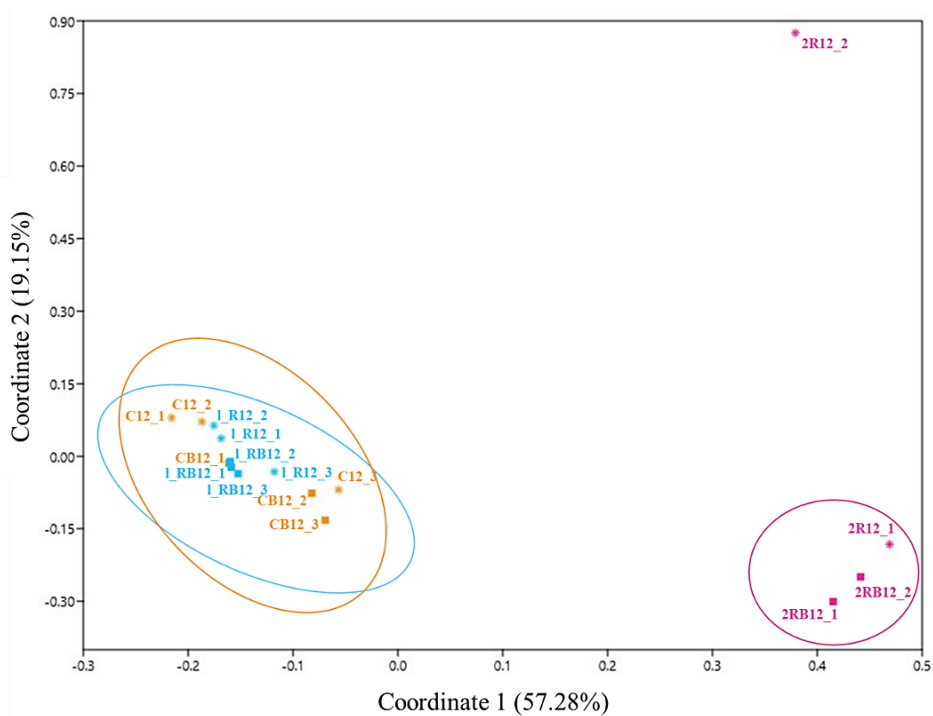


**Figure 3.** Principal coordinate analysis (PCoA) comparing the microbial community structure of the different 1.6 g/cm<sup>3</sup> compacted blocks after 1 year of anoxic incubation. The distance is based on the Bray-Curtis algorithm. Square (■): SRB-spiked treatments; Star (\*): non-spiked treatments; orange color: non-irradiated; blue color: late-irradiated (14 kGy); pink color: double-irradiated (28 kGy). Samples studied in triplicates except double-irradiated treatments (2R12, 2RB12). C: non-irradiated compacted treatments; B: SRB consortium; 1\_R: one-time irradiated treatments in the middle of the incubation time as late exposure (14 kGy); 2R: two-times irradiated treatments (28 kGy); 12: one year of anoxic incubation.

Only one replicate of the 2R12 treatment differed from the rest. Therefore, no dissimilarities were found between the non-irradiated samples (C12, CB12) and those irradiated once in the middle of the incubation period (1\_R12, 1\_RB12), either with or without the SRB consortium inoculated. Thus, the PCoA results suggested that late irradiation, along with an incubation period

both before and after irradiation exposure, minimized the differences in bacterial communities compared to unirradiated samples. These results were corroborated by studies of the microbial community profiles in each compacted bentonite treatment represented at phylum level in **Supplementary Figure S2** and at genus level in **Figure 4**.

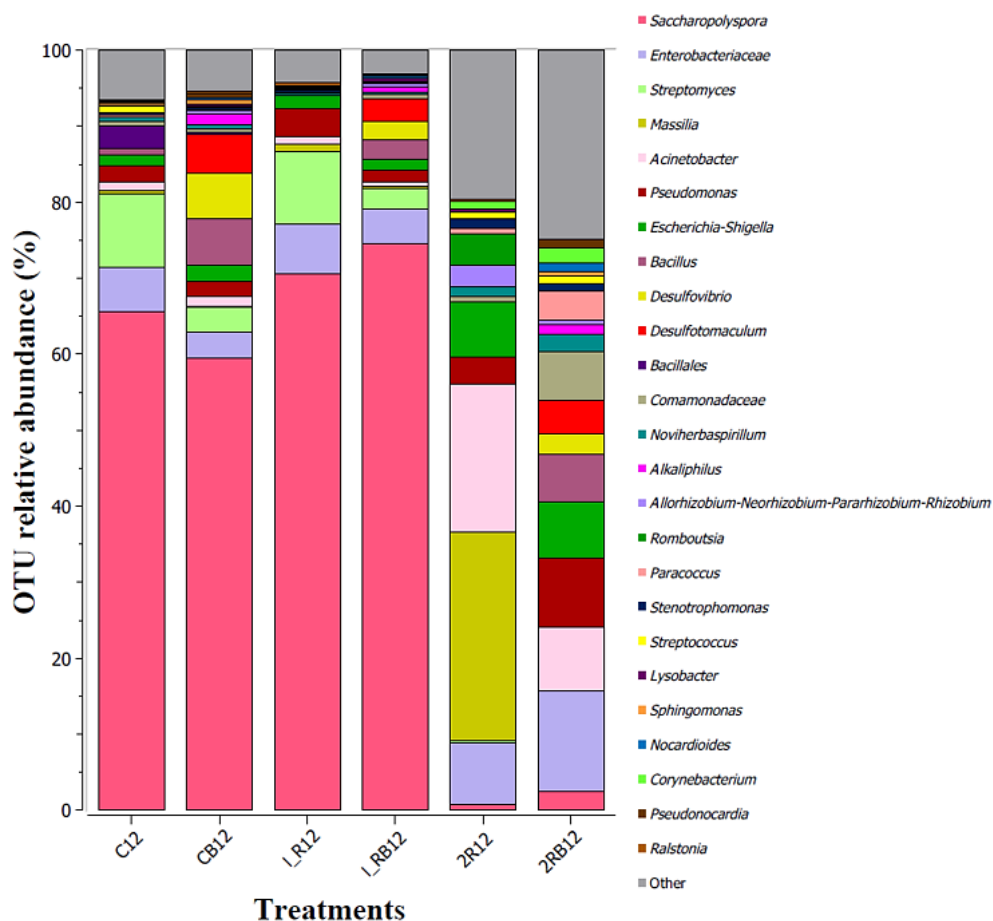


**Figure 4.** OTU relative abundances at genus level of the microbial communities in compacted bentonite after 1 year of anoxic incubation. Cut off: 0.20% of relative abundance. Stacked bars represent the mean values of biological triplicates (except 2R12 and 2RB12 in duplicate). C: non-irradiated compacted treatments; B: SRB consortium; l\_R: one-time irradiated treatments in the middle of the incubation time as late exposure (14 kGy); 2R: two-times irradiated treatments (28 kGy); 12: one year of anoxic incubation.

## CHAPTER 1

Overall, the most representative genus across all samples was *Saccharopolyspora* (57.68%), followed by unclassified Enterobacteriaceae (5.75%), *Streptomyces* (5.49%), *Massilia* (3.16%), *Acinetobacter* (3.12%), and *Pseudomonas* (2.80%). The communities of the non-irradiated (C12, CB12) and mid-incubation irradiated treatments (1\_R12, 1\_RB12) were dominated by *Saccharopolyspora*, with relative abundances greater than 50% in all cases (**Supplementary Table S2**). However, in the treatments irradiated twice, receiving a total cumulative dose of 28 kGy, its relative abundance decreased significantly annotating values of 0.84% in 2R12 and 2.49% in 2RB12. This actinobacterium has been described in the literature as resistant to challenging survival conditions, such as desiccation (Saygin et al. (2021); Shen et al. (2019)). Previous studies have identified several species of this bacterial genus isolated from deserts and various extremely dry soils. For instance, Saygin et al. (2021) identified four new *Saccharopolyspora* species from the Karakum desert. The characteristics of each strain were described, emphasizing the versatility of this genus and its high adaptability to harsh environmental conditions. On the other hand, Shen et al. (2019) reported that exposure to gamma radiation doses of 10 kGy reduced the population of *Saccharopolyspora erythrea* species by 99%. Therefore, high levels of total radiation doses appear to have a negative impact on this genus. However, its ability to form spores in adverse situations may have allowed it to withstand exposure to 14 kGy after a previous 6-month incubation period. Sporulation is a well-known mechanism of some microorganisms for radiation resistance and desiccation (Laskowska & Kuczyńska-Wiśnik, 2020). The previous incubation period, along with a subsequent other 6 months, would have allowed the bacterial community to adapt to the compaction conditions. This adaptation would have increased the relative abundance of the bacterial community compared to genera that were more affected. Additionally, sporulating cells

may have been able to withstand radiation exposure due to their approximately five times higher radiation tolerance than vegetative cells (van Gerwen et al., 1999). The post-radiation incubation period would have allowed the cells to recover from such exposure to gamma radiation. However, applying a double dose of 14 kGy, first prior incubation and then again after 6 months of incubation, would likely have been lethal to most of the bacterial community. The initial exposure would have prevented any chance of adaptation to the environment, resulting in a substantially magnified radiation effect. The subsequent exposure would have removed the strains that managed to survive the initial radiation dose.

*Streptomyces* was another of the most abundant genera in the unirradiated and late-irradiated samples, although at a lower relative abundance than *Saccharopolyspora*. This genus is gram-positive, filamentous, spore-forming actinobacteria that have been studied extensively in bibliography. Its characteristics are very similar to those mentioned above for *Saccharopolyspora*. Strains of *Streptomyces* are able to withstand harsh conditions such as desiccation and gamma radiation. It has been isolated and identified in a variety of soils, including deserts such as Sahara (Sivakala et al., 2021; Zerouki et al., 2021). In addition, studies such as Mao et al. (2007) described a new species of this genus, *S. radiopugnans*, which can resist up to 15 kGy of gamma radiation. Moussa et al. (2005) also described *S. albaduncus* and *S. erythogresius* species as resistant to gamma radiation doses up to 5 kGy.

In general, the profile of the communities present in the different treatments includes genera characteristic of soils (e.g. bentonite), most of them distinguishable for their presence in adverse environments with limited water and nutrients and even exposure to radiation. Among them, therefore, the genus *Massilia* (Ren et al., 2018), an unclassified member of the family

## CHAPTER 1

Enterobacteriaceae (Park et al., 2024), *Acinetobacter* (Gallego, 2016), *Pseudomonas* (Campos et al., 2010), *Bacillus* (Dose and Gill, 1995), among others, stood out. On the other hand, the presence of sulfate-reducing bacteria was very low, even below the detection limit of sequencing in the unirradiated non-consortium spiked bentonite treatment (C12). However, the SRB viability data mentioned above indicated that they were present, and they were able to grow and proliferate under favorable conditions. In all the consortium treatments (CB12, 1\_RB12 and 2RB12), two of the five strains initially added, *Desulfovibrio* and *Desulfotomaculum*, were detected (**Supplementary Table S2**).

The presence of these types of microorganisms with the ability to remain in dormant states and withstand adverse conditions would be mainly those that would be more likely to remain in such a hostile environment similar to that of the future nuclear waste repositories. By possibly remaining in these dormant states for long periods of time, they would be able to reactivate under more favorable conditions that will arise over the years in these future storage systems, thus favoring microbial activity. Therefore, knowledge of the microbial diversity profiles under different conditions of future repositories is crucial to ensure the long-term safety of these systems.

### **3.2.1. Changes in microbial abundance over time by qPCR**

The qPCR analyses were also performed on the 1-year samples (**Figure 5**). Based on the relative quantification of the 16S rRNA gene, the results supported the NGS data. The total bacterial content of the one-time irradiated treatments (1\_R12, 1\_RB12) was remarkably similar to that of the non-irradiated bentonite blocks (C12, CB12). However, a double radiation dose of 14 kGy was barely enough to obtain a signal and the qPCR data were nearly identical to the negative control. In addition, two specific sulfate-reducing

genes, *apsA* (adenosine-5'-phosphosulfate) and *dsrA* (dissimilatory sulfite reductase), were studied for the quantification of sulfate reducing bacteria. The abundance of FEBEX autochthonous SRB was very low as confirmed in the control without consortium (C12). Exposure to a total radiation dose of 14 kGy (1\_R12) was already enough to not be able to detect signal for either of the two genes *apsA* or *dsrA*. With double dose of irradiation (2R12), no signal was observed either. However, the SRB consortium (B) seemed to withstand the conditions of 14 kGy since a signal was obtained in the one-time irradiated treatment (1\_RB12). Although in a very low relative quantification, both genes were still detected as well in the SRB-spiked two-times irradiated treatment (2RB12). The presence of such DNA in the NGS analysis and the quantification of the genes under study did not imply the survival of these genera. However, it serves as a guide to understand the changes that bacterial communities were undergoing.

Due to the key role of this group of bacteria in long-term anaerobic corrosion of copper containers (Bengtsson and Pedersen, 2017), it is important to further investigate their behavior under different scenarios, despite their low abundance in the samples and low viability under harsh conditions such as those expected to be present in future DGRs (e.g. radiation, bentonite compaction).

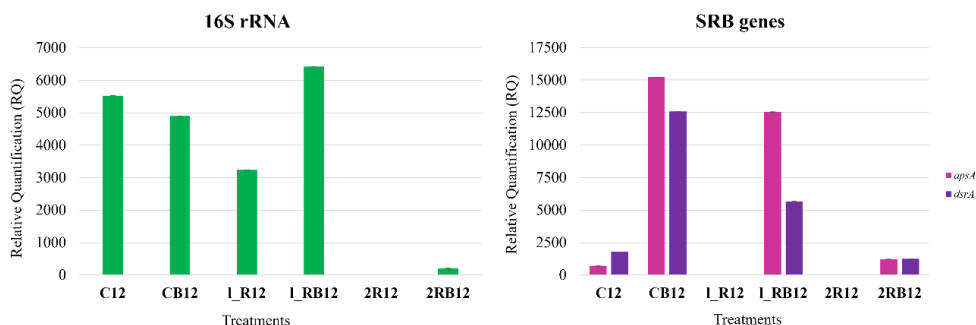


**Figure 5.** Relative quantification of total bacterial content (detected by 16S rRNA) and sulfate-reducing bacteria (detected by *apsA* and *dsrA*) in 1.6 g/cm<sup>3</sup> bentonite blocks in triplicate (except 2R12 and 2RB12 in duplicate) after one year of anoxic incubation. C: non-irradiated compacted treatments; B: SRB consortium; 1\_R: one-time irradiated treatments in the middle of the incubation time as late exposure (14 kGy); 2R: two-times irradiated treatments (28 kGy); 12: one year of anoxic incubation.

### 3.3. Shifts in bentonite mineralogical and chemical stability

FEBEX bentonite is an aluminum phyllosilicate consisting of a clayey material formed primarily from minerals of the smectite group, with montmorillonite being the major mineral (80-90% by weight). The structure of montmorillonite is characterized by a layered structure, each layer consisting of 3 sheets in a 2:1 ratio, i.e. two tetrahedral silica sheets sandwiched by an octahedral aluminum sheet (T-O-T structure). These layers have a negative charge that is balanced by cation exchange and are responsible for giving bentonite most of its physicochemical properties (Abdullahi & Audu, 2017; García-Romero et al., 2019). Among all the types of bentonites that exist according to their different properties, the company ENRESA in Spain has chosen FEBEX bentonite as its preferred option for future repositories. FEBEX bentonite has been extensively studied and is expected to be used as backfill material in future Spanish repositories as compacted blocks at a density of approximately 1.6 - 1.65 g/cm<sup>3</sup> (7<sup>o</sup> Plan General de Residuos Radiactivos, 2023; Huertas et al., 2021; Villar et al., 2006). Therefore, this work has focused on the simulation, at laboratory scale, of the future conditions estimated to occur in a Spanish DGR.

In the present work, from a mineralogical point of view, no appreciable changes were observed in any of the compacted bentonite treatments after 6 and 12 months of anoxic incubation by XRD (**Figure 6**). In all cases, XRD patterns maintained the main character of a dioctahedral two-layer hydrated Ca-Mg-montmorillonite (**Figure 6A**). In order to detect signs of bentonite

illitization, the samples with the longest treatment time, i.e. all those corresponding to 1 year of incubation, were analyzed by XRD oriented aggregates (OA-XRD). No evidence of illitization was observed in any of the samples, as no illite peaks were detected in any of the OA-XRD patterns. The smectites preserved their expansion property, as indicated for all samples by the (001) reflection around 17 Å in ethylene glycol (EG) patterns shown in **Figure 6B** (Fernández et al., 2022). Therefore, the stability of the bentonite remained intact after one year of anoxic incubation in the different treatments studied: gamma radiation at total cumulative doses of 14 and 28 kGy, compaction at 1.6 g/cm<sup>3</sup> and presence/absence of SRB bacteria. On the other hand, pH of each treatment was measured. It was noteworthy that no variation in pH was observed either in any of the treatments studied. The pH remained stable in a range of values between 7.8 and 8.3.

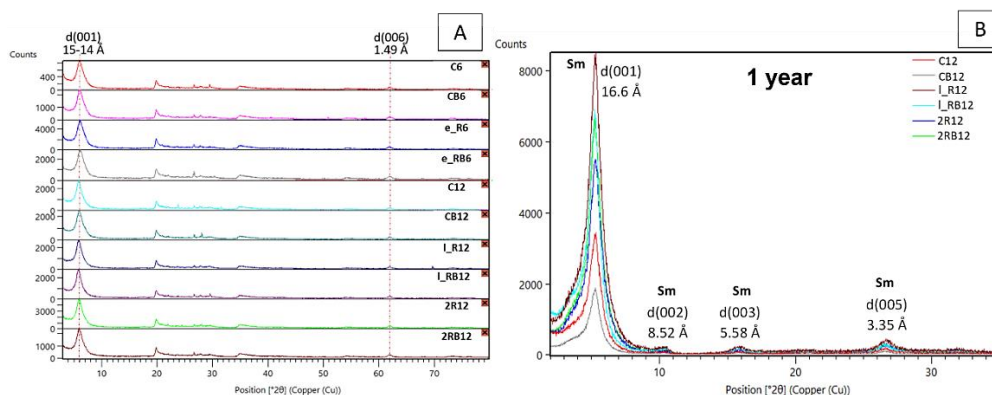


**Figure 6.** A. X-Ray diffraction (XRD) patterns of randomly oriented bulk bentonite samples after 6 and 1 year of anoxic incubation. B. X-Ray diffraction (XRD) patterns of oriented aggregates (OA) of 1-year samples after ethylene glycol exposure. Clay fraction < 2 μm. Glossary: C: non-irradiated compacted treatments; B: SRB consortium; e\_R: one-time irradiated treatments prior incubation time as early exposure (14 kGy); l\_R: one-time irradiated treatments in the middle of the incubation time as late exposure (14 kGy); 2R: two-times irradiated treatments (28 kGy); 6: six months of anoxic incubation; 12: one year of anoxic incubation.

## CHAPTER 1

Controversy exists in the published literature regarding the impact of gamma radiation on bentonite stability (Allard et al., 2009). Most studies indicate that significant changes in bentonite properties require very high doses of radiation (up to 12 kGy/h), which are not expected in future repositories (Chikkamath et al., 2021).

In this work, doses much higher than those estimated in a DGR have been applied, and yet, the mineralogy of the bentonite remained stable. Other factors, in addition to the radiation dose received, have been reported to influence the effect of radiation on the mineralogical stability of this clay. These factors include the water content present in the bentonite, which can induce radiolysis reactions, and the content of accessory minerals that could dissolve and alter properties (Gu et al., 2001; Dixon, 2019). On the other hand, microorganisms can impact the stability of the bentonite buffer by interacting with minerals, leading to weathering, dissolution, and the creation of new minerals (Meleshyn, 2014). More specifically, the bioreduction of Fe(III) is a significant process that transforms smectite into illite. Pedersen et al., (2017) reported that hydrogen sulfide produced by SRB and iron-reducing bacteria (IRB) could react with Fe(III), reducing it and potentially facilitating the illitization process. This is the reason why illitization is one of the main concerns since this process alters the desirable characteristics of smectite (Masurat et al., 2010). As previously mentioned, the presented results indicated no signs of an illitization process, even in the samples inoculated with SRB consortium (CB12, 1\_RB12, 2RB12). Therefore, longer incubation periods would be necessary to observe any significant impact of SRB on the mineralogy of bentonite. However, it is expected that there will be minimal microbial activity in future repositories, at least in the first few hundred years.

### 3.4. Copper surface characterization along the incubation time

Ensuring the long-term safety of future nuclear repositories is crucial for biosphere protection. Therefore, every component of the multisystem must be meticulously designed and thoroughly studied to guarantee the stability of the DGRs for periods as long as the estimated 100,000 years. Accordingly, one of the principal barriers will be the metal canister containing the radioactive waste, which must remain as intact as possible over time. This study has focused on the alteration of copper, a metal that has been proposed to be used by countries such as Finland and Sweden (Bennett & Gens, 2008). In general, copper can be altered by a variety of physical, chemical, and biological factors. These parameters include the presence of water, exposure to radiation, the activity of microorganisms, among others. In the present study, the copper disks corresponding to the different treatments were analyzed macroscopically by visual inspection and microscopically by environmental scanning electron microscopy (ESEM) and energy dispersive X-ray (EDX) microanalysis after 6 months and 1 year of incubation. In general, the disks that exhibited a more damaged appearance upon visual inspection were those that had not undergone irradiation as shown in **Figure 7** (C6, CB6, C12, CB12).

The results found by ESEM and EDX on the samples at both 6 months and 1 year followed the same trend of behavior according to the treatment. The only difference is that at one year the amount of corrosion products observed was higher. The surface of each sample was scanned using ESEM, resulting in a montage that integrated the frames of the whole surface. EDX maps were generated for the entire surface in order to identify the principal corrosion products and their distribution. **Supplementary Figure S3** and **Figure 8** illustrate the 6-month and 1-year surface EDX maps of each disk, respectively, analyzing elements such as Cu, O (representative of oxides), S (representative

## CHAPTER 1

of sulfur compounds), Si (for bentonite detection) and Cl (to detect chlorides). Based on the distribution of these elements on the EDX maps, each zone of interest was analyzed in more detail.

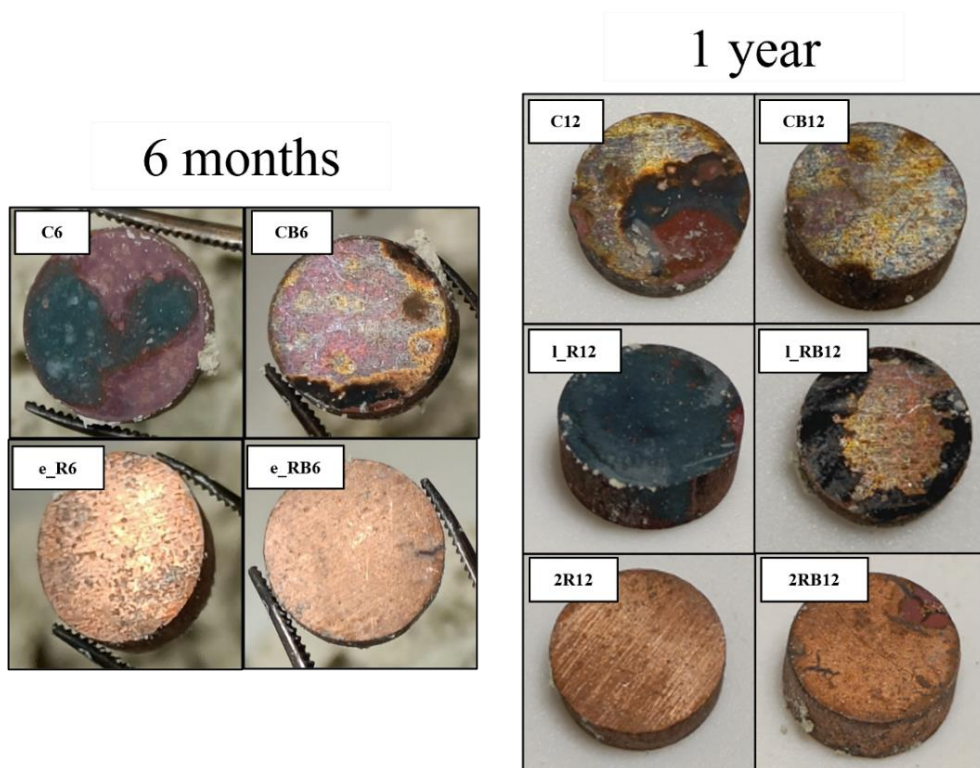


**Figure 7.** Copper disks after 6 months and 1 year of incubation within the different compacted bentonite treatments. Glossary: C: non-irradiated compacted treatments; B: SRB consortium; e\_R: one-time irradiated treatments prior incubation time as early exposure (14 kGy); 1\_R: one-time irradiated treatments in the middle of the incubation time as late exposure (14 kGy); 2R: two-times irradiated treatments (28 kGy); 6: six months of anoxic incubation; 12: one year of anoxic incubation.

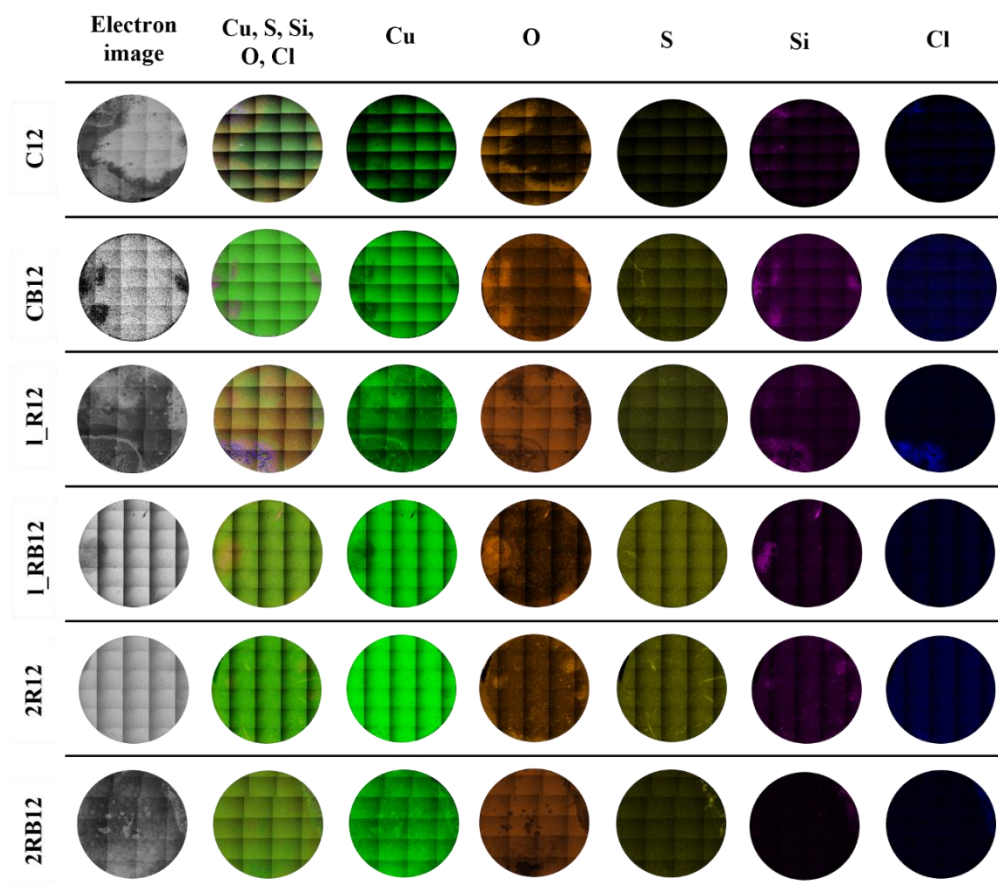


**Figure 8.** The EDX maps of the entire surface of each study Cu disk after one year of incubation. The first column corresponds to electron images and the second column to the summatory EDX map of all detected elements. The other columns correspond to Cu (green), O (orange), S (yellow), Si (pink), Cl (dark blue). Glossary: C: non-irradiated compacted treatments; B: SRB consortium; I\_R: one-time irradiated treatments in the middle of the incubation time as late exposure (14 kGy); 2R: two-times irradiated treatments (28 kGy); 12: one year of anoxic incubation.

**Table 7** describes the main corrosion products found in each study sample. A variety of precipitated copper oxides ( $\text{Cu}_x\text{O}$ ) of differing morphologies were identified in all samples at both six-month and one-year incubation times (**Fig. 9 and 10**). These copper oxides were particularly prevalent in the non-irradiated samples, which exhibited more pronounced surface damage, both with and without SRB consortium (C6, CB6, C12, CB12). In addition, as

## CHAPTER 1

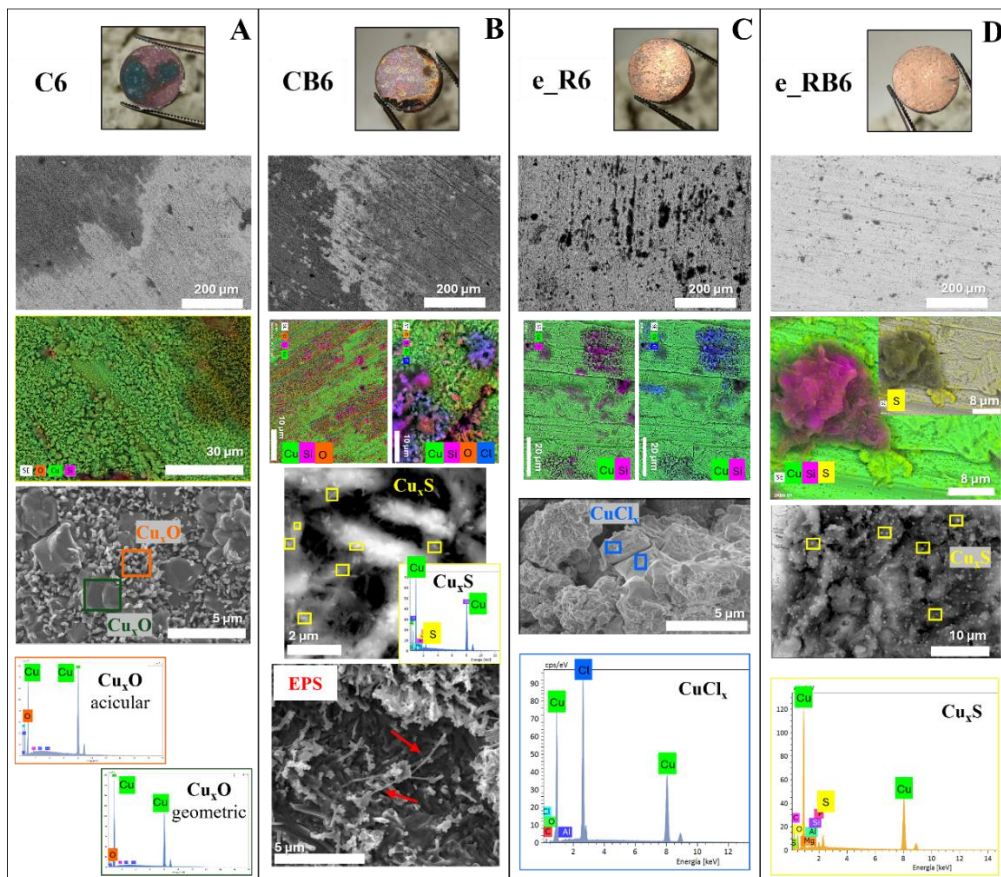
discussed in the previously mentioned microbiological results, the copper disks corresponding to the treatments irradiated after 6 months of incubation (1\_R12, 1\_RB12) were quite similar to those of the non-irradiated 1-year treatments (C12, CB12).

**Table 7.** Main corrosion products found in each study treatment at both 6 months and 1 year of incubation. Glossary: C: non-irradiated compacted treatments; B: SRB consortium; e\_R: one-time irradiated treatments prior incubation time as early exposure (14 kGy); l\_R: one-time irradiated treatments in the middle of the incubation time as late exposure (14 kGy); 2R: two-times irradiated treatments (28 kGy); 6: six months of anoxic incubation; 12: one year of anoxic incubation.

Treatment	Corrosion products
<b>C6</b>	$\text{Cu}_x\text{O}$
<b>CB6</b>	$\text{Cu}_x\text{O}$ / Cu-S in bentonite
<b>e_R6</b>	$\text{Cu}_x\text{O}$ / Cu-S in copper
<b>e_RB6</b>	$\text{Cu}_x\text{O}$ / Cu-S in copper and bentonite
<b>C12</b>	$\text{Cu}_x\text{O}$
<b>CB12</b>	$\text{Cu}_x\text{O}$ / Cu-S in bentonite
<b>1_R12</b>	$\text{Cu}_x\text{O}$ / Cu-S in copper
<b>1_RB12</b>	$\text{Cu}_x\text{O}$ / Cu-S in copper and bentonite
<b>2R12</b>	$\text{Cu}_x\text{O}$ / Cu-S in copper
<b>2RB12</b>	$\text{Cu}_x\text{O}$ / Cu-S in copper

One of the principal corrosion products of concern in relation to copper corrosion is copper sulfide (Bengtsson and Pedersen, 2017). For this reason, the S signal has been investigated in these Cu disks to identify Cu+S compounds. Nevertheless, the use of microscopy and EDX techniques does not allow an accurate identification of the precipitate nature, which could be a copper sulfide or a copper sulfate salt. Sulfur signal was detected in all treatments with SRB consortium, both at 6 months and 1 year of incubation

(CB6, CB12, e\_RB6, 1\_RB12, 2RB6). In addition to these inoculated samples, it was also detected in all irradiated treatments, regardless of incubation time and total radiation dose received. Upon closer examination of the zones on each disk that exhibited sulfur signals, the following observations were made. In the non-irradiated treatments (CB6, CB12) together with early irradiated (e\_RB6) and late-irradiated treatments (1\_RB12), all of them with SRB consortium, small Cu+S precipitates were observed, located exclusively within bentonite layers (**Figures 9B, 9D, 10B**). However, in the treatment with double doses of radiation + SRB consortium (2RB12), these sulfur precipitates were not found in the bentonite.



## CHAPTER 1

**Figure 9.** Environmental scanning electron microscopy (ESEM) and energy dispersive X-Ray (EDX) analysis of the copper disks corresponding to the 6-month incubation treatments. In the first line, photographs of the disks are shown before being analyzed. EDX maps and spectra detail the signal of the elements that correspond to the main corrosion products together with Cu signal. Cu is represented in green, O in orange, S in yellow, and Cl in dark blue. Additionally, the Si signal was illustrated in pink, representing traces of bentonite. **A.** C6 sample with Cu surface mainly covered by  $\text{Cu}_x\text{O}$  of different morphologies. **B.** CB6 sample with surface mainly covered by copper oxides in addition to small Cu+S precipitates within bentonite traces. EPS filaments are also indicated with red arrows. **C.** e\_R6 sample exhibiting a surface with minimal alteration, primarily coated with traces of bentonite. Copper chlorides precipitated between bentonite are also shown. **D.** e\_RB6 sample exhibiting a surface with minimal alteration primarily coated with traces of bentonite. Small Cu+S precipitates within bentonite traces are also shown. Glossary: C: non-irradiated compacted treatments; B: SRB consortium; e\_R: one-time irradiated treatments prior incubation time as early exposure (14 kGy); 6: six months of anoxic incubation.

On the other hand, in all irradiated samples, regardless of the presence of a consortium, Cu+S precipitates were also observed but to be located directly on the copper surface. These precipitates exhibited a distinct morphology and were larger in size compared to those observed in the bentonite (**Figure 10C**). Moreover, copper chloride salts, which precipitate mainly between bentonite layers, were also found in almost all samples. The presence of chloride precipitates was likely due to the composition of the FEBEX pore water (detailed in **Table 1**). **Figure 9C** showed an electron micrograph of the morphologies of these precipitated copper chlorides together with their EDX spectrum. In general, no bacterial cells were found as biofilms on the copper surface. However, some filaments similar to the structure of extracellular polymeric substances (EPS) were observed in the unirradiated + SRB consortium samples at both 6 months and 1 year (CB6, CB12). **Figure 9B** showed an electron image of such EPS filaments (red arrows) found in CB6 copper disk sample.

On the other hand, it should be noted that the Cu disks exhibiting minimal alterations based on surface corrosion products were those initially irradiated

with a dose of 14 kGy (e\_R6, e\_RB6) and those subjected to two irradiation exposure, accumulating a total dose of 28 kGy (2R12, 2RB12), as illustrated in **Figure 7** showing disks barely altered. ESEM analysis confirmed the minimal alteration of these disks' surfaces, revealing certain areas with precipitates of  $\text{Cu}_x\text{O}$  and  $\text{Cu+S}$ , as well as copper chlorides and traces of bentonite. In comparison to non-irradiated samples or those irradiated at mid-incubation time, the presence of these corrosion products was greatly limited, with most of the copper surface remaining unaltered. **Supplementary Figure S4** showed the surfaces of the Cu disks corresponding to the treatments after 6 months of incubation, showing a clear disparity in the amount of precipitated corrosion products.

Additionally, the copper disks after 6 months of incubation were analyzed by X-ray photoelectron spectroscopy (XPS). Complementary XPS was used to assess and compare each Cu disks surface composition. As mentioned above, the XPS analysis only covered 6-month Cu disks. On the surface of the samples, wide scans revealed the presence of Cu, C, O, Si, Na, Fe, Mg and Al. Apart from copper, all these elements probably corresponded to bentonite adhering to the surface of the disks. High-resolution scans conducted for the Cu 2p region revealed elemental copper peaks present on all samples, while also indicating the potential presence of CuO. XPS spectra for the Cu 2p region (region between 922-977 eV) on 6-month samples are illustrated in **Figure 11**. Cu  $2p_{3/2}$  and Cu  $2p_{1/2}$  were discerned at 934.21 eV and 954.17 eV, respectively, as two pronounced peaks. These conform to previously published data linked to elemental copper (Wagner et al., 1979) and were evident in each sample under study. In addition, according to the literature, the peaks observed at 943.49 eV and 962.89 eV, and the distance between Cu  $2p_{1/2}$  and Cu  $2p_{3/2}$  peaks (19.96 eV) corresponded to the presence of CuO (Wagner et al., 1979). These peaks were not present in the untreated Cu control.

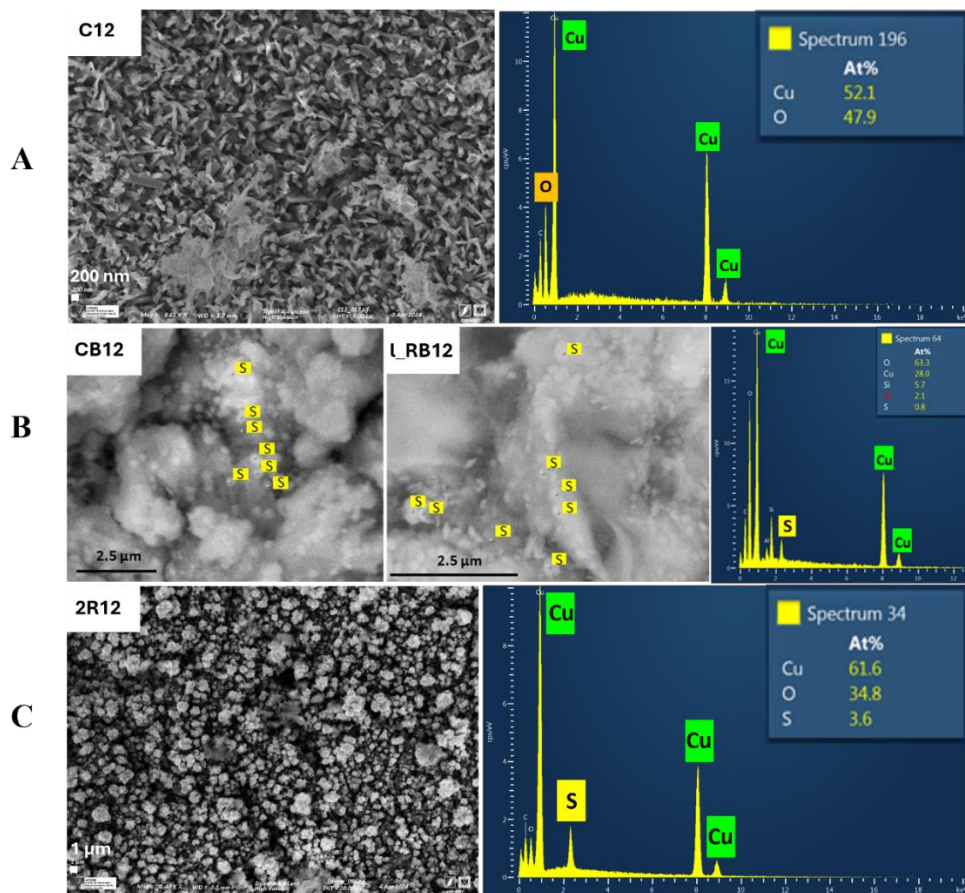


**Figure 10.** Environmental scanning electron microscopy (ESEM) and energy dispersive X-Ray (EDX) analysis of the copper disks corresponding to C12, CB12, l\_RB12 and 2RB12 treatments after 1 year of incubation. **A.** C12 sample with Cu surface mainly covered by  $\text{Cu}_x\text{O}$  of different morphologies. **B.** CB12 and l\_RB12 samples showing small Cu+S precipitates within bentonite traces. **C.** 2R12 surface showing Cu+S precipitates directly on copper surface.

The presence of Cu+S compounds in some of the Cu disks has been mentioned previously, highlighting small precipitates within bentonite layers when the SRB consortium was present, and bigger precipitates directly on the copper surface in all irradiated treatments. XPS analyses would elude identification of sulfur compounds present on copper surfaces. Krylova and Andrulėvičius, (2009) reported that peaks corresponding to CuS typically manifest at around 932.2 eV in high-resolution Cu 2p scans. However, if CuS were present, its

peak would overlap with the Cu 2p<sub>3/2</sub> peak, thereby making its presence unable to be confirmed solely through the Cu 2p high-resolution spectrum. Therefore, in this study, high-resolution scans were also conducted in the S 2p region within the range of 143 to 180 eV (**Fig. 11**). This XPS scans revealed the presence of sulfur on samples CB6 and e\_RB6. More specifically, these samples showed peaks around 163 eV, which are related to the presence of Cu<sub>2</sub>S (Martinez-Moreno et al., 2023; Yu et al., 1990). Additionally, the peak observed at 161.4 eV was attributed to CuS according to Kutty, (1991). Conversely, the peak observed around 154 eV in all disks corresponded to Si 2s, indicating the presence of SiO<sub>2</sub> belonging to the bentonite traces adhered to the copper surface (Clarke & Rizkalla, 1976). In the irradiated sample e\_R6, a smooth peak was observed around 168.9 eV, which was attributed to the presence of sulfate (Cai et al., 2009).

In the future repository for nuclear waste, oxygen will only be present during the initial years due to bacterial activity and mineral oxidation, after which its presence will be limited (King et al., 2017). In the present study, the incubation period was conducted under anoxic conditions. Nevertheless, the assembly of the blocks was conducted in the presence of oxygen. During this period, it was possible that the copper may have undergone a spontaneous passivation process to protect its surface. Furthermore, Burzan et al., (2022) reported the presence of oxygen molecules trapped between the pores of the bentonite, thus creating microaerophilic environments. According to this, along with the presence of pore water in the samples, which would also contribute oxygen molecules, would have facilitated the formation of copper oxides. In future high compacted bentonite barriers, some degree of saturation with water will initially exist, then some of the oxygen will be present as dissolved species as well. The most plausible reaction to be expected to have occurred is the formation of copper(I) oxide, as described by the following equation

## CHAPTER 1

$4\text{Cu} + \text{O}_2 \rightarrow 2\text{Cu}_2\text{O}$ , reported by Hall et al., (2021). The copper oxides could continue to oxidize, resulting in the formation of copper(II) oxides, as evidenced by the XPS analysis (**Fig. 11**). This process could occur in a similar reaction as the one described by Mahmoodi et al. (2018):  $2\text{Cu}_2\text{O} + \text{O}_2 \rightarrow 4\text{CuO}$ .

On the other hand, one of the most critical sources of corrosion would be the microbial activity. More specifically, by the activity of microorganisms involved in sulfate reduction, which are known as sulfate-reducing bacteria (SRB). This group of bacteria are frequently responsible for microbiologically influenced corrosion (MIC) damage through the production of  $\text{HS}^-$  that combined with  $\text{H}^+$  would result in  $\text{H}_2\text{S}$ . These bacteria coupled the oxidation of electron donors to the reduction of sulfate as terminal electron acceptor (Little et al., 2020; Thauer et al., 2007). In future DGR, bacteria would obtain electron donors from organic material derived from groundwater seepage, neighboring minerals, and organic material already present in bentonite or host rock. The viability of these group of bacteria was confirmed by the results shown in the most probable number using Postgate medium. As mentioned above, this group of bacteria was generally present and viable in the non-irradiated treatments over time and was quite negatively affected in the presence of gamma irradiation. The presence of bacteria, both bentonite indigenous SRB and those inoculated with the consortium, were associated with the bentonite layers. Hall et al., (2021) reported that microbial activity would mainly happen within the bentonite. The small precipitates with S signal localized between the bentonite layer in the non-irradiated treatments with SRB consortium could have a biotic origin. Thus, the copper would have corroded due to biogenic sulfides resulting in the formation of copper sulfides as described by the following equation:  $2\text{Cu} + \text{HS}^- + \text{H}^+ \rightarrow \text{Cu}_2\text{S} (\text{s}) + \text{H}_2 (\text{g})$  (Huttunen-Saarivirta et al., 2016). These precipitates were found only in

treatments with SRB viability. The XPS results confirmed the presence of  $\text{Cu}_2\text{S}$  in those treatments corresponding to 6 months of incubation.

On the other hand, precipitates with S signal directly on copper surface were also detected in all irradiated treatments. Li et al., (2021) reported that  $\gamma$ -radiation induced synthesis involved redox reactions between products of water radiolysis, radicals and active species, and dissolved metal salt precursors, resulting in precipitation of less soluble reaction products.

Furthermore, according to Hall et al., (2021), groundwater in a DGR environment will contain a variety of anions from the dissolution of host rock minerals, particularly chloride, sulfate, and carbonate. Therefore, the formation of copper salts containing these anions, such as copper sulfate and copper chloride, can be expected. The presence of these copper sulfides would occur in the more advanced stages of future repositories, when oxygen has been completely consumed and the oxic corrosion stage has ended. Hence, when sulfide production by SRB would begin in an anaerobic environment, these sulfides would be found with copper layers coated by oxides. The conversion of  $\text{Cu}_2\text{O}$  to  $\text{Cu}_2\text{S}$  has been documented by Smith et al., (2007). Accordingly, the oxide layers would act as a protective barrier to sulfide corrosion by reacting with existing corrosion products rather than with pure copper (Hall et al., 2021).

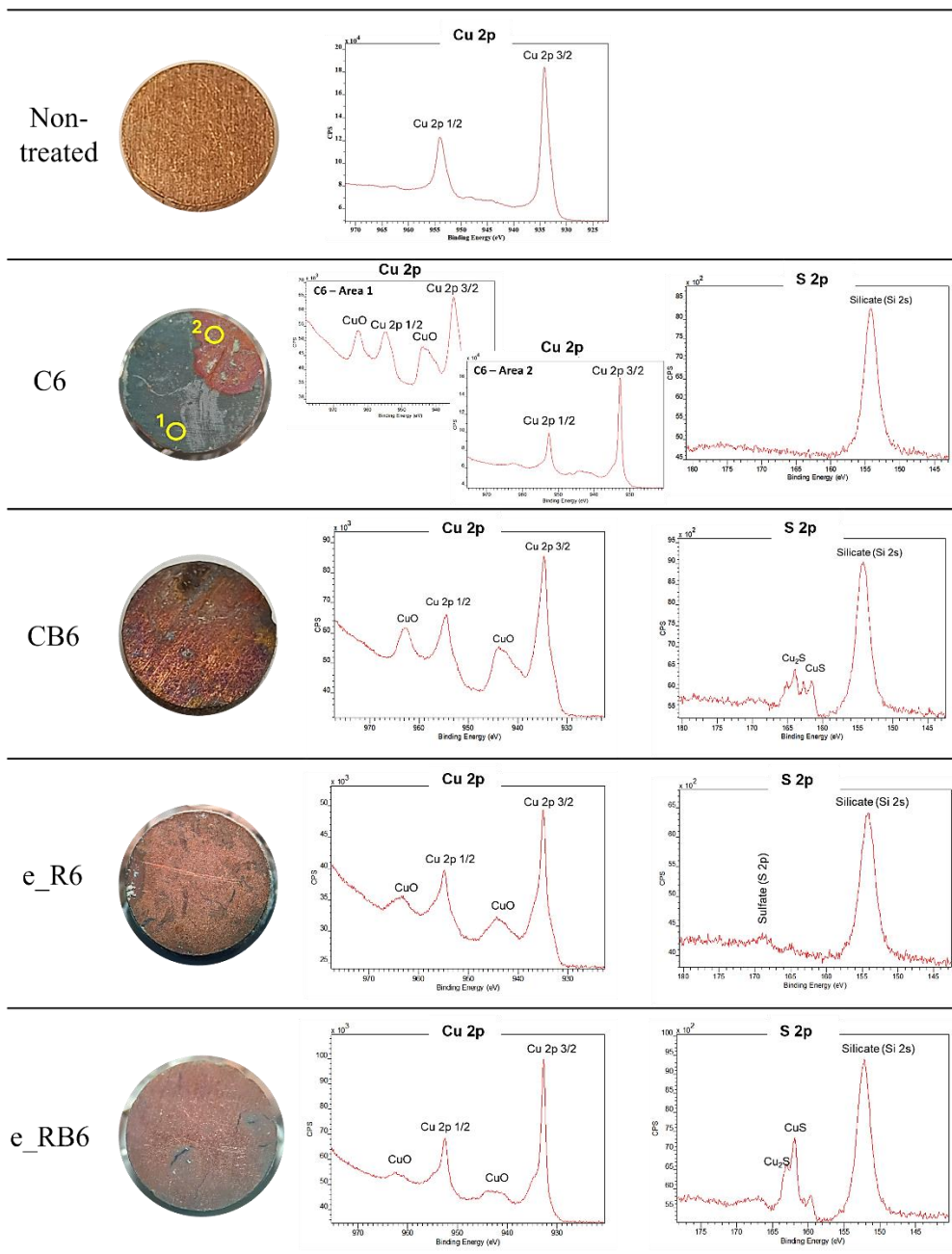


**Figure 11.** High-resolution XPS spectra of the Cu 2p (977 eV – 922 eV) and S 2p (180 eV – 143 eV) regions of the Cu surface before experimental set-up (non-treated) and after 6 months of incubation. Glossary: C: non-irradiated compacted treatments; B: SRB consortium; e\_R: one-time irradiated treatments prior incubation time as early exposure (14 kGy); 6: six months of anoxic incubation.

#### 4. Conclusions and future scope

The present study investigated the combined effect of high compaction density ( $1.6 \text{ g/cm}^3$ ) together with the presence of gamma radiation (total cumulative dose of 14 kGy or 28 kGy), pore water saturation conditions, the presence of sulfate-reducing bacteria and anoxic atmosphere, in FEBEX bentonite blocks. Additionally, small pure-copper disks were placed in the core of each bentonite block to analyze the corrosion in presence of the aforementioned conditions. A comprehensive analysis of various study times at different disciplinary levels has led to advance in the understanding of the microbial behavior and impact in conditions relevant to future nuclear repositories. Compaction conditions at  $1.6 \text{ g/cm}^3$ , combined with anoxic incubation and low nutrient availability, favor the viability of spore-forming microorganisms that are resistant to harsh environments, such as desiccation or nutrient scarcity. Following a six-month incubation period, all viable bacterial strains were identified as belonging to the family Bacillaceae, with the exception of the genus *Arthrobacter*. Genera of this family are known to persist in challenging environments, such as drought or nutrient deficiency, and to form endospores. Furthermore, the microbial diversity after one year of incubation also revealed the presence of genera resistant to these harsh conditions, including *Saccharopolyspora*, *Streptomyces*, *Massilia*, *Acinetobacter*, and *Pseudomonas*.

On the other hand, gamma radiation would negatively affect the viability of aerobic heterotrophic microorganisms and sulfate-reducing bacteria, at total cumulative doses of at least 14 kGy and 28 kGy with a dose rate of 0.66 Gy/h. However, the results presented in this study demonstrated that an incubation period prior to radiation exposure would favor the survival and resistance of these microorganisms. The results of treatments irradiated with 14 kGy after 6 months of incubation were very similar to those of non-irradiated treatments.

## CHAPTER 1

This emphasizes the significance of the fact that the same radiation dose can affect the microbiology differently depending on the *in vivo* developmental status of the microbial community. The copper corrosion results showed that the main corrosion products were copper oxides, which were present in all samples, mainly as CuO. The potential sources of oxygen could have included the bentonite compaction process, oxygen molecules entrapped within the pores of bentonite, and pore water. Gamma radiation would indirectly delay the biotic corrosion of copper by negatively affecting the microbiology of the bentonite. Furthermore, it appears to enhance the precipitation of salts, including potential copper sulfates.

On the other hand, the group of sulfate-reducing bacteria, which are the main agents involved in microbiologically influenced corrosion (MIC), would be implicated in the corrosion of Cu disks by producing potential biogenic copper sulfides, which were detected only in the bentonite. Finally, from a mineralogical perspective, neither gamma radiation nor any of the other experimental conditions had an adverse effect on the properties of FEBEX bentonite, which remained stable even after one year of incubation.

The findings presented here offer new insights and advances in the field of microbiology relevant to future nuclear repositories. It is of paramount importance to study the conditions that will be present in the DGRs in order to guarantee the safety of these engineering systems at all possible levels. In the future, both engineered barriers and microorganisms will face different conditions in a combined manner, rather than as independent factors. Consequently, the present study yields novel results, providing new multidisciplinary insights into the combined effects of gamma radiation with other parameters of interest.

## Funding

This research was supported by the grant ID 516514 funded by the FP6-EURATOM-NUWASTE WP ConCorD to MLM and by the grant FPU20/00583 from “Ministerio de Universidades” to the first author from the Spanish Government. In addition, this work has also been partially supported by the EURAD project that has received funding from H2020-EURATOM 1.2 under grant agreement ID 847593. MMH acknowledges EURAD Mobility Programme for the award of a Research and Training Grant at the Technical University of Liberec (Czech Republic).

## Acknowledgements

The authors acknowledge the assistance of Daniel García Muñoz Bautista Cerro, Dr. Isabel Guerra-Tschuschke and Dr. Isabel María Sánchez Almazo (Centro de Instrumentación Científica, University of Granada, Spain) for the sample preparation and microscopy assistance, respectively. Moreover, Klára Lísková for her guidance and training on the facilities at the Institute for Nanomaterials, Advanced Technology and Innovation – Technical University of Liberec. Finally, Pedro Valdivieso for his assistance in the radioactive installations of the Nayade facility of CIEMAT.

## References

- 7º Plan General de Residuos Radiactivos. (2023). Ministerio para la transición ecológica y el reto demográfico. <https://www.miteco.gob.es/es/energia/nuclear/residuos/plan-general.html>
- Abdullahi, S. L., and Audu, A. A. (2017). Comparative analysis on chemical composition of bentonite clays obtained from Ashaka and tango deposits in Gombe State, Nigeria. *ChemSearch Journal*, 8(2), 35-40.
- Allard, T., and Calas, G. (2009). Radiation effects on clay mineral properties. *Applied Clay Science*, 43(2), 143-149. <https://doi.org/10.1016/j.clay.2008.07.032>

## CHAPTER 1

- Anderson, T. F. (1951). Techniques For The Preservaation Of Three-Dimensional Structure In Preparing Specimens For The Electron Microscope. *Transactions of the New York Academy of Sciences*, 13(4 Series II), 130-134. <https://doi.org/10.1111/j.2164-0947.1951.tb01007.x>
- Ben-Dov, E., Brenner, A., & Kushmaro, A. (2007). Quantification of sulfate-reducing bacteria in industrial wastewater, by real-time polymerase chain reaction (PCR) using *dsrA* and *apsA* genes. *Microbial ecology*, 54, 439-451. <https://doi.org/10.1007/s00248-007-9233-2>
- Bengtsson, A., Pedersen, K. 2017. Microbial sulphide-producing activity in water saturated Wyoming MX-80, Asha and Calcigel bentonites at wet densities from 1500 to 2000 kg m<sup>-3</sup>. *Applied Clay Science*, 137, 203-212. <https://doi.org/10.1016/j.clay.2016.12.024>
- Bennett, D. G., & Gens, R. (2008). Overview of European concepts for high-level waste and spent fuel disposal with special reference waste container corrosion. *Journal of Nuclear Materials*, 379(1-3), 1-8. <https://doi.org/10.1016/j.jnucmat.2008.06.001>
- Burzan, N., Murad Lima, R., Frutschi, M., Janowczyk, A., Reddy, B., Rance, A., Diomidis, N., Bernier-Latmani, R., (2022). Growth and Persistence of an Aerobic Microbial Community in Wyoming Bentonite MX-80 Despite Anoxic in situ Conditions. *Frontiers in Microbiology*, 13. <https://doi.org/10.3389/fmicb.2022.858324>
- Cai, Y., Pan, Y., Xue, J., Sun, Q., Su, G., & Li, X. (2009). Comparative XPS study between experimentally and naturally weathered pyrites. *Applied Surface Science*, 255(21), 8750-8760. <http://dx.doi.org/10.1016/j.apsusc.2009.06.028>
- Callahan, B. J., McMurdie, P. J., Rosen, M. J., Han, A. W., Johnson, A. J. A., & Holmes, S. P. (2016). DADA2: High-resolution sample inference from Illumina amplicon data. *Nature methods*, 13(7), 581-583. <https://doi.org/10.1038/nmeth.3869>
- Campos, V. L., Valenzuela, C., Yarza, P., Kämpfer, P., Vidal, R., Zaror, C., ... & Rosselló-Móra, R. (2010). *Pseudomonas arsenicoxydans* sp nov., an arsenite-oxidizing strain isolated from the Atacama Desert. *Systematic and Applied Microbiology*, 33(4), 193-197. <https://doi.org/10.1016/j.syapm.2010.02.007>
- Černoušek, T., Shrestha, R., Kovářová, H., Špánek, R., Ševců, A., Sihelská, K., Kokinda, J., Stouřil, J., & Steinová, J. (2020). Microbially influenced corrosion of carbon steel in the presence of anaerobic sulphate-reducing bacteria. *Corrosion Engineering, Science and Technology*, 55(2), 127-137. <https://doi.org/10.1080/1478422X.2019.1700642>
- Chikkamath, S., Manjanna, J., Kabadagi, A., Patil, D., Tripathi, V. S., Kar, A. S., & Tomar, B. S. (2021). Gamma (<sup>60</sup>Co) irradiation and thermal effect on redox behavior of interlayer iron in montmorillonite. *Applied Clay Science*, 200, 105893. <https://doi.org/10.1016/j.clay.2020.105893>

- Claesson, M. J., Wang, Q., O'Sullivan, O., Greene-Diniz, R., Cole, J. R., Ross, R. P., & O'Toole, P. W. (2010). Comparison of two next-generation sequencing technologies for resolving highly complex microbiota composition using tandem variable 16S rRNA gene regions. *Nucleic acids research*, 38(22), e200-e200. <https://doi.org/10.1093/nar/gkq873>
- Clarke, T. A., & Rizkalla, E. N. (1976). X-ray photoelectron spectroscopy of some silicates. *Chemical Physics Letters*, 37(3), 523-526.
- Clifford, R. J., Milillo, M., Prestwood, J., Quintero, R., Zurawski, D. V., Kwak, Y. I., Waterman, P. E., Lesho, E. P. & Mc Gann, P. (2012). Detection of bacterial 16S rRNA and identification of four clinically important bacteria by real-time PCR. *PLoS one*, 7(11), e48558. <https://doi.org/10.1371/journal.pone.0048558>
- Dixon, D. A. (2019). Review of the T-H-M-C Properties of MX-80 Bentonite. Technical report NWMO-TR 2019-07, Nuclear Waste Management Organization, Toronto, Ontario, Canada.
- Dose, K., & Gill, M. (1995). DNA stability and survival of *Bacillus subtilis* spores in extreme dryness. *Origins of Life and Evolution of the Biosphere*, 25(1), 277-293. <https://doi.org/10.1007/BF01581591>
- Dowd, S. E., Callaway, T. R., Wolcott, R. D., Sun, Y., McKeegan, T., Hagevoort, R. G., & Edrington, T. S. (2008). Evaluation of the bacterial diversity in the feces of cattle using 16S rDNA bacterial tag-encoded FLX amplicon pyrosequencing (bTEFAP). *BMC microbiology*, 8(1), 1-8. <https://doi.org/10.1186/1471-2180-8-125>
- Engel, K., Ford, S.E., Binns, W.J., Diomidis, N., Slater, G.F., Neufeld, J.D., (2023). Stable microbial community in compacted bentonite after 5 years of exposure to natural granitic groundwater. *mSphere*, 8, e00048-23. <https://doi.org/10.1128/msphere.00048-23>
- Ewing, R. C., Whittleston, R. A., & Yardley, B. W. (2016). Geological disposal of nuclear waste: a primer. *Elements*, 12(4), 233-237. <https://doi.org/10.2113/gselements.12.4.233>
- Fernández, A. M., Marco, J. F., Nieto, P., León, F. J., Robredo, L. M., Clavero, M. Á., Cardona, A. I., Fernández, S., Svensson, D., Sellin, P. (2022). Characterization of Bentonites from the in situ ABM5 Heater Experiment at Äspö Hard Rock Laboratory, Sweden. *Minerals*, 12(4), 471. <https://doi.org/10.3390/min12040471>
- Fernandez, A.M., Rivas. P (2005). Pore water chemistry of saturated FEBEX bentonite compacted at different densities. *Advances in Understanding Engineered Barriers*. Alonso & Ledesma (eds). Taylor and Francis Group, London. Pg 505- 514 ISBN 04-1536-544-9.

## CHAPTER 1

- Gallego, L. (2016). *Acinetobacter baumannii*: Factors involved in its high adaptability to adverse environmental conditions. *Journal of Microbiology & Experimentation*, 3(2), 00085. <http://dx.doi.org/10.15406/jmen.2016.03.00085>
- García-Romero, E., María Manchado, E., Suárez, M., & García-Rivas, J. (2019). Spanish Bentonites: A review and new data on their geology, mineralogy, and crystal chemistry. *Minerals*, 9(11), 696. <https://doi.org/10.3390/min9110696>
- García-Siñeriz, J. L., Mazón, M. R., Kober, F., & Sakaki, T. (2019). Performance of THM monitoring instrumentation in FEBEX bentonite barrier after 18 years of operation under repository-like conditions. *Geomechanics for Energy and the Environment*, 17, 75-89. <https://doi.org/10.1016/j.gete.2018.09.008>
- Gu, B. X., Wang, L. M., Minc, L. D., Ewing, R. C. (2001). Temperature Effects on the Radiation Stability and Ion Exchange Capacity of Smectites. *Journal of Nuclear Materials*, 297, 345–54. [https://doi.org/10.1016/S0022-3115\(01\)00631-6](https://doi.org/10.1016/S0022-3115(01)00631-6)
- Guo, M. (2020). The electrochemical and corrosion study of copper for nuclear waste containers under deep geological disposal conditions (Doctoral dissertation, The University of Western Ontario (Canada)).
- Hall, D. S., Behazin, M., Binns, W. J., & Keech, P. G. (2021). An evaluation of corrosion processes affecting copper-coated nuclear waste containers in a deep geological repository. *Progress in Materials Science*, 118, 100766. <https://doi.org/10.1016/j.pmatsci.2020.100766>
- Hammer, O. (2001). PAST: paleontological statistics software package for education and data analysis. *Palaeontologia Electronica*. <http://palaeo-electronica.org>
- Haynes, H. M., Pearce, C. I., Boothman, C., & Lloyd, J. R. (2018). Response of bentonite microbial communities to stresses relevant to geodisposal of radioactive waste. *Chemical Geology*, 501, 58-67. <https://doi.org/10.1016/j.chemgeo.2018.10.004>
- Huertas, F., Fariña, P., Farias, J., García-Siñeriz, J.L., Villar, M.V., Fernández, A.M., Martín, P.L., Elorza, F.J., Gens, A., Sánchez, M., Lloret, A., Samper, J., Martínez, M. Á. (2021). Full-scale Engineered Barriers Experiment. Updated Final Report 1994-2004.
- Huertas, F., Fuentes-Santillana, J.L., Jullien, F., Rivas, P., Linares, J., Fariña, P., Ghoreychi, M., Jockwer, N., Kickmaier, W., Martínez, M.A., Samper, J., Alonso, E., Elorza, F.J. (2000). Full Scale Engineered Barriers Experiment for a Deep Geological Repository for High-level Radioactive Waste in Crystalline Host Rock. EC Final REPORT EUR 19147.
- Huttunen-Saarivirta, E., Rajala, P., & Carpén, L. (2016). Corrosion behaviour of copper under biotic and abiotic conditions in anoxic groundwater: Electrochemical study. *Electrochimica Acta*, 203, 350-365. <https://doi.org/10.1016/j.electacta.2016.01.098>

- IAEA. (2018). Status and trends in spent fuel and radioactive waste management. Vienna, International Atomic Energy Agency. Nuclear Energy Series No. NW-T-1.14, 74. Available at: [https://www-pub.iaea.org/MTCD/Publications/PDF/PUB1963\\_web.pdf](https://www-pub.iaea.org/MTCD/Publications/PDF/PUB1963_web.pdf)
- Jackson, M. L. (2005). Soil chemical analysis: advanced course: a manual of methods useful for instruction and research in soil chemistry, physical chemistry of soils, soil fertility, and soil genesis. UW-Madison Libraries parallel press, p. 930.
- Jung, K. W., Lim, S., & Bahn, Y. S. (2017). Microbial radiation-resistance mechanisms. *Journal of Microbiology*, 55, 499-507. <https://doi.org/10.1007/s12275-017-7242-5>
- King, F., Hall, D. S., & Keech, P. G. (2017). Nature of the near-field environment in a deep geological repository and the implications for the corrosion behaviour of the container. *Corrosion Engineering, Science and Technology*, 52(sup1), 25-30. <https://doi.org/10.1080/1478422X.2017.1330736>
- Krylova, V., Andrulevičius, M. (2009). Optical, XPS and XRD studies of semiconducting copper sulfide layers on a polyamide film. *International Journal of Photoenergy*, 2009(1), 304308. <https://doi.org/10.1155/2009/304308>
- Kutty, T. R. N. (1991). A controlled copper-coating method for the preparation of ZnS: Mn DC electroluminescent powder phosphors. *Materials Research Bulletin*, 26(5), 399-406. [https://doi.org/10.1016/0025-5408\(91\)90054-P](https://doi.org/10.1016/0025-5408(91)90054-P)
- Laskowska, E., & Kuczyńska-Wiśnik, D. (2020). New insight into the mechanisms protecting bacteria during desiccation. *Current Genetics*, 66(2), 313-318. <https://doi.org/10.1007/s00294-019-01036-z>
- Li, Z., Yang, Y., Relefors, A., Kong, X., Siso, G. M., Wickman, B., ... & Soroka, I. L. (2021). Tuning morphology, composition and oxygen reduction reaction (ORR) catalytic performance of manganese oxide particles fabricated by  $\gamma$ -radiation induced synthesis. *Journal of Colloid and Interface Science*, 583, 71-79. <https://doi.org/10.1016/j.jcis.2020.09.011>
- Little, B. J., Hinks, J., & Blackwood, D. J. (2020). Microbially influenced corrosion: Towards an interdisciplinary perspective on mechanisms. *International Biodeterioration & Biodegradation*, 154, 105062. <https://doi.org/10.1016/j.ibiod.2020.105062>
- Lopez-Fernández, M., Fernández-Sanfrancisco, O., Moreno-García, A., Martín-Sánchez, I., Sánchez-Castro, I., & Merroun, M. L. (2014). Microbial communities in bentonite formations and their interactions with uranium. *Applied geochemistry*, 49, 77-86. <https://doi.org/10.1016/j.apgeochem.2014.06.022>
- Mahmoodi, A., Solaymani, S., Amini, M., Nezafat, N. B., and Ghoranneviss, M. (2018). Structural, Morphological and Antibacterial Characterization of CuO Nanowires. *Silicon*, 10, 1427–143. <https://doi.org/10.1007/s12633-017-9621-2>

## CHAPTER 1

- Mandic-Mulec, I., Stefanic, P., & van Elsas, J. D. (2016). Ecology of bacillaceae. *The bacterial spore: From molecules to systems*, 59-85. <https://doi.org/10.1128/9781555819323.ch3>
- Mao, J., Tang, Q., Zhang, Z., Wang, W., Wei, D., Huang, Y., Liu, Z., Shi, Y., & Goodfellow, M. (2007). *Streptomyces radiopugnans* sp. nov., a radiation-resistant actinomycete isolated from radiation-polluted soil in China. *International journal of systematic and evolutionary microbiology*, 57(11), 2578-2582. <https://doi.org/10.1099/ijs.0.65027-0>
- Martinez-Moreno, M. F., Povedano-Priego, C., Morales-Hidalgo, M., Mumford, A. D., Ojeda, J. J., Jroundi, F., & Merroun, M. L. (2023). Impact of compacted bentonite microbial community on the clay mineralogy and copper canister corrosion: a multidisciplinary approach in view of a safe Deep Geological Repository of nuclear wastes. *Journal of Hazardous Materials*, 131940. <https://doi.org/10.1016/j.jhazmat.2023.131940>
- Martinez-Moreno, M.F., Povedano-Priego, C., Mumford, A.D., Morales-Hidalgo, M., Mijndonckx, K., Jroundi, F., Ojeda, J.J., Merroun, M.L., (2024). Microbial responses to elevated temperature: Evaluating bentonite mineralogy and copper canister corrosion within the long-term stability of deep geological repositories of nuclear waste. *Science of The Total Environment*, 915, 170149. <https://doi.org/10.1016/j.scitotenv.2024.170149>
- Masurat, P., Eriksson, S., and Pedersen, K. (2010). Evidence of Indigenous Sulphate-Reducing Bacteria in Commercial Wyoming Bentonite MX- 80. *Applied Clay Science*, 47(1-2), 51-57. <https://doi.org/10.1016/j.clay.2008.07.002>
- McMurdie, P. J., & Holmes, S. (2013). phyloseq: an R package for reproducible interactive analysis and graphics of microbiome census data. *PloS one*, 8(4), e61217. <https://doi.org/10.1371/journal.pone.0061217>
- Meleshyn, A. (2014). Microbial processes relevant for the long-term performance of high-level radioactive waste repositories in clays. *Geological Society, London, Special Publications*, 400(1), 179-194. <https://doi.org/10.1144/SP400.6>
- Moore, D. M., & Reynolds, R. C. (1997). X-ray Diffraction and the Identification and Analysis of Clay Minerals. New York: Oxford university press, Vol. 378.
- Morales-Hidalgo, M., Povedano-Priego, C., Martinez-Moreno, M. F., Ruiz-Fresneda, M. A., Lopez-Fernandez, M., Jroundi, F., & Merroun, M. L. (2024a). Insights into the Impact of Physicochemical and Microbiological Parameters on the Safety Performance of Deep Geological Repositories. *Microorganisms*, 12(5), 1025. <https://doi.org/10.3390/microorganisms12051025>
- Morales-Hidalgo, M., Povedano-Priego, C., Martinez-Moreno, M. F., Ojeda, J. J., Jroundi, F., & Merroun, M. L. (2024b). Long-term tracking of the microbiology of uranium-amended water-saturated bentonite microcosms: a mechanistic characterization of U speciation. *Journal of Hazardous Materials*, 476, 135044. <https://doi.org/10.1016/j.jhazmat.2024.135044>

- Moussa, L. A. A., Mansour, F. A., Serag, M. S., & Abou El-Nour, S. A. M. (2005). Effect of gamma radiation on the physiological properties and genetic materials of *Streptomyces albaduncus* and *S. erythrogresius*. *International Journal of Agriculture and Biology*, 7(2), 197-202.
- Neuwirth E. (2022). RColorBrewer: ColorBrewer Palettes. R package version 1.1–3, <  
<https://CRAN.R-project.org/package=RColorBrewer> >
- Park, S. Y., Zhang, Y., O’Loughlin, E. J., Jo, H. Y., Kwon, J. S., & Kwon, M. J. (2024). Temperature-dependent microbial reactions by indigenous microbes in bentonite under Fe(III)-and sulfate-reducing conditions. *Journal of hazardous materials*, 465, 133318. <https://doi.org/10.1016/j.jhazmat.2023.133318>
- Pedersen, K., Bengtsson, A., Blom, A., Johansson, L., & Taborowski, T. (2017). Mobility and reactivity of sulphide in bentonite clays—implications for engineered bentonite barriers in geological repositories for radioactive wastes. *Applied Clay Science*, 146, 495-502. <https://doi.org/10.1016/j.clay.2017.07.003>
- Pedersen, K., Motamedi, M., Karnland, O., Sandén, T., (2000). Mixing and sulphate-reducing activity of bacteria in swelling, compacted bentonite clay under high-level radioactive waste repository conditions. *Journal of Applied Microbiology*, 89, 1038–1047. <https://doi.org/10.1046/j.1365-2672.2000.01212.x>
- Pitonzio, B. J., Amy, P. S., & Rudin, M. (1999). Effect of gamma radiation on native endolithic microorganisms from a radioactive waste deposit site. *Radiation Research*, 152(1), 64-70. <https://doi.org/10.2307/3580050>
- Povedano-Priego, C., Jroundi, F., Morales-Hidalgo, M., Pinel-Cabello, M., Peula-Ruiz, E., Merroun, M. L., & Martín-Sánchez, I. (2024). Unveiling fungal diversity in uranium and glycerol-2-phosphate-amended bentonite microcosms: Implications for radionuclide immobilization within the Deep Geological Repository system. *Science of The Total Environment*, 908, 168284. <https://doi.org/10.1016/j.scitotenv.2023.168284>
- Povedano-Priego, C., Jroundi, F., Solari, P.L., Guerra-Tschuschke, I., Abad-Ortega, M. del M., Link, A., Vilchez-Vargas, R., Merroun, M.L. (2023). Unlocking the bentonite microbial diversity and its implications in selenium bioreduction and biotransformation: Advances in deep geological repositories. *Journal of Hazardous Materials*, 445, 130557. <https://doi.org/10.1016/j.jhazmat.2022.130557>
- Povedano-Priego, C., Jroundi, F., Lopez-Fernandez, M., Morales-Hidalgo, M., Martín-Sánchez, I., Huertas, F. J., Dopson, M. & Merroun, M. L. (2022). Impact of anoxic conditions, uranium(VI) and organic phosphate substrate on the biogeochemical potential of the indigenous bacterial community of bentonite. *Applied Clay Science*, 216, 106331. <https://doi.org/10.1016/j.clay.2021.106331>
- Povedano-Priego, C., Jroundi, F., Lopez-Fernandez, M., Shrestha, R., Spanek, R., Martín-Sánchez, I., Villar, M. V., Ševců, A., Dopson, M. & Merroun, M. L. (2021).

## CHAPTER 1

- Deciphering indigenous bacteria in compacted bentonite through a novel and efficient DNA extraction method: Insights into biogeochemical processes within the Deep Geological Disposal of nuclear waste concept. *Journal of Hazardous Materials*, 408, 124600. <https://doi.org/10.1016/j.jhazmat.2020.124600>
- Povedano-Priego, C., Jroundi, F., Lopez-Fernandez, M., Sánchez-Castro, I., Martín-Sánchez, I., Huertas, F. J., & Merroun, M. L. (2019). Shifts in bentonite bacterial community and mineralogy in response to uranium and glycerol-2-phosphate exposure. *Science of The Total Environment*, 692, 219-232. <https://doi.org/10.1016/j.scitotenv.2019.07.228>
- R Core Team. (2022). R: A language and environment for statistical computing. R Foundation for Statistical Computing, Vienna, Austria. <https://www.Rproject.org/>.
- Ren, M., Li, X., Zhang, Y., Jin, Y., Li, S., & Huang, H. (2018). *Massilia armeniaca* sp. nov., isolated from desert soil. *International Journal of Systematic and Evolutionary Microbiology*, 68(7), 2319-2324. <https://doi.org/10.1099/ijsem.0.002836>
- Robertson, C. E., Harris, J. K., Wagner, B. D., Granger, D., Browne, K., Tatem, B., Feazel, M. L., Park, K., Pace, N. R. & Frank, D. N. (2013). Explicite: graphical user interface software for metadata-driven management, analysis and visualization of microbiome data. *Bioinformatics*, 29(23), 3100-3101. <https://doi.org/10.1093/bioinformatics/btt526>
- Ruiz-Fresneda, M. A., Morales-Hidalgo, M., Povedano-Priego, C., Jroundi, F., Hidalgo-Iruela, J., Cano-Cano, M., Pérez-Muelas, E., Merroun, M. L., & Martín-Sánchez, I. (2024). Unlocking the key role of bentonite fungal isolates in tellurium and selenium bioremediation and biorecovery: Implications in the safety of radioactive waste disposal. *Science of The Total Environment*, 912, 169242. <https://doi.org/10.1016/J.SCITOTENV.2023.169242>
- Ruiz-Fresneda, M. A., Martínez-Moreno, M. F., Povedano-Priego, C., Morales-Hidalgo, M., Jroundi, F., & Merroun, M. L. (2023). Impact of microbial processes on the safety of deep geological repositories for radioactive waste. *Frontiers in Microbiology*, 14, 1134078. <https://doi.org/10.3389/fmicb.2023.1134078>
- Saygin, H., Ay, H., Guven, K., Inan-Bektas, K., Cetin, D., & Sahin, N. (2021). *Saccharopolyspora karakumensis* sp. nov., *Saccharopolyspora elongata* sp. nov., *Saccharopolyspora aridisoli* sp. nov., *Saccharopolyspora terrae* sp. nov. and their biotechnological potential revealed by genome analysis. *Systematic and applied microbiology*, 44(6), 126270. <https://doi.org/10.1016/j.syapm.2021.126270>
- Schloss, P. D., Westcott, S. L., Ryabin, T., Hall, J. R., Hartmann, M., Hollister, E. B., Lesniewski, R.A., Oakley, B.B., Parks, D.H., et al. (2009). Introducing mothur: open-source, platform-independent, community-supported software for describing and comparing microbial communities. *Applied and environmental microbiology*, 75(23), 7537-7541. <https://doi.org/10.1128/AEM.01541-09>

- Shen, Y., Zhuan, R., Chu, L., Xiang, X., Sun, H., & Wang, J. (2019). Inactivation of antibiotic resistance genes in antibiotic fermentation residues by ionizing radiation: Exploring the development of recycling economy in antibiotic pharmaceutical factory. *Waste Management*, 84, 141-146. <https://doi.org/10.1016/j.wasman.2018.11.039>
- Shrestha, R., Cerna, K., Spanek, R., Bartak, D., Cernousek, T., & Sevcu, A. (2022). The effect of low-pH concrete on microbial community development in bentonite suspensions as a model for microbial activity prediction in future nuclear waste repository. *Science of The Total Environment*, 808, 151861. <https://doi.org/10.1016/j.scitotenv.2021.151861>
- Shrestha, R., Černoušek, T., Stoužil, J., Kovářová, H., Sihelská, K., Špánek, R., Ševců, A. & Steinová, J. (2021). Anaerobic microbial corrosion of carbon steel under conditions relevant for deep geological repository of nuclear waste. *Science of The Total Environment*, 800, 149539. <https://doi.org/10.1016/j.scitotenv.2021.149539>
- Sivakala, K. K., Gutiérrez-García, K., Jose, P. A., Thinesh, T., Anandham, R., Barona-Gómez, F., & Sivakumar, N. (2021). Desert environments facilitate unique evolution of biosynthetic potential in *Streptomyces*. *Molecules*, 26(3), 588. <https://doi.org/10.3390/molecules26030588>
- Smith, J. M., Wren, J. C., Odziemkowski, M., & Shoosmith, D. W. (2007). The electrochemical response of preoxidized copper in aqueous sulfide solutions. *Journal of the Electrochemical Society*, 154(8), C431. <https://doi.org/10.1149/1.2745647>
- Thauer, R.K., Stackebrandt, E., Hamilton, W.A. (2007). Energy metabolism and phylogenetic diversity of sulphate-reducing bacteria. *Sulphate-reducing bacteria*, 1-38. <https://doi:10.1017/cbo9780511541490.002>
- Van Gerwen, S. J., Rombouts, F. M., Van't Riet, K., & Zwietering, M. H. (1999). A data analysis of the irradiation parameter D10 for bacteria and spores under various conditions. *Journal of food Protection*, 62(9), 1024-1032. <https://doi.org/10.4315/0362-028X-62.9.1024>
- Villar, M. V., Pérez del Villar, L., Martín, P. L., Pelayo, M., Fernández, A. M., Garralón, A., Cuevas, J., Leguey, S., Caballero, E., Huertas, F. J., Jiménez de Cisneros, C., Linares, J., Reyes, E., Delgado, A., Fernández-Soler, J. M., & Astudillo, J. (2006). The study of Spanish clays for their use as sealing materials in nuclear waste repositories: 20 years of progress. *Journal of Iberian Geology*, 32, 15–36.
- Wagner, C.D., Riggs, W.M., Davis, L.E., Moulder, J.F., Muilenberg, G.E. (1979). Handbook of X-ray photoelectron spectroscopy: a reference book of standard data for use in X-ray photoelectron spectroscopy. Perkin-Elmer Corporation: Eden Prairie, MN.
- Warnes G., Bolker B., Bonebakker L., Gentleman R., Huber W., Liaw A., Lumley T., Maechler M., Magnusson A., Moeller S., Schwartz M., Venables, B. (2022). gplots: Various R Programming Tools for Plotting Data. R package version 3.1.3. <https://CRAN.R-project.org/package=gplots>

## CHAPTER 1

- Yu, X. R., Liu, F., Wang, Z. Y., & Chen, Y. (1990). Auger parameters for sulfur-containing compounds using a mixed aluminum-silver excitation source. *Journal of Electron Spectroscopy and Related Phenomena*, 50(2), 159-166. [https://doi.org/10.1016/0368-2048\(90\)87059-W](https://doi.org/10.1016/0368-2048(90)87059-W)
- Zerouki, C., Bensalah, F., Kuittinen, S., Pappinen, A., & Turunen, O. (2021). Whole-genome sequencing of two *Streptomyces* strains isolated from the sand dunes of Sahara. *BMC genomics*, 22, 1-21. <https://doi.org/10.1186/s12864-021-07866-x>
- Zheng, L., & Fernández, A. M. (2023). Prediction of Long-Term Geochemical Change in Bentonite Based on the Interpretative THMC Model of the FEBEX In Situ Test. *Minerals*, 13(12), 1522. <https://doi.org/10.3390/min13121522>

Supplementary material for:

**Assessing the impact of radiation and high compaction on FEBEX bentonite: microbial, mineralogical, and copper corrosion studies**

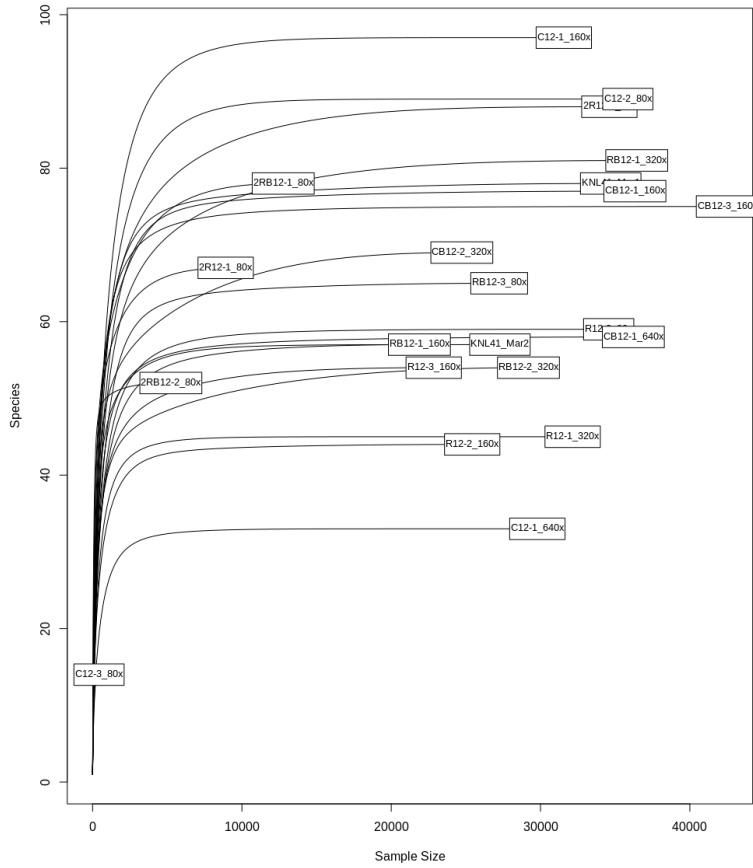
**Mar Morales-Hidalgo**<sup>1,\*</sup>, Marcos F. Martinez-Moreno<sup>1</sup>, Cristina Povedano-Priego<sup>1</sup>, Kateřina Černá<sup>2</sup>, Ana Maria Fernandez<sup>3</sup>, Ursula Alonso<sup>3</sup>, Adam D. Mumford<sup>4</sup>, Jesus Ojeda<sup>4</sup>, Fadwa Jroundi<sup>1</sup> and Mohamed L. Merroun<sup>1</sup>

<sup>1</sup>*Faculty of Sciences, Department of Microbiology, University of Granada, Granada, Spain.*

<sup>2</sup>*Technical University of Liberec, Institute for Nanomaterials, Advanced Technologies and Innovations, Bendlova 1407/7, 461 17 Liberec 1, Czech Republic*

<sup>3</sup>*Departamento de Impacto Ambiental de la Energia, CIEMAT, Avenida Complutense, 22-28040 Madrid, Spain*

<sup>4</sup>*Department of Chemical Engineering, Faculty of Science and Engineering, Swansea University, Swansea, United Kingdom*



**Supplementary Figure S1.** Rarefaction curves of the sequenced samples representing the richness and sample size. C: non-irradiated compacted treatments; B: SRB consortium; 1\_R: one-time irradiated treatments in the middle of the incubation time as late exposure (14 kGy); 2R: two-times irradiated treatments (28 kGy); 12: one year of anoxic incubation.

**Supplementary Table S1.** Phyla relative abundances of Bacteria and Archaea in 1-year bentonite blocks treatments in triplicates (except 2R12 and 2RB12 in duplicate). C: non-irradiated compacted treatments; B: SRB consortium; I\_R: one-time irradiated treatments in the middle of the incubation time as late exposure (14 kGy); 2R: two-times irradiated treatments (28 kGy); 12: one year of anoxic incubation.

Phyla	Relative abundances (%)					
	C12	CB12	I_R12	I_RB12	2R12	2RB12
Actinomycetota	76.66	64.81	81.64	78.34	5.06	11.54
Pseudomonadota	16.27	14.96	17.34	12.02	81.00	64.12
Bacillota	5.86	13.53	0.39	6.60	5.88	17.59
Thermodesulfobacteriota	0.05	5.86	0.08	2.49	0.00	2.65
Bacteroidota	0.54	0.40	0.23	0.22	1.23	1.66
Myxococcota	0.14	0.00	0.01	0.09	3.68	0.04
Chloroflexota	0.07	0.03	0.09	0.07	1.37	0.34
Acidobacteriota	0.05	0.18	0.03	0.03	0.39	0.88
Cyanobacteria	0.13	0.16	0.13	0.06	0.00	0.91
Verrucomicrobiota	0.03	0.03	0.00	0.00	0.89	0.06
Gemmatimonadota	0.12	0.03	0.06	0.03	0.00	0.07
Planctomycetota	0.05	0.00	0.01	0.01	0.27	0.07
Fusobacteriota	0.00	0.00	0.00	0.00	0.17	0.00
Bdellovibrionota	0.02	0.00	0.00	0.00	0.00	0.04
FCPU426	0.00	0.00	0.00	0.00	0.02	0.00
Patescibacteria	0.00	0.00	0.00	0.00	0.00	0.01
Methylomirabilota	0.00	0.00	0.01	0.01	0.00	0.00
Nitrospirota	0.01	0.00	0.00	0.00	0.01	0.00
GAL15	0.00	0.00	0.00	0.00	0.00	0.03
Halobacterota	0.00	0.00	0.00	0.00	0.04	0.00
Deinococcota	0.00	0.00	0.00	0.02	0.00	0.00

## CHAPTER 1

**Supplementary Table S2.** Percentages of relative abundances at genus level of 1-year bentonite blocks treatments. Treatments studied in triplicated (except 2R12 and 2RB12 in duplicate). Cut off:  $\geq 0.02\%$ . C: non-irradiated compacted treatments; B: SRB consortium; I\_R: one-time irradiated treatments in the middle of the incubation time as late exposure (14 kGy); 2R: two-times irradiated treatments (28 kGy); 12: one year of anoxic incubation.

Genera	Relative abundances (%)						
	Total	C12	CB12	I_R12	I_RB12	2R12	2RB12
<i>Saccharopolyspora</i>	57.68	65.58	59.49	70.56	74.54	0.84	2.49
<i>Enterobacteriaceae</i>	5.75	5.92	3.48	6.52	4.65	8.06	13.17
<i>Streptomyces</i>	5.49	9.55	3.26	9.60	2.60	0.22	0.08
<i>Massilia</i>	3.16	0.49	0.16	1.00	0.29	27.52	0.01
<i>Acinetobacter</i>	3.12	1.08	1.16	0.91	0.66	19.42	8.29
<i>Pseudomonas</i>	2.8	2.15	2.11	3.80	1.50	3.62	9.22
<i>Escherichia-Shigella</i>	2.45	1.40	2.10	1.63	1.49	7.16	7.38
<i>Bacillus</i>	2.37	0.91	6.12	0.00	2.44	0.00	6.20
<i>Desulfovibrio</i>	1.97	0.05	5.86	0.00	2.49	0.00	2.65
<i>Desulfotomaculum</i>	1.97	0.00	5.22	0.00	3.02	0.00	4.51
<i>Bacillales</i>	0.76	2.92	0.29	0.00	0.00	0.00	0.00
<i>Comamonadaceae</i>	0.69	0.63	0.38	0.06	0.57	0.72	6.32
<i>Noviherbaspirillum</i>	0.56	0.50	0.52	0.23	0.24	1.31	2.27
<i>Alkaliphilus</i>	0.54	0.00	1.48	0.00	0.69	0.04	1.36
<i>Allorhizobium-Neorhizobium-Pararhizobium-Rhizobium</i>	0.51	0.01	0.48	0.00	0.50	2.81	0.52
<i>Romboutsia</i>	0.43	0.07	0.00	0.00	0.00	4.13	0.00
<i>Paracoccus</i>	0.36	0.19	0.11	0.21	0.08	0.70	3.82

<i>Stenotrophomonas</i>	0.35	0.33	0.18	0.22	0.01	1.35	1.05
<i>Streptococcus</i>	0.34	0.81	0.14	0.00	0.07	0.73	0.91
<i>Sphingomonas</i>	0.28	0.32	0.60	0.17	0.01	0.00	0.64
<i>Lysobacter</i>	0.28	0.18	0.30	0.15	0.50	0.47	0.00
<i>Corynebacterium</i>	0.24	0.13	0.01	0.03	0.09	0.95	2.08
<i>Nocardioides</i>	0.24	0.16	0.28	0.20	0.26	0.04	1.06
<i>Pseudonocardia</i>	0.23	0.02	0.64	0.12	0.03	0.00	1.04
<i>Ralstonia</i>	0.22	0.12	0.27	0.40	0.13	0.26	0.00
<i>Hydrogenophilus</i>	0.19	0.56	0.05	0.00	0.00	0.49	0.00
<i>Methylobacterium-Methylorubrum</i>	0.18	0.00	0.07	0.00	0.21	0.68	1.48
<i>Staphylococcus</i>	0.17	0.05	0.08	0.01	0.05	0.00	3.03
<i>Sphingomonadaceae</i>	0.17	0.11	0.17	0.21	0.17	0.00	0.60
<i>Thiopseudomonas</i>	0.17	0.00	0.41	0.22	0.00	0.32	0.00
<i>Amycolatopsis</i>	0.16	0.08	0.22	0.09	0.16	0.00	0.92
<i>KD4-96</i>	0.16	0.00	0.00	0.04	0.05	1.27	0.27
<i>Arthrobacter</i>	0.15	0.08	0.21	0.12	0.04	0.15	0.73
uncultured	0.15	0.00	0.00	0.00	0.07	0.00	3.29
<i>Chloroplast</i>	0.14	0.12	0.16	0.13	0.06	0.00	0.91
uncultured	0.14	0.00	0.00	0.00	0.00	1.38	0.00
<i>Haliangium</i>	0.13	0.14	0.00	0.00	0.00	0.93	0.04
<i>Brevundimonas</i>	0.12	0.09	0.11	0.09	0.06	0.47	0.00
<i>Oxalobacteraceae</i>	0.11	0.12	0.09	0.03	0.00	0.45	0.20
<i>TRA3-20</i>	0.11	0.06	0.40	0.00	0.00	0.00	0.00
<i>Prauserella</i>	0.1	0.26	0.04	0.11	0.04	0.00	0.00

## CHAPTER 1

<i>Altererythrobacter</i>	0.1	0.05	0.12	0.02	0.05	0.00	1.09
<i>Photobacterium</i>	0.1	0.41	0.00	0.00	0.00	0.00	0.00
<i>Micrococcaceae</i>	0.09	0.05	0.07	0.05	0.13	0.32	0.00
<i>Cytophaga</i>	0.09	0.00	0.22	0.00	0.00	0.22	0.29
<i>Tepidanaerobacter</i>	0.09	0.00	0.00	0.00	0.00	0.94	0.00
<i>KD3-10</i>	0.09	0.00	0.00	0.00	0.00	0.85	0.00
<i>Muricoccus</i>	0.09	0.06	0.00	0.00	0.00	0.80	0.00
<i>Rhizobiaceae</i>	0.09	0.00	0.02	0.21	0.04	0.00	0.80
<i>PLTA13</i>	0.09	0.00	0.00	0.00	0.00	0.87	0.00
<i>Ahniella</i>	0.09	0.00	0.00	0.00	0.00	0.92	0.00
uncultured	0.08	0.05	0.13	0.02	0.02	0.31	0.07
uncultured	0.08	0.07	0.07	0.11	0.08	0.00	0.28
<i>Intrasporangiaceae</i>	0.08	0.00	0.00	0.00	0.05	0.26	1.10
<i>Saccharomonospora</i>	0.08	0.05	0.17	0.05	0.08	0.00	0.00
<i>Chryseobacterium</i>	0.08	0.32	0.00	0.00	0.00	0.00	0.00
<i>Bradyrhizobium</i>	0.08	0.07	0.00	0.12	0.04	0.35	0.00
<i>Rubellimicrobium</i>	0.08	0.06	0.10	0.04	0.06	0.20	0.00
<i>Novosphingobium</i>	0.08	0.06	0.02	0.32	0.00	0.00	0.00
uncultured	0.07	0.04	0.02	0.08	0.00	0.27	0.20
<i>Sanguibacter</i>	0.07	0.00	0.04	0.00	0.00	0.61	0.00
<i>Lysinibacillus</i>	0.07	0.00	0.00	0.36	0.00	0.00	0.00
<i>Paenibacillus</i>	0.07	0.29	0.01	0.00	0.00	0.00	0.00
<i>Rhodopseudomonas</i>	0.07	0.00	0.30	0.00	0.00	0.00	0.00
<i>Cellvibrionaceae</i>	0.07	0.00	0.27	0.00	0.06	0.00	0.00

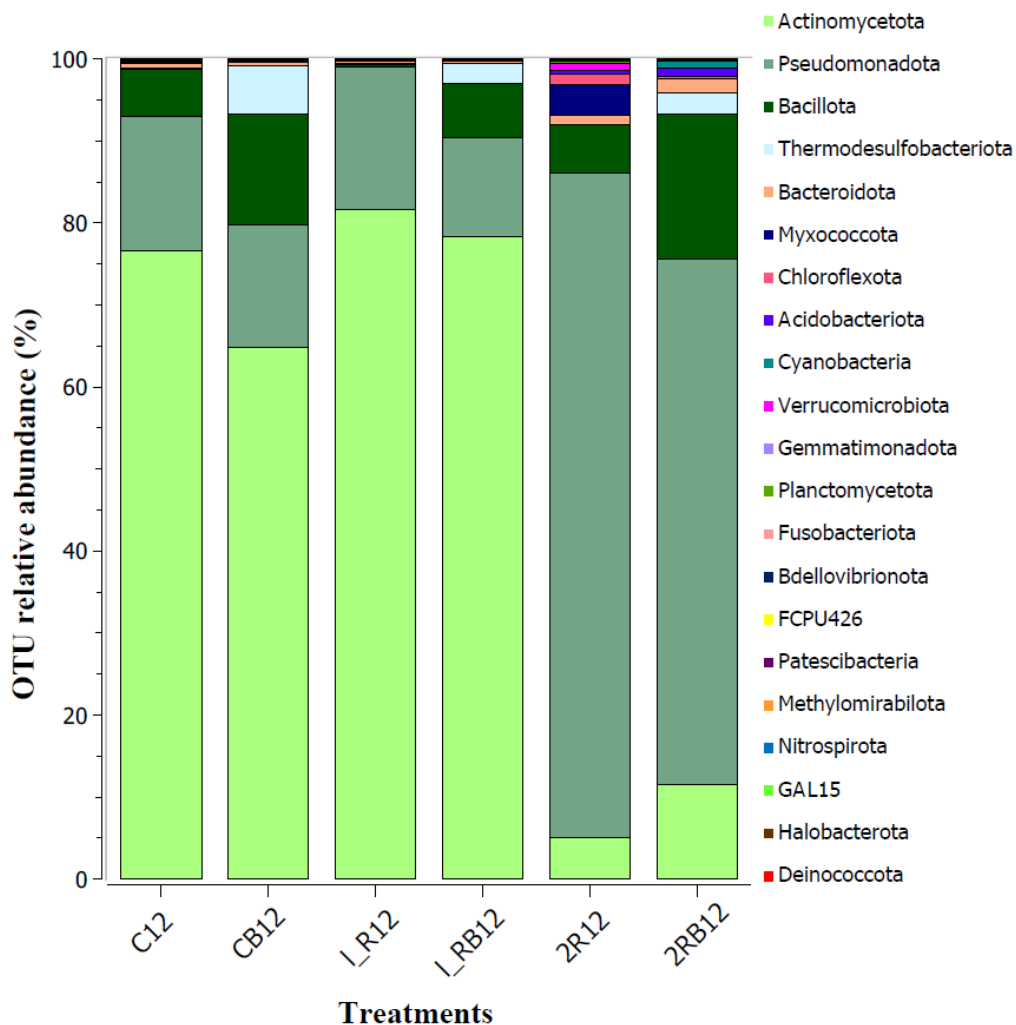
<i>Micrococcus</i>	0.06	0.14	0.00	0.00	0.00	0.30	0.00
<i>Pseudonocardiaceae</i>	0.06	0.00	0.04	0.17	0.09	0.00	0.00
<i>Pontibacter</i>	0.06	0.04	0.02	0.12	0.04	0.20	0.00
uncultured	0.06	0.00	0.00	0.00	0.02	0.58	0.00
<i>Cohnella</i>	0.06	0.25	0.00	0.00	0.00	0.00	0.00
<i>Rhodobacteraceae</i>	0.06	0.06	0.00	0.22	0.00	0.00	0.00
<i>Haemophilus</i>	0.06	0.27	0.00	0.00	0.00	0.00	0.00
<i>Pseudoxanthomonas</i>	0.06	0.01	0.26	0.00	0.00	0.00	0.00
<i>Promicromonospora</i>	0.05	0.00	0.00	0.03	0.07	0.35	0.00
<i>Solirubrobacter</i>	0.05	0.01	0.08	0.09	0.00	0.04	0.28
<i>Skermanella</i>	0.05	0.00	0.00	0.00	0.04	0.43	0.00
<i>Pandoraea</i>	0.05	0.00	0.00	0.00	0.00	0.00	1.14
<i>Marinomonas</i>	0.05	0.23	0.00	0.00	0.00	0.00	0.00
<i>Adhaeribacter</i>	0.04	0.01	0.07	0.02	0.07	0.00	0.00
<i>Hymenobacter</i>	0.04	0.00	0.00	0.01	0.03	0.00	0.76
<i>Gitt-GS-136</i>	0.04	0.04	0.02	0.04	0.02	0.08	0.00
<i>Oceanobacillus</i>	0.04	0.00	0.00	0.00	0.00	0.00	0.89
<i>Planococcaceae</i>	0.04	0.00	0.14	0.00	0.06	0.00	0.00
<i>Sarcina</i>	0.04	0.00	0.00	0.00	0.21	0.00	0.00
<i>Agathobacter</i>	0.04	0.17	0.00	0.00	0.00	0.00	0.00
<i>Anaerococcus</i>	0.04	0.00	0.00	0.00	0.06	0.00	0.68
<i>Pajaroellobacter</i>	0.04	0.00	0.00	0.01	0.00	0.39	0.00
<i>Curvibacter</i>	0.04	0.00	0.11	0.00	0.00	0.12	0.00
<i>Cellvibrio</i>	0.04	0.02	0.08	0.06	0.00	0.00	0.00

## CHAPTER 1

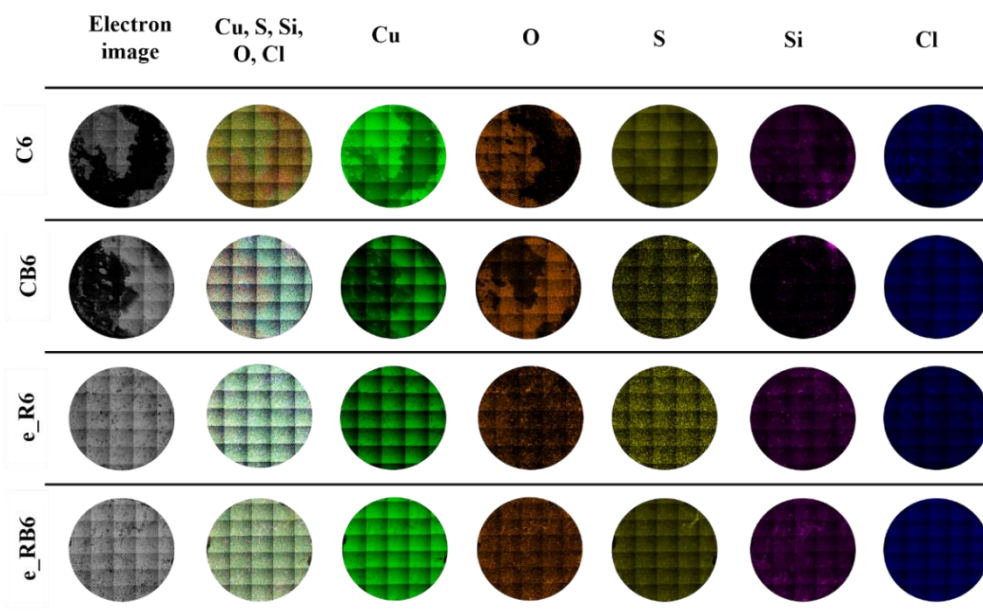
<i>Enhydrobacter</i>	0.04	0.04	0.00	0.00	0.00	0.00	0.65
<i>Bryobacter</i>	0.03	0.00	0.00	0.00	0.00	0.00	0.76
<i>Brachybacterium</i>	0.03	0.14	0.00	0.00	0.00	0.00	0.00
<i>Actinomadura</i>	0.03	0.00	0.00	0.00	0.02	0.26	0.00
<i>Flavobacterium</i>	0.03	0.04	0.00	0.06	0.00	0.04	0.03
<i>Longimicrobiaceae</i>	0.03	0.07	0.03	0.04	0.02	0.00	0.00
<i>Roseomonas</i>	0.03	0.09	0.00	0.00	0.04	0.00	0.00
<i>Aureimonas</i>	0.03	0.00	0.00	0.00	0.00	0.00	0.66
<i>Comamonas</i>	0.03	0.00	0.00	0.00	0.00	0.30	0.00
uncultured	0.03	0.00	0.00	0.00	0.00	0.30	0.00
uncultured	0.03	0.00	0.00	0.00	0.00	0.31	0.00
<i>Candidatus_Udaeobacter</i>	0.03	0.00	0.00	0.00	0.00	0.34	0.00
<i>Micromonospora</i>	0.02	0.00	0.00	0.02	0.00	0.15	0.14
<i>Nocardiodiaceae</i>	0.02	0.04	0.04	0.00	0.00	0.00	0.00
<i>Marmoricola</i>	0.02	0.03	0.00	0.04	0.00	0.00	0.23
<i>Pedobacter</i>	0.02	0.00	0.00	0.00	0.01	0.00	0.43
<i>Desulfuromonas</i>	0.02	0.00	0.00	0.08	0.00	0.00	0.00
<i>CAG-352</i>	0.02	0.08	0.00	0.00	0.00	0.00	0.00
<i>Fusobacterium</i>	0.02	0.00	0.00	0.00	0.00	0.17	0.00
<i>mle1-27</i>	0.02	0.00	0.00	0.00	0.09	0.00	0.00
<i>WD2101_soil_group</i>	0.02	0.00	0.00	0.01	0.01	0.19	0.02
<i>Phenylobacterium</i>	0.02	0.00	0.00	0.12	0.00	0.00	0.00
<i>Xanthobacteraceae</i>	0.02	0.02	0.06	0.00	0.00	0.00	0.00
<i>Qipengyuania</i>	0.02	0.00	0.10	0.00	0.00	0.00	0.00

<i>Sphingobium</i>	0.02	0.00	0.00	0.00	0.00	0.17	0.00
uncultured	0.02	0.00	0.00	0.00	0.13	0.00	0.00
<i>Gammaproteobacteria</i>	0.02	0.00	0.00	0.00	0.00	0.00	0.49
<i>Aeromonas</i>	0.02	0.02	0.00	0.02	0.00	0.00	0.32
<i>Ramlibacter</i>	0.02	0.03	0.00	0.00	0.07	0.00	0.00
<i>MND1</i>	0.02	0.00	0.02	0.00	0.00	0.16	0.00
<i>Pantoea</i>	0.02	0.00	0.00	0.10	0.00	0.00	0.00
<i>Pseudomonadaceae</i>	0.02	0.00	0.10	0.00	0.00	0.00	0.00
uncultured	0.02	0.00	0.00	0.00	0.13	0.00	0.00
<i>Chthoniobacter</i>	0.02	0.00	0.00	0.00	0.00	0.19	0.01
<i>Opitutus</i>	0.02	0.00	0.00	0.00	0.00	0.23	0.00

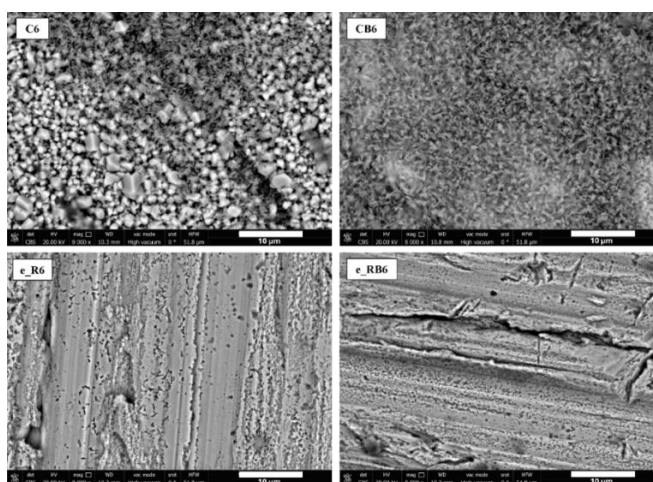
---



**Supplementary Figure S2.** OTU relative abundances at phylum level of the microbial communities in compacted bentonite after 1 year of anoxic incubation. Stacked bars represent the mean values of biological triplicates (except 2R12 and 2RB12 in duplicate). C: non-irradiated compacted treatments; B: SRB consortium; L\_R: one-time irradiated treatments in the middle of the incubation time as late exposure (14 kGy); 2R: two-times irradiated treatments (28 kGy); 12: one year of anoxic incubation.



**Supplementary Figure S3.** The EDX maps of the entire surface of each study Cu disk after six months of incubation. The first column corresponds to electron images and the second column to the summatory EDX map of all detected elements. The other columns correspond to Cu (green), O (orange), S (yellow), Si (pink), Cl (dark blue). Glossary: C: non-irradiated compacted treatments; B: SRB consortium; e\_R: one-time irradiated treatments prior incubation time as early exposure (14 kGy); 6: six months of anoxic incubation.



**Supplementary Figure S4.** ESEM images of 6-month treatments Cu disks surfaces. Magnitude: 8,000X. Glossary: C: non-irradiated compacted treatments; B: SRB consortium; e\_R: one-time irradiated treatments prior incubation time as early exposure (14 kGy); 6: six months of anoxic incubation.

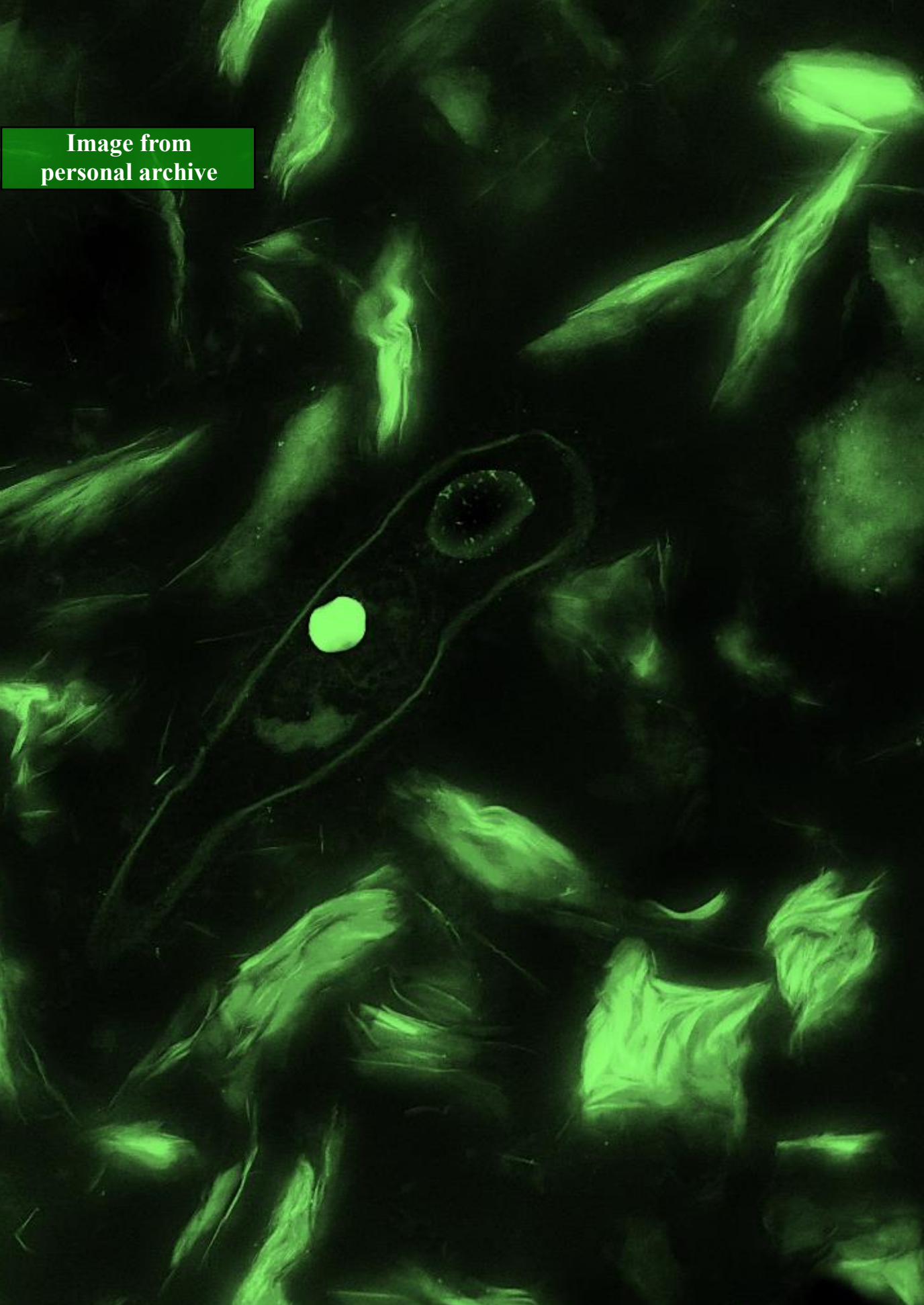
## CHAPTER 1

**Supplementary Table S3.** Summary table of the main results obtained by treatment. T.0 N: non-incubated non-irradiated powdered bentonite; T.0 IR: non-incubated irradiated powdered bentonite (14 kGy); C: non-irradiated compacted treatments; B: SRB consortium; e\_R: one-time irradiated treatments prior incubation time as early exposure (14 kGy); l\_R: one-time irradiated treatments in the middle of the incubation time as late exposure (14 kGy); 2R: two-times irradiated treatments (28 kGy); 6: six months of anoxic incubation; 12: one year of anoxic incubation. +: presence; -: absence; /: non-studied.

Treatment	Viability of heterotrophs	Viability of SRB	Copper oxides	Copper sulfides	Possible copper sulfates
T.0 N	+	+	/	/	/
T. 0 IR	-	-	/	/	/
C6	+	+	+	-	-
CB6	+	+	+	+	-
e_R6	-	-	+	-	+
e_RB6	+	+	+	+	+
C12	+	+	+	-	-
CB12	+	+	+	+	-
l_R12	+	-	+	-	+
l_RB12	+	-	+	+	+
2R12	-	-	+	-	+
2RB12	-	-	+	-	+



Image from  
personal archive



## *Chapter 2*

### High temperature impact on bentonite microbial communities: A study of Se(IV) biogeochemical cycle

#### Authors

**Mar Morales-Hidalgo\***, Cristina Povedano-Priego, Marcos F. Martinez-Moreno, Fadwa Jroundi and Mohamed L. Merroun

---

*Faculty of Sciences, Department of Microbiology, University of Granada, Granada, Spain*

## CHAPTER 2

**Abstract**

The deep geological repository (DGR) is the globally accepted option for storing highly radioactive waste, being bentonite clay the preferred backfilling and sealing material. In such DGRs, nuclear waste will generate significant heat, reaching temperatures of 60 °C or higher for the first few hundred years. Moreover, among the radionuclides stored,  $^{79}\text{Se}$  is one of the critical element, as identified by safety assessments. Evaluating the role of bentonite indigenous microorganisms in retarding radionuclide mobility, if a leak occurs in the system, is of high interest for DGR safety issues. Therefore, in this study Spanish bentonite microcosms saturated with equilibrium water were treated with Se(IV) as an inactive analog for  $^{79}\text{Se}$ , and amended with acetate, lactate, sulfate, and a bacterial consortium. Such microcosms aimed to simulate a system failure scenario with organic-rich groundwater seepage and high temperature of 60 °C under anoxic conditions. Following a period of two months of incubation, the elevated temperature conditions facilitated the presence of bentonite autochthonous thermophilic genera such as *Clostridium*, *Pseudomonas*, *Caloribacterium*, *Thermaerobacter* or *Brockia*. Besides, the presence of the bacterial consortium had a strong impact on the microbial communities, leading to the dominance of *Stenotrophomonas* and *Pseudomonas*. A high influence of the bacterial consortium on the Se reduction as well was observed, as shown by the color shift to the orange after only 4 days of incubation. Additionally, ICP-MS (inductively coupled plasma mass spectrometry) data indicated a reduction of nearly 100% of soluble Se(IV) after two months. However, in non-consortium microcosms, the percentage of reduction was much slower (~6.7%), but still occurred. Accordingly, at that time, scanning transmission electron microscopy (STEM) coupled with energy dispersive X-ray (EDX) results confirmed the reduction of Se(IV) to form Se(0) nanoparticles (NPs) with different morphologies or Se+Fe nanoaggregates likely corresponding to the mineral ferroselite ( $\text{FeSe}_2$ ). Thus, bentonite microbial communities would affect the biogeochemical cycle of Se through the immobilization of this critical radionuclide retarding its mobility at DGR barriers.

**Keywords:** *Bentonite, Selenium, Nuclear waste repository, Microbial diversity, Electron microscopy.*

## CHAPTER 2

## 1. Introduction

It is estimated that high-level radioactive waste (HLW) will emit radiation for periods of time lasting up to hundreds of thousands of years. Confinement of these HLW in future deep geological repository (DGR) systems represents the optimal approach for the management of these hazardous waste, ensuring thus the biosphere protection. These DGRs consists of multi-barrier systems located between 500 -1,000 meters underground in geologically stable formations (Tondel & Lindahl, 2019). The barriers include as artificial ones, a metallic container (e.g. copper, carbon steel, titanium) that directly contains the waste, in addition to another barrier made of bentonite, as filling and sealing material, that would act as a safeguard against potential system failures (WNA, 2023). Bentonite is a clay-based material considered for its use as a buffer in a number of DGR concepts, including those in Finland, Sweden, Spain, Switzerland, and Canada (Haynes et al., 2018; Morales-Hidalgo et al., 2024). The bentonite will be employed in a compacted state at densities that vary between companies, with an average of approximately  $1.6 \text{ g/cm}^3$ . Once the repository is closed, the canister-bentonite interface will go through four distinct phases over the next thousand years. Initially, during the first few decades, the surface of the metal canister will experience dry and oxic conditions with high temperatures. This will be followed by an oxic atmosphere and water unsaturated buffer material phase, lasting several hundred years. In the subsequent few hundred years, oxygen will be depleted, resulting in an anoxic environment with still unsaturated conditions. Ultimately, a cold, anoxic, and enduring phase with saturated conditions resulting from groundwater infiltrations will prevail (King et al., 2017). Depending on the DGR model of each country, the average maximum temperature on the surface of the metal container would be expected to reach around  $100 \text{ }^\circ\text{C}$ . Therefore, most of disposal agencies (POSIVA, SKB, ANDRA, NWMO) have established this temperature as the exposure limit for

## CHAPTER 2

scenarios involving a bentonite buffer, in order to prevent this barrier from drying out, thermal alterations such as illitization, and to minimize *in situ* canister corrosion rates (Morales-Hidalgo et al., 2024a; Hicks et al., 2009; Haynes et al., 2018). These elevated temperatures will persist for several decades until it begins to gradually decline over periods of up to thousands of years, during which the system will remain at temperatures above 70-60 °C (King et al., 2017). Ensuring the integrity of these systems requires extensive multidisciplinary studies conducted over many years. Although current predictive models do not expect fully saturated water conditions, except for the latest years of the repository, it is essential to investigate a wide range of potential scenarios considering both realistic and worst-case perspectives, in order to be prepared for possible system failures in future nuclear repositories. Potentially critical scenarios may include corrosion of metal containers and the consequent leakage of radioactive waste, loss of bentonite compaction properties, groundwater seepage including organic matter, and microorganism activity, among others.

In the event of such worst-case scenario, microorganisms would play a crucial role. The presence of water, organic matter sources, and uncompacted bentonite conditions would stimulate their activity, conditioning thus the DGR safety. Moreover, in case of radionuclides' release from the canisters, microorganisms could contribute to their mobilization or immobilization through various microbial processes including biosorption, bioaccumulation, biomineralization, and biotransformation, among others (Merroun & Selenska-Pobell, 2008; Ruiz-Fresneda et al., 2023). In the HLW, it is expected the presence of the radioisotope  $^{79}\text{Se}$  as one of the most critical element, for its long half-life ranging from  $6.5 \times 10^4$  to  $1.13 \times 10^6$  years (Atwood, 2010). This  $\beta$ -radiation emitting radioisotope is generated during the fission of  $^{235}\text{U}$  and other fissile radionuclides such as  $^{239}\text{Pu}$  (Hassan et al., 2021). Additionally, it

can be formed during the neutron activation of  $^{78}\text{Se}$  present in the materials used for constructing nuclear fission reactors. Consequently,  $^{79}\text{Se}$  is only found in significant quantities associated with irradiated nuclear fuels and radioactive waste (Atwood, 2010; Jörg et al, 2010). Furthermore, the chemical toxicity of Se is closely linked to its oxidation state, as demonstrated in previous studies performed by Ruiz-Fresneda et al. (2018, 2020). The oxidized states, Se(VI) and Se(IV), are more toxic, more soluble and therefore more bioavailable than the reduced states, Se(0) and Se(-II)(Ruiz-Fresneda et al., 2020). As recently reported by Povedano-Priego et al. (2023), the presence of Se(IV) has been shown to exert a significant impact on the native microbial communities of Spanish bentonite. The presence of Se in bentonite can influence the microbial composition by increasing the number of bacteria that are able to tolerate this metalloid. These bacteria, including *Pseudomonas*, *Stenotrophomonas*, and *Desulfosporosinus*, may develop a variety of Se detoxification mechanisms. Furthermore, there is evidence that microbial reduction of Se can occur under both anaerobic and aerobic conditions by a wide range of microbes (Lampis et al., 2014). For example, bacterial strains such as *Bacillus* sp., *Rhodobacter*, *Stenotrophomonas maltophilia*, *Stenotrophomonas bentonitica* BII-R7, and *Shewanella oneidensis*, among others, have been previously studied as Se bioreducers (Prakash et al., 2009; Antonioli et al., 2007; Ruiz-Fresneda et al., 2018, 2019, 2020; Di Gregorio et al., 2005; Li et al., 2014).

During the initial years of the repository, the anticipated high temperatures would restrict microbial activity and could impact the diversity of the microbial communities especially those naturally occurring in the bentonite. Nevertheless, it is possible that certain microorganisms remain active under such conditions. At high temperatures, cell membranes become more fluid, and critical macromolecules can be denaturalized (DNA, RNA, proteins), resulting in the loss of viability. However, some microorganisms can mitigate these

## CHAPTER 2

effects by (i) synthesizing heat-resistant proteins, (ii) rapidly regenerating sensitive molecules, and (iii) producing spores that remain viable for long durations (Haynes et al., 2018). According to Bartak et al. (2024), several thermophilic species (e.g., *Caldinitratiruptor* and *Brockia*) and thermotolerant spore-forming genera (e.g., *Thermincola* and *Bacillus*) were identified in bentonite treated at 90 °C. Additionally, they established this temperature as a threshold for inhibiting microbial activity and growth in all tested bentonite suspensions. Since temperature stress stands as a significant factor controlling the microbial activity and, consequently, impacting the microorganisms in the future repositories, investigating this stress from a microbiological point of view would be crucial to obtain more reliable predictions about the microbial activities occurring under different scenarios in future DGRs.

In light of the aforementioned considerations, the present study aimed at simulating one of the most adverse scenarios that could arise in the event of a system failure at an early stage, where temperature is a key factor. This worst-case scenario would involve the loss of bentonite compaction resulting from the seepage of nutrient-enriched groundwater, along with the leakage of radionuclides, specifically selenium, from the metallic copper container. Previous studies have focused on assessing the effect of Se on the bentonite microbial communities (Povedano-Priego et al., 2023). However, here for the first time, we further explore the influence of high temperature in these conditions and in the presence of copper plates simulating the metal containers. For this purpose, water-saturated bentonite microcosms were prepared with Spanish bentonite, doped with electron donors and acceptor, together with Se(IV) as an inactive chemical analog of  $^{79}\text{Se}$ . Furthermore, some treatments included a bacterial consortium to facilitate the study of processes under accelerated conditions of microbial activity. Therefore, this study aimed to investigate, using a multidisciplinary approach, the impact of selenium on the

microbial communities of Spanish bentonite, under high temperature conditions (60 °C). All these clues would help to assess the influence of these microorganisms on the geochemical evolution of the metalloid during an early stage (lasting 2 months) of anoxic incubation.

## **2. Materials and methods**

### **2.1. Bentonite collection**

Spanish bentonite was collected from a geological site called “El Cortijo de Archidona” in Almeria (Spain), in February 2021. Sampling was conducted, using a soil auger, under aseptic conditions to prevent contamination with exogenous microorganisms. The depth of extraction was approximately 90 centimeters. The samples were stored at 4 °C in the laboratory until their use.

### **2.2. Experimental setup of water-saturated bentonite microcosms**

Prior to the elaboration of the water-saturated bentonite microcosms, it was necessary to ensure the dryness and the grain size homogeneity of the bentonite. Therefore, the samples were maintained in a laminar flow hood for a period of three to four days, at room temperature. In addition, in order to reduce the grain size and homogenize the bentonite, a carbon steel nonstick roller pin was employed under sterile conditions.

Water-saturated bentonite microcosms were elaborated in 250 mL borosilicate glass bottles, containing 50 g of bentonite dry powder, and a final volume of 230 mL of equilibrium water with electron donors and acceptor. Equilibrium water was prepared by mixing bentonite with distilled water in a ratio of 1:100 (g:mL). The mixture was incubated at 28 °C under agitation at 180 rpm for 24 hours. Subsequently, the supernatant was collected by centrifugation at 10,000 xg for 5 minutes, and then sterilized by autoclave. The major elements composition of this equilibrium water was determined by Inductively Coupled

## CHAPTER 2

Plasma-Mass Spectroscopy (ICP-MS) with a NexION 300D spectrometer. The data is provided in **Supplementary Table S1**. Sodium acetate ( $C_2H_3NaO_2$ ) and sodium lactate ( $NaC_3H_5O_3$ ) were added as electron donors at final concentrations of 30 mM and 10 mM, respectively. These electron donors aim to stimulate the growth of bentonite microbial communities, including sulfate-reducing bacteria (SRB). Additionally, 20 mM of sodium sulfate was added as the final electron acceptor for the SRB. Stock solutions were prepared with distilled water and autoclaved at 121 °C for 22 minutes. Some microcosms received a selenium treatment (Se) by adding a final concentration of 2 mM sodium selenite ( $Na_2SeO_3$ ), in order to study its effects on bentonite microbial diversity. Se stock solution (1 M) was prepared and sterilized by filtration through 0.22  $\mu$ m pore-sized nitrocellulose filters and stored at 4 °C until further use.

Furthermore, a second batch of microcosms was prepared using heat-shocked bentonite (Bst). For that purpose, tyndallization method was employed which consists of a moist heating treatment in cycles of 110 °C for 45 minutes, three days in succession. This process is able to reduce most of the microorganisms present in the bentonite. Although this method is not optimal for the complete sterilization of bentonite, the objective of these treatments was to analyze the possible abiotic processes in comparison with those observed in natural bentonite microcosms.

Moreover, a bacterial consortium (C) composed of four genera, previously identified in other studies to belong to the bacterial community of the Spanish bentonite, was also added to some microcosms as a treatment (Lopez-Fernandez et al., 2018, 2014; Povedano-Priego et al., 2019, 2021), with the aim to accelerate the microbial processes. This consortium included *Stenotrophomonas bentonitica* BII-R7, *Bacillus* sp. BII-C3, *Pseudomonas*

*putida* ATCC33015, and *Amycolatopsis ruanii* NCIMB14711. The culture media and incubation conditions of this consortium are described in detail in Morales-Hidalgo et al. (2024b).

On the other hand, all microcosms included three plates of pure metallic copper, provided by the Centro de Instrumentación Científica (CIC, UGR), with dimensions of 8 mm in height, 15 mm in width, and 2 mm in thickness. Prior to their inclusion into each microcosm, the plates were subjected to a chemical cleaning and sterilization process following the protocol detailed by Guo M. (2020). These Cu plates were added for the copper corrosion studies, which will be presented in **Chapter 3** of this doctoral thesis.

These microcosms were incubated under conditions relevant to the future nuclear waste repository: anoxic atmosphere, high temperature (60 °C), and darkness. Anoxic conditions were achieved by using butyl rubber stoppers and bubbling the microcosms with N<sub>2</sub> for 20 minutes, as molecular nitrogen displaces oxygen molecules (**Supplementary Fig. S1**). Altogether, 8 treatments were considered and prepared in triplicate as biological replicates obtaining a total of 24 microcosms. The designation of each treatment is indicated in **Table 1** and the detailed experimental setup workflow is presented in **Figure 1**.

## CHAPTER 2

**Table 1.** Different experimental conditions of water-saturated bentonite microcosms. B: natural bentonite; Bst: heat-shocked bentonite; C: bacterial consortium; Se: sodium selenite (2 mM).

Sample Name	Natural bentonite (B)	Heat-shocked bentonite (Bst)	Bacterial consortium (C)	Selenium (Se)
<b>B</b>	+	-	-	-
<b>BC</b>	+	-	+	-
<b>Bst</b>	-	+	-	-
<b>BstC</b>	-	+	+	-
<b>BSe</b>	+	-	-	+
<b>BCSe</b>	+	-	+	+
<b>BstSe</b>	-	+	-	+
<b>BstCSe</b>	-	+	+	+

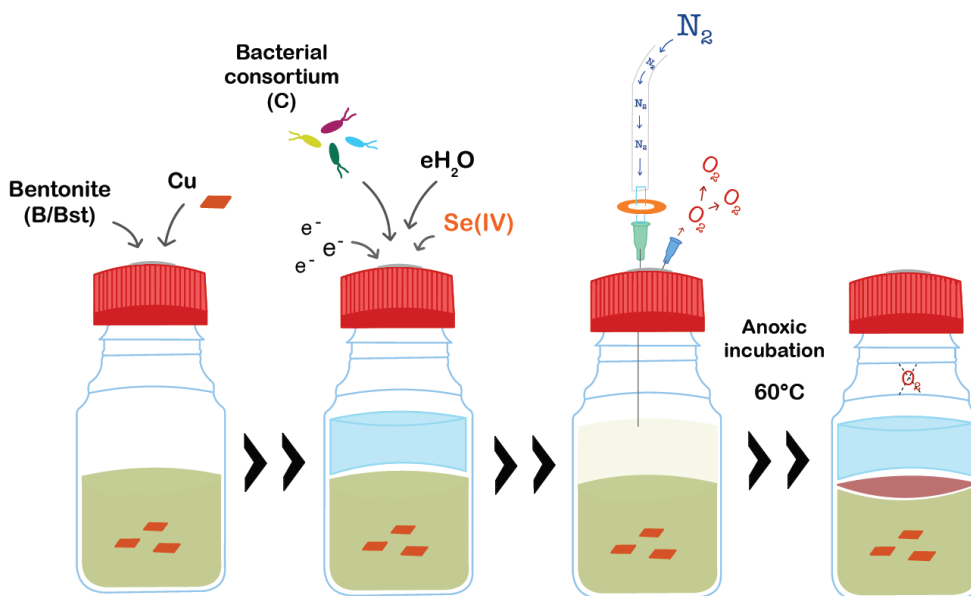


**Figure 1.** Microcosms experimental workflow and  $N_2$  degassing process to obtain anoxic conditions. B: natural bentonite; Bst: heat-shocked bentonite; C: bacterial consortium;  $e^-$ : electron donors and acceptor;  $eH_2O$ : equilibrium water;  $Se(IV)$ : sodium selenite (2 mM).

## **2.3. Diversity studies of the bentonite microbial communities**

### **2.3.1. Bentonite DNA extractions and sequencing**

The DNA extractions from each microcosm sample were conducted in accordance with the protocol established by Povedano-Priego et al. (2021), which is based on the traditional phenol-chloroform method. Briefly, ~500  $\mu\text{L}$  of slurry bentonite was added to 1.5 mL screw tubes containing sterilized glass beads to achieve the mechanical lysis. Furthermore, chemical lysis was conducted by adding 400  $\mu\text{L}$  of 0.12 M  $\text{NaH}_2\text{PO}_4$ , 600  $\mu\text{L}$  of lysis buffer, lysozyme (10 mg/mL), and proteinase K (20 mg/mL). Once DNA is precipitated following the phenol-chloroform steps, impurities were removed using 80% ethanol. Finally, the DNA concentration was quantified using a Qubit 3.0 Fluorometer (Life Technology).

Regarding the sequencing, amplification and, bioinformatic analysis of the extracted DNA, they were conducted at StabVida Company (Caparica, Portugal, <https://www.stabvida.com/es>). Libraries of 16S rRNA gene were constructed by amplifying the V3-V4 variable regions using the universal primers 341F (5'-CCTACGGGNGGCWGCAG-3') and 785R (5'-GACTACHVGGGTATCTAATCC-3') (Thijs et al., 2017). Before amplification, the DNA samples underwent quality control to ensure high integrity. They were then purified using the Sera-Mag Select kit (Cytiva), and the libraries were then sequenced on the Illumina MiSeq platform using the MiSeq Reagent Kit v3 and 300bp paired-end reads.

### **2.3.2. Bioinformatics and statistical analyses**

The generated raw data were processed and analyzed with QIIME2 v2022.2 (Caporaso et al., 2010). The DADA2 plugin was used to eliminate low-quality regions, dereplicate reads, and filter out chimeras (Callahan et al., 2016). Alpha rarefaction curves were generated, and the reads were grouped into operational

## CHAPTER 2

taxonomic units (OTUs) and classified by taxon using the SILVA (release 138 QIIME) database (clustering threshold of 99% similarity). Explicet 2.10.5 software was used to obtain relative abundances of the taxa and alpha diversity indices (Robertson et al., 2013). To compare the similarity between samples at the genus level, a principal coordinate analysis (PCoA) was conducted using the Past 4.04 software (Hammer, 2021), based on the Bray-Curtis algorithm. In addition, a heatmap was generated to depict the differences between the bentonite treatments, focusing only on genera with a relative abundance of  $\geq 1.8\%$ . This was achieved by plotting the heatmap.2 function from the gplots v.3.0.1.1, phyloseq, and RColorBrewer packages in the R v.4.2.1 software (McMurdie and Holmes, 2013; Warnes et al., 2022; Neuwirth, 2022; R Core Team, 2022).

### **2.4. Microscopic and spectroscopic characterization of the selenium reduced nanoprecipitates**

To characterize the products resulting from Se-treated microcosms, the intermediate layer formed between the bentonite and the supernatant was collected and prepared according to the procedure described by Povedano-Priego et al., (2023). For this purpose, the Se samples (BCSe, BstCSe, BSe, BstSe) were analyzed by high-resolution transmission electron microscopy with high-angle annular dark-field (HAADF) imaging (Thermo Fisher Scientific TALOS F200X and FEI TITAN G2) coupled to energy dispersive X-ray spectroscopy (EDX) microanalysis, with an acceleration voltage of 200 kV or 300 kV was used. The crystallinity of Se nanoparticles was analyzed using selected-area electron diffraction (SAED) and high-resolution transmission electron microscopy (HRTEM) combined with fast fourier transform (FFT).

This microscopic and spectroscopic characterizations were carried out on samples with incubation times of 4 and 14 days as the first stages of the experiment and after 2 months as the main study time.

### **2.5. Analyses of the supernatant: pH and soluble selenium depletion**

The biochemical changes occurring in pH and in the concentration of soluble selenium in each treatment were analyzed by collecting 5 mL of the supernatant of each microcosm, i.e., the liquid phase, under anoxic conditions inside an anoxic glove box. The pH of the 24 bentonite microcosms was measured in triplicate using a multi-parameter probe HQd Field Case HACH previously calibrated using commercially available reference solutions (pH 4.00 and 7.00). The pH measurements were conducted at 0, 4, 14, 30, and 60 days of anoxic incubation at 60 °C. For each study time, the supernatants were collected from the three replicates of each treatment.

The concentration of soluble Se(IV) present in the aforementioned supernatants was determined via inductively coupled plasma-mass spectrometry (ICP-MS), employing a NexION 300D spectrometer. Five mL of each sample were acidified (4% HNO<sub>3</sub>) before measurements. The determination of this parameter was carried out in all microcosms at time 0 and after 2 months of anoxic incubation.

## **3. Results and discussion**

### **3.1. Visual color changes throughout the incubation time**

Throughout the 2 months of anoxic incubation at 60 °C, visually observable color changes were tracked in the different microcosms. **Figure 2** shows the changes observed in one of the replicates of each treatment before (T. 0) and at 4, 14, 30, and 60 days of incubation.

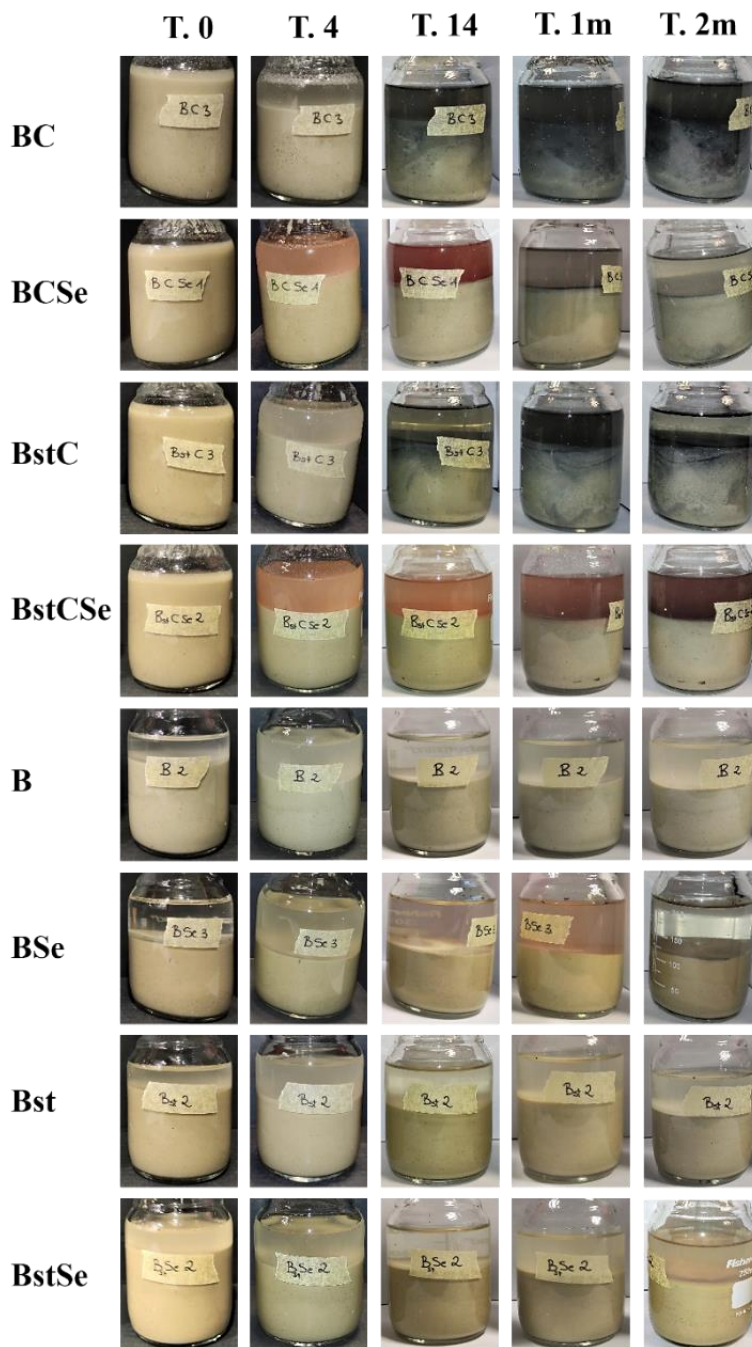


**Figure 2.** Visual color changes throughout the incubation time of water-saturated bentonite microcosms before (T. 0) and after 4, 14, 30 (1 month) and 60 days (2 months) of anoxic incubation at 60 °C. B: natural bentonite; Bst: heat-shocked bentonite; C: bacterial consortium; Se: sodium selenite (2 mM).

The most evident color changes were observed in the treatments inoculated with the bacterial consortium. In the case of selenium treatments (BCSe, BstCSe), an orange color was observed after four days, particularly in the supernatant area. The color intensified gradually over time, becoming darker red after 60 days in BstCSe. In addition, specifically in the BCSe sample, the red color mixed with blackish tones after 30 days of incubation. The reddish orange color is indicative of the presence of Se(0), which would suggest that a reduction of Se(IV) to Se(0) would have occurred in these microcosms (Ruiz-Fresneda et al., 2018; Povedano-Priego et al., 2023). The presence of the bacterial consortium (C) would have accelerated the reduction of selenite, as three out of the four strains, *Stenotrophomonas*, *Pseudomonas*, and *Bacillus*, are known to reduce this metalloid (Ruiz-Fresneda et al., 2020; Tenedezai et al., 2021; Borah et al., 2021).

In particular, the strain *Stenotrophomonas bentonitica* BII-R7 has been reported to exhibit the capacity to reduce selenite at concentrations up to 200 mM in agar medium in the presence of oxygen, and it can also reduce this metalloid under anaerobic conditions (Ruiz-Fresneda et al., 2018; 2019). Moreover, these two treatments, BCSe and BstCSe, appeared to exhibit the same Se reduction capacity, at the macroscopic level, despite the difference of natural or heat-shocked bentonite. This is because the bacterial consortium was added after the tyndallization of the bentonite, reinforcing the hypothesis that the reduction of Se(IV) in these microcosms was mainly due to the bacterial consortium. The Se-treatments without the consortium addition (BSe, BstSe) required a longer incubation time to observe the orange color. In the case of natural bentonite (BSe), the color began to be visible after one month of incubation, while the heat-shocked ones (BstSe) required at least two months to reach the same tone. This indicates a reduction of selenium due to the indigenous microorganisms of the Spanish bentonite. In all the Se-treatments,

but more specifically in the one with Se-treated heat-shocked bentonite (BstSe), an abiotic reduction of this metalloid may also be considered.

On the other hand, the treatments amended with the bacterial consortium but without the metalloid addition (BC, BstC), also exhibited color changes. In these cases, the bentonite-supernatant interphase, and the supernatant adopted a blackish color. The BCSe treatment also adopted this color after 30 days of incubation. This black color change would be associated with the production of hydrogen sulfide ( $H_2S$ ), as a consequence of the bacterial activity. This  $H_2S$  could react with the iron present in bentonite and result in the formation of black precipitates of reduced iron compounds (Miettinen et al., 2022; Matschiavelli et al., 2019). It should be noted that during the processing of the samples, there was a strong smell of rotten eggs in the microcosms where a more intense black color was obtained. This odor has been reported to be characteristic of the presence of  $H_2S$  (Daldal et al., 2010; Martinez-Moreno et al., 2024b). The presence of sulfides in the system is a key factor to consider regarding the corrosion of metal canisters, particularly those made of copper. The main biotic source of sulfide production are sulfate-reducing bacteria. This bacterial group can reduce the sulfate, added to the microcosms, to sulfides (Martinez-Moreno et al., 2024b; Hall et al., 2021). These can then interact with copper plates, resulting in copper sulfides, one of the most critical corrosion products.

### **3.2. Soluble Se(IV) reduction and pH changes in microcosms' supernatant**

To further study the selenium dynamics during the incubation time within the different treatments, the presence of soluble Se(IV) in the supernatants of Se-treated microcosms (BCSe, BstCSe, BSe, and BstSe) was analyzed by ICP-MS. A final concentration of 2 mM sodium selenite was added to each microcosm at time 0. All ICP-MS measurements were conducted in triplicate

(biological replicates). The supernatants of the Se-treated microcosms were initially analyzed at time 0 to establish a baseline of 100% Se(IV) presence. After a two-month anoxic incubation at 60 °C, the supernatants were reanalyzed to determine the remaining percentage of soluble selenite in each treatment (**Fig. 3**).

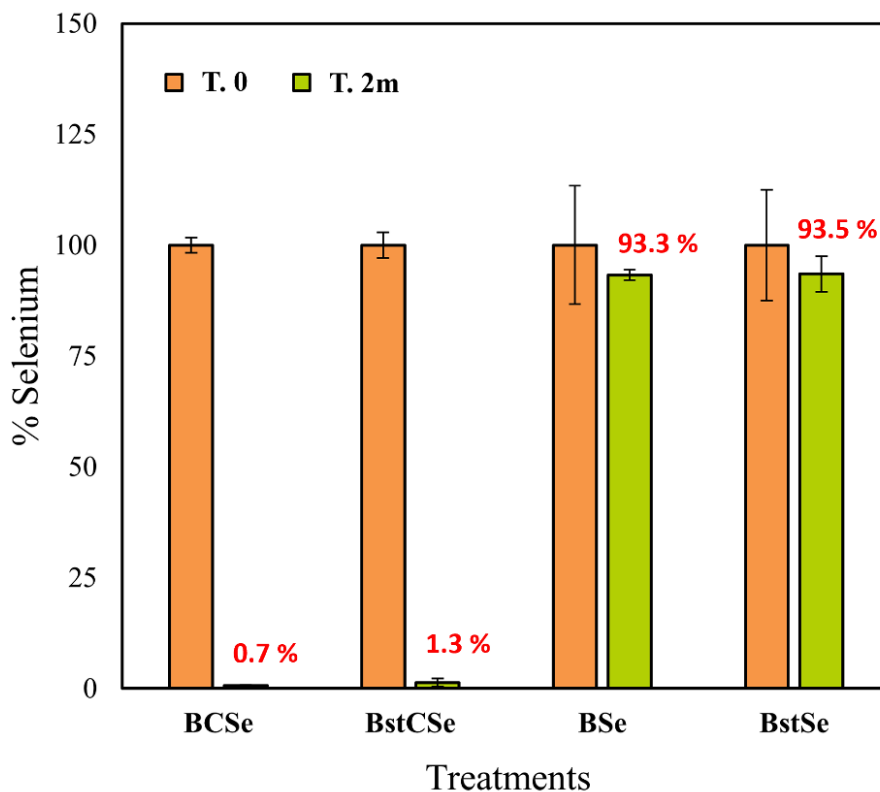


**Figure 3.** Percentage of soluble Se(IV) present in the supernatants of Se-treated water-saturated bentonite microcosms before (T. 0) and after 2 months (T. 2m) of anoxic incubation at 60 °C. Measurements were performed in triplicate using ICP-MS. Data showed the mean values with standard deviations measured from three independent replicates. Time 0 measurements were taken as a reference representing the 100% Se(IV) present. B: natural bentonite; Bst: heat-shocked bentonite; C: bacterial consortium; Se: sodium selenite (2 mM).

The two treatments with inoculated consortium, BCSe and BstCSe, exhibited the highest reduction values for Se(IV) after 2 months of incubation. The soluble Se(IV) detected in the supernatants was only 0.7% and 1.3%,

## CHAPTER 2

respectively, indicating that in two months, nearly 100% of the added selenite had been reduced or transformed into insoluble forms. The inoculation of this bacterial consortium was intended to simulate a scenario where the microbial activity conditions were elevated. Nevertheless, the reduction was less pronounced in the treatments lacking the consortium, with almost all the added selenium still present in the solutions. In the case of natural bentonite (BSe), the percentage of soluble Se(IV) detected at two months was 93.3%, while in the heat-shocked bentonite (Bst), it was 93.5%.

These results were in alignment with the color changes noted in the microcosms (**Fig. 2**). According to the orange color observed throughout the incubation time in the supernatant of the amended-consortium microcosms, the reduction of Se(IV) to Se(0) likely started within the first few days, at least by day 4 of incubation, as previously shown in **Figure 2**. However, in the treatments without the amended consortium, the rate of selenium reduction was lower, with a slight orange hue beginning to be subtly observed after one month of incubation in treatment BSe and after two months in treatment BstSe. The presented results demonstrated that the activity and presence of bacteria were crucial for the reduction of Se(IV). Consortium strains such as *Stenotrophomonas* and *Pseudomonas*, which have been previously reported to be able to reduce Se(IV), would have participated in the reduction (Macy et al., 1989; Ruiz-Fresneda et al., 2019). These results are also consistent with a similar study conducted at 28 °C, where Povedano-Priego et al. (2023) also observed greater Se reduction in samples inoculated with the same bacterial consortium. Here, despite the high temperature conditions, the reduction of this metalloid by the consortium was not affected. Additionally, the presence of lactate and acetate would have favored the growth of both native and consortium bacteria by serving as carbon and energy sources (Sanchez-Castro et al., 2017; Freikowski et al., 2010; Gonzalez-Gil et al., 2016; Yang et al.,

2019). Overall, these results elucidate that Se reduction process could occurred naturally by stimulating the native bacteria of the bentonite.

From the beginning of the incubation period, the pH values in the supernatants of the different treatments were also measured (**Fig. 4**). At time 0, the pH of the microcosm's supernatants was slightly alkaline, ranging from 7.78 to 8.56. After 4 days of incubation, the pH of the samples dropped to below 8. These slightly alkaline values were maintained throughout the incubation period, with the average pH values after 2 months being  $7.31 \pm 0.14$ .

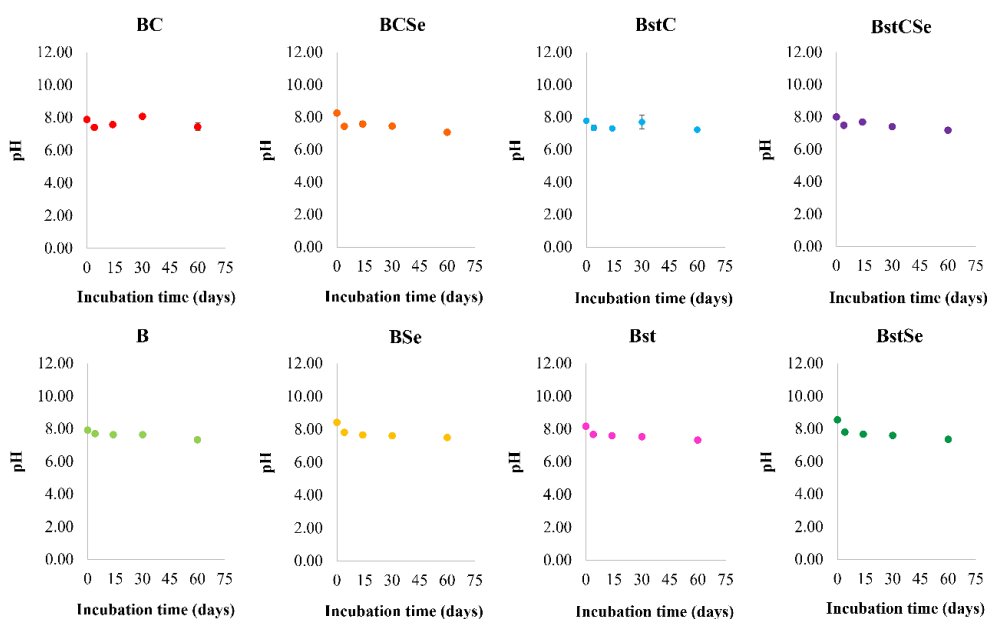


**Figure 4.** pH measurements of the supernatants of water-saturated bentonite microcosms before (T.0) and after 4, 14, 30 and 60 days of incubation in anaerobiosis at 60 °C. The measurements were carried out in triplicate for each study time and treatment. Data showed the mean values with standard derivations measured from three independent replicates. B: natural bentonite; Bst: heat-shocked bentonite; C: bacterial consortium; Se: sodium selenite (2 mM).

In general, the samples followed the same trend, and no differences were observed between the treatments. All supernatants were supplemented at the beginning of the experiment with sodium acetate, sodium lactate, and sodium

sulfate. The difference was the addition of Se(IV) and the bacterial consortium. However, the presence of these factors did not seem to affect the pH dynamics. This minimal decrease in pH values over time could be attributed to several factors, including the dissolution of minerals such as calcite, the presence of microbial metabolites produced during the incubation time such as CO<sub>2</sub>, methane, and hydrogen, and even the ionic exchange that occurs between bentonite and the amended solvents (acetate, lactate, sulfate) (Fernandez-Diaz et al., 2014; Povedano-Priego et al., 2019; Bagnoud et al., 2016).

### **3.3. Tracking the changes in Se chemical speciation over the incubation time by transmission electron microscopy**

To characterize the Se(IV) reduction products, the bentonite-supernatant interphase of the different Se-treated samples (BCSe, BstCSe, BSe and BstSe) was analyzed using HAADF-STEM coupled with EDX. To elucidate the processes associated with the color changes observed in the microcosms (**Fig. 2**), different sampling times (after 4 days, 14 days, and 2 months of incubation) were studied. Due to the insolubility of Se(0), its physico-chemical properties and crystalline structure were identified using SAED and lattice spacing measurements obtained through HRTEM combined with Fast Fourier Transform (FFT). The two treatments without amended consortium, BSe and BstSe, did not show any color changes in the microcosms for at least one month. By electron microscopy, no Se reduction was detected in these samples after 4 days neither 14 days of incubation at 60 °C. Only bentonite was observed, with EDX microanalyses detecting Si, Al, Fe, and Mg signals exclusively (data not shown). However, after 2 months, nanoparticles of Se(0) were found, where a slight orange hue was observed in the microcosms (**Fig. 2**) and the data of ICP-MS showed a low reduction of Se(IV) (**Fig. 3**). In



## CHAPTER 2

**Figure 5.** Scanning transmission microscopy-high-angle annular dark-field imaging (STEM-HAADF) images of BSe and BstSe microcosms after 2-month anoxic incubation at 60 °C (A). The EDX maps with the elemental distribution of Se in pink color and Si, as representative of bentonite, in yellow color (B). The SAED patterns (C) and high-resolution images including the d-spacing (D). EDX spectra (E). Glossary: B: natural bentonite; Bst: heat-shocked bentonite; Se: sodium selenite (2 mM); *m*-Se: monoclinic Se.

Some of the Se nanoparticles detected in the BSe sample also exhibited a small Fe signal in the EDX spectrum (**Fig. 5E**). Nevertheless, no such Fe signal was observed in the BstSe sample. The crystalline nature of the reduced Se was assessed utilizing both SAED (**Fig. 5C**) and HRTEM (**Fig. 5D**) analyses. Across all nanoparticles examined, the selenium exhibited a distinct crystalline structure. The lattice spacing observed at high resolution (**Fig. 5D**) showed values of 0.297 nm and 0.299 nm, corresponding to the (430) and (100) planes of the monoclinic Se (*m*-Se). In these non-consortium treatments, abiotic transformations of Se could be more easily elucidated. These abiotic interactions include adsorption to mineral surfaces such as calcite, magnesium-containing minerals, magnetite, iron oxide, and apatites (Moore et al., 2016), and reduction by minerals such as pyrite (FeS<sub>2</sub>) and siderite (FeCO<sub>3</sub>) or others containing Fe(II), leading to the formation of Se(0) and even minerals such as FeSe<sub>2</sub> (Hoving et al., 2019; Breynaert et al., 2010; Badaut et al., 2012; He et al., 2018; Olegario et al., 2010). In the case of Spanish bentonite, known as FEBEX, Fernandez et al. (2000) reported that the pyrite content is almost zero. However, this bentonite does have other accessory minerals, including quartz, plagioclase, cristobalite, calcite, among others (Fernandez & Villar, 2010). Furthermore, Garcia-Romero et al. (2019) conducted a comparative study between different Spanish bentonites indicating its richness in Si, Al, Fe, and Mg. This study highlighted that the Al+Fe<sup>3+</sup> content in the clays from Cortijo de Archidona, such as those of the present study, was higher. Abiotic processes would have been better elucidated in the most "sterile" treatment, i.e., the one with heat-shocked bentonite without consortium (BstSe). In this treatment,

reduced Se was only found in the extracellular space. Due to the complexity of these ternary bentonite/microorganism/metalloid systems, it cannot be guaranteed whether the reduction occurred abiotically or biotically, leaving the discussions as hypotheses. Therefore, the biotic reduction of Se(IV) by autochthonous microorganisms in the bentonite, stimulated by the presence of the amended electron donors, acetate and lactate, should also be considered (Martinez-Moreno et al., 2024b). In addition, in the Bst treatment, the main microorganisms involved would be spore formers with the ability to withstand high temperatures (heat shock treatment) and tolerate Se.

Regarding the samples inoculated with the consortium, BCSe and BstCSe, both exhibited a consistent pattern in visual color changes and the percentage of Se(IV) reduction detected by ICP-MS (**Fig. 2 and Fig. 3**). Both treatments showed an intense orange coloration from day 4 of incubation, which persisted as the color gradually darkened to a dark red after 2 months. Following a 4-day incubation period, the BCSe treatment resulted in the predominant formation of Se nanospheres at the intracellular level (**Fig. 6A, 6B**). The SAED pattern of some nanospheres indicated a weakly crystalline structure (**Fig. 6C**), which was confirmed by the lattice spacing measurements using HRTEM (**Fig. 6D**). The measured lattice spacing of 0.316 nm corresponded specifically to the (132) plane of *m*-Se. Other nanospheres were also examined but did not present any SAED pattern, indicating their amorphous nature (*a*-Se) (data not shown). At 14 days of incubation, in addition to the detection of intracellular Se(0) nanospheres of mainly amorphous structure, nanoparticles were also detected in the extracellular space. These extracellular nanoparticles exhibited monoclinic crystalline structures (**Fig. 6C**). The most significant change was observed after two months in the BCSe microcosm. At this incubation time, larger nanoparticles were observed aggregated, which led to the formation of different morphologies, including hexagonal and spherical shapes (**Fig. 6A**).

## CHAPTER 2

The EDX spectra of these nanoaggregates showed Se signal in addition to a more pronounced Fe signal than the one observed previously in the BSe sample (Fig. 6E and 5E). SAED pattern measurements revealed lattice spacings of 0.244 nm, 0.301 nm, 0.201 nm, and 0.305 nm.

### BCSe

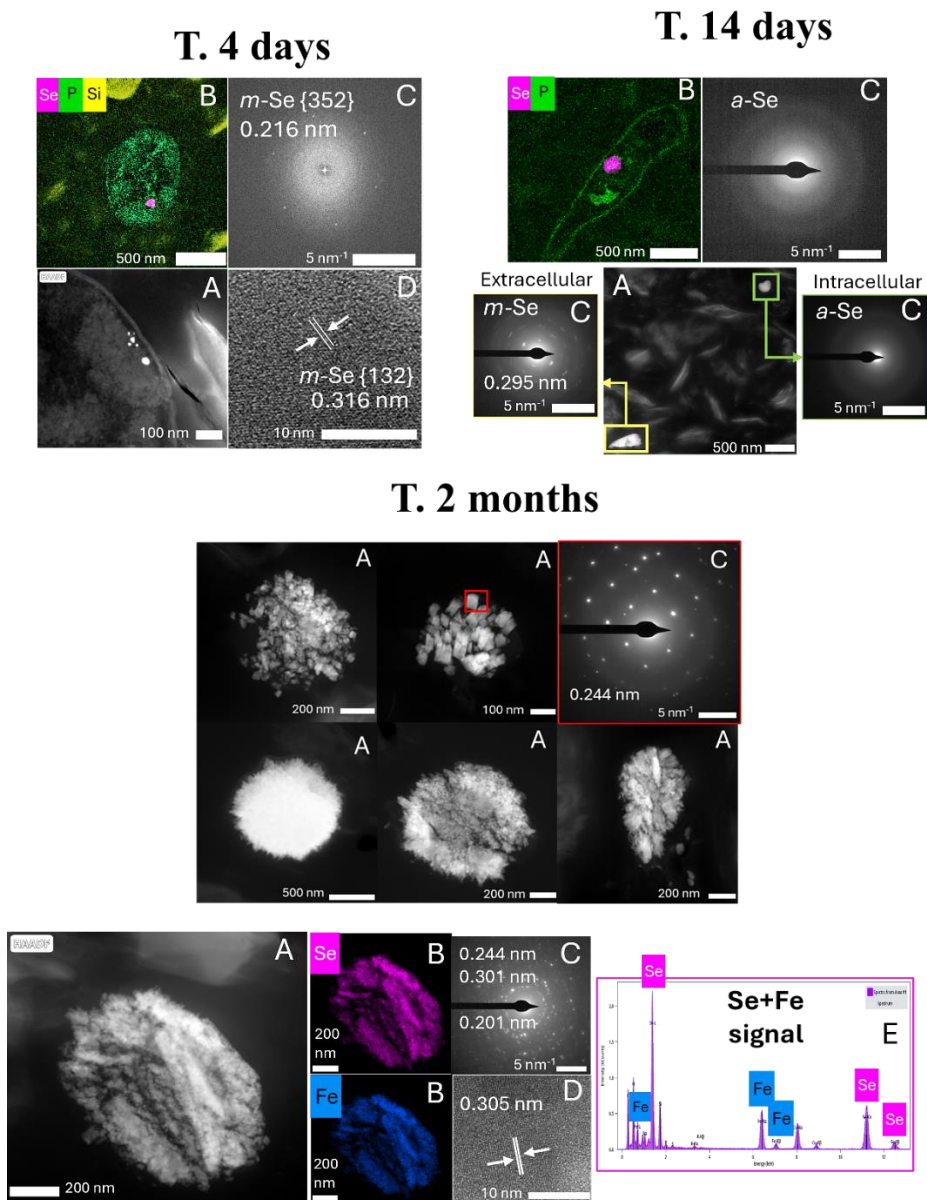


**Figure 6.** Scanning transmission microscopy-high-angle annular dark-field imaging (STEM-HAADF) images of BCSe treatment after 2-month anoxic incubation at 60 °C (A). The EDX maps with the elemental distribution of Se in pink color, P in green color, Fe in dark blue color and Si in yellow color as representative of bentonite (B). The SAED patterns (C) and high-resolution images together with d-spacing (D). EDX spectra (E). Glossary: B: natural bentonite; Bst: heat-shocked bentonite; C: bacterial consortium; Se: sodium selenite 2 mM; *m*-Se: monoclinic Se; *a*-Se: amorphous Se.

Given that the composition of these nanoaggregates was not only selenium, the formation of ferroselite ( $\text{FeSe}_2$ ), a mineral composed of iron and selenium, might have occurred. Interestingly, the spacings measured by SAED, corresponding to the planes (111), (011), (121), and (011), respectively, fitted very well with those of ferroselite (**Fig. 6C**). In this study, we propose a hypothesis regarding the potential formation of the ferroselite mineral. Given that the incubation occurred within an anaerobic and reducing environment, the hypothetical mechanism might have unfolded as follows: initially, Se(IV) could have undergone a reduction to Se(0), mediated by bacteria. As known, certain bacteria, such as *Pseudomonas* and *Stenotrophomonas*, possess the capacity to reduce Fe(III), present in the bentonite smectites, to Fe(II) (Naganuma et al., 2015; Pinel-Cabello et al., 2021). Afterwards, these Fe(II) could react with Se(0), leading to the formation of iron selenide, according to the following reaction:  $\text{Fe}^{2+} + 2\text{Se}^0 + 2e^- \leftrightarrow \text{FeSe}_2$  (Howard, 1977). This iron selenide is a mineral phase recognized as ferroselite. However, more specific techniques such as RAMAN or EXAFS/XANES spectroscopies are further required to confirm the exact mineral phase of these selenium and iron precipitates. The potential abiotic origin of Se+Fe formations also has to be considered. Warren (1968) successfully synthesized ferroselite under controlled pH conditions between 7 and 9 and at a temperature of 80 °C. Nevertheless, in the present study, these Se+Fe formations were only detected in microcosms with high bacterial activity and not in the "most sterile" treatment, which involved heat-shocked bentonite and the absence of a

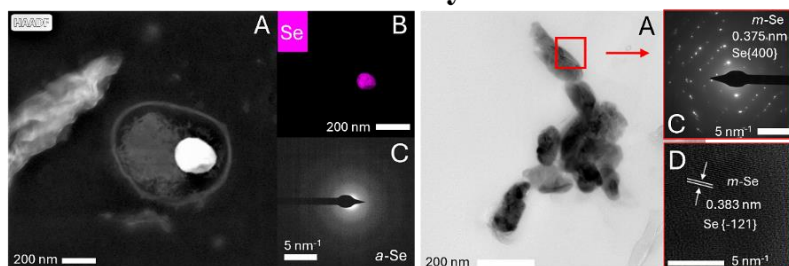
## CHAPTER 2

consortium (Bst). Therefore, if their origin were abiotic, these formations should have appeared in the different experimental treatments regardless of bacterial activity. The reduction of a metal/metalloid soluble and toxic oxidation state to insoluble forms, such as Se(0), or the formation of new minerals such as ferroselite, is of great interest in the case of DGR system failure. In this context, the bentonite microorganisms would act as an additional barrier by retaining the leakage in localized areas, thus preventing its spread to the rest of the system.

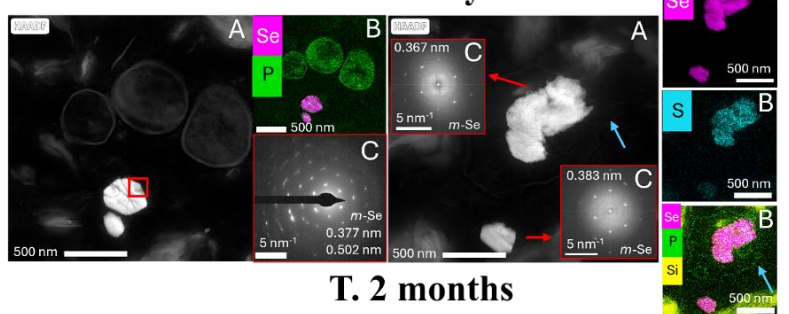
Similarly, the microscopic analyses of the BstCSe sample showed comparable results to those of BCSe. At the 4 and 14-day times, both intracellular nanospheres with an amorphous structure and extracellular crystalline nanoparticles were detected (**Fig. 7A, 7B, 7C, and 7D**). These reduced Se(0) products showed only a Se signal at these incubation times. In addition, some bacterial cells containing intracellular nanoparticles, showed a lysed cell surface (**light blue arrow in Fig. 7A and 7B**). Once more, the lattice spacings of selenium nanoparticles were measured by SAED and HRTEM, annotating the following values: 0.383 nm, 0.377 nm, 0.502 nm, and 0.367 nm. These d-spacings corresponded to the monoclinic Se planes, specifically (-121), (310), (210), and (040), respectively. After 2 months of incubation, the extracellular nanoaggregates were also observed. Interestingly, some nanoparticles showed only a Se signal by EDX, while others presented signals for both Se and Fe (**Fig. 7E**).

## BstCSe

T. 4 days



T. 14 days



T. 2 months

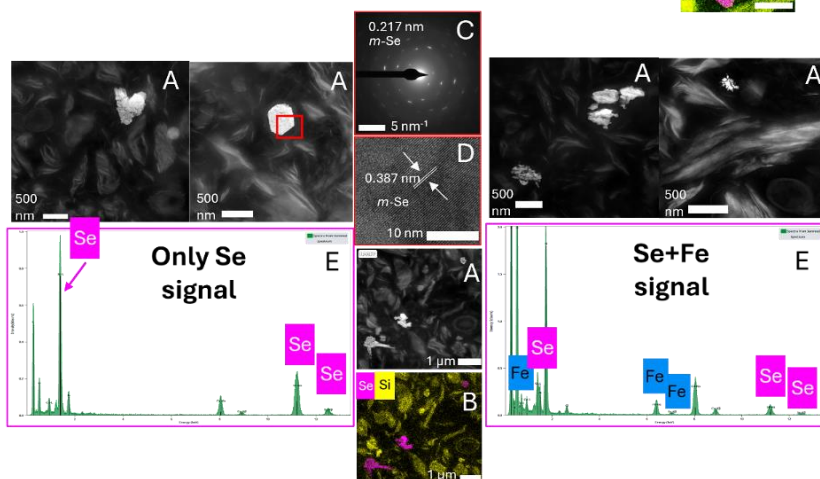


**Figure 7.** Scanning transmission microscopy-high-angle annular dark-field imaging (STEM-HAADF) images of BstCSe treatment after 2-month anoxic incubation at 60 °C (A). The EDX maps with the elemental distribution of Se in pink color, P in green color, and Si in yellow color as representative of bentonite (B). The SAED patterns (C) and high-resolution images together with d-spacing (D). EDX spectra (E). Light blue arrow: lysed cell wall. Glossary: B: natural bentonite; Bst: heat-shocked bentonite; C: bacterial consortium; Se: sodium selenite (2 mM); *m*-Se: monoclinic Se; *a*-Se: amorphous Se.

## CHAPTER 2

The selenite bioreduction can be achieved by an intracellular process involving molecules and/or enzymes, such as glutathione (which contains reduced -SH thiol groups), reduced thioredoxin, nitrite reductase, selenite/ate reductase, sulfite reductase, and fumarate reductase (Lampis et al., 2014). Once reduced, Se(0) can be accumulated intracellularly, within the cell wall, or be excreted to the external medium. The results obtained in this work demonstrated the presence of Se nanoparticles or nanoaggregates near the bacterial cells or even within the cells. Furthermore, the current study has also identified the presence of intracellularly reduced Se(0) within lysed bacterial cell walls (**light blue arrow in Fig. 7A**). All these findings were consistent with those published by Povedano-Priego et al. (2023), where a similar study was conducted under moderate temperature conditions of 28 °C, using complex bentonite/microorganism/selenium conditions. Nevertheless, to the best of our knowledge, this is the first study to demonstrate Se reduction in these complex ternary systems and under high-temperature conditions.

Furthermore, selenium exists in three distinct allotropic forms: trigonal (*t*-Se), monoclinic (*m*-Se), and amorphous (*a*-Se) phases. Among these, trigonal Se stands out as the most thermodynamically stable phase, characterized by a crystalline structure wherein Se atoms are bound together by covalent bonds. Conversely, the amorphous form is considered the least stable (Chen et al., 2010). In this study, the majority of intracellular nanospheres exhibited an amorphous or weakly crystalline structure, consistent with the *m*-Se phase. However, as the incubation period was longer, the extracellular nanoparticles exhibited increased size and a tendency to cluster or aggregate. The crystalline structure of these nanoaggregates was more consistent, showing lattice spacings, in agreement with the allotropic phase of monoclinic selenium. These results suggested that reduced selenium may have undergone changes in the arrangements of its atoms over time. Previous studies have demonstrated

the existence of bacteria capable of producing amorphous selenium nanospheres (Eswayah et al., 2017; Li et al., 2014). However, Ruiz-Fresneda et al. (2018) reported a time-dependent transformation process of *a*-Se nanospheres to *t*-Se nanostructures with different morphologies formed by the bacterium *S. bentonitica* BII-R7. Their proposed mechanism suggested that this transformation to *t*-Se nanostructures takes place after intracellularly formed *a*-Se nanospheres and their release from the cells, likely through cell lysis. This theory gained support from the presence of Se nanoparticles near the lysed cells, also observed in this study (**light blue arrow in Fig. 7A**). Subsequently, upon release into the extracellular space, these nanospheres initiate fusion and aggregation, ultimately culminating in the crystallization to form various *t*-Se nanostructures. The microscopic analyses of this study are in accordance with such proposed mechanism. Furthermore, Povedano-Priego et al. (2023) also identified intermediate phases of *m*-Se nanostructures. These *m*-Se aggregates may represent a phase preceding the ordering of the atoms according to *t*-Se. Consequently, further long-term studies have been proposed to be conducted under the same conditions in order to elucidate and confirm whether the incubation time is involved in the allotropic transformation process of the reduced Se.

Overall, these results obtained by state-of-the-art microscopic techniques (STEM/HAADF, HRTEM, EDX) revealed the impact of bentonite microorganisms on the chemical speciation of Se. The inoculated bacterial consortium accelerated the reduction process of Se(IV), leading to the formation of Se(0) intracellular nanospheres in the early phases, and nanoaggregates of Se and Se+Fe after 2 months of incubation at 60 °C. These processes seemed to occur at a slower rate in the microcosms without the consortium, which may indicate the involvement of the native bentonite microbial communities. The presence of the consortium in these microcosms

## CHAPTER 2

allowed to progress in the understanding of the occurrences in a scenario with high microbial activity. Due to the insoluble and stable nature of Se(0) or mineral phases as FeSe<sub>2</sub>, the reduction of soluble Se(IV) would interestingly favor the bioimmobilization of this metalloid in the event of leakage. Biotic processes appear to be the most likely mechanisms responsible for the reduction of Se(IV) and the formation of Se(0) nanostructures in the studied bentonite microcosms. However, abiotic transformations of Se could also have occurred.

### **3.4. Analysis of the microbial communities incubated at high temperature: implications on selenium reduction**

#### **3.4.1. Statistical analyses: principal coordinate (PCoA) and heatmap analyses**

Total DNA from all treatments was extracted and sequenced in triplicate after 2 months of incubation under anoxic conditions at 60 °C. This study incubation time was selected to highlight the early shifts occurred in the microbial communities as well as the biogeochemical changes undergone by selenium. Some replicates were excluded from the bioinformatic diversity analysis due to their failure during the DNA sequencing step (BCSe\_2, BstC\_3 and BstSe\_1). Beside identifying the bacterial communities developed under high-temperature incubation conditions, comparing the different bentonite treatments helped to determine, among them, the most tolerant bacteria to selenium (Se) and those better adapted to withstand extreme heat, such as the tyndallization process (Bst).

After amplification of the V3-V4 variable regions of the 16S rRNA gene, a total of 601 phlotypes were identified and classified into 35 different phyla and 471 genera. The Good's coverage values (> 0.99% in all cases) indicated that the sequencing depth was sufficient to fully cover all sequences in the

bacterial community. Alpha diversity was analyzed using the Sobs, ShannonH, SimpsonD, and ShannonE indices with a bootstrap of 100 (see **Table 2**). Overall, according to the diversity indices, high bacterial diversity (ShannonD and SimpsonD) and a uniform distribution of OTUs (ShannonE) within the microcosms' microbial communities were revealed. In a more detail, these indices indicated a higher diversity in the samples without a bacterial consortium (BSe > Bst > B > BstSe > BCSe > BC > BstC > BstCSe) in comparison to those amended with, suggesting that the presence of such consortium enhance the dominance of a few species over the others.

**Table 2.** Richness (Sobs), diversity (ShannonH and SimpsonD), and evenness (ShannonE) indices of the bacterial communities of the different treatments incubated for 2 months at 60 °C. B: natural bentonite; Bst: heat-shocked bentonite; C: bacterial consortium; Se: sodium selenite (2 mM).

<b>Sample</b>	<b>Sobs</b>	<b>ShannonH</b>	<b>ShannonE</b>	<b>SimpsonD</b>
<b>BC</b>	94.86	3.36	0.51	0.81
<b>BCSe</b>	145.00	3.19	0.45	0.76
<b>BstC</b>	86.92	3.55	0.55	0.84
<b>BstCSe</b>	65.85	2.43	0.40	0.70
<b>B</b>	303.46	4.52	0.55	0.89
<b>BSe</b>	456.83	6.07	0.69	0.96
<b>Bst</b>	306.62	4.41	0.54	0.86
<b>BstSe</b>	203.89	3.91	0.51	0.87

A principal coordinate analysis (PCoA) based on the Bray-Curtis distance highlighted the differences and similarities between the samples (**Fig. 8**). After 2 months of incubation at high temperature, the samples grouped into three distinct clusters. The first one included all treatments with the consortium (BC, BstC, BCSe, BstCSe), incorporating those with selenium (Se) and either natural (B) or heat-shocked bentonite (Bst). However, in the absence of the

## CHAPTER 2

bacterial consortium, differences were observed between the natural and heat-shocked bentonite treatments. Except for the replicates B\_3 and BSe\_1, which deviated from the trend, the remaining samples clearly grouped into treatments with natural bentonite (B, BSe) and those with heat-shocked bentonite (Bst, BstSe).

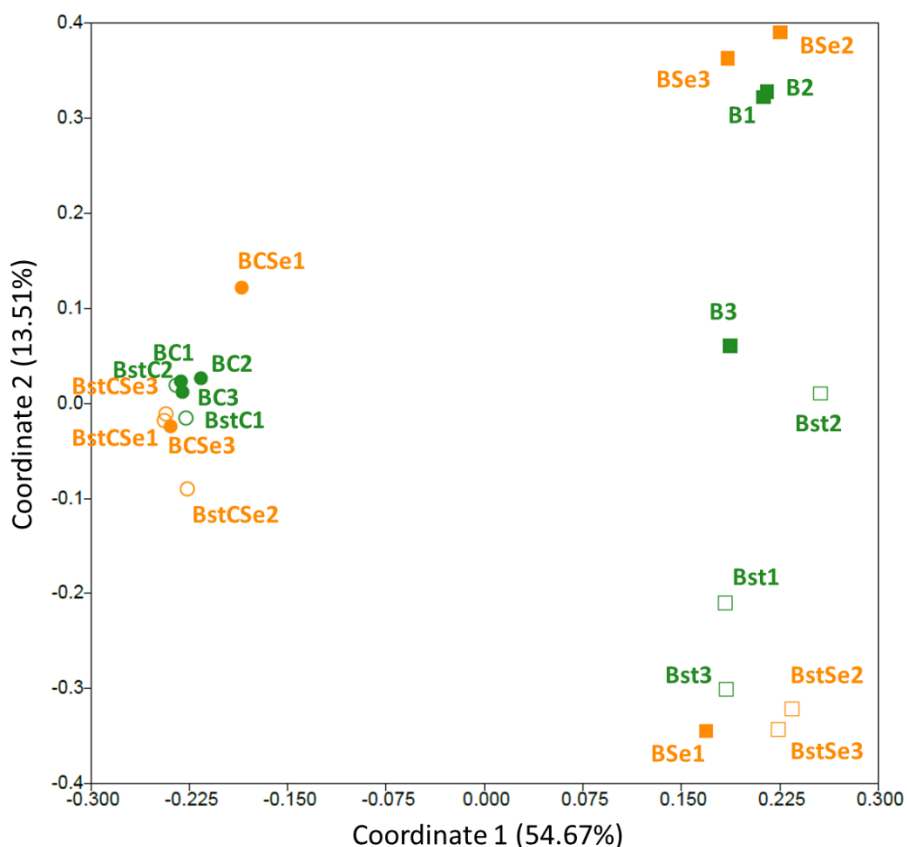


**Figure 8.** Principal coordinate analysis (PCoA) comparing the microbial community structure of the different water-saturated bentonite microcosms after 2 months of anoxic incubation at 60 °C. The distance is based on the Bray-Curtis algorithm. Treatments studied in triplicates, except for BstC, BCSe and BstSe in duplicate. Square (■□): non-consortium treatments; Circle (●○): amended consortium treatments; Filled square (■) and filled circle (●): natural bentonite; Empty square (□) and empty circle (○): heat-shocked bentonite; Green color: non-Se treatments; Orange color: Se(IV) treatments. B: natural bentonite; Bst: heat-shocked bentonite; C: bacterial consortium; Se: sodium selenite (2 mM).

The PCoA results suggested a clear effect of the bacterial consortium on the overall bentonite community. Accordingly, Povedano-Priego et al. (2023) also reported differences between treatments with and without the consortium, as well as differences between some treatments with and without Se. In addition, Martinez-Moreno et al. (2024b) discussed the effect of the same bacterial consortium, noting that such treatments were completely separated from the other two groups, differentiating as well between natural and heat-shocked bentonite. Together with the present results, all this evidence supports the previously observed effect of both the consortium and Se(IV) on bentonite bacterial communities.

To further identify the OTUs (at genus level) contributing to the differences and similarities between the samples, a heatmap was constructed (**Fig. 9**). Here again, a clear grouping of the samples was revealed, which agreed with the PCoA results mentioned above. The diversity in the consortium treatments (C) was mainly dominated by two strains, *Pseudomonas* and *Stenotrophomonas*. However, in those without the amended consortium, the genera distribution was more homogeneous, with no single genus showing strong dominance over the others. In the microcosms with natural bentonite (B), *Pseudomonas* showed a more pronounced relative abundance compared to the other genera, while in the heat-shocked ones (Bst), *Bacillus* exhibited slightly higher relative abundance.

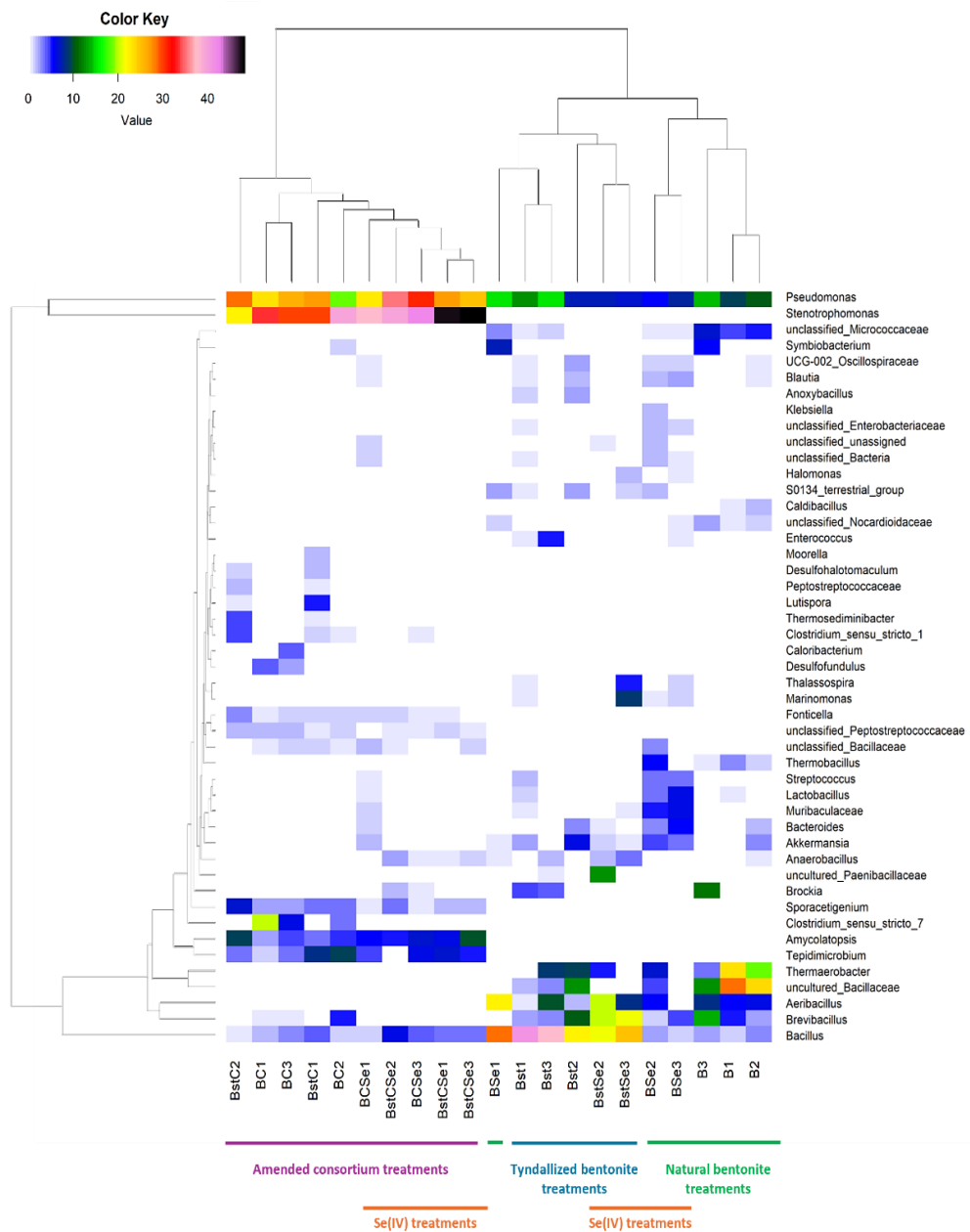


**Figure 9.** Heatmap of relative abundances and microbial distribution of the water-saturated bentonite samples based on Manhattan distance after 2 months of anoxic incubation at 60 °C. Cut off: 1.8%. Colors represent the varying levels of relative abundance for each genus. Treatments studied in triplicates except BstC, BCSe and BstSe in duplicate. B: natural bentonite; Bst: heat-shocked bentonite; C: bacterial consortium; Se: sodium selenite (2 mM).

The distribution of the samples in the heatmap also revealed further grouping based on Se treatments, with samples treated with the metalloid grouping together within each cluster. Specifically, treatments with both the consortium and Se were grouped together (BCSe and BstCSe), as well as those with Se but without the consortium (BSe and BstSe). Since Se is toxic to some microorganisms, its presence could have modified the community according to genera more or less tolerant to this metalloid. To identify these communities in more detail, an exhaustive study of the bacterial diversity in each treatment was conducted.

### **3.4.2. Analysis of the distribution of microbial communities**

Across all the treatments, the most abundant phyla were Pseudomonadota (52.44%), Bacillota (40.91%), and Actinomycetota (4.67%). These phyla are mainly related to the four genera of the amended bacterial consortium, *Pseudomonas*, *Stenotrophomonas*, *Bacillus* and *Amycolatopsis*, respectively. Furthermore, other phyla with low relative abundance were also present, including Bacteroidota (0.79%), Verrucomicrobiota (0.35%), Chloroflexota (0.22%), and Gemmatimonadota (0.15%), among others. The relative abundances of the different phyla are presented in **Supplementary Table S2** and **Supplementary Figure S2**. In addition, the annotated phylotypes were further grouped at genus level into 471 OTUs (**Supplementary Table S3**).

#### **3.4.2.1. Impact of the temperature on the bentonite bacterial community**

Overall, the most abundant genera were *Stenotrophomonas* (29.75%), *Pseudomonas* (21.31%), *Clostridium* (7.57%), *Bacillus* (4.31%), *Tepidimicrobium* (3.98%), *Amycolatopsis* (3.51%), *Brevibacillus* (2.90%) and *Sporacetigenium* (2.48%). In general, these genera demonstrated the greatest resilience to anoxic incubation conditions at 60 °C. The OTUs relative abundance at genus level of each treatment in triplicate (except BstC, BCSe

and BstSe in duplicate) are represented in **Figure 10** and detailed in **Supplementary Table S3**.

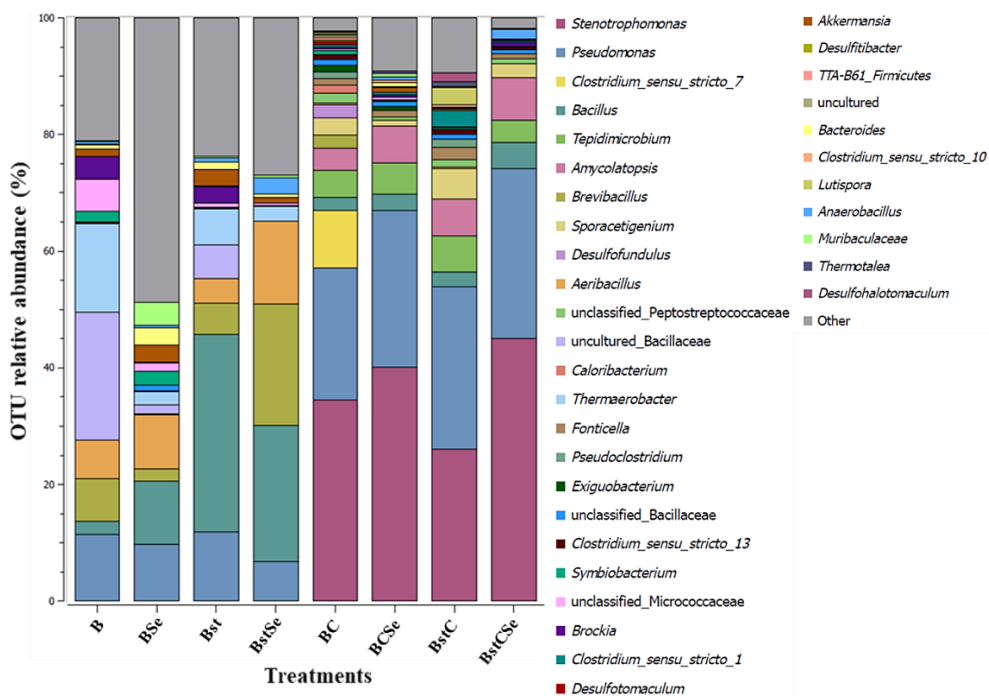


**Figure 10.** OTU relative abundances at genus level of the microbial communities in water-saturated bentonite microcosms after 2 months of anoxic incubation at 60 °C. Cut off: 0.19% of relative abundance. Stacked bars represent the mean values of biological triplicates (except BstC, BCSe and BstSe in duplicate). B: natural bentonite; Bst: heat-shocked bentonite; C: bacterial consortium; Se: sodium selenite (2 mM).

Since the incubation was carried out at a high temperature, it was possible to detect the presence of thermophilic autochthonous bacterial genera in the Spanish bentonite. Among these genera were the aforementioned *Pseudomonas*, *Clostridium*, *Bacillus*, and *Tepidimicrobium*, along with others with lower percentages of relative abundance but also of interest, including *Aeribacillus*, *Caloribacterium*, *Thermaerobacter*, *Brockia*, *Thermotalea*, *Thermobacillus*, *Thermosediminibacter*, and *Thermacetogenium*. *Tepidimicrobium* was detected in all treatments and showed a higher relative abundance in Bst (33.88%). The genus *Aeribacillus* was also detected in all

treatments, except in BCSe and BstCSe, with the highest relative abundance observed in BstSe (14.16%). Regarding *Caloribacterium* and *Thermaerobacter*, the first one was detected only in BC with a percentage of 1.41%, while the second one was present in the treatments without consortium, standing out in B with a relative abundance of 15.19%. The relative abundances of other thermophilic genera such as *Brockia*, *Thermotalea*, and *Thermobacillus* were generally lower in the total community, with higher percentages observed in treatments B (3.91%), BstC (0.91%), and BSe (1.96%), respectively. In a recent study, Martinez-Moreno et al. (2024) reported the presence of *Pseudomonas* in Spanish bentonites compacted at 1.7 g/cm<sup>3</sup> and incubated for one year at 60 °C. Furthermore, the ability of the other genera to withstand such high temperature was demonstrated in the literature. For example, *Clostridium* was reported to grow at 60 °C (Shiratori et al., 2009), *Tepidimicrobium* at 62 °C (Slobodkin et al., 2006), and *Bacillus* at 58 °C (Combet-Blanc et al., 1995). The other thermophilic genera are more specific bacteria with high temperature requirements for their optimal growth: *Caloribacterium* can grow up to 65 °C (Slobodkina et al., 2012), *Thermaerobacter* up to 80 °C (Takai et al., 1999), *Thermobacillus* up to 63 °C (Touzel et al., 2000), *Thermosediminibacter* up to 78 °C (Lee et al., 2005), and *Thermacetogenium* with an optimal temperature of 58 °C (Hattori et al., 2000). The presence of thermophilic bacteria in bentonites is particularly important to consider for the safety of future DGR since these bacteria are well-adapted to survive the high temperatures expected during the early stages of the repository. In general, thermophilic microorganisms are capable of employing a range of adaptation mechanisms to withstand the critical stress factor of high temperatures. These mechanisms include synthesizing heat-resistant proteins, rapidly regenerating sensitive molecules, and producing spores that can remain viable for extended periods of time (Haynes et al., 2018). Therefore, these heat-

## CHAPTER 2

resistant bacterial genera would remain viable during the DGR phases of high temperatures and could become active at any time under favorable conditions, such as the infiltration of groundwater with electron donors or the presence of sulfate in the case of SRB. Depending on the metabolism of each heat-resistant bacterium, the DGR environment could be altered by its activity, potentially resulting in system failures such as gas production leading to increased pressure, corrosion of the metallic canisters, or changes in the stability of the bentonite.

### **3.4.2.2. Bacterial community in the heat-shocked bentonite treatments: BstC, BstCSe, Bst, BstSe**

The effect of the heat shock (tyndallization) was also evident. While some genera may have been favored by these heat-shock treatment, others may have experienced a negative impact. For example, the relative abundance of *Bacillus* was higher in the Bst (33.88%) and BstSe (23.25%) treatments compared to the non-heat-shocked B (2.34%) and BSe (10.90%) treatments. *Sporacetigenium* also showed higher relative abundance values in the BstC (5.18%) and BstCSe (2.31%) treatments compared to the BC (2.90%) and BCSe (1%) treatments. *Brevibacillus* was also relatively higher in BstSe (20.85%) compared to BSe (2.07%). In contrast, other genera decreased in abundance when the heat-shock treatment was applied to the bentonite. This was the case of uncultured\_Bacillaceae, whose relative abundance decreased in Bst treatment (5.80%) compared to B treatment (21.88%). Another example was *Exiguobacterium*, which was detected at 1.12% and 0.82% in the BC and BCSe treatments, respectively, but disappeared in the related heat-shock-treated samples (BstC and BstCSe).

The resistance of these genera to very high temperatures (110 °C), although for a short period of time, may be mainly attributed to the formation of spores

(Haynes et al., 2018). In general, spore-forming bacteria, such as those detected in this study, likely undergo sporulation as a survival mechanism when facing harsh environmental conditions (Den Besten et al., 2018). This intricate process, extensively discussed by Eijlander et al. (2014), converts the bacterial cells into dormant endospores, allowing them to remain inactive for extended periods of time. In the present research, molecular analyses of the bacterial diversity do not permit the determination of viability of these communities, since only DNA was studied. The possibility exists that many of the spore-forming genera present in the different bentonite treatments, such as *Bacillus*, *Brevibacillus* and *Sporacetigenium*, were in a latent state allowing them to withstand these harsh tested conditions.

Understanding the role of spore-forming microorganisms in DGR systems is critical since, as previously discussed, they have the capability to survive in a dormant state under challenging repository conditions for prolonged periods of time. The present findings are crucial in assessing the microbial contribution to the safety of future repositories. Despite the conditions in DGRs, being typically harsh and inhibitory to microbial activity, bacteria can potentially be reactivated from dormant states under favorable conditions that support their growth.

#### **3.4.2.3. Impact of the bacterial consortium: BC, BCSe, BstC, BstCSe**

The impact of each treatment on the microbial communities was reflected in the observed changes in the relative abundances of the microbial genera (**Figure 10, Supplementary Table S3**). As previously indicated in PCoA and heatmap analyses, the presence of the bacterial consortium (C) resulted in a modification of the structure of the microbial communities, with the consortium genera exhibiting dominance over the remaining bacteria. In particular, the genera *Stenotrophomonas* and *Pseudomonas* were the most

## CHAPTER 2

prevalent in all inoculated treatments. *Stenotrophomonas* was present at relative abundances of 34.48% in BC, 40.11% in BCSe, 26% in BstC, and 45.05% in BstCSe. *Pseudomonas* also showed high relative abundances, though slightly lower than those of the first one, with percentages of 22.62% in BC, 26.81% in BCSe, 27.91% in BstC, and 29.13% in BstCSe. Because the consortium created dominance in these amended samples, the rest of the bacterial diversity was masked and appeared in much lower percentages. Aside from the other consortium genera, such as *Bacillus* and *Amycolatopsis*, other genera were also identified like *Tepidimicrobium*, with relative abundances of 4.62% in BC, 5.34% in BCSe, 6.15% in BstC, and 3.84% in BstCSe, and *Sporacetigenium*, with abundances ranging from 1% to 5.18% depending on the treatment.

In terms of DGR safety, the consortium treatment aimed to accelerate what would naturally occur with bentonite microbial communities since the four strains included in the consortium are naturally present in Spanish bentonite (Lopez-Fernandez et al., 2018, 2014; Povedano-Priego et al., 2019, 2021). Essentially, it simulated conditions of heightened microbial activity that would typically progress more slowly in a DGR environment. Therefore, in this research, the impact of this consortium was primarily observed in terms of altering the chemical speciation of selenium, as discussed earlier using microscopic and spectroscopic techniques. Specifically, the strains of this consortium (*Stenotrophomonas*, *Pseudomonas* and *Bacillus*) might have been the main ones involved in the immobilization of Se(IV) by its reduction to Se(0) since these bacteria possess the ability to detoxify Se, as evidenced by previous studies (Avendaño et al., 2016; Tendenedzai et al., 2020; Ruiz-Fresneda et al., 2019, 2020; Yu et al., 2018).

#### 3.4.2.4. Effect of Selenium on the bacterial populations in treatments: BCSe, BstCSe, BSe, BstSe

Additionally, the presence of selenium in some microcosms seems to have an impact on the bentonite bacterial communities. Once more, the two strains of the amended consortium, *Stenotrophomonas* and *Pseudomonas*, stood out for their tolerance to selenium. For instance, the relative abundance of *Stenotrophomonas* increased by 5.63% in the BCSe treatment compared to BC, and by 19.05% in BstCSe compared to BstC. Instead, *Pseudomonas* increased its relative abundance by 4.19% in BCSe compared to BC and by 1.22% in BstCSe compared to BstC. Furthermore, the *Bacillus* genus exhibited higher relative abundance values in the BstCSe (4.48%) compared to the non-metalloid BstC (2.56%) treatment. According to the existing literature, species of all three genera have been reported to be capable of bioreducing Se(IV) to Se(0) under anoxic conditions, resulting in the formation of reddish-colored nanoparticles (Switzer Blum et al., 1998, Macy et al., 1989; Ruiz-Fresneda et al., 2019). These findings are consistent with the previously mentioned macroscopic color changes observed in the microcosms, specifically in the BCSe and BstCSe treatments, in which the bacterial consortium and selenium were included (**Fig. 2**). After only 4 days of incubation, the supernatants of the three replicates of these microcosms turned orange. Furthermore, these findings align with the microscopy results, which also showed the presence of Se(0) nanoparticles at all studied time points (4 days, 14 days, and 2 months). All the results are therefore fully consistent, underscoring the key role of the consortium bacterial strains in the reduction of the metalloid. To the best of our knowledge, there are no studies on selenium reduction by these genera at high temperatures. This is the first work describing the high potential of such bacterial consortium to reduce Se(IV) under anoxic conditions and at a temperature, relevant to the DGR system, as high as 60 °C.

## CHAPTER 2

On the other hand, there were also non-consortium genera that were favored by the presence of Se(IV), for instance, *Aeribacillus* and *Symbiobacterium*. The first one increased its relative abundance by 9.96% in the BstSe compared to Bst treatment, while the second one showed a higher relative abundance in BSe (2.38%) compared to B (1.91%) treatment. In addition, in these treatments without consortium addition, the *Pseudomonas* and *Bacillus* genera were also detected, both in the Se and Se-free treatments. The use of sodium acetate or sodium lactate as electron and carbon sources in these microcosms could have stimulated the growth of these bacteria, as previously reported (Martinez-Moreno et al., 2024b; Gonzalez-Gil et al., 2016; Yang et al., 2019). There are no studies linking the *Aeribacillus* genus with Se(IV) reduction. However, *Symbiobacterium* were previously detected in Se-contaminated environments (Povedano-Priego et al., 2023; Aoyagi et al., 2021). These genera, along with others, including *Pseudomonas* and *Bacillus*, may have contributed to the reduction of Se(IV) in these treatments without the consortium (BSe, BstSe), although at a slower rate. In this context, color changes in these microcosms were observed more subtly after one month of incubation in the case of natural bentonite (BSe) or two months for heat-shocked bentonite (BstSe) (**Fig. 2**).

In contrast, certain genera appeared to be negatively influenced by the presence of selenium, exhibiting a reduction in their relative abundance in the Se-treated microcosms. For example, uncultured\_Bacillaceae dropped in BSe (1.63%) compared to B (21.88%); *Thermaerobacter* decreased in BSe (2.22%) relative to B (15.19%); unclassified\_Micrococaceae was reduced in BSe (1.51%) compared to B (5.39%); and *Sporacetigenium* showed a reduction in BstCSe (2.37%) compared to BstC (5.18%). Heatmap results, previously detailed in **Figure 9**, showed an effect of Se on microbial communities, suggesting that the presence of this metalloid may have acted as a stressor agent for certain genera. This research has investigated Se as an inactive chemical analogue of

the radionuclide  $^{79}\text{Se}$ , simulating a leak of this highly dangerous nuclear waste. The results showed that the autochthonous bentonite communities include both Se-tolerant and Se-sensitive bacteria. The presence of bacterial genera most resistant to this metalloid would act as an additional barrier, preventing Se(IV)-filtration into the surrounding environment by reducing and immobilizing it as insoluble Se(0) nanoparticles (Ruiz-Fresneda et al., 2018; Povedano-Priego et al., 2023). Furthermore, bacteria involved in the reduction of Fe(III) in smectite, such as *Stenotrophomonas* and *Pseudomonas*, would facilitate the formation of more stable mineral phases, such as ferroselite, thereby also immobilizing the leakage of waste into the system (Pinel-Cabello et al., 2021; Naganuma et al., 2015). These findings were consistent with previous microscopy data, which showed both intracellular and extracellular Se(0) nanoparticles, as well as Se+Fe nanoaggregates that likely corresponded to ferroselite. Therefore, these Se-tolerant bacteria, along with iron-reducing bacteria (IRB), would decrease the bioavailability of this toxic form in the environment. This would reduce the exposure of more sensitive bacteria and also help contain the leakage within the other DGR barriers.

Overall, the findings of this research are important to consider in case of a system failure in a DGR. They highlight the bacterial response to harsh conditions such as selenium leakage, high temperatures, and groundwater infiltration. It is crucial to acknowledge the microbial activity of bacteria that can enter dormancy or survive under harsh conditions within nuclear repositories. While some bacterial activity consequences, such as those observed in this study concerning selenium leakage, may be advantageous, others such as gas or sulfides production could pose risks to the safety of DGRs.

### 4. Environmental implications

The deep geological repository concept is a system that will undergo various phases throughout its active lifetime. One of the principal challenges confronting these future DGRs is the assurance of their multilevel safety over time scales of hundreds of thousands of years. For this reason, it is crucial to investigate realistic repository scenarios but also to comprehend the consequences at different levels in the event of system failure. One of the most extreme potential worst scenarios is the leakage of waste from the metal container and the seepage of groundwater loaded with organic matter, which would facilitate and intensify the bacterial activity. In the context of this scenario, the findings in the present study advanced in elucidating the behavior of bentonite microbial communities in the event of a selenium waste leakage during the initial phase of the nuclear repositories, where high temperatures are expected.

### 5. Conclusions

Based on the results discussed above, using a combination of a state-of-the-art microbiological, microscopic, and spectroscopic techniques, we demonstrated that incubation at 60 °C favored the presence of native bentonite genera capable of withstanding high temperatures, such as *Pseudomonas*, *Clostridium*, *Bacillus*, *Tepidimicrobium*, *Brockia*, *Caloribacterium*, and *Thermotalea*, among others. In addition, a strong impact of the inoculated bacterial consortium on the bentonite microbial communities was evidenced, with two out of the four genera included, namely *Stenotrophomonas* and *Pseudomonas*, being dominant. These consortium microcosms changed their color to orange within the first days of incubation, indicative of the presence of Se(0), and by the end of the experiment, the percentage of soluble Se(IV) was very low. STEM-HAADF results elucidated a process of reduced selenium

transformation over time. In the earliest phases of incubation, the Se(0) detected was mainly intracellular, exhibiting amorphous or weakly monoclinic crystalline phase. However, as incubation time advanced, Se(0) appeared to be released in the extracellular space forming aggregates of Se(0) nanoparticles. Furthermore, larger nanoaggregates of Fe+Se composition, as possible ferroselite minerals, were found in those treatments with high bacterial activity, while no such precipitates were found in the heat-shocked bentonite treatment without consortium. The present study proposes a hypothetical mechanism indicating that Fe- and Se-reducing bacteria may play a crucial role in the formation of this mineral ferroselite. In addition, the absence of the consortium further slowed down the Se reduction processes.

In this study, for the first time, the behavior of indigenous microbial communities in bentonite was highlighted under high-temperature conditions and in the presence of Se as a toxic metalloid. Finally, despite the elevated temperatures, certain bacteria would facilitate the immobilization of this metalloid by reducing it into insoluble Se(0) or by forming minerals such as FeSe<sub>2</sub>, in the event of waste leakage. The chemical transformation of amorphous Se(0) into crystalline phases would also ensure the stability of these insoluble precipitates. Thus, bentonite microbial communities would affect the biogeochemical cycle of Se through the immobilization of this critical radionuclide retarding its mobility at DGR barriers.

### **Funding**

The present work was supported by the grant RTI2018–101548-B-I00 “ERDF A way of making Europe” to MLM from the “Ministerio de Ciencia, Innovación y Universidades” (Spanish Government) and by the grant FPU20/00583 from “Ministerio de Universidades” to the first author from the Spanish Government.

### Acknowledgements

The authors would like to thank Dr. F. Javier Huertas (IACT, Spain) for his guidance and assistance in collecting the bentonite from the El Cortijo de Archidona site (Almería, Spain). Moreover, Daniel García Muñoz Bautista Cerro and Cecilia de la Prada (Centro de Instrumentación Científica, University of Granada, Spain) for the sample preparation and microscopy assistance, respectively.

### References

- Antonioli, P., Lampis, S., Chesini, I., Vallini, G., Rinalducci, S., Zolla, L., & Righetti, P. G. (2007). *Stenotrophomonas maltophilia* SeITE02, a new bacterial strain suitable for bioremediation of selenite-contaminated environmental matrices. *Applied and Environmental Microbiology*, 73(21), 6854-6863. <https://doi.org/10.1128/AEM.00957-07>
- Aoyagi, T., Mori, Y., Nanao, M., Matsuyama, Y., Sato, Y., Inaba, T., ... & Hori, T. (2021). Effective Se reduction by lactate-stimulated indigenous microbial communities in excavated waste rocks. *Journal of Hazardous Materials*, 403, 123908. <https://doi.org/10.1016/j.jhazmat.2020.123908>
- Atwood, D. A. (Ed.). (2010). *Radionuclides in the Environment*. Chichester, Reino Unido: John Wiley & Sons.
- Avendaño, R., Chaves, N., Fuentes, P., Sánchez, E., Jiménez, J. I., & Chavarría, M. (2016). Production of selenium nanoparticles in *Pseudomonas putida* KT2440. *Scientific Reports*, 6, 37155. <https://doi.org/10.1038/srep37155>
- Badaut, V., Schlegel, M. L., Descostes, M., & Moutiers, G. (2012). In situ time-resolved X-ray near-edge absorption spectroscopy of selenite reduction by siderite. *Environmental Science & Technology*, 46(19), 10820-10826. <https://doi.org/10.1021/es301611e>
- Bagnoud, A., De Bruijn, I., Andersson, A. F., Diomidis, N., Leupin, O. X., Schwyn, B., & Bernier-Latmani, R. (2016). A minimalistic microbial food web in an excavated deep subsurface clay rock. *FEMS Microbiology Ecology*, 92(1), fiv138. <https://doi.org/10.1093/femsec/fiv138>
- Bartak, D., Bedrníková, E., Kašpar, V. et al. (2024). Survivability and proliferation of microorganisms in bentonite with implication to radioactive waste geological disposal: strong effect of temperature and negligible effect of pressure. *World Journal of Microbiology and Biotechnology*, 40, 41. <https://doi.org/10.1007/s11274-023-03849-0>

- Borah, S. N., Goswami, L., Sen, S., Sachan, D., Sarma, H., Montes, M., Peralta-Videa, J. R., Pakshirajan, K. & Narayan, M. (2021). Selenite bioreduction and biosynthesis of selenium nanoparticles by *Bacillus paramycoides* SP3 isolated from coal mine overburden leachate. *Environmental Pollution*, 285, 117519. <https://doi.org/10.1016/j.envpol.2021.117519>
- Breynaert, E., Scheinost, A. C., Dom, D., Rossberg, A., Vancluysen, J., Gobechiya, E., Kirschhock, C.E.A., Maes, A. (2010). Reduction of Se(IV) in boom clay: XAS solid phase speciation. *Environmental Science & Technology*, 44(17), 6649-6655. <https://doi.org/10.1021/es100569e>
- Callahan, B.J., McMurdie, P.J., Rosen, M.J., Han, A.W., Johnson, A.J., Holmes, S.P. (2016). DADA2: High-resolution sample inference from Illumina amplicon data. *Nature Methods*, 13(7), 581-3. <https://doi.org/10.1038/nmeth.3869>
- Caporaso, J.G., Kuczynski, J., Stombaugh, J., Bittinger, K., Bushman, F.D., Costello, E.K., Fierer, N., Peña, A.G., Goodrich, J.K., Gordon, J.I., Huttley, G.A., Kelley, S.T., Knights, D., Koenig, J.E., Ley, R.E., Lozupone, C.A., McDonald, D., Muegge, B.D., Pirrung, M., Reeder, J., Sevinsky, J.R., Turnbaugh, P.J., Walters, W.A., Widmann, J., Yatsunencko, T., Zaneveld, J., Knight, R. (2010). QIIME allows analysis of high-throughput community sequencing data. *Nature Methods*, 7(5), 335-6. <https://doi.org/10.1038/nmeth.f.303>
- Checinska, A., Paszczynski, A., & Burbank, M. (2015). *Bacillus* and other spore-forming genera: variations in responses and mechanisms for survival. *Annual review of food science and technology*, 6, 351-369. <https://doi.org/10.1146/annurev-food-030713-092332>
- Chen, H., Shin, D. W., Nam, J. G., Kwon, K. W., & Yoo, J. B. (2010). Selenium nanowires and nanotubes synthesized via a facile template-free solution method. *Materials Research Bulletin*, 45(6), 699-704. <https://doi.org/10.1016/j.materresbull.2010.02.016>
- Combet-Blanc, Y., Ollivier, B., Streicher, C., Patel, B. K. C., Dwivedi, P. P., Pot, B., ... & Garcia, J. L. (1995). *Bacillus thermoamylovorans* sp. nov., a moderately thermophilic and amylolytic bacterium. *International Journal of Systematic and Evolutionary Microbiology*, 45(1), 9-16. <https://doi.org/10.1099/00207713-45-1-9>
- Den Besten, H. M., Wells-Bennik, M. H., & Zwietering, M. H. (2018). Natural diversity in heat resistance of bacteria and bacterial spores: impact on food safety and quality. *Annual Review of Food Science and Technology*, 9, 383-410. <https://doi.org/10.1146/annurev-food-030117-012808>
- Di Gregorio, S., Lampis, S., & Vallini, G. (2005). Selenite precipitation by a rhizospheric strain of *Stenotrophomonas* sp. isolated from the root system of *Astragalus bisulcatus*: a biotechnological perspective. *Environment International*, 31(2), 233-241. <https://doi.org/10.1016/j.envint.2004.09.021>

## CHAPTER 2

- Eijlander, R. T., de Jong, A., Krawczyk, A. O., Holsappel, S., & Kuipers, O. P. (2014). SporeWeb: an interactive journey through the complete sporulation cycle of *Bacillus subtilis*. *Nucleic acids research*, 42(D1), D685-D691. <https://doi.org/10.1093/nar/gkt1007>
- Eswayah, A. S., Smith, T. J., Scheinost, A. C., Hondow, N., & Gardiner, P. H. (2017). Microbial transformations of selenite by methane-oxidizing bacteria. *Applied Microbiology and Biotechnology*, 101(17), 6713-6724. <https://doi.org/10.1007/s00253-017-8380-8>
- Fernández, A. M., & Villar, M. V. (2010). Geochemical behaviour of a bentonite barrier in the laboratory after up to 8 years of heating and hydration. *Applied Geochemistry*, 25(6), 809-824. <https://doi.org/10.1016/j.apgeochem.2010.03.001>
- Fernández, A. M., Cuevas, J., & Rivas, P. (2000). Pore water chemistry of the FEBEX bentonite. *MRS Online Proceedings Library (OPL)*, 663, 573. <https://doi.org/10.1557/PROC-663-573>
- Fernández-Díaz, A.M. (2004). Caracterización y modelización del agua intersticial de materiales arcillosos: estudio de la bentonita de Cortijo de Archidona. PhD Thesis. Universidad Autónoma de Madrid Editorial CIEMAT, p. 505.
- Freikowski, D., Winter, J., & Gallert, C. (2010). Hydrogen formation by an arsenate-reducing *Pseudomonas putida*, isolated from arsenic-contaminated groundwater in West Bengal, India. *Applied microbiology and biotechnology*, 88, 1363-1371. <https://doi.org/10.1007/s00253-010-2856-0>
- García-Romero, E., María Manchado, E., Suárez, M., & García-Rivas, J. (2019). Spanish bentonites: a review and new data on their geology, mineralogy, and crystal chemistry. *Minerals*, 9(11), 696. <https://doi.org/10.3390/min9110696>
- Gonzalez-Gil, G., Lens, P.N.L., Saikaly, P.E. (2016). Selenite reduction by anaerobic microbial aggregates: microbial community structure, and proteins associated to the produced selenium spheres. *Frontiers in Microbiology*, 7. <https://doi.org/10.3389/fmicb.2016.00571>
- Guo, M. (2020). The electrochemical and corrosion study of copper for nuclear waste containers under deep geological disposal conditions (Doctoral dissertation, The University of Western Ontario (Canada)).
- Hall, D. S., Behazin, M., Binns, W. J., & Keech, P. G. (2021). An evaluation of corrosion processes affecting copper-coated nuclear waste containers in a deep geological repository. *Progress in Materials Science*, 118, 100766. <https://doi.org/10.1016/j.pmatsci.2020.100766>
- Hammer, O. (2001). PAST: paleontological statistics software package for education and data analysis. *Palaeontologia Electronica*. <http://palaeo-electronica.org>

- Hassan, R. S., Abass, M. R., Eid, M. A., & Abdel-Galil, E. A. (2021). Sorption of some radionuclides from liquid waste solutions using anionic clay hydrotalcite sorbent. *Applied Radiation and Isotopes*, 178, 109985. <https://doi.org/10.1016/j.apradiso.2021.109985>
- Hattori, S., Kamagata, Y., Hanada, S., & Shoun, H. (2000). *Thermacetogenium phaeum* gen. nov., sp. nov., a strictly anaerobic, thermophilic, syntrophic acetate-oxidizing bacterium. *International Journal of Systematic and Evolutionary Microbiology*, 50(4), 1601-1609. <https://doi.org/10.1099/00207713-50-4-1601>
- Haynes, H. M., Pearce, C. I., Boothman, C., & Lloyd, J. R. (2018). Response of bentonite microbial communities to stresses relevant to geodisposal of radioactive waste. *Chemical Geology*, 501, 58-67. <https://doi.org/10.1016/j.chemgeo.2018.10.004>
- He, J., Shi, Y., Yang, X., Zhou, W., Li, Y., & Liu, C. (2018). Influence of Fe(II) on the Se(IV) sorption under oxic/anoxic conditions using bentonite. *Chemosphere*, 193, 376-384. <https://doi.org/10.1016/j.chemosphere.2017.10.143>
- Hicks, T.W., White, M.J., Hooker, P.J. (2009). Role of bentonite in determination of thermal limits on geological disposal facility design. *Nuclear*, 0883-1.
- Hoving, A. L., Münch, M. A., Bruggeman, C., Banerjee, D., & Behrends, T. (2019). Kinetics of selenite interactions with Boom Clay: adsorption–reduction interplay. *Geological Society, London, Special Publications*, 482(1), 225-239. <https://doi.org/10.1144/SP482-2018-60>
- Howard III, J. H. (1977). Geochemistry of selenium: formation of ferroselite and selenium behavior in the vicinity of oxidizing sulfide and uranium deposits. *Geochimica et Cosmochimica Acta*, 41(11), 1665-1678. [https://doi.org/10.1016/0016-7037\(77\)90176-4](https://doi.org/10.1016/0016-7037(77)90176-4)
- Jörg, G., Bühnenmann, R., Hollas, S., Kivel, N., Kossert, K., Van Winckel, S., & Gostomski, C. L. V. (2010). Preparation of radiochemically pure <sup>79</sup>Se and highly precise determination of its half-life. *Applied Radiation and Isotopes*, 68(12), 2339-235. <https://doi.org/10.1016/j.apradiso.2010.05.006>
- King, F. (2017). Nuclear waste canister materials: Corrosion behavior and long-term performance in geological repository systems. In *Geological Repository Systems for Safe Disposal of Spent Nuclear Fuels and Radioactive Waste*; Woodhead Publishing: Sawston, UK, pp. 365–408. <https://doi.org/10.1016/B978-0-08-100642-9.00013-X>
- Lampis, S., Zonaro, E., Bertolini, C., Bernardi, P., Butler, C. S., & Vallini, G. (2014). Delayed formation of zero-valent selenium nanoparticles by *Bacillus mycoides* SeITE01 as a consequence of selenite reduction under aerobic conditions. *Microbial Cell Factories*, 13(1), 1-14. <https://doi.org/10.1186/1475-2859-13-35>
- Lee, Y. J., Wagner, I. D., Brice, M. E., Kevbrin, V. V., Mills, G. L., Romanek, C. S., & Wiegel, J. (2005). *Thermosediminibacter oceani* gen. nov., sp. nov. and *Thermosediminibacter*

## CHAPTER 2

- litoriperuensis* sp. nov., new anaerobic thermophilic bacteria isolated from Peru Margin. *Extremophiles*, 9, 375-383. <https://doi.org/10.1007/s00792-005-0453-4>
- Li, D. B., Cheng, Y. Y., Wu, C., Li, W. W., Li, N., Yang, Z. C., Tong, Z. H., & Yu, H. Q. (2014). Selenite reduction by *Shewanella oneidensis* MR-1 is mediated by fumarate reductase in periplasm. *Scientific Reports*, 4(1), 1-7. <https://doi.org/10.1038/srep03735>
- Lopez-Fernandez, M., Romero-González, M., Günther, A., Solari, P. L., & Merroun, M. L. (2018). Effect of U(VI) aqueous speciation on the binding of uranium by the cell surface of *Rhodotorula mucilaginosa*, a natural yeast isolate from bentonites. *Chemosphere*, 199, 351-360. <https://doi.org/10.1016/j.chemosphere.2018.02.055>
- Lopez-Fernandez, M., Fernández-Sanfrancisco, O., Moreno-García, A., Martín-Sánchez, I., Sánchez-Castro, I., & Merroun, M. L. (2014). Microbial communities in bentonite formations and their interactions with uranium. *Applied geochemistry*, 49, 77-86. <https://doi.org/10.1016/j.apgeochem.2014.06.022>
- Macy, J. M., Michel, T. A., & Kirsch, D. G. (1989). Selenate reduction by a *Pseudomonas* species: a new mode of anaerobic respiration. *FEMS Microbiology Letters*, 61(1-2), 195-198. <https://doi.org/10.1111/j.1574-6968.1989.tb03577.x>
- Martinez-Moreno, M.F., Povedano-Priego, C., Mumford, A.D., Morales-Hidalgo, M., Mijndonckx, K., Jroundi, F., Ojeda, J.J., Merroun, M.L., (2024). Microbial responses to elevated temperature: Evaluating bentonite mineralogy and copper canister corrosion within the long-term stability of deep geological repositories of nuclear waste. *Science of The Total Environment*, 915, 170149. <https://doi.org/10.1016/j.scitotenv.2024.170149>
- Martinez-Moreno, M. F., Povedano-Priego, C., Morales-Hidalgo, M., Mumford, A. D., Aranda, E., Vilchez-Vargas, R., ... & Merroun, M. L. (2024b). Microbial influence in Spanish bentonite slurry microcosms: unveiling a-year long geochemical evolution and early-stage copper corrosion related to nuclear waste repositories. *Environmental Pollution*, 124491. <https://doi.org/10.1016/j.envpol.2024.124491>
- Matschiavelli, N., Kluge, S., Podlech, C., Standhaft, D., Grathoff, G., Ikeda-Ohno, A., ... & Cherkouk, A. (2019). The year-long development of microorganisms in uncompacted bavarian bentonite slurries at 30 and 60 °C. *Environmental Science & Technology*, 53, 10514–10524. <https://doi.org/10.1021/acs.est.9b02670>
- McMurdie, P.J., Holmes, S. (2013). Phyloseq: a R package for reproducible interactive analysis and graphics of microbiome census data. *PLoS One*, 8, e61217. <https://doi.org/10.1371/journal.pone.0061217>
- Merroun, M. L., & Selenska-Pobell, S. (2008). Bacterial interactions with uranium: an environmental perspective. *Journal of Contaminant Hydrology*, 102(3-4): 285-295. <https://doi.org/10.1016/j.jconhyd.2008.09.019>

- Miettinen, H., Bomberg, M., Bes, R., Tiljander, M., & Vikman, M. (2022). Transformation of inherent microorganisms in Wyoming-type bentonite and their effects on structural iron. *Applied Clay Sciences*, 221, 106465. <https://doi.org/10.1016/j.clay.2022.106465>
- Moore, R. C., Rigali, M. J., & Brady, P. (2016). Selenite sorption by carbonate substituted apatite. *Environmental Pollution*, 218, 1102-1107. <https://doi.org/10.1016/j.envpol.2016.08.063>
- Morales-Hidalgo, M., Povedano-Priego, C., Martinez-Moreno, M. F., Ruiz-Fresneda, M. A., Lopez-Fernandez, M., Jroundi, F., & Merroun, M. L. (2024a). Insights into the Impact of Physicochemical and Microbiological Parameters on the Safety Performance of Deep Geological Repositories. *Microorganisms*, 12(5), 1025. <https://doi.org/10.3390/microorganisms12051025>
- Morales-Hidalgo, M., Povedano-Priego, C., Martinez-Moreno, M. F., Ojeda, J. J., Jroundi, F., & Merroun, M. L. (2024b). Long-term tracking of the microbiology of uranium-amended water-saturated bentonite microcosms: a mechanistic characterization of U speciation. *Journal of Hazardous Materials*, 476, 135044. <https://doi.org/10.1016/j.jhazmat.2024.135044>
- Naganuma, T., Sato, M., Hoshii, D., Amano-Murakami, Y., Iwatsuki, T., & Mandernack, K. W. (2006). Isolation and characterization of *Pseudomonas* strains capable of Fe(III) reduction with reference to redox response regulator genes. *Geomicrobiology Journal*, 23(3-4), 145-155. <https://doi.org/10.1080/01490450600596565>
- Neuwirth E. (2022). RColorBrewer: ColorBrewer Palettes. R package version 1.1–3, <<https://CRAN.R-project.org/package=RColorBrewer>>.
- Olegario, J. T., Yee, N., Miller, M., Szczepaniak, J., & Manning, B. (2010). Reduction of Se(VI) to Se(-II) by zerovalent iron nanoparticle suspensions. *Journal of Nanoparticle Research*, 12(6), 2057-2068. <https://doi.org/10.1007/s11051-009-9764-1>
- Pinel-Cabello, M., Jroundi, F., López-Fernández, M., Geffers, R., Jarek, M., Jauregui, R., ... & Merroun, M. L. (2021). Multisystem combined uranium resistance mechanisms and bioremediation potential of *Stenotrophomonas bentonitica* BII-R7: transcriptomics and microscopic study. *Journal of Hazardous Materials*, 403, 123858. <https://doi.org/10.1016/j.jhazmat.2020.123858>
- Povedano-Priego, C.; Jroundi, F.; Solari, P.L.; Guerra-Tschuschke, I.; Abad-Ortega, M.D.M.; Link, A.; Vilchez-Vargas, R.; and Merroun, M.L. (2023). Unlocking the bentonite microbial diversity and its implications in selenium bioreduction and biotransformation: Advances in deep geological repositories. *Journal Hazardous Material*, 445, 130557. <https://doi.org/10.1016/j.jhazmat.2022.130557>
- Povedano-Priego, C., Jroundi, F., Lopez-Fernandez, M., Shrestha, R., Spanek, R., Martín-Sánchez, I., Villar, M. V., Ševců, A., Dopson, M. & Merroun, M. L. (2021). Deciphering indigenous bacteria in compacted bentonite through a novel and efficient DNA extraction method: Insights into biogeochemical processes within the Deep

## CHAPTER 2

- Geological Disposal of nuclear waste concept. *Journal of Hazardous Materials*, 408, 124600. <https://doi.org/10.1016/j.jhazmat.2020.124600>
- Povedano-Priego, C., Jroundi, F., Lopez-Fernandez, M., Sánchez-Castro, I., Martín-Sánchez, I., Huertas, F. J., & Merroun, M. L. (2019). Shifts in bentonite bacterial community and mineralogy in response to uranium and glycerol-2-phosphate exposure. *Science of The Total Environment*, 692, 219-232. <https://doi.org/10.1016/j.scitotenv.2019.07.228>
- Prakash, N. T., Sharma, N., Prakash, R., Raina, K. K., Fellowes, J., Pearce, C. I., Lloyd, J. R., & Patrick, R. A. D. (2009). Aerobic microbial manufacture of nanoscale selenium: exploiting nature's bio-nanomineralization potential. *Biotechnology Letters*, 31(12), 1857. <https://doi.org/10.1007/s10529-009-0096-0>
- R Core Team. (2022). R: A language and environment for statistical computing. R Foundation for Statistical Computing, Vienna, Austria. <https://www.Rproject.org/>
- Robertson, C. E., Harris, J. K., Wagner, B. D., Granger, D., Browne, K., Tatem, B., Feazel, M. L., Park, K., Pace, N. R. & Frank, D. N. (2013). Explicite: graphical user interface software for metadata-driven management, analysis and visualization of microbiome data. *Bioinformatics*, 29(23), 3100-3101. <https://doi.org/10.1093/bioinformatics/btt526>
- Ruiz-Fresneda, M. A., Martínez-Moreno, M. F., Povedano-Priego, C., Morales-Hidalgo, M., Jroundi, F., & Merroun, M. L. (2023). Impact of microbial processes on the safety of deep geological repositories for radioactive waste. *Frontiers in Microbiology*, 14, 1134078. <https://doi.org/10.3389/fmicb.2023.1134078>
- Ruiz-Fresneda, M. A., Eswayah, A. S., Romero-Gonzalez, M., Gardiner, P. H., Solari, P. L., & Merroun, M. L. (2020). Chemical and structural characterization of SeIV biotransformations by *Stenotrophomonas bentonitica* into Se0 nanostructures and volatile Se species. *Environmental Science: Nano*, 5, 2103–2116. <https://doi.org/10.1039/D0EN00507J>
- Ruiz-Fresneda, M. A., Gomez-Bolivar, J., Delgado-Martin, J., Abad-Ortega, M. D. M., Guerra-Tschuschke, I., & Merroun, M. L. (2019). The Bioreduction of Selenite under Anaerobic and Alkaline Conditions Analogous to Those Expected for a Deep Geological Repository System. *Molecules*, 24(21), 3868. <https://doi.org/10.3390/molecules24213868>
- Ruiz-Fresneda, M. A., Martín, J. D., Bolívar, J. G., Cantos, M. V. F., Bosch-Estévez, G., Moreno, M. F. M., & Merroun, M. L. (2018). Green synthesis and biotransformation of amorphous Se nanospheres to trigonal 1D Se nanostructures: impact on Se mobility within the concept of radioactive waste disposal. *Environmental Science: Nano*, 5(9), 2103-2116. <https://doi.org/10.1039/C8EN00221E>
- Sánchez-Castro, I., Ruiz-Fresneda, M. A., Bakkali, M., Kämpfer, P., Glaeser, S. P., Busse, H. J., ... & Merroun, M. L. (2017). *Stenotrophomonas bentonitica* sp. nov., isolated from

- bentonite formations. *International journal of systematic and evolutionary microbiology*, 67(8), 2779-2786. <https://doi.org/10.1099/ijsem.0.002016>
- Shiratori, H., Sasaya, K., Ohiwa, H., Ikeno, H., Ayame, S., Kataoka, N., ... & Ueda, K. (2009). *Clostridium clariflavum* sp. nov. and *Clostridium caenicola* sp. nov., moderately thermophilic, cellulose-/cellobiose-digesting bacteria isolated from methanogenic sludge. *International journal of systematic and evolutionary microbiology*, 59(7), 1764-1770. <https://doi.org/10.1099/ijms.0.003483-0>
- Slobodkin, A. I., Tourova, T. P., Kostrikina, N. A., Lysenko, A. M., German, K. E., Bonch-Osmolovskaya, E. A., & Birkeland, N. K. (2006). *Tepidimicrobium ferriphilum* gen. nov., sp. nov., a novel moderately thermophilic, Fe(III)-reducing bacterium of the order Clostridiales. *International journal of systematic and evolutionary microbiology*, 56(2), 369-372. <https://doi.org/10.1099/ijms.0.63694-0>
- Slobodkina, G. B., Kolganova, T. V., Kostrikina, N. A., Bonch-Osmolovskaya, E. A., & Slobodkin, A. I. (2012). *Caloribacterium cisternae* gen. nov., sp. nov., an anaerobic thermophilic bacterium from an underground gas storage reservoir. *International journal of systematic and evolutionary microbiology*, 62(Pt\_7), 1543-1547. <https://doi.org/10.1099/ijms.0.033076-0>
- Switzer Blum, J., Burns Bindi, A., Buzzelli, J., Stolz, J. F., & Oremland, R. S. (1998). *Bacillus arsenicoselenatis*, sp. nov., and *Bacillus selenitireducens*, sp. nov.: two haloalkaliphiles from Mono Lake, California that respire oxyanions of selenium and arsenic. *Archives of microbiology*, 171, 19-30. <https://doi.org/10.1007/s002030050673>
- Takai, K., Inoue, A., & Horikoshi, K. (1999). *Thermaerobacter marianensis* gen. nov., sp. nov., an aerobic extremely thermophilic marine bacterium from the 11000 m deep Mariana Trench. *International Journal of Systematic and Evolutionary Microbiology*, 49(2), 619-628. <https://doi.org/10.1099/00207713-49-2-619>
- Tenededzai, J. T., Brink, H. G., & Chirwa, E. M. (2021). Formation of Elemental Selenium Nanoparticles (SeNPs) from the Reduction of Selenite (SeO<sub>3</sub><sup>2-</sup>) by a Pure Culture of *Pseudomonas Stutzeri* NT-i. *Chemical Engineering Transactions*, 86, 193-198. <https://doi.org/10.3303/CET2186033>
- Tenededzai, J. T., Chirwa, E. M., & Brink, H. G. (2020). Reduction of Selenite by use of *Pseudomonas stutzeri* NT-I Cell-free Extract. *Chemical Engineering Transactions*, 79, 373-378. <http://hdl.handle.net/2263/80531>
- Thijs, S., Op De Beeck, M., Beckers, B., Truyens, S., Stevens, V., Van Hamme, J. D., Weyens, N. & Vangronsveld, J. (2017). Comparative evaluation of four bacteria-specific primer pairs for 16S rRNA gene surveys. *Frontiers in microbiology*, 8, 494. <https://doi.org/10.3389/fmicb.2017.00494>
- Tondel, M., & Lindahl, L. (2019). Intergenerational ethical issues and communication related to high-level nuclear waste repositories. *Current Environmental Health Reports*, 6, 338-343. <https://doi.org/10.1007/s40572-019-00257-1>

## CHAPTER 2

- Touzel, J. P., O'Donohue, M., Debeire, P., Samain, E., & Breton, C. (2000). *Thermobacillus xylanilyticus* gen. nov., sp. nov., a new aerobic thermophilic xylan-degrading bacterium isolated from farm soil. *International journal of systematic and evolutionary microbiology*, 50(1), 315-320. <https://doi.org/10.1099/00207713-50-1-315>
- Warnes G., Bolker B., Bonebakker L., Gentleman R., Huber W., Liaw A., Lumley T., Maechler M., Magnusson A., Moeller S., Schwartz M., Venables, B. (2022). *gplots: Various R Programming Tools for Plotting Data*. R package version 3.1.3. <https://CRAN.R-project.org/package=gplots>
- Warren, C. G. (1968). The synthesis of ferroselite from an aqueous solution at low temperature. *Economic Geology*, 63(4), 418-419. <https://doi.org/10.2113/gsecongeo.63.4.418>
- WNA. World Nuclear Association. 2023. Storage and disposal of radioactive waste. <https://www.world-nuclear.org/>
- Yang, S., Li, S., Jia, X. (2019). Production of medium chain length polyhydroxyalkanoate from acetate by engineered *Pseudomonas putida* KT2440. *Journal of Industrial Microbiology and Biotechnology*, 46, 793–800. <https://doi.org/10.1007/s10295-019-02159-5>
- Yu, Q., Boyanov, M. I., Liu, J., Kemner, K. M., & Fein, J. B. (2018). Adsorption of selenite onto *Bacillus subtilis*: The overlooked role of cell envelope sulfhydryl sites in the microbial conversion of Se(IV). *Environmental Science & Technology*, 52(18), 10400-10407. <https://doi.org/10.1021/acs.est.8b02280>

Supplementary material for:

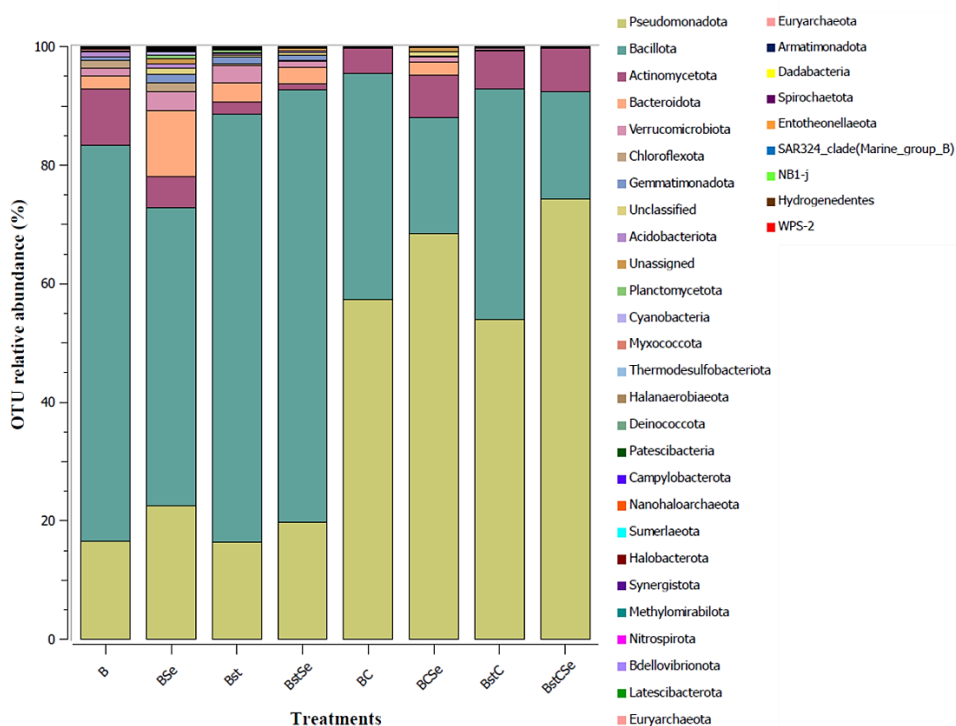
**High temperature impact on bentonite microbial communities: A study  
of Se(IV) biogeochemical cycle**

**Mar Morales-Hidalgo**<sup>1</sup>, Cristina Povedano-Priego<sup>1</sup>, Marcos F. Martinez-  
Moreno<sup>1</sup>, Fadwa Jroundi<sup>1</sup>, Mohamed L. Merroun<sup>1</sup>

<sup>1</sup>*Faculty of Science, Department of Microbiology, University of Granada, Granada,  
Spain.*



**Supplementary Figure S1.** Water-saturated bentonite microcosms of different treatments bubbling with N<sub>2</sub> to get anoxic conditions.



**Supplementary Figure S2.** Relative abundances of phyla belonging to Archaea and Bacteria in water-saturated bentonite microcosms after 2 months of anoxic incubation at 60 °C. Stacked bars represent the mean values of biological triplicates (except BstC, BCSe and BstSe in duplicate). B: natural bentonite; Bst: heat-shocked bentonite; C: bacterial consortium; Se: sodium selenite (2 mM).

**Supplementary Table S1.** ICP-MS analysis of the major element's composition of the equilibrium water.

Element/unit (PPB)																						
Be	Sc	V	Cr	Mn	Co	Ni	Cu	Zn	As	Se	Y	Mo	Cd	In	Sn	Sb	Ba	Tl	Pb	Bi	Th	U
0.01	1.61	3.87	0.33	12.10	0.16	0.94	3.52	15.30	6.76	6.01	0.43	0.47	0.03	0.01	1.21	1.09	2.04	0.01	1.95	4.62	0.32	3.12

**Supplementary Table S2.** Percentages of relative abundances at phylum level of the microbial communities in water-saturated bentonite microcosms after 2 months of anoxic incubation at 60 °C. Treatments studied in triplicated (except BstC, BCSe and BstSe in duplicate). B: natural bentonite; Bst: heat-shocked bentonite; C: bacterial consortium; Se: sodium selenite (2 mM).

Phyla	Relative abundances (%)								
	Total	B	BSe	Bst	BstSe	BC	BCSe	BstC	BstCSe
Pseudomonadota	52.44	16.48	22.58	16.36	19.74	57.26	68.46	53.97	74.23
Bacillota	40.91	66.91	50.23	72.26	72.98	38.21	19.57	38.93	18.13
Actinomycetota	4.67	9.47	5.33	2.05	1.07	4.33	7.13	6.36	7.42
Bacteroidota	0.79	2.14	11.01	3.24	2.78	0.01	2.24	0.23	0.10
Verrucomicrobiota	0.35	1.42	3.24	2.91	0.98	0.01	0.84	0.26	0.06
Chloroflexota	0.22	1.27	1.43	0.30	0.19	0.11	0.10	0.00	0.03
Gemmatimonadota	0.15	0.53	1.51	1.20	0.78	0.00	0.00	0.00	0.00
Unclassified	0.10	0.10	1.03	0.27	0.42	0.02	0.80	0.07	0.00
Acidobacteriota	0.08	0.74	0.75	0.24	0.27	0.00	0.02	0.01	0.01
Unassigned	0.08	0.00	0.85	0.10	0.47	0.01	0.68	0.14	0.00
Planctomycetota	0.05	0.12	0.59	0.43	0.02	0.01	0.01	0.00	0.01

## CHAPTER 2

Cyanobacteria	0.04	0.16	0.52	0.26	0.10	0.00	0.12	0.01	0.01
Myxococcota	0.03	0.22	0.20	0.11	0.04	0.01	0.00	0.00	0.00
Thermodesulfobacteriota	0.02	0.22	0.20	0.03	0.02	0.00	0.00	0.00	0.00
Halanaerobiaeota	0.01	0.02	0.03	0.00	0.03	0.01	0.00	0.00	0.00
Deinococcota	0.01	0.03	0.06	0.01	0.00	0.01	0.00	0.00	0.00
Patescibacteria	0.01	0.03	0.09	0.14	0.00	0.00	0.00	0.00	0.00
Campylobacterota	< 0.01	0.00	0.05	0.00	0.01	0.00	0.03	0.00	0.00
Nanohaloarchaeota	< 0.01	0.00	0.01	0.00	0.00	0.00	0.00	0.00	0.00
Sumerlaeota	< 0.01	0.02	0.00	0.01	0.00	0.00	0.00	0.00	0.00
Halobacterota	< 0.01	0.00	0.00	0.00	0.00	0.00	0.00	0.00	0.00
Synergistota	< 0.01	0.02	0.03	0.00	0.00	0.00	0.00	0.00	0.00
Methylomirabilota	< 0.01	0.00	0.02	0.00	0.00	0.00	0.00	0.00	0.00
Nitrospirota	< 0.01	0.05	0.03	0.03	0.01	0.00	0.00	0.00	0.00
Bdellovibrionota	< 0.01	0.00	0.01	0.00	0.06	0.00	0.00	0.00	0.00
Latescibacterota	< 0.01	0.00	0.04	0.00	0.00	0.00	0.00	0.00	0.00
Euryarchaeota	< 0.01	0.00	0.03	0.00	0.00	0.00	0.00	0.00	0.00
Armatimonadota	< 0.01	0.01	0.02	0.02	0.02	0.00	0.00	0.00	0.00
Dadabacteria	< 0.01	0.01	0.01	0.00	0.00	0.00	0.00	0.00	0.00
Spirochaetota	< 0.01	0.00	0.04	0.00	0.00	0.00	0.00	0.00	0.00
Entotheonellaeota	< 0.01	0.00	0.01	0.00	0.00	0.00	0.00	0.00	0.00
SAR324_clade(Marine_group_B)	< 0.01	0.00	0.00	0.02	0.00	0.00	0.00	0.00	0.00
NB1-j	< 0.01	0.00	0.01	0.00	0.00	0.00	0.00	0.00	0.00
Hydrogenedentes	< 0.01	0.01	0.00	0.00	0.00	0.00	0.00	0.00	0.00

**Supplementary Table S3.** Percentages of relative abundances at genus level of the microbial communities in water-saturated bentonite microcosms after 2 months of anoxic incubation at 60 °C. Treatments studied in triplicated (except BstC, BCSe and BstSe in duplicate). Cut off:  $\geq 0.02\%$ . B: natural bentonite; Bst: heat-shocked bentonite; C: bacterial consortium; Se: sodium selenite (2 mM).

Genera	Relative abundances (%)								
	Total	B	BSe	Bst	BstSe	BC	BCSe	BstC	BstCSe
<i>Stenotrophomonas</i>	29.75	0.00	0.02	0.02	0.00	34.48	40.11	26.00	45.05
<i>Pseudomonas</i>	21.31	11.39	9.71	11.77	6.84	22.62	26.81	27.91	29.13
<i>Clostridium_sensu_stricto_7</i>	7.57	0.00	0.00	0.00	0.00	9.89	0.00	0.00	0.00
<i>Bacillus</i>	4.31	2.34	10.90	33.88	23.25	2.19	2.90	2.56	4.48
<i>Tepidimicrobium</i>	3.98	0.00	0.00	0.00	0.00	4.62	5.34	6.15	3.84
<i>Amycolatopsis</i>	3.51	0.00	0.01	0.00	0.02	3.80	6.25	6.26	7.27
<i>Brevibacillus</i>	2.90	7.20	2.07	5.42	20.85	2.30	0.00	0.00	0.00
<i>Sporacetigenium</i>	2.48	0.00	0.00	0.00	0.00	2.90	1.00	5.18	2.31
<i>Desulfofundulus</i>	1.72	0.00	0.00	0.00	0.00	2.24	0.00	0.00	0.00
<i>Aeribacillus</i>	1.45	6.68	9.31	4.20	14.16	0.34	0.00	0.30	0.00
unclassified_Peptostreptococcaceae	1.32	0.00	0.03	0.00	0.00	1.61	0.56	1.32	0.93
uncultured_Bacillaceae	1.25	21.88	1.63	5.80	0.00	0.00	0.00	0.00	0.00
<i>Caloribacterium</i>	1.08	0.00	0.00	0.00	0.00	1.41	0.00	0.00	0.00
<i>Thermaerobacter</i>	1.05	15.19	2.22	6.14	2.50	0.00	0.00	0.00	0.00
<i>Fonticella</i>	0.98	0.02	0.04	0.01	0.00	1.13	1.10	2.15	0.84
<i>Pseudoclostridium</i>	0.97	0.00	0.00	0.00	0.00	1.22	0.00	1.36	0.00
<i>Exiguobacterium</i>	0.88	0.09	0.04	0.04	0.00	1.12	0.82	0.00	0.00
unclassified_Bacillaceae	0.82	0.16	0.97	0.10	0.18	0.92	0.81	0.77	0.67

## CHAPTER 2

<i>Clostridium_sensu_stricto_13</i>	0.75	0.01	0.02	0.00	0.00	0.92	0.27	0.90	0.38
<i>Symbiobacterium</i>	0.73	1.91	2.38	0.18	0.00	0.70	0.00	0.28	0.00
unclassified_Micrococcaceae	0.56	5.39	1.51	0.68	0.50	0.26	0.41	0.07	0.12
<i>Brockia</i>	0.52	3.91	0.00	2.85	0.00	0.27	0.46	0.14	0.75
<i>Clostridium_sensu_stricto_1</i>	0.46	0.03	0.04	0.01	0.00	0.46	0.43	2.73	0.27
<i>Desulfotomaculum</i>	0.35	0.01	0.00	0.02	0.00	0.45	0.00	0.01	0.00
<i>Akkermansia</i>	0.33	1.28	3.00	2.85	0.93	0.00	0.84	0.26	0.05
<i>Desulfitibacter</i>	0.30	0.03	0.00	0.00	0.00	0.39	0.00	0.00	0.00
<i>TTA-B61_Firmicutes</i>	0.29	0.00	0.00	0.00	0.00	0.38	0.00	0.00	0.00
uncultured	0.27	0.00	0.00	0.00	0.00	0.34	0.05	0.20	0.03
<i>Bacteroides</i>	0.23	0.74	2.99	1.26	0.55	0.00	0.73	0.13	0.04
<i>Clostridium_sensu_stricto_10</i>	0.23	0.00	0.01	0.02	0.00	0.26	0.47	0.36	0.24
<i>Lutispora</i>	0.22	0.02	0.02	0.02	0.02	0.17	0.00	2.98	0.01
<i>Anaerobacillus</i>	0.21	0.43	0.40	0.67	2.74	0.02	0.55	0.08	1.58
<i>Muribaculaceae</i>	0.20	0.23	3.91	0.37	0.51	0.00	0.57	0.02	0.02
<i>Thermotalea</i>	0.20	0.00	0.00	0.00	0.00	0.20	0.36	0.91	0.20
<i>Desulfohalotomaculum</i>	0.19	0.00	0.00	0.00	0.00	0.18	0.01	1.60	0.00
<i>Lactobacillus</i>	0.18	0.35	3.16	0.58	0.35	0.00	0.38	0.00	0.05
uncultured_Paenibacillaceae	0.18	0.00	0.00	0.27	6.43	0.00	0.00	0.00	0.00
<i>Clostridium_sensu_stricto_8</i>	0.16	0.06	0.07	0.10	0.07	0.15	0.15	0.94	0.03
<i>Thermobacillus</i>	0.16	1.81	1.96	0.07	0.00	0.00	0.00	0.00	0.00
<i>Marinomonas</i>	0.16	0.18	0.72	0.19	4.48	0.00	0.21	0.00	0.00
<i>Clostridium_sensu_stricto_3</i>	0.15	0.00	0.00	0.00	0.00	0.19	0.00	0.03	0.00

<i>Sphingomonas</i>	0.15	0.90	1.19	0.53	0.20	0.04	0.04	0.01	0.00
<i>Tepidanaerobacter</i>	0.15	0.00	0.00	0.00	0.00	0.20	0.00	0.00	0.00
<i>Streptococcus</i>	0.14	0.23	2.33	0.64	0.21	0.00	0.29	0.02	0.04
<i>Blautia</i>	0.13	0.46	1.48	0.77	0.35	0.00	0.31	0.09	0.01
<i>S0134_terrestrial_group</i>	0.13	0.27	1.40	1.15	0.73	0.00	0.00	0.00	0.00
<i>UCG-002_Oscillospiraceae</i>	0.12	0.45	0.97	1.18	0.24	0.00	0.30	0.11	0.01
<i>Actinotalea</i>	0.12	0.28	0.21	0.04	0.02	0.12	0.06	0.00	0.00
unclassified_Nocardioidaceae	0.12	1.42	0.87	0.05	0.13	0.02	0.06	0.00	0.01
<i>Thalassospira</i>	0.11	0.08	0.51	0.23	2.65	0.00	0.23	0.00	0.00
<i>Sedimentibacter</i>	0.11	0.00	0.00	0.00	0.00	0.14	0.00	0.13	0.00
unclassified_Lachnospiraceae	0.11	0.08	0.37	0.31	0.07	0.09	0.06	0.18	0.00
<i>Peptostreptococcaceae</i>	0.11	0.00	0.00	0.00	0.00	0.09	0.05	1.26	0.19
unclassified_Bacteria	0.10	0.10	1.03	0.27	0.42	0.02	0.80	0.07	0.00
unclassified_Firmicutes	0.09	0.00	0.00	0.00	0.00	0.12	0.00	0.00	0.00
<i>Enterococcus</i>	0.09	0.00	0.50	1.94	0.03	0.00	0.08	0.00	0.00
uncultured_Symbiobacteraceae	0.08	0.00	0.00	0.03	0.01	0.10	0.00	0.16	0.00
<i>Anaerolinea</i>	0.08	0.30	0.21	0.04	0.09	0.07	0.04	0.00	0.02
<i>Kocuria</i>	0.08	0.25	0.21	0.04	0.04	0.07	0.05	0.00	0.00
<i>Thermosediminibacter</i>	0.08	0.00	0.00	0.00	0.00	0.00	0.00	2.76	0.00
unclassified	0.08	0.00	0.85	0.10	0.47	0.01	0.68	0.14	0.00
<i>Ureibacillus</i>	0.07	0.46	0.00	0.23	0.00	0.06	0.00	0.04	0.00
<i>Alistipes</i>	0.07	0.22	0.77	0.44	0.22	0.00	0.15	0.05	0.01
<i>Anaerosolibacter</i>	0.07	0.05	0.02	0.00	0.02	0.06	0.12	0.31	0.09

## CHAPTER 2

unclassified_Enterobacteriaceae	0.07	0.15	1.11	0.28	0.12	0.00	0.07	0.00	0.01
<i>Anoxybacillus</i>	0.06	0.06	0.17	1.16	0.00	0.00	0.16	0.00	0.15
<i>Subdoligranulum</i>	0.06	0.24	0.60	0.39	0.13	0.00	0.16	0.02	0.00
<i>Nocardioides</i>	0.06	0.59	0.31	0.13	0.10	0.01	0.02	0.00	0.02
<i>Thermacetogenium</i>	0.06	0.00	0.00	0.00	0.00	0.07	0.00	0.00	0.00
<i>Faecalibacterium</i>	0.06	0.13	0.86	0.40	0.07	0.00	0.10	0.05	0.07
<i>Moorella</i>	0.05	0.00	0.00	0.00	0.00	0.02	0.00	1.01	0.00
<i>Lachnospira</i>	0.05	0.22	0.39	0.40	0.14	0.00	0.11	0.05	0.00
<i>Escherichia-Shigella</i>	0.05	0.14	0.77	0.08	0.15	0.00	0.08	0.01	0.02
<i>Caldibacillus</i>	0.05	0.86	0.00	0.13	0.00	0.00	0.25	0.01	0.13
<i>Veillonella</i>	0.04	0.08	0.67	0.09	0.06	0.00	0.05	0.00	0.00
<i>Muribaculum</i>	0.04	0.04	0.77	0.08	0.06	0.00	0.05	0.00	0.01
<i>Lachnoclostridium</i>	0.04	0.01	0.73	0.21	0.06	0.00	0.02	0.02	0.03
<i>Enterobacter</i>	0.04	0.09	0.84	0.14	0.05	0.00	0.01	0.01	0.00
<i>Skermanella</i>	0.04	0.11	0.17	0.02	0.03	0.03	0.04	0.01	0.00
<i>[Eubacterium]_hallii_group</i>	0.04	0.10	0.41	0.30	0.07	0.00	0.08	0.03	0.01
<i>Chloroplast</i>	0.04	0.13	0.49	0.24	0.08	0.00	0.12	0.01	0.01
uncultured_Peptococcaceae	0.04	0.00	0.01	0.04	0.01	0.04	0.00	0.06	0.03
<i>Halomonas</i>	0.04	0.04	0.31	0.04	1.04	0.00	0.06	0.01	0.00
<i>Prevotella</i>	0.03	0.06	0.38	0.15	0.04	0.00	0.08	0.00	0.02
unclassified_Peptostreptococcales-Tissierellales	0.03	0.00	0.00	0.00	0.00	0.01	0.10	0.18	0.21
<i>Gitt-GS-136_Chloroflexi</i>	0.03	0.32	0.17	0.04	0.04	0.00	0.01	0.00	0.00
uncultured_Vicinamibacterales	0.03	0.43	0.20	0.01	0.03	0.00	0.00	0.00	0.00

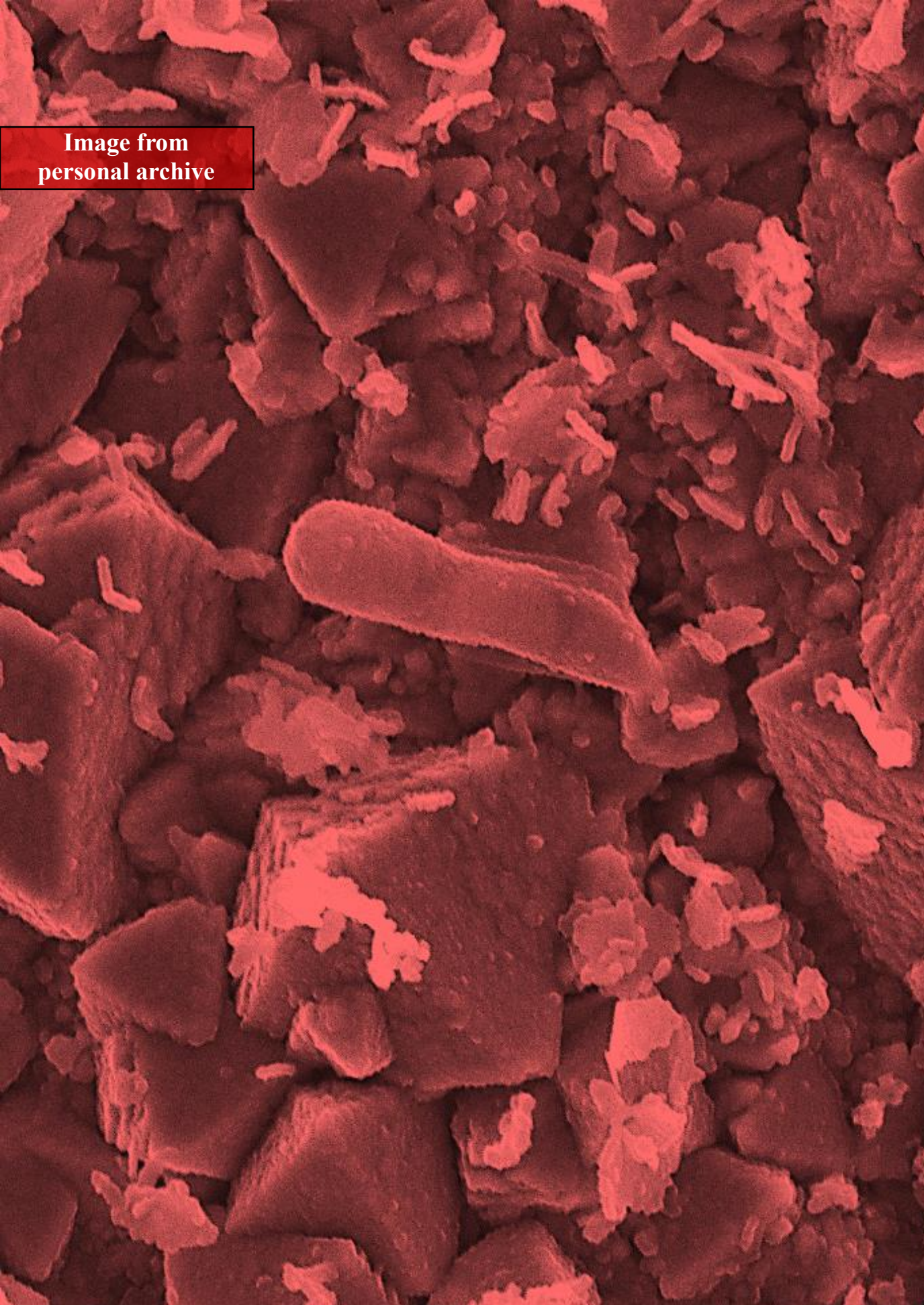
<i>Thermincola</i>	0.03	0.01	0.06	0.08	0.05	0.03	0.00	0.00	0.00
<i>Klebsiella</i>	0.03	0.03	0.72	0.00	0.00	0.00	0.00	0.00	0.00
<i>Noviherbaspirillum</i>	0.03	0.29	0.22	0.03	0.08	0.01	0.01	0.00	0.00
<i>Idiomarina</i>	0.03	0.01	0.15	0.04	0.88	0.00	0.00	0.00	0.00
<i>Bryobacter</i>	0.03	0.15	0.25	0.12	0.15	0.00	0.02	0.00	0.01
<i>Bifidobacterium</i>	0.03	0.03	0.48	0.20	0.07	0.00	0.02	0.01	0.00
<i>Collinsella</i>	0.03	0.10	0.30	0.23	0.07	0.00	0.09	0.02	0.00
<i>Parabacteroides</i>	0.03	0.07	0.26	0.22	0.08	0.00	0.07	0.02	0.00
<i>[Eubacterium]_coprostanoligenes_group</i>	0.03	0.09	0.25	0.28	0.04	0.00	0.06	0.01	0.00
unclassified_Comamonadaceae	0.03	0.42	0.24	0.03	0.05	0.00	0.00	0.00	0.01
<i>Curvibacter</i>	0.02	0.03	0.13	0.37	0.00	0.00	0.00	0.00	0.00
<i>JG30-KF-CM45_Thermomicrobiales</i>	0.02	0.16	0.11	0.01	0.02	0.01	0.01	0.00	0.00
<i>Garciella</i>	0.02	0.00	0.00	0.00	0.00	0.02	0.00	0.08	0.00
<i>Vibrio</i>	0.02	0.01	0.22	0.15	0.18	0.00	0.08	0.00	0.00
<i>Flavisolibacter</i>	0.02	0.07	0.07	0.03	0.02	0.01	0.01	0.00	0.00
<i>NK4A214_group_Oscillospiraceae</i>	0.02	0.08	0.14	0.12	0.04	0.00	0.04	0.01	0.00
<i>[Ruminococcus]_torques_group</i>	0.02	0.07	0.29	0.02	0.08	0.00	0.05	0.01	0.01
<i>[Eubacterium]_eligens_group</i>	0.02	0.03	0.18	0.17	0.06	0.00	0.04	0.01	0.00
uncultured_Caldilineaceae	0.02	0.08	0.13	0.05	0.00	0.02	0.02	0.00	0.00
<i>Porphyrobacter</i>	0.02	0.13	0.06	0.01	0.02	0.02	0.02	0.00	0.01
unclassified_Hungateiclostridiaceae	0.02	0.00	0.00	0.02	0.01	0.02	0.00	0.00	0.01
<i>Anaerostipes</i>	0.02	0.06	0.30	0.16	0.06	0.00	0.05	0.00	0.00
<i>Sphaerobacter</i>	0.02	0.00	0.51	0.00	0.00	0.00	0.00	0.00	0.00

## CHAPTER 2

<i>Ramlibacter</i>	0.02	0.00	0.13	0.05	0.00	0.01	0.00	0.01	0.00
uncultured_Microtrichales	0.02	0.15	0.15	0.03	0.02	0.01	0.00	0.00	0.00
<i>Pontibacter</i>	0.02	0.30	0.24	0.03	0.00	0.00	0.00	0.00	0.00
<i>Agathobacter</i>	0.02	0.03	0.17	0.16	0.05	0.00	0.04	0.00	0.00
uncultured_Lachnospiraceae	0.02	0.03	0.02	0.03	0.00	0.03	0.01	0.00	0.00
unclassified_Tannerellaceae	0.02	0.00	0.30	0.07	0.05	0.00	0.03	0.00	0.00
<i>Maribacter</i>	0.02	0.00	0.12	0.07	0.47	0.00	0.03	0.00	0.00
<i>Intestinibacter</i>	0.02	0.02	0.35	0.05	0.01	0.00	0.00	0.00	0.00
<i>Desulfosporosinus</i>	0.02	0.01	0.03	0.00	0.00	0.02	0.00	0.00	0.00
<i>Candidatus_Heliomonas</i>	0.02	0.00	0.00	0.00	0.00	0.00	0.00	0.66	0.00
<i>Phascolarctobacterium</i>	0.02	0.05	0.20	0.16	0.02	0.00	0.04	0.01	0.00
<i>Thermanaeromonas</i>	0.02	0.00	0.00	0.00	0.00	0.02	0.00	0.21	0.00
<i>Anaeromyxobacter</i>	0.02	0.15	0.03	0.06	0.02	0.01	0.00	0.00	0.00
WD2101_soil_group	0.02	0.04	0.14	0.10	0.02	0.01	0.00	0.00	0.01
<i>Microvirga</i>	0.02	0.09	0.06	0.03	0.02	0.01	0.03	0.00	0.00
uncultured_Rhizobiales_Incertae_Sedis	0.02	0.07	0.04	0.05	0.00	0.01	0.01	0.00	0.00
<i>Rubellimicrobium</i>	0.02	0.21	0.19	0.02	0.01	0.01	0.01	0.00	0.00
<i>Ruegeria</i>	0.02	0.00	0.09	0.03	0.41	0.00	0.07	0.00	0.00
<i>Glaciecola</i>	0.02	0.02	0.26	0.05	0.16	0.00	0.16	0.00	0.00
<i>Marinobacter</i>	0.02	0.01	0.23	0.02	0.46	0.00	0.00	0.00	0.00
<i>Pseudoalteromonas</i>	0.02	0.00	0.10	0.06	0.39	0.00	0.00	0.00	0.00
<i>Cellvibrionaceae</i>	0.02	0.01	0.24	0.00	0.20	0.00	0.19	0.00	0.00



Image from  
personal archive



## *Chapter 3*

High-temperature microbial corrosion of copper by sulfate-reducing bacteria in water-saturated bentonite microcosms and its relevance to nuclear waste deep geological repositories

### *Authors*

Mar Morales-Hidalgo<sup>\*</sup>, Cristina Povedano-Priego, Marcos F. Martinez-Moreno, Fadwa Jroundi and Mohamed L. Merroun

---

---

*Faculty of Sciences, Department of Microbiology, University of Granada, Granada, Spain*

## CHAPTER 3

**Abstract**

To guarantee the long-term safety of the multi-barrier repository system, it is essential to investigate the possible outcomes in the event of system failure. One of the key barriers in a deep geological repository (DGR) is the metal canister, which may be made of copper and is designed to contain the nuclear waste. There is currently a lack of information on the impact of microorganisms on its corrosion under system failure conditions. Therefore, his study focuses on investigating copper corrosion, the viability of sulfate-reducing bacteria (SRB) and bentonite stability under conditions of high temperature (60 °C), high microbial activity, groundwater seepage with electron donors/acceptors, and selenium (Se) leakage. A multidisciplinary approach was employed, integrating microbiological analyses with microscopic and spectroscopic characterization of copper surface using VP-FESEM (variable pressure-field emission scanning electron microscope), EDX (energy-dispersive X-ray), and RAMAN spectroscopy. In addition, mineralogical based techniques such as XRD (X-ray diffraction) and XRF (X-ray fluorescence) assessed bentonite stability. After two-month incubation period under anoxic conditions, viable SRB cells were detected in all treatments using the most probable number (MPN) method, with higher counts in the absence of the bacterial consortium. Moreover, Se negatively impacted the MPN g<sup>-1</sup> of bentonite in non-consortium treatments. Next-generation sequencing identified *Desulfosporosinus*, *Desulfotomaculum*, and *Desulfohalotomaculum* as the most abundant viable SRB genera. Microscopy and spectroscopy data highlighted important microbial impact on copper corrosion, particularly in treatments involving amended bacterial consortium, revealing the formation of copper(I) oxides and potential copper sulfides. Selenium treatments exhibited lower corrosion, likely due to competitive inhibition between sulfate and selenite for HS<sup>-</sup>. Elemental composition of bentonite and swelling capacity remained stable, indicating no remarkable alteration. To the best of our knowledge, this is the first study to investigate copper corrosion under such complex conditions, highlighting interactions between Spanish bentonite, microorganisms, copper, and selenium at high temperatures.

**Keywords:** *Copper, corrosion, Sulfate-reducing bacteria, Bentonite, Temperature, Selenium.*

## CHAPTER 3

## 1. Introduction

Metal canisters play a key role in the safe performance of deep geological repository (DGR), a multi-barrier system designed for the disposal of high-level waste (HLW) or spent fuel (SF) (King et al., 2024). There has been a general consensus that, after closure, the DGR environment will shift from being initially warm and oxidizing to a prolonged period of cool and anoxic conditions. This evolutionary process will have a pronounced impact on the types of corrosion and their corresponding rates (King et al., 2017). It is anticipated that the canisters will undergo time-dependent degradation due to corrosion. In addition, their long-term performance would depend on the intrinsic properties of the engineered barriers, particularly those of the clay-based buffer such as bentonite barrier (King et al., 2024). Companies such as POSIVA (Finland), SKB (Sweden) and NWMO (Canada) have proposed using copper-coated metal as the preferred material for canisters (Jonsson et al., 2018; Bennett and Gens, 2008; McMurry et al., 2004). These metallic canisters will be surrounded by a protective barrier buffer, typically composed of compacted bentonite in most DGR models, and safely stored deep underground at several hundred meters. Bentonite offers advantageous properties for canisters, including mechanical support that ensures stability, low permeability to minimize groundwater infiltration, high ion exchange capacity for retaining radionuclides in case of a leakage, high plasticity and swelling ability to self-seal cracks in canisters, good thermal conductivity, and optimal compaction properties (García-Romero et al., 2019; Martínez-Moreno et al., 2023). Such multi-system would guarantee the secure and safe disposal of nuclear waste over very long timescales. Furthermore, the expected phases following the repository closure will influence the corrosion of copper canisters. These phases include the presence/absence of oxygen, water activity, radiation effects, and microbiologically influenced corrosion (MIC) (Hall et al., 2021).

## CHAPTER 3

In the case of MIC corrosion, sulfate-reducing bacteria (SRB) would be the main bacterial group involved. More specifically, SRB would act through the well-known mechanism of chemical microbiologically influenced corrosion (CMIC), where corrosion is indirectly caused by the byproducts of microbial metabolism (Little et al., 2020). The SRB use sulfate as a final electron acceptor, resulting in the production of sulfide, which reacts with copper to form copper sulfides (Huttunen-Saarivirta et al., 2016). High levels of dissolved sulfate ions in deep underground water sources could support the survival of these SRB. Additionally, nutrients might be obtained from natural organic materials within the clay, fracture fluids, or surrounding minerals (Hall et al., 2021; Morales-Hidalgo et al., 2024a). This bacterial group has previously been identified in Spanish bentonite under a variety of conditions, including different levels of compaction, incubation periods, temperatures and the presence of water (Martinez-Moreno et al., 2023;2024; Povedano-Priego et al., 2023; Morales-Hidalgo et al., 2024b). In a study published in 2024, Martinez-Moreno et al. reported the viability of SRB in Spanish bentonite compacted at a density of 1.7 g/cm<sup>3</sup> after one year of incubation at 60 °C. They demonstrated the viability of SRB in Postgate culture medium incubated at 30 °C, while no growth was obtained when the same medium was incubated at 60 °C.

Another important factor that should be considered in future repositories is the temperature. According to predictive models based on the DGR designs of each country, the surface temperature of the canister is projected to gradually increase, reaching a peak of approximately 100 °C within the first few decades (King et al., 2024). After reaching this peak, the temperature would then gradually begin to decline. Therefore, the effect of temperature is crucial to consider in relation to the stability of the repository barriers, including the metal canister, bentonite material, and even the microbial diversity and

activity. The primary source of heat would come from the radionuclides, including  $^{90}\text{Sr}$  and  $^{137}\text{Cs}$ , present in the stored radioactive waste (Forsberg, 2000). Furthermore, while  $^{235}\text{U}$  would be one of the most prevalent stored radionuclides, other elements resulting from its fission, such as  $^{79}\text{Se}$ , would also be significant due to their extended half-life of up to one million years (Frechou et al., 2007).

To ensure the long-term and multi-level safety of the multi-barrier nuclear repository system, it is crucial to study potential consequences in the event of system failure. This study has aimed to elucidate the processes related to copper corrosion and the viability of the main bacterial group involved, SRB, under conditions of high temperature (60 °C), high microbial activity, groundwater seepage with electron donors/acceptors, and selenium leakage, using sodium selenite as an inactive chemical analogue of  $^{79}\text{Se}$ . The effect of selenium at 60 °C on the bentonite bacterial communities has been studied in detail in **Chapter 2**. However, this chapter focused on the metal canister barrier, which, in case of failure, would release the stored radionuclides into the surrounding environment. Furthermore, under these conditions, the stability of bentonite is necessary to analyze to ascertain whether its advantageous physicochemical and mechanical properties are still preserved. Therefore, we present a multidisciplinary study that combines culture-dependent and molecular microbiological analyses of viable SRB together with microscopic and spectroscopic characterization of the copper plate surface using techniques such as variable pressure scanning electron microscopy (VP-FESEM), EDX, and RAMAN spectroscopy. Additionally, X-ray diffraction (XRD) and X-ray fluorescence (XRF) have been employed for the analysis of bentonite stability. To the best of our knowledge, this is the first investigation of copper corrosion under such complex conditions of quaternary systems, which includes the interaction of Spanish bentonite, microorganisms,

## CHAPTER 3

copper, and selenium, alongside elevated temperatures, high bacterial activity, and water hyper-saturation.

### **2. Materials and methods**

#### **2.1. Sampling and processing of bentonite clay**

The bentonite utilized in this study was collected from the geological site known as "El Cortijo de Archidona", situated within the region of Almeria in southern Spain. The clay collection and processing in the laboratory was conducted as described in detail in **Chapter 2** of this Ph.D. thesis.

Both natural (B) and heat-shocked bentonite (Bst) were investigated. No pre-treatments were necessary for the natural bentonite, while a tyndallization treatment (a moist heat process with temperature cycles of 110 °C for 45 minutes over three consecutive days) was employed to obtain the heat-shocked one, in order to minimize the presence of microorganisms and to better elucidate abiotic processes.

#### **2.2. Assembly of water-saturated bentonite microcosms and incubation conditions**

Water-saturated bentonite microcosms were prepared and assembled as described in the previous chapter (**Chapter 2**). A total of 8 treatments, each with 3 independent replicates, were prepared. Each microcosm was prepared using 50 g of water saturated dry powdered bentonite in a final volume of 230 mL.

The bentonite used was either natural (B) or heat-shocked (Bst), depending on the treatment. The volume of all the microcosms consisted of equilibrium water, as well as the electron donors and acceptor: sodium acetate 30 mM, sodium lactate 10 mM, and sodium sulfate 20 mM. The electron acceptor sodium sulfate was included to specifically promote SRB activity. The major

components of the equilibrium water were analyzed in detail in the **Chapter 2** using ICP-MS (Inductively Coupled Plasma Mass Spectrometry).

Only the treatments involving selenium (Se) included 2 mM sodium selenite. This Se-treatment aimed to investigate the impact of this metalloid on the bacterial communities of bentonite (**Chapter 2**) and on copper corrosion. A 1 M stock solution was prepared and sterilized using 0.22  $\mu\text{m}$  nitrocellulose filters for filtration. Additionally, a bacterial consortium was inoculated into the microcosms as another treatment (C). This consortium was composed of four genera, previously identified in other studies to belong to the bacterial community of the Spanish bentonite (Lopez-Fernandez et al., 2018, 2014; Povedano-Priego et al., 2019, 2021), with the aim to represent high microbial activity. This consortium included *Stenotrophomonas bentonitica* BII-R7, *Bacillus* sp. BII-C3, *Pseudomonas putida* ATCC33015, and *Amycolatopsis ruanii* NCIMB14711. The culture media and incubation conditions of this consortium are described in detail in Morales-Hidalgo et al. (2024b).

In total, 24 microcosms were prepared. The experimental setup is detailed in **Figure 1** and the different experimental conditions of water-saturated bentonite microcosms are specified in **Table 1**. To establish anoxic conditions during the incubation period, the microcosms were bubbled with nitrogen gas in order to displace the oxygen present. This was achieved by utilizing needles through butyl rubber stoppers, with 22  $\mu\text{m}$  nitrocellulose filters to prevent contamination, and a flow of  $\text{N}_2$ . All the microcosms were bubbled for at least 20 minutes. Sampling of the different treatments was always conducted inside an anaerobic glove box.

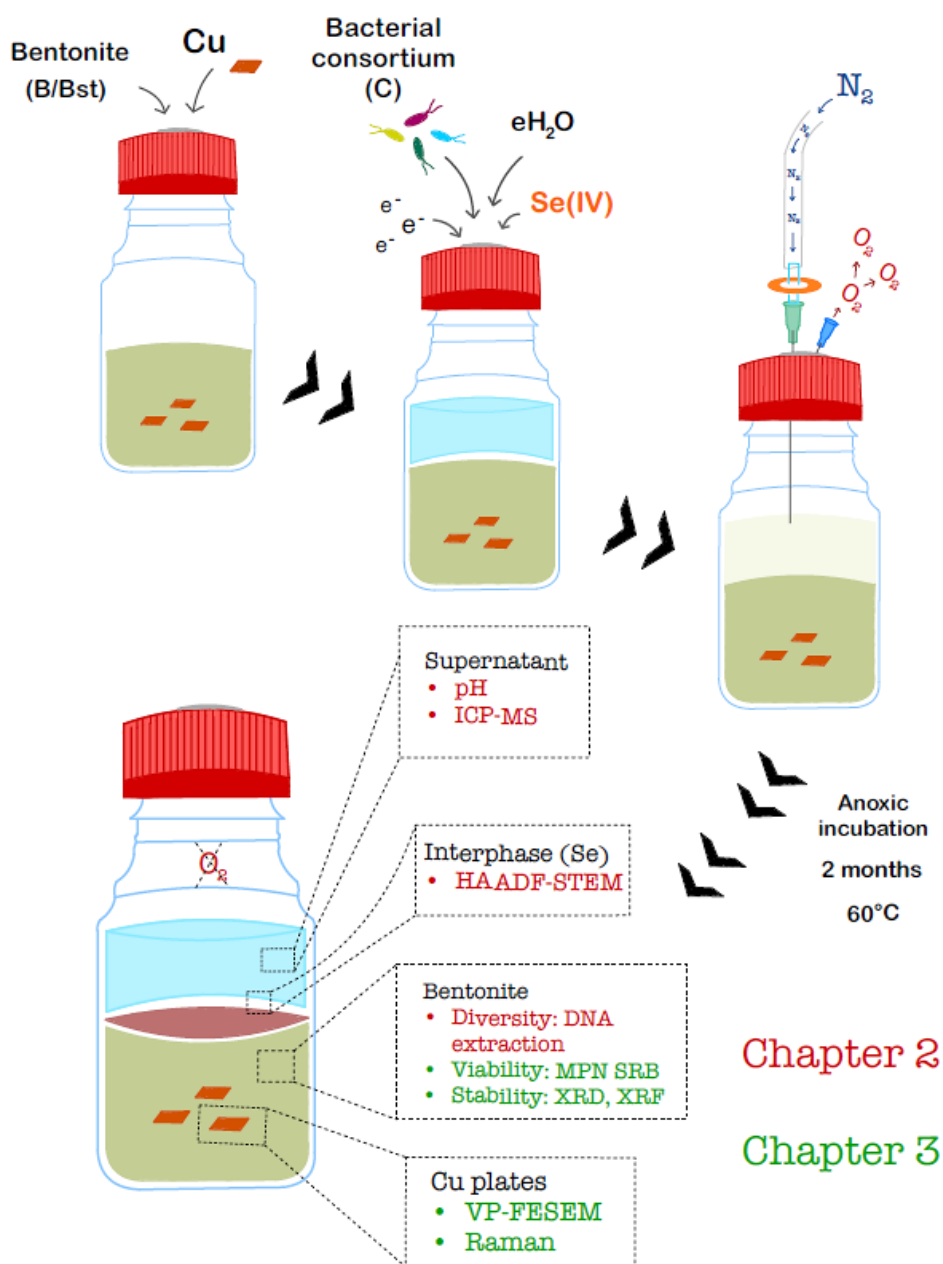


**Figure 1.** Workflow of the microcosm's experimental setup, including the N<sub>2</sub> degassing process to achieve anoxic conditions and the sampling of different components. B: natural bentonite; Bst: heat-shocked bentonite; C: bacterial consortium; e<sup>-</sup>: electron donors and acceptors; eH<sub>2</sub>O: equilibrium water; Se(IV): sodium selenite (2 mM). The red color represents the techniques used in Chapter 2, while the green color represents the techniques used in the present chapter (Chapter 3).

**Table 1.** Different experimental conditions of water-saturated bentonite microcosms. B: natural bentonite; Bst: heat-shocked bentonite; C: bacterial consortium; Se: sodium selenite (2 mM).

Sample Name	Natural bentonite (B)	Heat-shocked bentonite (Bst)	Bacterial consortium (C)	Selenium (Se)
<b>B</b>	+	-	-	-
<b>BC</b>	+	-	+	-
<b>Bst</b>	-	+	-	-
<b>BstC</b>	-	+	+	-
<b>BSe</b>	+	-	-	+
<b>BCSe</b>	+	-	+	+
<b>BstSe</b>	-	+	-	+
<b>BstCSe</b>	-	+	+	+

### 2.2.1. Copper plates

To carry out corrosion analysis, each microcosm included pure copper (Cu) plates (> 99%), representing the material that would be used for future metal canisters. The Cu plates were provided by the Centro de Instrumentación Científica (CIC, UGR), with dimensions of 8 mm in height, 15 mm in width, and 2 mm in thickness (**Fig. 2**). To remove impurities and organic residues from the surface of the Cu plates, a chemical cleaning treatment was conducted following the protocol detailed by Guo, M. (2020). Briefly, the Cu plates were first degreased by sonication for five minutes in an absolute ethanol solution. Subsequently, they were cleaned with MilliQ ultrapure water to remove any residual ethanol. Additionally, another sonication process for five minutes was conducted by immersing the plates in 10 mM nitric acid. This cleaning treatment cycle was repeated three times consecutively. Finally, the plates were dried under a nitrogen gas atmosphere.

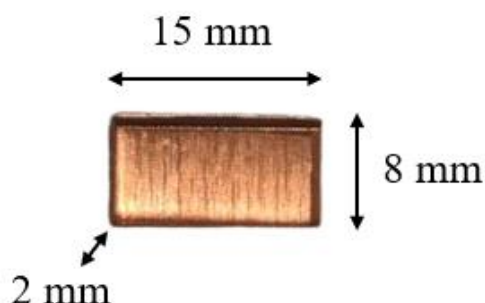


**Figure 2.** Dimensions of pure copper plates (> 99%).

### **2.3. Microbiological analysis: viability of sulfate-reducing bacteria**

#### **2.3.1. Quantifying the viable sulfate-reducing bacteria through the most probable number (MPN)**

Due to the key role of sulfate-reducing bacteria in copper corrosion, the viability of this bacterial group was studied and quantified using the most probable number (MPN) method, following the protocol from Biotechnology Solutions (Houston, USA, <https://biotechnologysolutions.com>). The viability of SRB in all treatments (BC, BCSe, BstC, BstCSe, B, BSe, Bst, BstSe) after 2-month incubation at 60 °C was studied by mixing bentonite from the three corresponding replicates in an anoxic atmosphere inside a glove box. Subsequently, 0.5 g of water-saturated bentonite was weighed and mixed with 4.5 mL of 0.9% N<sub>2</sub>-bubbled sodium chloride solution in serum bottles. The mixture was kept under agitation at 180 rpm for 24 hours to disperse the microbial cells from the clay. Then, 0.5 mL of the suspension was transferred to 10 mL serum bottles pre-filled with 4.5 mL of anoxic Postgate's Medium (DSMZ Medium 63, [www.dsmz.de/](http://www.dsmz.de/)). Decimal dilutions up to 10<sup>-4</sup> were then elaborated in triplicate. Finally, the serum bottles were sealed and incubated at 28 °C, static, and in the dark for a total period of 30 days. The presence of

black precipitates in the medium after the specified incubation time indicated the viability of sulfate-reducing bacteria. The MPN was assessed by correlating the number of bottles showing positive results with the reference table supplied by Biotechnology Solutions (MPN Method, <https://biotechnologysolutions.com>).

### **2.3.2. Molecular identification of viable bacterial communities from most probable number**

In order to analyze the viable microbial diversity, total DNA was extracted from one positive bottle from each treatment using the DNAeasy PowerSoil Pro Kit (Qiagen, <https://www.qiagen.com/us>). Then, the DNA concentrations were determined using a Qubit 3.0 Fluorometer (Life Technology).

The extracted DNA was purified, amplified, and sequenced at the StabVida Company (Caparica, Portugal, <https://www.stabvida.com/es>) following the same procedure detailed in **Chapter 2**. Briefly, the variable regions V3-V4 of the 16S rRNA gene were amplified for the construction of the libraries using the universal primers 341F (5'-CCTACGGGG GNGGCWGCAG-3') and 785R (5'-GACTACHVGGGGGTATCTAATCC-3') (Thijs et al., 2017). The DNA was purified using the Sera-Mag Select kit (Cytiva) and sequenced on the Illumina MiSeq platform using the MiSeq v3 reagent kit, generating paired-end reads of 300 bp each. The raw reads were analyzed using QIIME2 v2022.2 (Caporaso et al., 2010) and denoised using the DADA2 plugin to eliminate low-quality regions, dereplicate reads, and filter out chimeras (Callahan et al., 2016). After generating rarefaction curves to evaluate the number of sequences obtained, the reads were grouped into operational taxonomic units (OTUs) and classified into taxa using the SILVA database (release 138 QIIME) with a clustering threshold of 99% similarity. Percent relative abundances along with

## CHAPTER 3

alpha diversity indices were obtained using Explicit 2.10.5 software (Robertson et al., 2013).

### **2.4. Microscopic and spectroscopic characterization of copper corrosion products**

After 2 months of anoxic incubation, the surfaces of copper plates collected from the different treatments were analyzed to study signs of corrosion using variable pressure-field emission scanning electron microscopy (VP-FESEM) on a Zeiss Supra 40VP equipped with secondary electrons (SE, InLens) and backscattered electrons (BSE) detectors. This VP-FESEM microscope is connected to a microanalysis system (Aztec 2.2) that provides elemental composition by energy dispersive X-ray (EDX) and also equipped with a *Renishaw In Via* Raman spectrometer, fitted with a Nd:YAG 532 nm laser and a near-infrared diode 785 nm laser, with maximum powers of 500 mW and 100 mW, respectively (Guerra and Cardell, 2015). After sampling, the Cu plates were prepared for VP-FESEM according to the procedure detailed in Martinez-Moreno et al. (2023). Briefly, the plates were fixed with 2.5% glutaraldehyde in cacodylate buffer, followed by washing and post-fixing with osmium tetroxide and dehydration with ethanol. Finally, the plates were dried using the critical point drying (CPD) method and metallized with carbon.

### **2.5. Mineralogical and chemical analysis of bentonite stability**

Mineralogical changes, particularly shifts in the basal reflection of smectite, resulting from different treatments were analyzed using X-ray diffraction (XRD). Specifically, oriented aggregates (OA) of each treatment (a mixture of the three replicates) were prepared by diluting bentonite in distilled water at a ratio of 0.1:1 (w/v) and sonicating the mixture for 10 minutes to disperse clay particles. A small amount of the mixture was then deposited on a circular glass holder and air-dried to form a thin layer suitable for analysis. For ethylene

glycol (EG) analysis, the samples were exposed to EG for 24 hours at 60 °C. Then, oriented aggregates of the < 2 µm fraction were analyzed using a PANalytical X'Pert Pro diffractometer (CuK $\alpha$  radiation, 45 kV, 40 mA) equipped with an X'Celerator solid-state linear detector (0.008° 2 $\theta$  step increment; 10 s/step counting time). The OA samples were analyzed both in air-dried and ethylene glycol-treated (EG) conditions to identify clay shifts using HighScore software.

The elemental composition of the different treatments was also studied using X-ray fluorescence analysis (XRF), which were conducted with a PANalytical Zetium instrument, using a rhodium anode ceramic X-ray tube equipped with an ultra-thin high transmission beryllium front window.

### **3. Results and discussion**

#### **3.1. Effect of different physico-chemical parameters on viability of sulfate-reducing bacteria**

##### **3.1.1. Determination of the most probable number of SRB**

After 2 months of anoxic incubation at 60 °C and given the key role of sulfate-reducing bacteria in copper corrosion, the viability of this bacterial group was analyzed using the MPN method in the different treatments. The presence of viable SRB was positive in all treatments, to a greater or lesser extent (**Table 2**). The order from highest to lowest SRB MPN per gram of bentonite was as follows: B > BSe > Bst > BC = BCSe > BstC = BstCSe > BstSe.

In general, in the non-consortium treatments, the abundance of SRB was found to be greater than in treatments where the consortium was present. Specifically, the sample of natural bentonite without the consortium (B) exhibited the highest cell count per gram of bentonite, scoring a value of > 1.26 x 10<sup>4</sup> MPN g<sup>-1</sup>, while in the heat-shocked bentonite (Bst) a value of 2.25 x 10<sup>3</sup> MPN g<sup>-1</sup> was obtained. In contrast, in treatments BC and BstC, the abundance of SRB

## CHAPTER 3

was found to be lower annotating values of  $3.60 \times 10^2$  and  $8.55 \times 10^1$  MPNg<sup>-1</sup>, respectively. As discussed in the previous **Chapter 2**, the genera of the bacterial consortium *Stenotrophomonas*, *Pseudomonas*, and *Bacillus*, prevail in microcosms incubated at 60 °C for a period of two months. This was mainly observed in the treatments in which the consortium had been inoculated. The dominance of the consortium and its high activity in those treatments could have hindered the growth of other genera with lower relative abundances. The elevated metabolic activity of the consortium would have facilitated the accelerated consumption of the amended electron donors, consequently limiting the availability of resources for the proliferation of other bacteria, such as SRB, present in the microcosms with lower relative abundances.

**Table 2.** Viable SRB in water-saturated bentonite microcosms incubated at 60 °C for 2 months determined by most probable number (MPN) of cells per gram of bentonite (MPN g<sup>-1</sup>). All the values were calculated considering the initial suspension for cell's dispersion (0.5 g of bentonite in 4.5 mL of 0.9% NaCl solution). B: natural bentonite; Bst: heat-shocked bentonite; C: bacterial consortium; Se(IV): sodium selenite (2 mM).

Sample	XYZ pattern*	MPN value**	3PB dilution***	MPN g <sup>-1</sup> bentonite
BC	223	4	10 <sup>-1</sup>	$3.60 \times 10^2$
BCSe	232	4	10 <sup>-1</sup>	$3.60 \times 10^2$
BstC	320	9.5	10 <sup>0</sup>	$8.55 \times 10^1$
BstCSe	320	9.5	10 <sup>0</sup>	$8.55 \times 10^1$
B	333	> 140	10 <sup>-1</sup>	$> 1.26 \times 10^4$
BSe	331	45	10 <sup>-1</sup>	$4.05 \times 10^3$
Bst	330	25	10 <sup>-1</sup>	$2.25 \times 10^3$
BstSe	110	0.7	10 <sup>-1</sup>	$6.30 \times 10^1$

\*XYZ pattern: number of positive bottles after 3PB dilution

\*\*MPN value: MPN data from the reference table

\*\*\*3PB dilution: dilution with 3 positive bottles prior to XYZ pattern

However, in the absence of the consortium, and therefore under conditions of its lower dominance with respect to bacterial genera, the proliferation of this bacterial group could have been favored. In fact, the addition of lactate and sulfate was aimed at stimulating SRB. The preferred electron donor (lactate) is oxidized by this bacterial group yielding electrons to sulfate for its reduction to sulfide (Santos et al., 2022). According to Matschiavelli et al. (2019), SRB could carry out incomplete oxidation of lactate via the acetyl-CoA metabolic pathway, resulting in the production of acetate.

Conversely, selenium appears to also influence the viability of SRB. When comparing the consortium treatments (BC, BstC) with their selenium analogues (BCSe, BstCSe), minimal differences were observed (**Table 2**). Once again, the bacterial consortium likely accounts for this similarity. The aforementioned bacterial strains, dominant in these treatments, were the primary reducers of Se(IV) to Se(0) in these microcosms (Macy et al., 1989; Ruiz-Fresneda et al., 2019). This result was detailed and discussed previously in **Chapter 2**. In this case, the rapid detoxification of soluble and toxic selenite to insoluble and less toxic elemental selenium by the consortium strains may have facilitated the viability of SRB. However, in treatments lacking the consortium (BSe, BstSe), a decrease in the viability of this bacterial group in the presence of selenium was observed. In these non-consortium treatments, the reduction rates of Se were considerably slower (**Chapter 2**). As evidenced in the literature, certain SRB genera are capable of detoxifying specific levels of Se (Tomei et al., 1995). Nonetheless, the results presented here suggested a possible negative effect of Se(IV) on the viability of the SRB community. Furthermore, competition between sulfate and selenite reduction could have influenced the growth of these microorganisms, as this metalloid can also act as a final electron acceptor under anaerobic conditions (Hockin and Gadd, 2003; Shi et al., 2020; Staicu and Barton, 2021).

## CHAPTER 3

Lastly, the heat shock treatment (tyndallization) also had a negative effect on the MPN of SRB. All the treatments involving heat-shocked bentonite (BstC, BstCSe, Bst, BstSe) showed a lower number of cells per gram of bentonite compared to natural bentonite treatments (BC, BCSe, B, BSe). The objective of this heat shock treatment was to reduce the number of microorganisms in the samples, consequently also affecting the SRB group.

In general, these results highlight the ability of this bacterial group to withstand high temperatures and remain viable, until favorable conditions reappear (presence of nutrients, temperature 28 °C). In the same way, Martinez-Moreno et al. (2024) suggested the viability of SRB in compacted bentonite blocks incubated at 60 °C. This viability was only detected when incubation in Postgate medium was carried out at 30 °C, but not at 60 °C. An explanation to these results could be that members of this bacterial group may withstand high temperatures through spore formation or by entering a dormant state (desiccated cells) (Grigoryan et al., 2018; Masurat et al., 2010). Furthermore, the important role of bentonite, acting as a thermal buffer, could have provided in the microcosms, cooler zones where the activity of these bacteria would have been facilitated. Moreover, the presented results also suggested a negative impact on the MPN of SRB of both the bacterial consortium, which simulates very high activity, and selenium, simulating a waste leakage. Therefore, identifying the main viable bacterial groups is crucial for understanding the microbial activity and biochemical processes occurring over the time.

### **3.1.2. Bacterial diversity characterization of the viable SRB from MPN experiment**

Total DNA was extracted from Postgate-positive cultures to molecularly identify the main viable SRB genera after two months of anoxic incubation under high temperature conditions. It should be noted that other bacterial

genera not belonging to the sulfate-reducing group may have also grown in Postgate medium due to the consumption of compounds such as lactate, yeast extract, and ascorbic acid, among others. The relative abundances of the viable genera are illustrated in **Figure 3**, and the percentages are provided in **Supplementary Table S1**. The predominant SRB genera across all samples were *Desulfosporosinus* (26.77%), *Desulfotomaculum* (10.69%), and *Desulfohalotomaculum* (6.41%). The relative abundance of the three main SRB genera has been plotted for each treatment in **Supplementary Figure S1**.

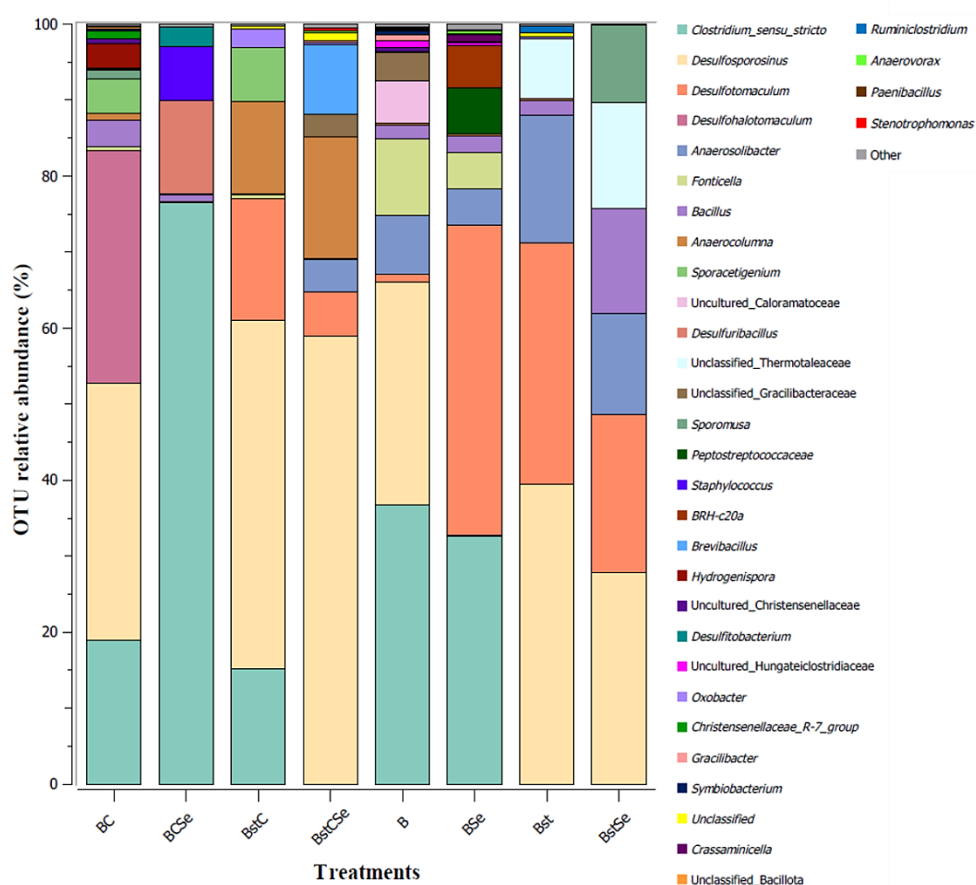


**Figure 3.** OTU relative abundances at genus level of the viable bacteria grown in positive Postgate medium from MPN experiment. Cut off: > 0.07% of relative abundance. B: natural bentonite; Bst: heat-shocked bentonite; C: bacterial consortium; Se: sodium selenite (2 mM).

## CHAPTER 3

When considering the percentage of total relative abundance, *Clostridium* was the most prevalent genus (28.18%). Although *Clostridium* is not typically considered a reference genus among the SRB group, some species within this genus are capable of reducing sulfate, and thus are considered as sulfate-reducing bacteria. For instance, the species *Clostridium nigrificans* has been documented to exhibit both sulfate reduction and thermophilic characteristics, with an optimal growth temperature of 55 °C. Nevertheless, strains of this species have been observed to thrive at temperatures approaching 35 °C (Campbell et al., 1956). In addition, most species of the *Clostridium* genus are acetogenic and utilize the acetyl-CoA pathway for the reductive synthesis of acetate from CO<sub>2</sub> as a means of energy conservation and terminal electron acceptance (Wood and Ljungdahl, 1991; Drake, 1994). They can also ferment lactate, which is present in the Postgate medium, into acetate (Tang et al., 1989). On the other hand, this genus also exhibited very high relative abundances in the Se treatments of 76.57% in BCSe and 32.56% in BSe. Previous studies, such as Bao et al. (2013), also reported on the ability of this genus to reduce Se oxyanions such as selenite and selenate.

Regarding the genus *Desulfosporosinus*, this is a well-known SRB naturally present in the Spanish bentonite, as previously reported by Martinez-Moreno et al. (2023) and Povedano-Priego et al. (2023). Previous physiological experiments demonstrated that cultured *Desulfosporosinus* species reduce sulfate while incompletely oxidizing lactate to produce acetate and CO<sub>2</sub> (Robertson et al., 2001; Mayeux et al., 2013; Aoyagi et al., 2021). In this study, although its relative abundance was reduced in the BSe treatment (0.13%) compared to B (29.38%), in other treatments with Se, such as BstSe and BstCSe, *Desulfosporosinus* presented higher percentages, with values of 27.85% and 58.97%, respectively. Accordingly, Povedano-Priego et al. (2023) identified this genus in microcosms of Spanish bentonite treated with Se and

incubated at 30 °C. Moreover, it has been commonly found under selenium-reducing conditions in different soils and sediments (Sánchez-Andrea et al., 2011; Liu et al., 2018).

On the other hand, the *Desulfotomaculum* genus includes numerous thermophilic and even hyper-thermophilic species, with optimal growth temperatures ranging from 30 to 65 °C. Surprisingly, some of these species can withstand maximum temperatures up to 140 °C (O'sullivan et al., 2015; Sass and Cypionka, 2004). However, their survival at these extreme temperatures is primarily attributed to the formation of spores. If considering the SRB *Desulfohalotomaculum*, the available published information is notably scarce, since this genus was reclassified in 2018 as a novel species, after being previously considered to belong to the genus *Desulfotomaculum* (Watanabe et al., 2018). This genus was only detected in the BC treatment, with a relative abundance of 30.63%. In the other treatments, it was below the sequencing detection limit (i.e., below 0.01%).

As previously mentioned, other strains not belonging to the SRB group have been enriched in the Postgate medium by utilizing different compounds. For instance, *Anaerosolibacter* has been identified as a bacterium native to Spanish bentonite. Actually, it was previously identified and isolated from 1.7 g/cm<sup>3</sup> compacted blocks of Spanish bentonite incubated for 1 year at 60 °C (Martinez-Moreno et al., 2024). Despite not being classified as a member of the SRB group, this genus encompasses species such as *Anaerosolibacter carboniphilus*, possessing the capacity to utilize sulfate and other compounds as electron acceptors (Hong et al., 2015). It has also been identified in hot springs in Sri Lanka, where temperatures were relatively high (Samarasinghe et al., 2021). Another identified genus was *Fonticella*, a non-spore forming, thermophilic, strictly anaerobic bacterium with growth temperatures ranging

## CHAPTER 3

between 45-70 °C (Fraj et al., 2013). The relative abundances of this genus decreased in the presence of selenium, being undetected in BCSe and BstCSe, and decreasing in BSe compared to B from 10.03% to 4.84%, respectively. Although this genus has previously been detected in both MX80 and Spanish bentonites (Gilmour et al., 2021; Morales-Hidalgo et al., 2024b), there is a lack of information about its interaction with selenium; however, the current results suggested a sensitivity to the presence of this metalloid.

Other genera, such as *Bacillus* and *Anaerocolumna*, were also identified as viable in Postgate medium across all treatments, with the exception of *Anaerocolumna* in BstSe. In the case of *Bacillus*, Combet-Blanc et al. (1995) reported growth at temperatures of 58 °C. With respect to *Anaerocolumna*, this bacterium has also been reported to produce H<sub>2</sub> under thermophilic incubation conditions of 50 °C (Kim et al., 2024).

From all the mentioned above, the SRB group was the most prevalent among the viable genera that grew in Postgate across the eight treatments, although other strains that were capable or not of sulfate reduction were also enriched. Many of these abundant genera exhibited the capacity to withstand elevated temperatures, such as 60 °C, throughout the 2-month incubation time and remain viable. The fact that they withstood the harsh conditions and remained viable did not imply that they were active. However, it suggested that under favorable conditions, they could become active again. This finding highlighted the resilience of native bentonite bacteria, which were capable of thriving in challenging conditions, such as high temperatures and the presence of toxic metalloids, in the potential failure scenarios of the future repository system.

### 3.2. Corrosion of copper plates surface

#### 3.2.1. Visual surface changes

The surface alterations of the copper plates after two months of anoxic incubation at 60 °C were observed macroscopically prior to their preparation for microscopy. **Figure 4** shows the surface appearance of the Cu plates collected from each treatment. Notably, the Cu surfaces corresponding to the consortium treatments (BC, BstC) exhibited a significantly darker and more blackish coloration compared to both non-consortium treatments (B, Bst) and the untreated unincubated control plate.

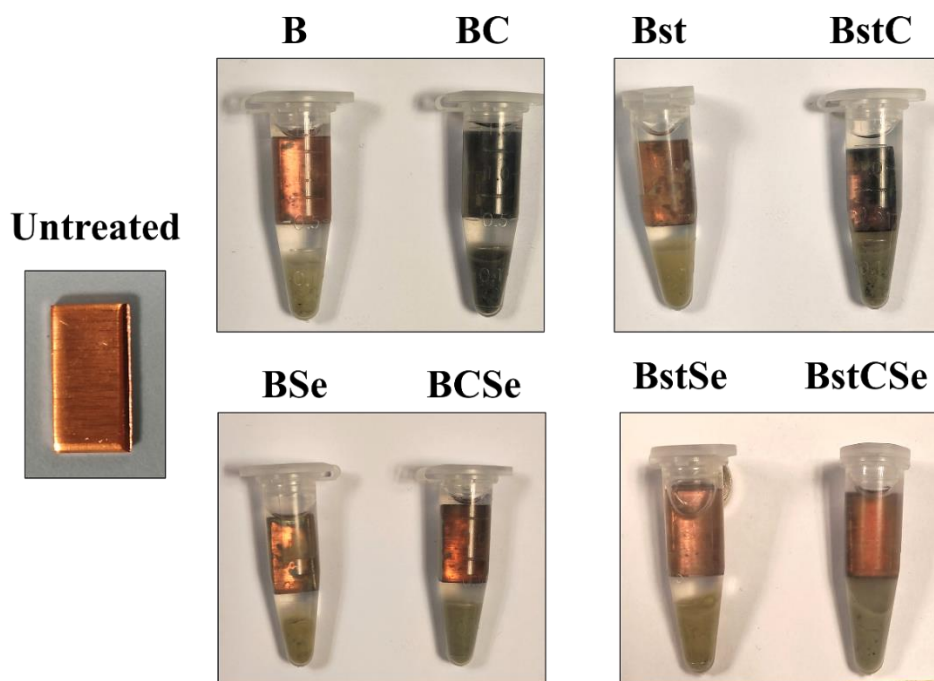


**Figure 4.** Copper plates corresponding to each treatment after 2 months of anoxic incubation at 60 °C inside water-saturated bentonite microcosms. Each Cu plate is immersed in 2.5% glutaraldehyde fixative prior to preparation for electron microscopy. Untreated: unincubated and untreated control copper plate; B: natural bentonite; Bst: heat-shocked bentonite; C: bacterial consortium; Se: sodium selenite (2 mM).

On the other hand, if comparing the four treatments inoculated with the consortium, those containing selenium showed a less darkened surface (BCSe, BstCSe). Interestingly, the visually less damaged Cu plates were those corresponding to the treatments without consortium (B, BSe, Bst, BstSe), and more specifically the Cu plate corresponding to the heat-shocked bentonite with selenium (BstSe).

### **3.2.2. Microscopic and spectroscopic characterization of the copper surface and corrosion products**

The metal surfaces were analyzed using microscopic and spectroscopic techniques (VP-FESEM, EDX, and Raman) to identify the signs and products of corrosion. To establish a non-corrosion reference, an unincubated and untreated pure copper plate, which was chemically cleaned according to the specified methodology, was analyzed as control (**Supplementary Fig. S2**). The surface appeared completely homogeneous, and at higher magnifications, streaks resulting from the plate cutting and polishing were discernible. EDX spectrum indicated a purely copper surface with a minimal oxygen (O) signal (< 1%) in some areas. The carbon signal was attributed to the metallization process during sample preparation for VP-FESEM. The main corrosion products in the different treatments, as identified by scanning electron microscopy, are detailed in **Table 3**. Then, each treatment will be discussed in detail, ordered from the one with the highest alteration to the ones with the lowest alteration in terms of the corrosion products occurrence.

The BC treatment, which involved natural bentonite and the inoculated consortium, exhibited the most significant visual changes in the surface, appearing completely black (**Fig. 4**). In accordance, a full altered surface was

also observed at the microscopic level, with detached copper layers, as shown in the EDX maps in **Figure 5**.

**Table 3.** Main corrosion products found in each study treatment detected by electron scanning microscopy. B: natural bentonite; Bst: heat-shocked bentonite; C: bacterial consortium; Se: sodium selenite (2 mM).

Treatment	Corrosion products
<b>BC</b>	$\text{Cu}_2\text{O}$ , $\text{Cu}_x\text{S}$
<b>BstC</b>	$\text{Cu}_2\text{O}$ , $\text{Cu}_x\text{O}$ , $\text{Cu}_x\text{S}$
<b>BCSe</b>	$\text{Cu}_x\text{O}$
<b>BstCSe</b>	$\text{Cu}_x\text{O}$
<b>B</b>	$\text{Cu}_x\text{O}$
<b>Bst</b>	O signal – no precipitates – passivation layer
<b>BSe</b>	O signal – no precipitates – passivation layer
<b>BstSe</b>	O signal – no precipitates – passivation layer



+ corrosion products

- corrosion products

## BC

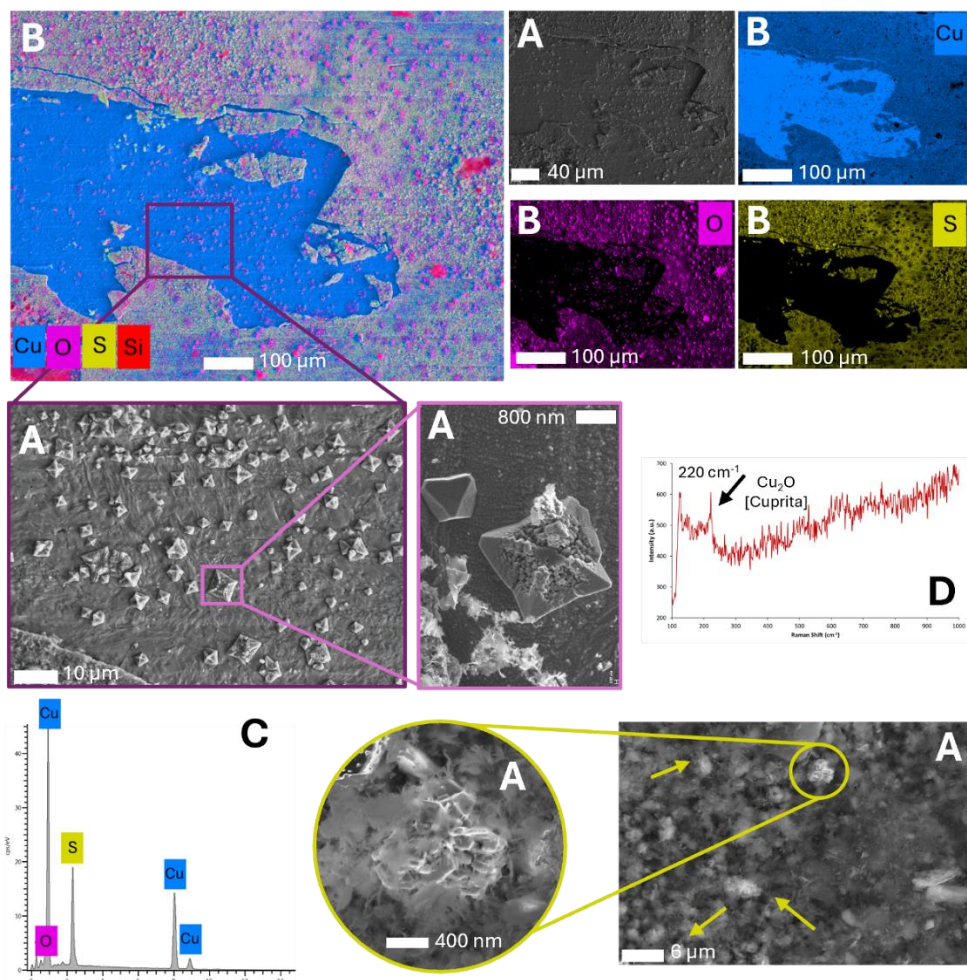


**Figure 5.** Variable pressure scanning electron microscopy (VP-FESEM) images of the copper plate from BC treatment (natural bentonite amended with bacterial consortium) after 2-month anoxic incubation at 60 °C (A). The EDX maps with the elemental distribution of Cu (in blue color), O (in pink color), S (in yellow color) and Si (in red color) (B). EDX spectrum (C). Raman spectrum derived from copper oxide precipitate (D).

The detachment of these layers exposed an unaltered copper surface, which was reflected in the elemental EDX map of Cu (blue), showing an intense coloration in that area (Fig. 5A, 5B). No such coloration was detected in the corresponding EDX maps of oxygen (O, pink) and sulfur (S, yellow) (Fig. 5B).

Instead, the non-detached areas were predominantly covered by a copper oxides crust. Upon closer inspection at higher magnifications, octahedral or pyramidal morphology precipitates composed of smaller particles were observed. The EDX spectra of these precipitates revealed the peaks of only O and Cu (data not shown), suggesting its nature as copper oxides. Raman spectroscopy showed a peak at  $220\text{ cm}^{-1}$  (**Fig. 5D**), which, according to the literature, identified and confirmed these precipitates as copper(I) oxide, known as cuprite (Montoya et al., 2017). Furthermore, in the aforementioned altered area, the S signal in the EDX map was also intense, indicating the presence of this element (**Fig. 5B**). At higher magnifications, precipitates with a “desert rose” mineral-type morphology and high Cu and S composition were identified (**Fig. 5C**). Due to the low intensity of the O peak in the EDX spectrum, it was suggested that these precipitates probably corresponded to copper sulfides ( $\text{Cu}_x\text{S}$ ), which are the main corrosion products of SRBs. To further identify the  $\text{Cu}_x\text{S}$  precipitates, raman analysis was attempted. However, the structure of such precipitates appeared to be weak and burned with the Raman laser, making it impossible to obtain a more accurate identification.

The treatment corresponding to heat-shocked bentonite and consortium (BstC), also presented an altered and darkened surface. Microscopic analysis revealed a completely damaged surface covered by corrosion products (**Fig. 6**). “Patches” were observed on the Cu surface, from which cuspids emerged, and EDX spectra revealed that these cusps corresponded to accumulations of copper oxides (**Fig. 6C**). Additionally, bentonite remnants were detected to be adhered to the plate surface and corrosion products. EDX spectrum of bentonite primarily identified peaks of silicon (Si), aluminum (Al), and magnesium (Mg).

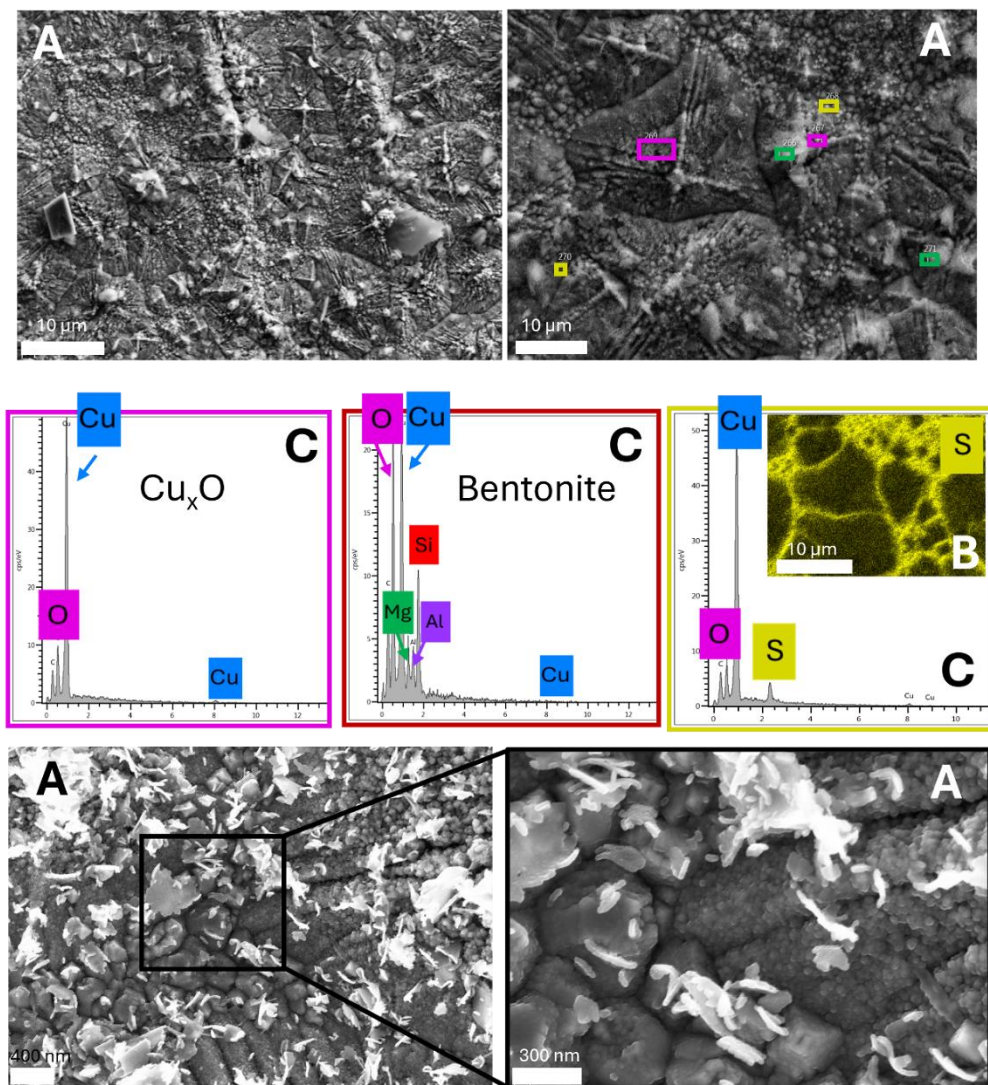


**Figure 6.** Variable pressure scanning electron microscopy (VP-FESEM) images of the copper plate from BstC treatment (heat-shocked bentonite with bacterial consortium amended) after 2-month of anoxic incubation at 60 °C (A). The EDX maps with the elemental distribution of S (in yellow color) (B). EDX spectra (C).

The S signal was primarily identified along the boundaries of these “patches”, as indicated by the EDX signal in the maps and spectrum, which exhibited heightened intensity in those areas (**Fig. 6B, 6C**). At higher magnifications, precipitates were observed in these limiting zones between the “patches” of

copper oxides (**Fig. 6A**). The  $\text{Cu}_x\text{S}$  compounds appeared to be formed from copper oxides that conform the “patches”.

Copper oxides may have a biotic or abiotic origin. Bacteria in the microcosms can contribute to the alteration of the system, thereby facilitating the formation of these copper oxides. Despite the anoxic conditions maintained within the microcosms, oxygen can still be derived from different sources, including trapped molecules within the bentonite pores (Burzan et al., 2022) and from the equilibrium water (Huttunen-Saarivirta et al., 2016). Hall et al. (2021) reported that the formation of copper oxides under relevant repository conditions would be according to the **reaction 1**. The present work is consistent with this reaction, as the results have shown the formation of copper(I) oxides. On the other hand, the formation of copper sulfides represents another potential microbiologically induced corrosion process. As mentioned earlier, SRBs are primarily responsible for the formation of copper sulfides under anoxic conditions. Microbiological results of this study demonstrated the presence of viable sulfate-reducing bacteria after the 2-month incubation period at high temperature. These results identified *Desulfosporosinus*, *Desulfotomaculum*, and *Desulfohalotomaculum* as the predominant viable genera. The viability of SRB after this incubation time could justify the involvement of this bacterial group in copper corrosion processes over the 2-month period. These bacteria utilize sulfate as a final electron acceptor, leading to the formation of sulfide according to the **reaction 2** (Dou et al., 2020). The consumption of lactate by SRB as an electron donor has been previously reported (e.g.: Matschiavelli et al., 2019). This consumption would contribute electrons to the sulfate reduction process, thereby facilitating the formation of sulfides. The corrosion of copper by SRB is known to be indirect process, as these bacteria produce sulfide ( $\text{HS}^-$ ), which then directly reacts with the copper. This reaction between sulfide and copper

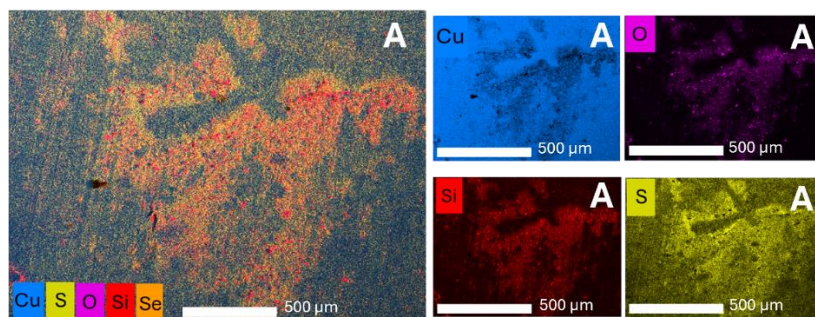
## CHAPTER 3

can take place in two different ways. On the one hand,  $\text{HS}^-$  could react with pure copper, giving rise to copper sulfides following the **reaction 3** also detailed by Dou et al., 2020. On the other hand, if the copper is already oxidized,  $\text{HS}^-$  could also react with the  $\text{Cu}_2\text{O}$ , leading to the formation of  $\text{Cu}_2\text{S}$ . This latest process would follow the **reaction 4** reported by Salehi Alaei et al., (2023).

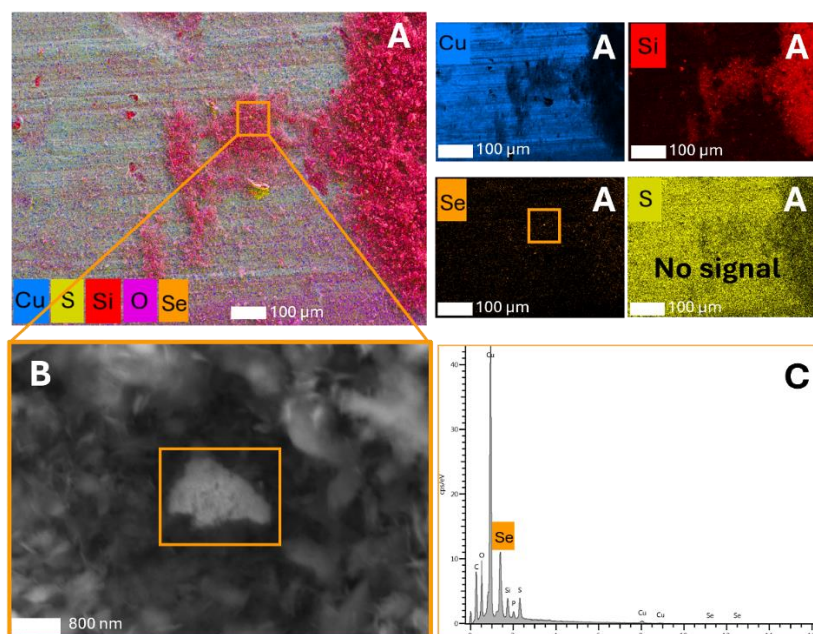
The presence of Se also had an impact on the copper corrosion. In Se-treatments with the bacterial consortium (BCSe, BstCSe), less altered surface areas were observed compared to the analogous treatments without selenium (BC, BstC). The surface of the copper plates corresponding to both treatments was mainly covered by bentonite remnants, as shown by the EDX maps for Si (**Fig. 7**). The detection of O was predominantly linked to the Si signal, suggesting a correlation with bentonite (**Fig. 7A**). Precipitates related to copper oxides, similar to those found in the BC and BstC samples, were not observed. In contrast, the presence of an oxidized surface was determined, which may be indicative of the formation of a passivation layer on the copper surface, as a result of exposure to oxygen molecules. Regarding the S signal, which is mainly associated with the formation of copper sulfides, it was identified only in the BCSe sample and was mainly associated with bentonite (**Fig. 7A**). In the BstCSe sample, the EDX map for S showed only a background signal, with no sulfur detected in any other area (**Fig. 7A**). The abundance of Se precipitates was relatively low, although a few were detected and consistently present in areas where bentonite was deposited (**Fig. 7B, 7C**). As previously discussed in **Chapter 2**, the presence of Se precipitates may be associated with the activity of bacteria involved in the reduction of Se(IV) to Se(0). In the context of these treatments, the bacterial consortium would have been the primary factor engaged in the reduction of selenium. This is due to the presence of genera such as *Stenotrophomonas* and *Pseudomonas*, which possess the capability to

reduce this metalloid (Macy et al., 1989; Ruiz-Fresneda et al., 2019). The findings of the present study demonstrated that the addition of Se would reduce the impact of microbial activity on copper corrosion. This phenomenon was likely due to the competition between Se(IV) and Cu for the sulfide, produced by SRBs, as the final electron acceptor (Hockin and Gadd (2003). The reaction of selenite with  $\text{HS}^-$  could result in the removal of available sulfide molecules, thereby reducing the likelihood of their reaction with copper. Hockin and Gadd (2003) detailed the **reaction 5** in which  $\text{HS}^-$  could react with selenite.

### BCSe

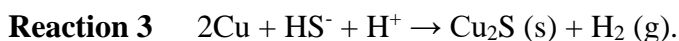


### BstCSe



## CHAPTER 3

**Figure 7.** Variable pressure scanning electron microscopy (VP-FESEM) images of the copper plate from BC and BstCSe treatments after 2-month of anoxic incubation at 60 °C (**A**). The EDX maps with the elemental distribution of Cu (in blue color), O (in pink color), S (in yellow color), Si (in red color) and Se (in orange color) (**B**). EDX spectrum (**C**). B: natural bentonite; Bst: heat-shocked bentonite; C: bacterial consortium; Se: sodium selenite (2 mM).



In treatments with less microbial activity, specifically those lacking consortium B, Bst, BSe, and BstSe, the alteration of the Cu surface was significantly lower. This reduction in surface alteration was evident both macroscopically (**Fig. 4**) and microscopically (**Fig. 8**). The Cu surfaces exhibited minimal corrosion products, with the streaks from cutting and polishing the plates clearly visible, similar to those in the untreated control (**Fig. 8, Supplementary Fig. 2**). In sample B, the presence of small copper oxide precipitates was observed at higher magnifications (**Fig. 8A**). In contrast, these precipitates were not observed in the other treatments (BSe, Bst, and BstSe), where only the possible spontaneously formed passivation layer was detected, as indicated by EDX, which showed only O and Cu peaks (**Fig. 8A, 8B**).

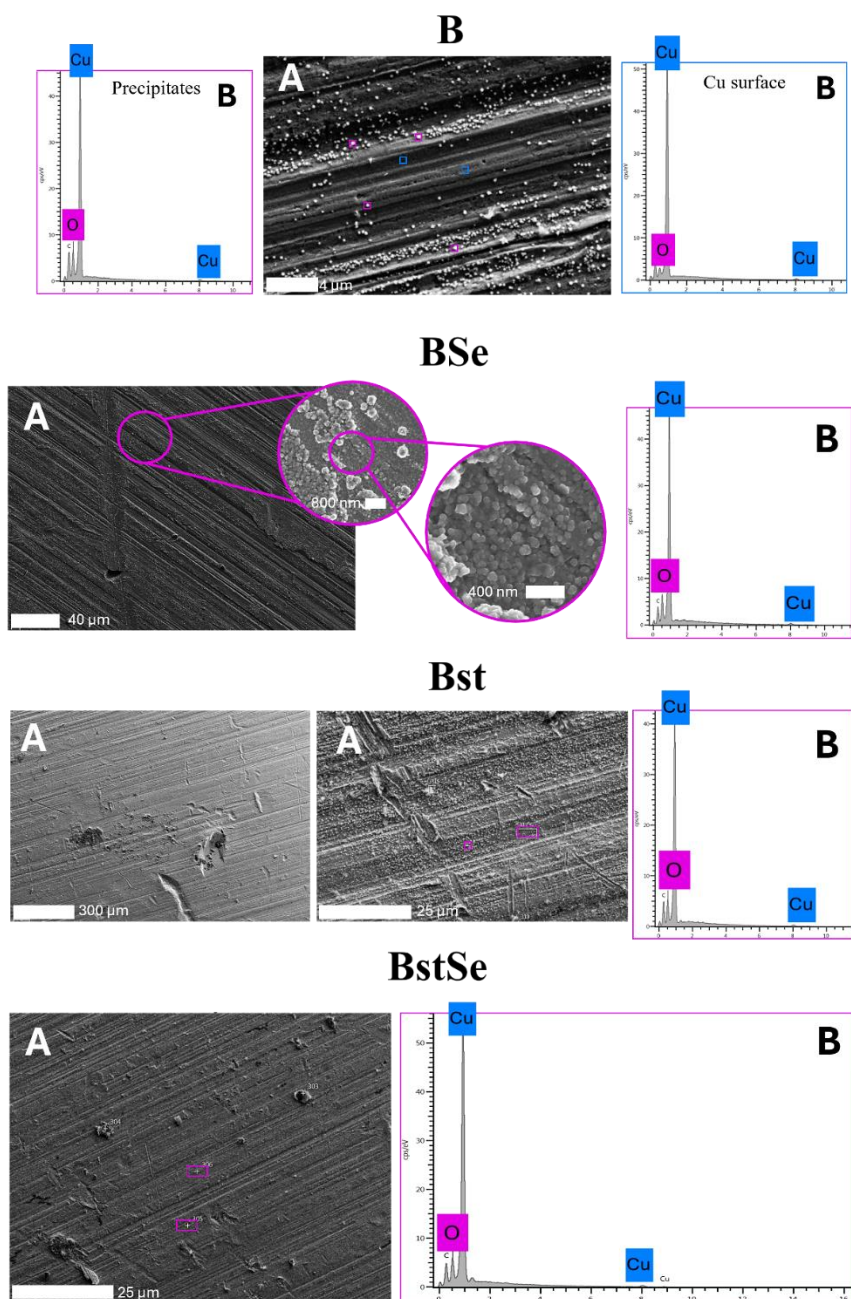


**Figure 8.** Variable pressure scanning electron microscopy (VP-FESEM) images of the copper plate from non-consortium treatments, B, BSe, Bst and BstSe, after 2-month of anoxic incubation at 60 °C (A). EDX spectra (B). B: natural bentonite; Bst: heat-shocked bentonite; Se: sodium selenite (2 mM).

## CHAPTER 3

These results enhance the hypothesis that microbial activity would accelerate the processes associated with the copper corrosion. MPN data (**Table 2**) showed higher SRB quantification in the absence of the bacterial consortium. However, if considering only treatments with the presence of the consortium, the characterization of the Cu surfaces showed higher corrosion products. In addition, bacterial cells were detected together with extracellular polymeric substances (EPS) in all consortium samples suggesting the possibility to form biofilms (**Fig. 9**). These cells were always associated with bentonite. As previously showed in **Chapter 2**, the presence of the consortium would have competed with the proliferation of other bacteria, including SRBs, by dominating the microbial communities. Nevertheless, a lower number of SRB would not imply a lower activity within the microcosm's environment. Based on the present results, the bacterial consortium would have enhanced the activity of SRB linked with favorable conditions for greater copper corrosion.

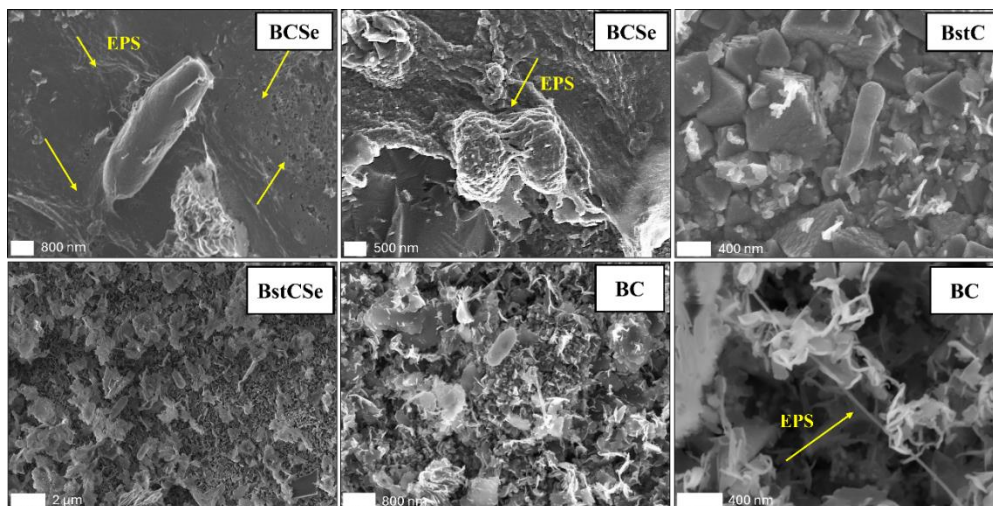


**Figure 9.** Bacterial cells together with extracellular polymeric substances (EPS, yellow arrow) on Cu plates corresponding to the four bacterial consortium treatments. B: natural bentonite; Bst: heat-shocked bentonite; C: bacterial consortium; Se: sodium selenite (2 mM).

### 3.3. Changes in bentonite mineralogy and chemical stability

The selection of bentonite clay as a filling and sealing barrier in the future Spanish DGR is attributed to its favorable physicochemical characteristics, which are expected to provide optimal properties to the multi-barrier system. These characteristics include thermal and chemical stability, swelling and leak retention capacity, mechanical stability, among other beneficial attributes (7<sup>th</sup> General Radioactive Waste Plan, 2023; Huertas et al., 2021; Villar et al., 2006). In Spain, it has been agreed to use bentonite as a barrier in compacted blocks with a density of approximately 1.65 g/cm<sup>3</sup> (Morales-Hidalgo et al., 2024a). In this study, a scenario of system failure was simulated where the bentonite barrier would have entirely lost its compaction density and transformed into a slurry phase.

In the present work, the bentonite was subjected to various treatments, including the inoculation with a bacterial consortium, tyndallization (heat-shocked bentonite), and Se(IV) presence, for two months of anoxic incubation at 60 °C. It was then analyzed by XRD using the oriented aggregate (OA) technique, including ethylene glycol (EG) exposure, to elucidate mineralogical changes in the clay. The OA-XRD patterns, with and without EG exposure, exhibited no discernible changes between the treatments under study and the untreated unincubated natural bentonite (NB) (**Fig, 10**).

The observed differences in peak intensity between treatments were primarily associated to variations in the amount of sample used for X-ray diffraction analysis. The OA-XRD patterns showed a dominant phase corresponding to smectite (montmorillonite), which is the main mineral phase in Spanish bentonite (Villar et al., 2021). Other accessory minerals were also detected and identified, corresponding to albite, feldspar, quartz and plagioclase. Lopez-Fernandez et al. (2015) quantified the mineral phases of Spanish bentonite

## CHAPTER 3

from Cortijo de Archidona: ~84% of montmorillonite, 3% of quartz, and 12% of plagioclase (albite). Moreover, these findings are consistent with those reported by Martinez-Moreno et al. (2024), demonstrating no mineralogical changes in Spanish bentonite blocks compacted to a density of 1.7 g/cm<sup>3</sup> and incubated at 60 °C for one year under anoxic conditions. One of the most important properties of bentonite is its swelling and expansion capacity. This property arises from its ability to exchange cations in the crystalline structure, enabling the absorption of significant amounts of water within the interlayer spaces. As indicated by the reflection (001) around 17 Å in the ethylene glycol (EG) OA-XRD pattern, the dioctahedral Spanish bentonite maintained its expansion capacity in all the treatments previously incubated at 60 °C. This stability in swelling capacity indicated that no illitization-related processes have occurred (Martinez-Moreno et al., 2024; Fernández et al., 2022).

Additionally, the chemical characterization of the samples by XRF also revealed no remarkable differences between the 2-month incubated treatments and compared to the unincubated and untreated reference bentonite (NB) (**Supplementary Table S2**). The predominant oxides identified in the different samples were silicon dioxide (SiO<sub>2</sub>) and aluminum oxide (Al<sub>2</sub>O<sub>3</sub>). Overall, the elemental chemical composition was consistent with the data reported in previous studies, including those by Lopez-Fernandez et al. (2015) and Martinez-Moreno et al. (2024), which observed no significant changes between different samples of Spanish bentonite.

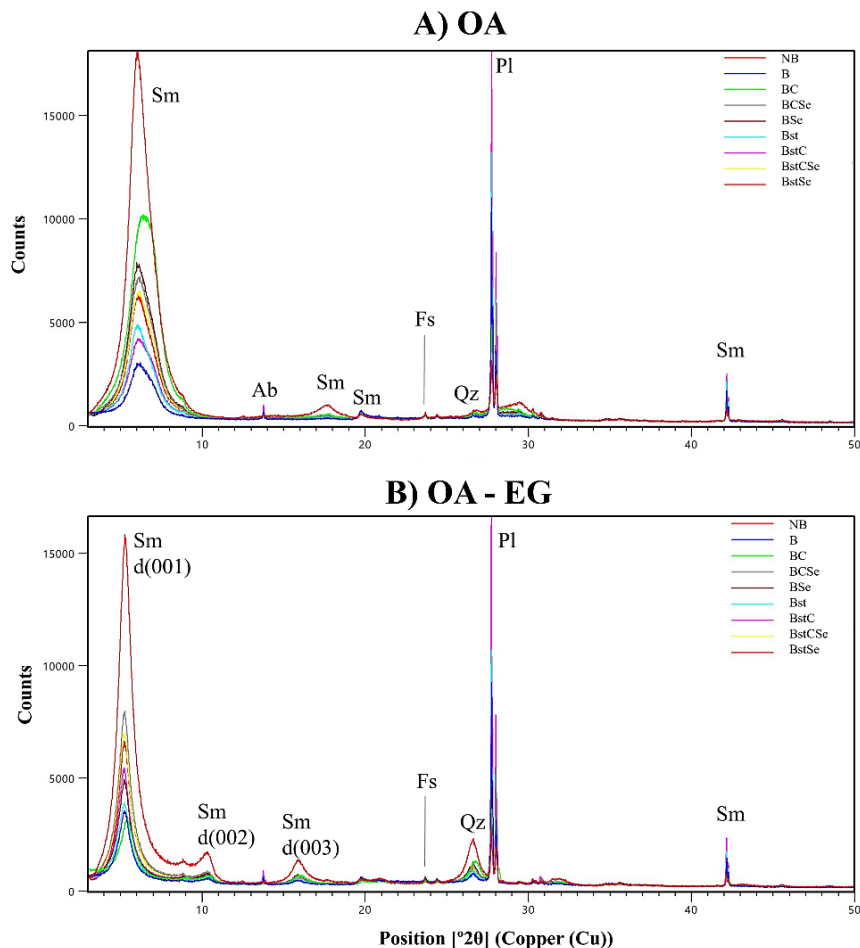


**Figure 10.** X-Ray diffraction (XRD) patterns of oriented aggregates (OA) of bentonite samples before (NB) and after two months of anoxic incubation at 60 °C (A). X-Ray diffraction (XRD) patterns of oriented aggregates (OA) of the same samples after 24 h of exposure to ethylene glycol (EG) (B). NB: untreated unincubated natural bentonite; B: natural bentonite; Bst: heat-shocked bentonite; C: bacterial consortium; Se: sodium selenite (2 mM). Sm: smectite; Ab: albite; Fs: feldspar; Qz: quartz; Pg: plagioclase.

The stability of the bentonite buffer can be compromised by microorganisms, which could interact with minerals, leading to processes such as weathering, dissolution, and the formation of new minerals (Meleshyn, 2014). In this context, a key process is the bioreduction of Fe(III), which favour the illitization of the smectite. Pedersen et al. (2017) observed that sulfide

produced by SRB and iron-reducing bacteria (IRB) can react with Fe(III) of the smectite, reducing it to Fe(II) and potentially favouring the illitization. This illitization process is particularly concerning because it can alter the beneficial properties of smectite as previously mentioned (Masurat et al., 2010; Kaufhold and Dohrmann, 2010). However, in the current study, despite observing evidences of bacterial activity and SRB viability after high-temperature incubation, there was no evidence of smectite illitization or destabilization. Consequently, despite the aggressive conditions studied here, longer incubation periods or more severe study parameters would still be required to destabilize this critically important artificial barrier for future radioactive waste storage.

#### **4. Key findings and conclusions**

The present study aimed to elucidate the processes related to copper corrosion and the viability of SRB, the main bacterial group involved, under conditions of DGR system failure. Additionally, the mineralogical and chemical stability of bentonite under these specified conditions were evaluated. After a two-month incubation period under anoxic atmosphere at 60 °C, all treatments were positive for viable SRB cells, showing a higher number in the absence of the bacterial consortium. The consortium strains are expected to dominate the community, potentially limiting the proliferation of other microbial communities, including SRBs, through resource competition. Taxonomic identification by next-generation sequencing of the 16S rRNA gene indicated that *Desulfosporosinus*, *Desulfotomaculum*, and *Desulfohalotomaculum* were the most abundant SRB genera across all treatments. These bacteria would be the main contributors to sulfate reduction and the subsequent production of sulfides, such as hydrogen sulfide, which could induce the copper corrosion. In addition to these, other genera such as *Clostridium*, *Anaerobaculum*, and

*Fonticella* were also identified as viable, being species capable of utilizing sulfate as a final electron acceptor and tolerating high temperatures. On the other hand, state-of-the-art microscopy and spectroscopic techniques including VP-FESEM, EDX and Raman, suggested the great impact that microorganisms can have on the copper corrosion under these oxygen-free and high temperature conditions. The Cu plates from the amended bacterial consortium microcosms (BC and BstC) exhibited the highest levels of corrosion. As identified by electron microscopy and raman spectroscopy, significant alterations were observed on the surfaces of these plates, with the formation of copper(I) oxides, in addition to the presence of potential copper sulfides ( $\text{Cu}_x\text{S}$ ). Although the bacterial consortium is not directly involved in copper corrosion, the current results indicated that its presence and activity may enhance that of SRB, which by sulfate reduction could potentially favor the conditions for copper alteration. Conversely, corrosion was observed to be remarkably lower in the Se treatments. This phenomenon may be attributed to the competition between copper and selenite for  $\text{HS}^-$ , which is produced primarily by SRBs. The presence of selenite, acting as final electron acceptor, would compete with copper, thereby reducing the probability of sulfide reacting with the metal and consequently resulting in a reduction in the formation of copper sulfides. The hypothesis linking microbial involvement to the observed negative impact on copper alteration is further reinforced by the following results. Furthermore, microscopy analyses revealed that the lowest alteration on the Cu plates surface occurred in those treatments initially expected to have lower microbial activity, i.e. those without the consortium (B, Bst, BSe, BstSe). Accordingly, only an oxygen signal was detected on the copper surface, corresponding to the spontaneous passivation layer, along with small precipitates of copper oxides in the case of treatment B.

## CHAPTER 3

Finally, no remarkable changes were observed in the bentonite elemental composition showing the mineralogical and chemical stability of this clay. Additionally, no alterations in the swelling capacity of the smectite were indicated by the exposure to ethylene glycol, suggesting thus the absence of an illitization process.

### **Funding**

The present work was supported by the grant RTI2018–101548-B-I00 “ERDF A way of making Europe” to MLM from the “Ministerio de Ciencia, Innovación y Universidades” (Spanish Government) and by the grant FPU20/00583 from “Ministerio de Universidades” to the first author from the Spanish Government.

### **Acknowledgements**

The authors would like to thank Dr. F. Javier Huertas (IACT, Spain) for his guidance and assistance in collecting the bentonite from the El Cortijo de Archidona site (Almería, Spain). Daniel García Muñoz Bautista Cerro and Isabel Guerra-Tschuschke (Centro de Instrumentación Científica, University of Granada, Spain) for the sample preparation and microscopy assistance, respectively. Moreover, Prof. Antonio Sánchez-Navas (Department of Mineralogy and Petrology, University of Granada, Spain) for his help and training on the diffractometer.

### **References**

- 7º Plan General de Residuos Radiactivos. (2023). Ministerio para la transición ecológica y el reto demográfico. <https://www.miteco.gob.es/es/energia/nuclear/residuos/plan-general.html>
- Aoyagi, T., Mori, Y., Nanao, M., Matsuyama, Y., Sato, Y., Inaba, T., ... & Hori, T. (2021). Effective Se reduction by lactate-stimulated indigenous microbial communities in

- excavated waste rocks. *Journal of Hazardous Materials*, 403, 123908. <https://doi.org/10.1016/j.jhazmat.2020.123908>
- Bao, P., Huang, H., Hu, Z. Y., Häggblom, M. M., & Zhu, Y. G. (2013). Impact of temperature, CO<sub>2</sub> fixation and nitrate reduction on selenium reduction, by a paddy soil *Clostridium* strain. *Journal of Applied Microbiology*, 114(3), 703-712. <https://doi.org/10.1111/jam.12084>
- Bennett, D. G., & Gens, R. (2008). Overview of European concepts for high-level waste and spent fuel disposal with special reference waste container corrosion. *Journal of Nuclear Materials*, 379(1-3), 1-8. <https://doi.org/10.1016/j.jnucmat.2008.06.001>
- Burzan, N., Murad Lima, R., Fruttschi, M., Janowczyk, A., Reddy, B., Rance, A., Diomidis, N., Bernier-Latmani, R., (2022). Growth and Persistence of an Aerobic Microbial Community in Wyoming Bentonite MX-80 Despite Anoxic in situ Conditions. *Frontiers in Microbiology*, 13. <https://doi.org/10.3389/fmicb.2022.858324>
- Callahan, B.J., McMurdie, P.J., Rosen, M.J., Han, A.W., Johnson, A.J., Holmes, S.P. (2016). DADA2: High-resolution sample inference from Illumina amplicon data. *Nature Methods*, 13(7), 581-3. <https://doi.org/10.1038/nmeth.3869>
- Campbell Jr, L. L., Frank, H. A., & Hall, E. R. (1957). Studies on thermophilic sulfate reducing bacteria i. *Sporovibrio desulfuricans* as *Clostridium nigrificans*: Identification of. *Journal of Bacteriology*, 73(4), 516-521.
- Caporaso, J.G., Kuczynski, J., Stombaugh, J., Bittinger, K., Bushman, F.D., Costello, E.K., Fierer, N., Peña, A.G., Goodrich, J.K., Gordon, J.I., Huttley, G.A., Kelley, S.T., Knights, D., Koenig, J.E., Ley, R.E., Lozupone, C.A., McDonald, D., Muegge, B.D., Pirrung, M., Reeder, J., Sevinsky, J.R., Turnbaugh, P.J., Walters, W.A., Widmann, J., Yatsunenko, T., Zaneveld, J., Knight, R. (2010). QIIME allows analysis of high-throughput community sequencing data. *Nature Methods*, 7(5), 335-6. <https://doi.org/10.1038/nmeth.f.303>
- Combet-Blanc, Y., Ollivier, B., Streicher, C., Patel, B. K. C., Dwivedi, P. P., Pot, B., ... & Garcia, J. L. (1995). *Bacillus thermoamylovorans* sp. nov., a moderately thermophilic and amyolytic bacterium. *International Journal of Systematic and Evolutionary Microbiology*, 45(1), 9-16. <https://doi.org/10.1099/00207713-45-1-9>
- Dou, W., Pu, Y., Han, X., Song, Y., Chen, S., & Gu, T. (2020). Corrosion of Cu by a sulfate reducing bacterium in anaerobic vials with different headspace volumes. *Bioelectrochemistry*, 133, 107478. <https://doi.org/10.1016/j.bioelechem.2020.107478>
- Drake, H.L. (1994). Acetogenesis, Acetogenic Bacteria, and the Acetyl-CoA “Wood/Ljungdahl” Pathway: Past and Current Perspectives. In: Drake, H.L. (eds) Acetogenesis. Chapman & Hall Microbiology Series. Springer, Boston, MA. [https://doi.org/10.1007/978-1-4615-1777-1\\_1](https://doi.org/10.1007/978-1-4615-1777-1_1)

## CHAPTER 3

- Fernández, A. M., Marco, J. F., Nieto, P., León, F. J., Robredo, L. M., Clavero, M. Á., Cardona, A. I., Fernández, S., Svensson, D., Sellin, P. (2022). Characterization of Bentonites from the in situ ABM5 Heater Experiment at Äspö Hard Rock Laboratory, Sweden. *Minerals*, 12(4), 471. <https://doi.org/10.3390/min12040471>
- Forsberg, C. W. (2000). Rethinking high-level waste disposal: Separate disposal of high-heat radionuclides ( $^{90}\text{Sr}$  and  $^{137}\text{Cs}$ ). *Nuclear technology*, 131(2), 252-268. <https://doi.org/10.13182/NT00-A3115>
- Fraj, B., Ben Hania, W., Postec, A., Hamdi, M., Ollivier, B., & Fardeau, M. L. (2013). *Fonticella tunisiensis* gen. nov., sp. nov., isolated from a hot spring. *International journal of systematic and evolutionary microbiology*, 63(Pt\_6), 1947-1950. <https://doi.org/10.1099/ijs.0.041947-0>
- Frechou, C., Aguerre, S., Degros, J. P., Kerlau, G., & Grangeon, T. (2007). Improvement of a radiochemical separation for selenium 79: Applications to effluents and nuclear wastes. *Talanta*, 72(3), 1166-1171. <https://doi.org/10.1016/j.talanta.2007.01.011>
- García-Romero, E., María Manchado, E., Suárez, M., & García-Rivas, J. (2019). Spanish Bentonites: A review and new data on their geology, mineralogy, and crystal chemistry. *Minerals*, 9(11), 696. <https://doi.org/10.3390/min9110696>
- Gilmour, K. A., Davie, C. T., & Gray, N. (2021). An indigenous iron-reducing microbial community from MX80 bentonite—a study in the framework of nuclear waste disposal. *Applied Clay Science*, 205, 106039. <https://doi.org/10.1016/j.clay.2021.106039>
- Grigoryan, A. A., Jalique, D. R., Medihala, P., Stroes-Gascoyne, S., Wolfaardt, G. M., McKelvie, J., & Korber, D. R. (2018). Bacterial diversity and production of sulfide in microcosms containing uncompacted bentonites. *Heliyon*, 4(8). <https://doi.org/10.1016/j.heliyon.2018.e00722>
- Guerra, I., and Cardell, C. (2015). Optimizing use of the structural chemical analyser (variable pressure FESEM-EDX Raman spectroscopy) on micro-size complex historical paintings characterization. *Journal of Microscopy*, 260, 47–61. <https://doi.org/10.1111/jmi.12265>
- Guo, M. (2020). The electrochemical and corrosion study of copper for nuclear waste containers under deep geological disposal conditions (Doctoral dissertation, The University of Western Ontario (Canada)).
- Hall, D. S., Behazin, M., Binns, W. J., & Keech, P. G. (2021). An evaluation of corrosion processes affecting copper-coated nuclear waste containers in a deep geological repository. *Progress in Materials Science*, 118, 100766. <https://doi.org/10.1016/j.pmatsci.2020.100766>
- Hockin, S. L., & Gadd, G. M. (2003). Linked redox precipitation of sulfur and selenium under anaerobic conditions by sulfate-reducing bacterial biofilms. *Applied and*

- Environmental Microbiology*, 69(12), 7063-7072.  
<https://doi.org/10.1128/AEM.69.12.7063-7072.2003>
- Hong, H., Kim, S. J., Min, U. G., Lee, Y. J., Kim, S. G., Roh, S. W., ... & Rhee, S. K. (2015). *Anaerosolibacter carboniphilus* gen. nov., sp. nov., a strictly anaerobic iron-reducing bacterium isolated from coal-contaminated soil. *International Journal of Systematic and Evolutionary Microbiology*, 65(Pt\_5), 1480-1485.  
<https://doi.org/10.1099/ijs.0.000124>
- Huertas, F., Fariña, P., Farias, J., García-Siñeriz, J.L., Villar, M.V., Fernández, A.M., Martín, P.L., Elorza, F.J., Gens, A., Sánchez, M., Lloret, A., Samper, J., Martínez, M. Á. (2021). Full-scale Engineered Barriers Experiment. Updated Final Report 1994-2004.
- Huttunen-Saarivirta, E., Rajala, P., & Carpén, L. (2016). Corrosion behaviour of copper under biotic and abiotic conditions in anoxic ground water: electrochemical study. *Electrochimica Acta*, 203, 350-365.  
<https://doi.org/10.1016/j.electacta.2016.01.098>
- Jonsson, M., Emilsson, G., & Emilsson, L. (2018). Mechanical design analysis for the canister. Posiva SKB Report, 4, 147.
- Kaufhold, S., & Dohrmann, R. (2010). Stability of bentonites in salt solutions: II. Potassium chloride solution—Initial step of illitization? *Applied Clay Science*, 49(3), 98-107.  
<https://doi.org/10.1016/j.clay.2010.04.009>
- Kim, G., Yang, H., Lee, J., & Cho, K. S. (2024). Comparative analysis of hydrogen production and bacterial communities in mesophilic and thermophilic consortia using multiple inoculum sources. *Chemosphere*, 350, 141144.  
<https://doi.org/10.1016/j.chemosphere.2024.141144>
- King, F., Hall, D. S., & Keech, P. G. (2017). Nature of the near-field environment in a deep geological repository and the implications for the corrosion behaviour of the container. *Corrosion Engineering, Science and Technology*, 52(sup1), 25-30.  
<https://doi.org/10.1080/1478422X.2017.1330736>
- King, F., Kolář, M., Briggs, S., Behazin, M., Keech, P., & Diomidis, N. (2024). Review of the Modelling of Corrosion Processes and Lifetime Prediction for HLW/SF Containers—Part 2: Performance Assessment Models. *Corrosion and Materials Degradation*, 5(2), 289-339. <https://doi.org/10.3390/cmd5020013>
- Little, B. J., Hinks, J., & Blackwood, D. J. (2020). Microbially influenced corrosion: Towards an interdisciplinary perspective on mechanisms. *International biodeterioration & biodegradation*, 154, 105062. <https://doi.org/10.1016/j.ibiod.2020.105062>
- Liu, J., Taylor, J. C., & Baldwin, S. A. (2018). Removal of selenate from brine using anaerobic bacteria and zero valent iron. *Journal of environmental management*, 222, 348-358.  
<https://doi.org/10.1016/j.jenvman.2018.05.095>

## CHAPTER 3

- Lopez-Fernandez, M., Romero-González, M., Günther, A., Solari, P. L., & Merroun, M. L. (2018). Effect of U(VI) aqueous speciation on the binding of uranium by the cell surface of *Rhodotorula mucilaginosa*, a natural yeast isolate from bentonites. *Chemosphere*, 199, 351-360. <https://doi.org/10.1016/j.chemosphere.2018.02.055>
- Lopez-Fernandez, M., Cherkouk, A., Vilchez-Vargas, R., Jauregui, R., Pieper, D., Boon, N., ... & Merroun, M. L. (2015). Bacterial diversity in bentonites, engineered barrier for deep geological disposal of radioactive wastes. *Microbial ecology*, 70, 922-935. <https://doi.org/10.1007/s00248-015-0630-7>
- Lopez-Fernandez, M., Fernández-Sanfrancisco, O., Moreno-García, A., Martín-Sánchez, I., Sánchez-Castro, I., & Merroun, M. L. (2014). Microbial communities in bentonite formations and their interactions with uranium. *Applied geochemistry*, 49, 77-86. <https://doi.org/10.1016/j.apgeochem.2014.06.022>
- Macy, J. M., Michel, T. A., & Kirsch, D. G. (1989). Selenate reduction by a *Pseudomonas* species: a new mode of anaerobic respiration. *FEMS Microbiology Letters*, 61(1-2), 195-198. <https://doi.org/10.1111/j.1574-6968.1989.tb03577.x>
- Martinez-Moreno, M.F., Povedano-Priego, C., Mumford, A.D., Morales-Hidalgo, M., Mijndonckx, K., Jroundi, F., Ojeda, J.J., Merroun, M.L., (2024). Microbial responses to elevated temperature: Evaluating bentonite mineralogy and copper canister corrosion within the long-term stability of deep geological repositories of nuclear waste. *Science of the Total Environment*, 915, 170149. <https://doi.org/10.1016/j.scitotenv.2024.170149>
- Martinez-Moreno, M. F., Povedano-Priego, C., Morales-Hidalgo, M., Mumford, A. D., Ojeda, J. J., Jroundi, F., & Merroun, M. L. (2023). Impact of compacted bentonite microbial community on the clay mineralogy and copper canister corrosion: a multidisciplinary approach in view of a safe Deep Geological Repository of nuclear wastes. *Journal of Hazardous Materials*, 131940. <https://doi.org/10.1016/j.jhazmat.2023.131940>
- Masurat, P., Eriksson, S., and Pedersen, K. (2010). Evidence of Indigenous Sulphate-Reducing Bacteria in Commercial Wyoming Bentonite MX- 80. *Applied Clay Science*, 47(1-2), 51-57. <https://doi.org/10.1016/j.clay.2008.07.002>
- Matschiavelli, N., Kluge, S., Podlech, C., Standhaft, D., Grathoff, G., Ikeda-Ohno, A., ... & Cherkouk, A. (2019). The year-long development of microorganisms in uncompacted bavarian bentonite slurries at 30 and 60 °C. *Environmental science & technology*, 53(17), 10514-10524. <https://doi.org/10.1021/acs.est.9b02670>
- Mayeux, B., Fardeau, M. L., Bartoli-Joseph, M., Casalot, L., Vinsot, A., & Labat, M. (2013). *Desulfosporosinus burensis* sp. nov., a spore-forming, mesophilic, sulfate-reducing bacterium isolated from a deep clay environment. *International journal of systematic and evolutionary microbiology*, 63(Pt\_2), 593-598. <https://doi.org/10.1099/ijs.0.035238-0>

- McMurry, J., Dixon, D. A., Garroni, J. D., Ikeda, B. M., Stroes-Gascoyne, S., Baumgartner, P., & Melnyk, T. W. (2004). Evolution of a Canadian deep geologic repository (No. 06819-REP, pp. 01200-100092). Ontario Power Generation Report.
- Meleshyn, A. (2014). Microbial processes relevant for the long-term performance of high-level radioactive waste repositories in clays. *Geological Society, London, Special Publications*, 400(1), 179-194. <https://doi.org/10.1144/SP400.6>
- Montoya, N., Montagna, E., Lee, Y., Doménech-Carbó, M. T., & Doménech-Carbó, A. (2017). Raman spectroscopy characterization of 10-cash productions from the late Chinese emperors to the Republic. *Journal of Raman Spectroscopy*, 48(10), 1337-1345. <https://doi.org/10.1002/jrs.5218>
- Morales-Hidalgo, M., Povedano-Priego, C., Martinez-Moreno, M. F., Ruiz-Fresneda, M. A., Lopez-Fernandez, M., Jroundi, F., & Merroun, M. L. (2024a). Insights into the Impact of Physicochemical and Microbiological Parameters on the Safety Performance of Deep Geological Repositories. *Microorganisms*, 12(5), 1025. <https://doi.org/10.3390/microorganisms12051025>
- Morales-Hidalgo, M., Povedano-Priego, C., Martinez-Moreno, M. F., Ojeda, J. J., Jroundi, F., & Merroun, M. L. (2024b). Long-term tracking of the microbiology of uranium-amended water-saturated bentonite microcosms: a mechanistic characterization of U speciation. *Journal of Hazardous Materials*, 476, 135044. <https://doi.org/10.1016/j.jhazmat.2024.135044>
- O'sullivan, L. A., Roussel, E. G., Weightman, A. J., Webster, G., Hubert, C. R., Bell, E., ... & Parkes, R. J. (2015). Survival of *Desulfotomaculum* spores from estuarine sediments after serial autoclaving and high-temperature exposure. *The ISME journal*, 9(4), 922-933. <https://doi.org/10.1038/ismej.2014.190>
- Pedersen, K., Bengtsson, A., Blom, A., Johansson, L., & Taborowski, T. (2017). Mobility and reactivity of sulphide in bentonite clays—implications for engineered bentonite barriers in geological repositories for radioactive wastes. *Applied Clay Science*, 146, 495-502. <https://doi.org/10.1016/j.clay.2017.07.003>
- Povedano-Priego, C.; Jroundi, F.; Solari, P.L.; Guerra-Tschuschke, I.; Abad-Ortega, M.D.M.; Link, A.; Vilchez-Vargas, R.; and Merroun, M.L. (2023). Unlocking the bentonite microbial diversity and its implications in selenium bioreduction and biotransformation: Advances in deep geological repositories. *Journal Hazardous Material*, 445, 130557. <https://doi.org/10.1016/j.jhazmat.2022.130557>
- Povedano-Priego, C., Jroundi, F., Lopez-Fernandez, M., Shrestha, R., Spanek, R., Martín-Sánchez, I., Villar, M. V., Ševců, A., Dopson, M. & Merroun, M. L. (2021). Deciphering indigenous bacteria in compacted bentonite through a novel and efficient DNA extraction method: Insights into biogeochemical processes within the Deep Geological Disposal of nuclear waste concept. *Journal of Hazardous Materials*, 408, 124600. <https://doi.org/10.1016/j.jhazmat.2020.124600>

## CHAPTER 3

- Robertson, C. E., Harris, J. K., Wagner, B. D., Granger, D., Browne, K., Tatem, B., Feazel, M. L., Park, K., Pace, N. R. & Frank, D. N. (2013). Explicit: graphical user interface software for metadata-driven management, analysis and visualization of microbiome data. *Bioinformatics*, 29(23), 3100-3101. <https://doi.org/10.1093/bioinformatics/btt526>
- Robertson, W. J., Bowman, J. P., Franzmann, P. D., & Mee, B. J. (2001). *Desulfosporosinus meridiei* sp. nov., a spore-forming sulfate-reducing bacterium isolated from gasoline-contaminated groundwater. *International Journal of Systematic and Evolutionary Microbiology*, 51(1), 133-140. <https://doi.org/10.1099/00207713-51-1-133>
- Ruiz-Fresneda, M. A., Gomez-Bolivar, J., Delgado-Martin, J., Abad-Ortega, M. D. M., Guerra-Tschuschke, I., & Merroun, M. L. (2019). The Bioreduction of Selenite under Anaerobic and Alkaline Conditions Analogous to Those Expected for a Deep Geological Repository System. *Molecules*, 24(21), 3868. <https://doi.org/10.3390/molecules24213868>
- Salehi Alaei, E., Guo, M., Chen, J., Behazin, M., Bergendal, E., Lilja, C., ... & Noël, J. J. (2023). The transition from used fuel container corrosion under oxic conditions to corrosion in an anoxic environment. *Materials and Corrosion*, 74(11-12), 1690-1706. <https://doi.org/10.1002/maco.202313757>
- Samarasinghe, S.N., Wanigatunge, R.P. & Magana-Arachchi, D.N. (2021). Bacterial Diversity in a Sri Lankan Geothermal Spring Assessed by Culture-Dependent and Culture-Independent Approaches. *Current Microbiology*, 78, 3439-3452. <https://doi.org/10.1007/s00284-021-02608-4>
- Sánchez-Andrea, I., Rodríguez, N., Amils, R., & Sanz, J. L. (2011). Microbial diversity in anaerobic sediments at Rio Tinto, a naturally acidic environment with a high heavy metal content. *Applied and environmental microbiology*, 77(17), 6085-6093. <https://doi.org/10.1128/AEM.00654-11>
- Sanchez-Castro, I., Ruiz-Fresneda, M. A., Bakkali, M., Kämpfer, P., Glaeser, S. P., Busse, H. J., ... & Merroun, M. L. (2017). *Stenotrophomonas bentonitica* sp. nov., isolated from bentonite formations. *International journal of systematic and evolutionary microbiology*, 67(8), 2779-2786. <https://doi.org/10.1099/ijsem.0.002016>
- Santos, A. M. D., Costa, J. M., Braga, J. K., Flynn, T. M., Brucha, G., Sancinetti, G. P., & Rodriguez, R. P. (2022). Lactate as an effective electron donor in the sulfate reduction: impacts on the microbial diversity. *Environmental Technology*, 43(20), 3149-3160. <https://doi.org/10.1080/09593330.2021.1916092>
- Sass, H., & Cypionka, H. (2004). Isolation of sulfate-reducing bacteria from the terrestrial deep subsurface and description of *Desulfovibrio cavernae* sp. nov. *Systematic and applied microbiology*, 27(5), 541-548. <https://doi.org/10.1078/0723202041748181>
- Shi, L. D., Lv, P. L., Niu, Z. F., Lai, C. Y., & Zhao, H. P. (2020). Why does sulfate inhibit selenate reduction: Molybdenum deprivation from Mo-dependent selenate

- reductase. *Water Research*, 178, 115832.  
<https://doi.org/10.1016/j.watres.2020.115832>
- Staicu, L. C., & Barton, L. L. (2021). Selenium respiration in anaerobic bacteria: Does energy generation pay off? *Journal of Inorganic Biochemistry*, 222, 111509.  
<https://doi.org/10.1016/j.jinorgbio.2021.111509>
- Tang, I. C., Okos, M. R., & Yang, S. T. (1989). Effects of pH and acetic acid on homoacetic fermentation of lactate by *Clostridium formicoaceticum*. *Biotechnology and bioengineering*, 34(8), 1063-1074. <https://doi.org/10.1002/bit.260340807>
- Thijs, S., Op De Beeck, M., Beckers, B., Truyens, S., Stevens, V., Van Hamme, J. D., Weyens, N. & Vangronsveld, J. (2017). Comparative evaluation of four bacteria-specific primer pairs for 16S rRNA gene surveys. *Frontiers in microbiology*, 8, 494.  
<https://doi.org/10.3389/fmicb.2017.00494>
- Tomei, F. A., Barton, L. L., Lemanski, C. L., Zocco, T. G., Fink, N. H., & Sillerud, L. O. (1995). Transformation of selenate and selenite to elemental selenium by *Desulfovibrio desulfuricans*. *Journal of Industrial Microbiology*, 14, 329-336.  
<https://doi.org/10.1007/BF01569947>
- Villar, M. V., Martín, P. L., Pelayo, M., Ruiz, B., Rivas, P., Alonso, E., ... & Velasco, V. (2021). FEBEX. Bentonite: origin, properties and fabrication of blocks. ENRESA Technical publication N° 05/98.
- Villar, M. V., Pérez del Villar, L., Martín, P. L., Pelayo, M., Fernández, A. M., Garralón, A., Cuevas, J., Leguey, S., Caballero, E., Huertas, F. J., Jiménez de Cisneros, C., Linares, J., Reyes, E., Delgado, A., Fernández-Soler, J. M., & Astudillo, J. (2006). The study of Spanish clays for their use as sealing materials in nuclear waste repositories: 20 years of progress. *Journal of Iberian Geology*, 32, 15–36.
- Watanabe, M., Kojima, H., & Fukui, M. (2018). Review of *Desulfotomaculum* species and proposal of the genera *Desulfallas* gen. nov., *Desulfofundulus* gen. nov., *Desulfofarcimen* gen. nov. and *Desulfohalotomaculum* gen. nov. *International Journal of Systematic and Evolutionary Microbiology*, 68(9), 2891-2899.  
<https://doi.org/10.1099/ijsem.0.002915>
- Wood, H. G., & Ljungdahl, L. G. (1991). Autotrophic character of the acetogenic bacteria. *Variations in autotrophic life*, 1, 201-250.

## CHAPTER 3

Supplementary material for:

**High-temperature microbial corrosion of copper by sulfate-reducing bacteria in water-saturated bentonite microcosms and its relevance to nuclear waste deep geological repositories**

**Mar Morales-Hidalgo**<sup>1</sup>, Cristina Povedano-Priego<sup>1</sup>, Marcos F. Martinez-Moreno<sup>1</sup>, Fadwa Jroundi<sup>1</sup>, Mohamed L. Merroun<sup>1</sup>

<sup>1</sup>*Faculty of Science, Department of Microbiology, University of Granada, Granada, Spain.*

## CHAPTER 3

**Supplementary Table S1.** Percentages of relative abundances at genus level of the viable bacteria grown in positive Postgate medium from MPN experiment. B: natural bentonite; Bst: heat-shocked bentonite; C: bacterial consortium; Se: sodium selenite (2 mM).

Genera	Relative abundances (%)								
	Total	BC	BCSe	BstC	BstCSe	B	BSe	Bst	BstSe
<i>Clostridium_sensu_stricto</i>	28.18	18.99	76.57	15.17	0.00	36.69	32.56	0.00	0.00
<i>Desulfosporosinus</i>	26.77	33.70	0.00	45.87	58.97	29.38	0.13	39.45	27.85
<i>Desulfotomaculum</i>	10.69	0.00	0.02	15.99	5.76	1.04	40.91	31.83	20.73
<i>Desulfohalotomaculum</i>	6.41	30.63	0.00	0.00	0.00	0.00	0.00	0.00	0.00
<i>Anaerosolibacter</i>	4.74	0.00	0.00	0.00	4.29	7.76	4.68	16.77	13.28
<i>Fonticella</i>	3.46	0.51	0.00	0.51	0.00	10.03	4.84	0.00	0.00
<i>Bacillus</i>	2.66	3.58	0.91	0.09	0.12	1.76	2.15	1.89	13.82
<i>Anaerocolumna</i>	2.55	0.84	0.21	12.19	16.04	0.31	0.30	0.24	0.00
<i>Sporacetigenium</i>	1.50	4.58	0.00	7.05	0.00	0.00	0.00	0.00	0.00
Uncultured_Caloramatoceae	1.46	0.00	0.00	0.00	0.00	5.57	0.00	0.00	0.00
<i>Desulfuribacillus</i>	1.40	0.00	12.19	0.00	0.00	0.00	0.00	0.00	0.00
Unclassified_Thermotaleaceae	1.33	0.00	0.00	0.00	0.00	0.00	0.00	7.92	13.97
Unclassified_Gracilibacteraceae	1.21	0.00	0.00	0.00	2.94	3.74	0.00	0.00	0.00
<i>Sporomusa</i>	0.91	1.05	0.00	0.00	0.00	0.00	0.00	0.00	10.18
<i>Peptostreptococcaceae</i>	0.89	0.22	0.00	0.00	0.00	0.00	6.01	0.00	0.00
<i>Staphylococcus</i>	0.82	0.00	7.15	0.00	0.00	0.00	0.00	0.00	0.00
<i>BRH-c20a</i>	0.79	0.00	0.00	0.00	0.00	0.04	5.53	0.00	0.00
<i>Brevibacillus</i>	0.74	0.06	0.00	0.00	9.16	0.00	0.00	0.00	0.00
<i>Hydrogenispora</i>	0.69	3.28	0.00	0.00	0.00	0.00	0.00	0.00	0.00
Uncultured_Christensenellaceae	0.31	0.68	0.00	0.00	0.00	0.59	0.07	0.00	0.00

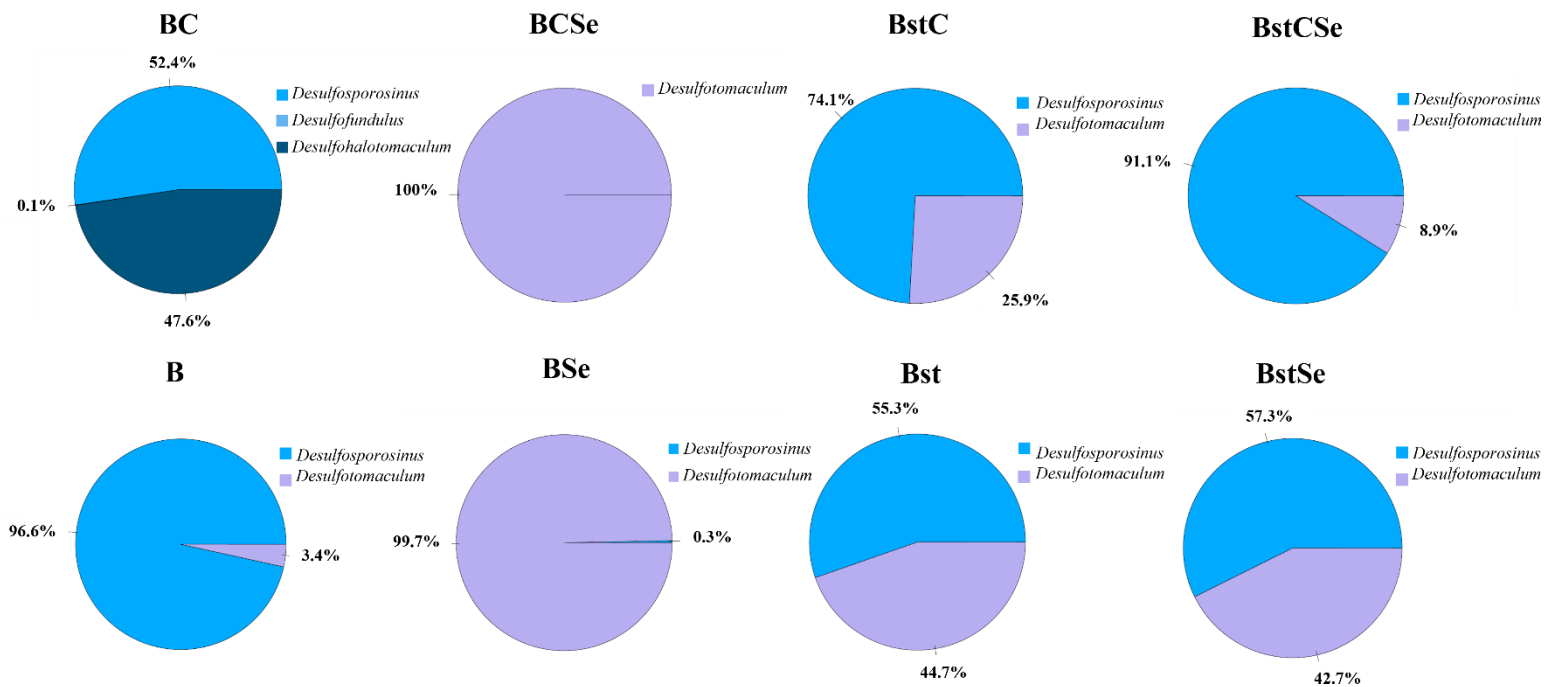
<i>Desulfitobacterium</i>	0.30	0.00	2.56	0.00	0.00	0.00	0.00	0.00	0.00
Uncultured_Hungateiclostridiaceae	0.28	0.00	0.00	0.00	0.00	0.88	0.35	0.00	0.00
<i>Oxobacter</i>	0.23	0.00	0.00	2.52	0.20	0.01	0.00	0.25	0.00
<i>Christensenellaceae_R-7_group</i>	0.22	1.01	0.00	0.00	0.00	0.03	0.04	0.00	0.00
<i>Gracilibacter</i>	0.21	0.00	0.00	0.00	0.35	0.70	0.00	0.00	0.00
<i>Symbiobacterium</i>	0.20	0.27	0.00	0.00	0.00	0.50	0.07	0.00	0.00
Unclassified	0.14	0.00	0.00	0.41	0.96	0.00	0.02	0.50	0.09
<i>Crassaminicella</i>	0.13	0.00	0.00	0.00	0.00	0.00	0.92	0.00	0.00
Unclassified_Bacillota	0.10	0.21	0.00	0.00	0.00	0.18	0.07	0.00	0.00
<i>Ruminiclostridium</i>	0.09	0.10	0.00	0.00	0.00	0.10	0.00	0.86	0.00
<i>Anaerovorax</i>	0.08	0.00	0.00	0.00	0.25	0.00	0.43	0.00	0.00
<i>Paenibacillus</i>	0.08	0.03	0.00	0.00	0.00	0.15	0.19	0.00	0.08
<i>Stenotrophomonas</i>	0.08	0.01	0.00	0.01	0.45	0.18	0.00	0.00	0.00
Unclassified_Christensenellaceae	0.06	0.00	0.00	0.00	0.00	0.16	0.10	0.18	0.00
Uncultured_Symbiobacteraceae	0.05	0.00	0.00	0.00	0.12	0.02	0.26	0.00	0.00
<i>Sedimentibacter</i>	0.04	0.00	0.38	0.00	0.00	0.00	0.00	0.00	0.00
<i>Salimesophilobacter</i>	0.02	0.00	0.00	0.00	0.00	0.00	0.15	0.00	0.00
<i>Tepidimicrobium</i>	0.02	0.05	0.00	0.09	0.00	0.00	0.00	0.00	0.00
<i>Pseudomonas</i>	0.01	0.00	0.00	0.01	0.11	0.00	0.00	0.00	0.00
<i>Alkaliphilus</i>	0.01	0.00	0.00	0.00	0.00	0.00	0.06	0.09	0.00
<i>Kocuria</i>	0.01	0.00	0.00	0.00	0.00	0.03	0.00	0.00	0.00
<i>Anaerobacterium</i>	0.01	0.00	0.00	0.00	0.00	0.03	0.00	0.00	0.00
Unclassified_Micrococcaceae	0.01	0.00	0.00	0.00	0.00	0.02	0.00	0.00	0.00
Unclassified_Peptostreptococcaceae	0.01	0.04	0.00	0.00	0.00	0.00	0.00	0.00	0.00

## CHAPTER 3

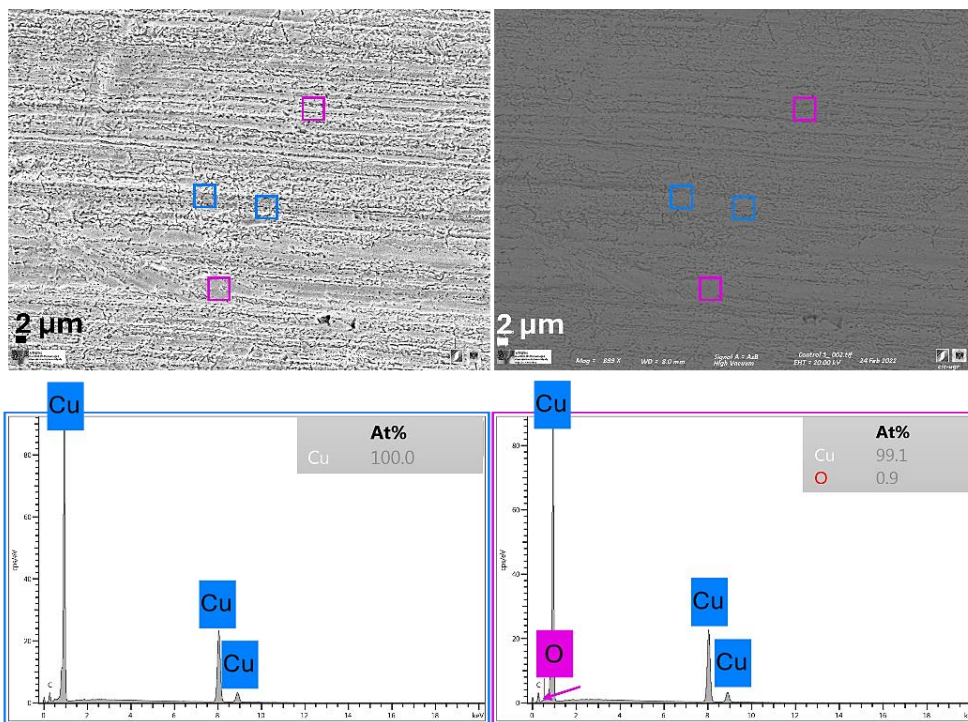
Unclassified_Lachnospiraceae	0.01	0.02	0.00	0.00	0.00	0.00	0.05	0.00	0.00
<i>Exiguobacterium</i>	0.01	0.03	0.00	0.00	0.00	0.00	0.00	0.00	0.00
Unclassified_Clostridiaceae	0.01	0.00	0.00	0.00	0.00	0.04	0.00	0.00	0.00
<i>Desulfofundulus</i>	0.01	0.04	0.00	0.00	0.00	0.00	0.00	0.00	0.00
<i>Amycolatopsis</i>	0.01	0.02	0.00	0.01	0.11	0.00	0.00	0.00	0.00
<i>Pelosinus</i>	0.01	0.07	0.00	0.00	0.00	0.00	0.00	0.00	0.00
<i>Paenisporosarcina</i>	0.01	0.00	0.00	0.00	0.04	0.02	0.00	0.00	0.00
<i>Dermacoccus</i>	0.01	0.00	0.00	0.00	0.08	0.00	0.00	0.00	0.00
Uncultured_Bacillota	0.01	0.00	0.00	0.00	0.00	0.00	0.11	0.00	0.00
Unclassified	0.01	0.00	0.00	0.02	0.02	0.00	0.00	0.02	0.01
<i>Massilia</i>	0.00	0.00	0.00	0.00	0.00	0.01	0.00	0.00	0.00
Unclassified_Veillonellales-Selenomonadales	0.00	0.00	0.00	0.06	0.00	0.00	0.00	0.00	0.00
<i>Desulfofarcimen</i>	0.00	0.00	0.00	0.00	0.00	0.00	0.00	0.00	0.00
<i>Streptococcus</i>	0.00	0.00	0.00	0.00	0.00	0.01	0.00	0.00	0.00
<i>Thermaerobacter</i>	0.00	0.00	0.00	0.00	0.00	0.01	0.00	0.00	0.00

**Supplementary Table S2.** Chemical elemental composition (%) by X-ray fluorescence (XRF) of bentonite samples before (NB) and after two months of anoxic incubation at 60 °C. LOI: Loss on ignition. NB: untreated unincubated natural bentonite; B: natural bentonite; Bst: heat-shocked bentonite; C: bacterial consortium; Se: sodium selenite (2 mM).

Sample	SiO <sub>2</sub>	Al <sub>2</sub> O <sub>3</sub>	Fe <sub>2</sub> O <sub>3</sub>	MnO	MgO	CaO	Na <sub>2</sub> O	K <sub>2</sub> O	TiO <sub>2</sub>	P <sub>2</sub> O <sub>5</sub>	LOI
<b>NB</b>	60.61	16.51	3.91	0.05	3.98	4.62	1.72	1.55	0.25	0.07	6.52
<b>BC</b>	60.03	18.03	4.19	0.03	4.69	2.86	1.68	1.09	0.26	0.05	6.53
<b>BstC</b>	61.31	17.18	4.04	0.03	3.86	3.35	1.89	1.56	0.25	0.07	6.40
<b>B</b>	60.41	16.38	3.82	0.05	4.09	4.82	1.60	1.43	0.24	0.06	6.36
<b>Bst</b>	61.27	16.65	3.94	0.04	3.96	4.08	1.75	1.63	0.23	0.07	6.20
<b>BCSe</b>	61.76	16.78	3.68	0.04	4.59	3.10	1.35	1.18	0.19	0.05	6.50
<b>BstSe</b>	61.51	17.03	4.09	0.03	3.87	3.36	1.84	1.62	0.24	0.06	6.29
<b>BSe</b>	61.44	16.90	3.71	0.04	4.60	3.12	1.38	1.17	0.20	0.05	6.59
<b>BstCSe</b>	60.67	16.24	3.87	0.05	3.90	4.31	1.68	1.56	0.26	0.07	6.60
<b>Average</b>	61.00 ± 0.59	16.86 ± 0.53	3.92 ± 0.17	0.04 ± 0.01	4.17 ± 0.35	3.74 ± 0.73	1.65 ± 0.19	1.42 ± 0.21	0.24 ± 0.03	0.06 ± 0.001	6.44 ± 0.14

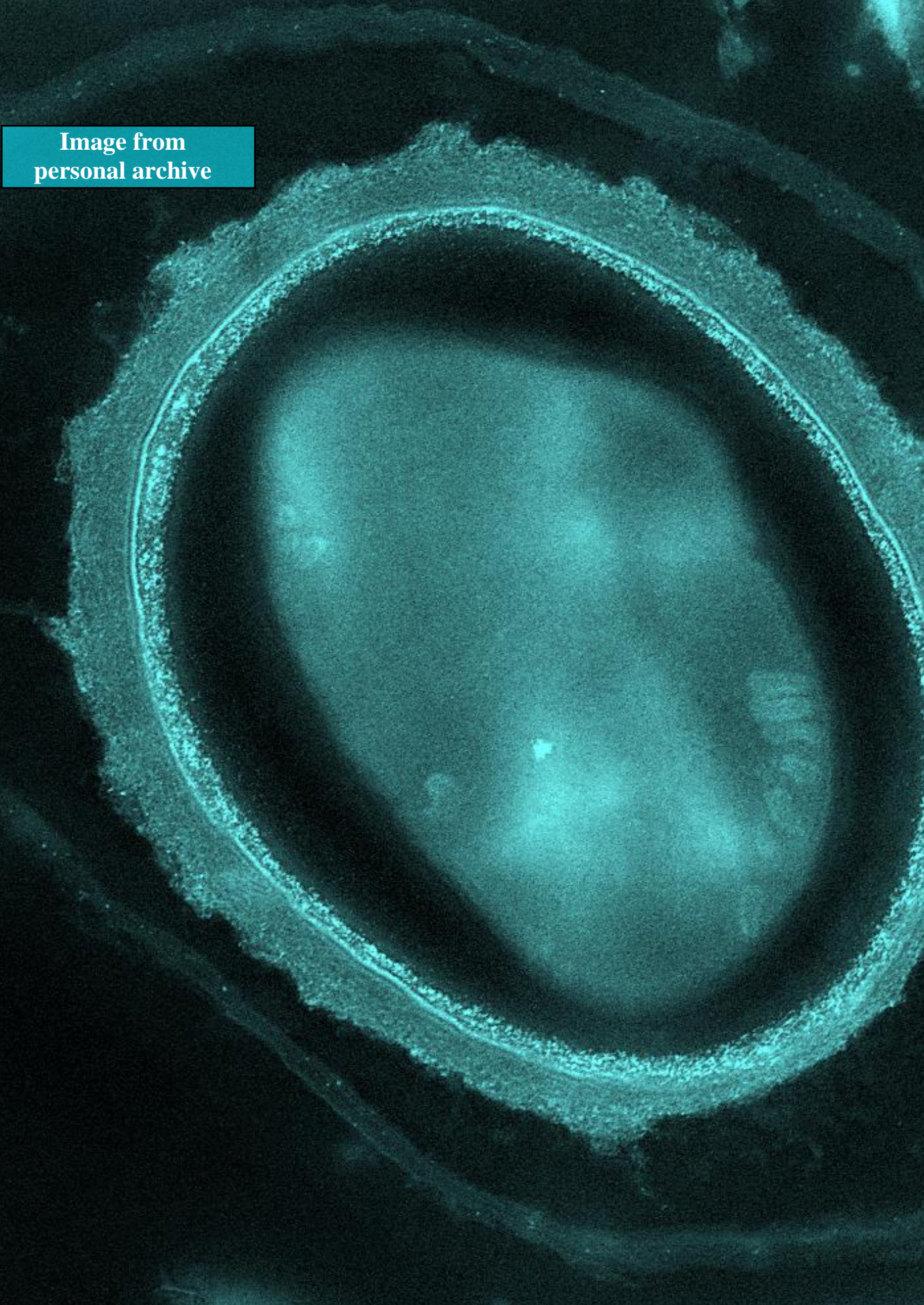


**Supplementary Figure S1.** Representation of the relative abundance of the three main viable SRB genera (*Desulfosporosinus*, *Desulfotomaculum* and *Desulfohalotomaculum*) from the MPN experiment for each treatment under study. B: natural bentonite; Bst: heat-shocked bentonite; C: bacterial consortium; Se: sodium selenite (2 mM).



**Supplementary Figure S2.** Variable pressure scanning electron microscopy (VP-FESEM) images of the control copper plate (untreated, unincubated) and the respective EDX spectra.

Image from  
personal archive





## Chapter 4

### Long-term tracking of the microbiology of uranium-amended water-saturated bentonite microcosms: A mechanistic characterization of U speciation

#### Authors

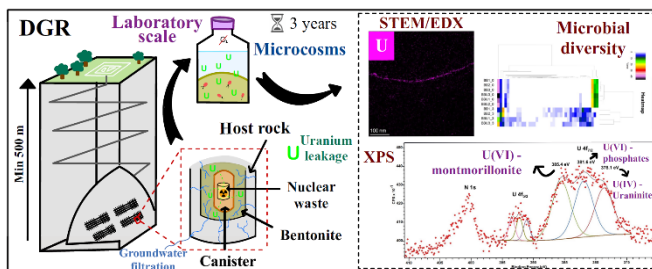
**Mar Morales-Hidalgo<sup>1,\*</sup>**, Cristina Povedano-Priego<sup>1</sup>, Marcos F. Martínez-Moreno<sup>1</sup>, Jesus J. Ojeda<sup>2</sup>, Fadwa Jroundi<sup>1</sup>, Mohamed L. Merroun<sup>1</sup>

<sup>1</sup>Faculty of Sciences, Department of Microbiology, University of Granada, Granada, Spain.

<sup>2</sup>Department of Chemical Engineering, Faculty of Science and Engineering, Swansea University, Swansea, United Kingdom

This chapter has been published in *Journal of Hazardous Materials*: <https://doi.org/10.1016/j.jhazmat.2024.135044>

IF: 12.2 / Q1 / D1



## CHAPTER 4

**Abstract**

Deep geological repositories (DGRs) stand out as one of the optimal options for managing high-level radioactive waste (HLW) such as uranium (U) in the near future. Here, we provide novel insights into microbial behavior in the DGR bentonite barrier, addressing potential worst-case scenarios such as waste leakage (e.g., U) and groundwater infiltration of electron rich donors in the bentonite. After a three-year anaerobic incubation, Illumina sequencing results revealed a bacterial diversity dominated by anaerobic and spore-forming microorganisms mainly from the phylum Firmicutes. Highly U tolerant and viable bacterial isolates from the genera *Peribacillus*, *Bacillus*, and some SRB such as *Desulfovibrio* and *Desulfosporosinus*, were enriched from U-amended bentonite. The results obtained by XPS and XRD showed that U was present as U(VI) and as U(IV) species. Regarding U(VI), we have identified biogenic U(VI) phosphates,  $U(VO_2) \cdot (PO_4)_2$ , located in the inner part of the bacterial cell membranes in addition to U(VI)-adsorbed to clays such as montmorillonite. Biogenic U(IV) species as uraninite may be produced as result of bacterial enzymatic U(VI) reduction. These findings suggest that under electron donor-rich water-saturation conditions, bentonite microbial community can control U speciation, immobilizing it, and thus enhancing future DGR safety if container rupture and waste leakage occurs.

**Keywords:** *DGR; Bentonite slurry; Uranium; Long-term incubation, Microbial diversity; Sulfate-reducing bacteria.*

## CHAPTER 4

## 1. Introduction

Nuclear energy is currently gaining global attention for the production of electricity with no greenhouse gas emissions to combat climate change (Othman, S. A. 2023). The main challenge associated with nuclear energy is the proper and safer disposal of radioactive waste. Since 1980, the United Nations have the commitment to protect future generations from the damage related to these types of residues. Over the past few decades, several approaches have been proposed to manage high-level radioactive waste (HLW). Deep geological repositories (DGRs) have emerged as the internationally preferred and safest option for the final disposal of the HLW, as a result of intensive investigation in this area that have lasted for over forty years (Tondel & Lindahl, 2019). DGR consists of a multi-barrier system composed of geological (host rock) and geo-technical barriers (metal canisters and filling/sealing materials) placed at a depth of few hundred meters (World Nuclear Association, 2021). Upon closure, the repository environment will undergo a transition process from relatively short initial oxic phase of about 100 years to stable reducing conditions due to factors such as low sub-surface oxygen, microbial metabolism, and mineral dissolution (Duro et al., 2014). Several countries such as Finland, Sweden, Switzerland, France, and Spain have selected bentonite as the most suitable backfilling and sealing material, since it serves to seal up the DGR upon saturation with groundwater (Ruiz-Fresneda et al., 2023; Hall et al., 2021). Moreover, the bentonite barrier is also very important since it could act as a radionuclide sorbent retarding, thus, their migration in case of a leakage (Kuleshova et al., 2014). As far as Spain is concerned, bentonite from “El Cortijo de Archidona” located in Almeria has been extensively studied and its use is currently being considered by the ENRESA company (Empresa Nacional de Residuos Radiactivos, S.A.) as the preferred sealing material for

## CHAPTER 4

future Spanish DGRs (Villar et al., 2006). Microorganisms are able to inhabit and influence all types of environments on Earth, including future DGRs. Several research studies have reported the high microbial diversity in bentonites including the Spanish one (Lopez-Fernandez et al. 2014, 2015, 2018; Bengtsson and Pedersen 2017; Burzan et al., 2022). This microbial diversity will include autochthonous microorganisms and those accidentally introduced during the construction of the repository. For example, anaerobic bacterial groups such as sulfate-reducing (SRB) and iron-reducing bacteria (IRB), can potentially be active under DGR conditions and cause corrosion in future metallic canisters, as well as induce changes in the mineralogy of the backfill and sealing material (Masurat et al., 2010; Povedano-Priego et al., 2021; Martinez-Moreno et al., 2023). Therefore, the study of both the diversity of microorganisms and their metabolic activity is crucial to evaluate the safety performance of HLW repositories during their lifespan (up to 100,000 years depending on the model) (Yang et al., 2019). It is well-documented that microbes can interact with heavy metals, including the most critical and principally stored radionuclides, i.e. uranium, through several mechanisms such as bioaccumulation, biosorption, biotransformation or biomineralization (Martinez-Rodriguez et al., 2023; Lopez-Fernandez et al., 2020; Ruiz-Fresneda et al., 2020; Merroun et al., 2006; Merroun & Selenska-Pobell 2008). In the case of a breakdown in the multi-barrier disposal system, uranium has the potential to migrate through rock fractures and groundwater, eventually finding its way into the biosphere. The two main oxidation states of U are U(VI), as the oxidized form, and U(IV), as the reduced one. U(VI) possess higher solubility and, therefore, higher toxicity to the microbial cells compared to U(IV) (Lakaniemi et al., 2019). Lopez-Fernandez et al., (2014) showed that, in the case of Spanish bentonite, the presence of uranium enriches U-tolerant bacterial strains from the phyla Proteobacteria,

Firmicutes, and Actinobacteria. In the same study, isolated strains such as *Arthrobacter*, *Pseudomonas*, *Sphingomonas* and *Micrococcus* tolerated a minimum of 2 mM of uranyl nitrate. It is also well-known that SRB are present in bentonites, where they may play a critical role in the biogeochemical cycle of uranium (Martinez-Moreno, et al., 2023; You et al., 2021).

Previous studies have focused on assessing the effect of uranium on the microbial community of unsaturated bentonite, reporting the enrichment of genera such as *Clostridium*, *Sulfurimonas*, *Desulfovibrio* and *Pseudomonas* (Lopez-Fernandez et al., 2018; Povedano-Priego et al., 2019; 2022). However, little is known about this uranium effect in a water-saturated environment. Therefore, we have aimed to take a few steps further in our study by simulating one of the worst scenarios that could occur in a repository: total filtration of groundwater (super-saturation), the presence of electron donors (such as sodium acetate), uranium leakage (such as uranyl acetate) and microorganism activity (by inoculation of a specific bacterial consortium). Povedano-Priego et al. (2023) studied similar conditions in their research, but in the presence of selenium. Furthermore, to the best of our knowledge, this is the first time that the impact of long-term incubation (3 years) has been studied in bentonite slurries. Therefore, we have aimed to firstly investigate alterations in the microbiology of bentonite following a 3-year exposure to uranium, with a specific focus on assessing the viability of heterotrophic microorganisms and sulfate-reducing bacteria, and secondly examine changes in the chemical speciation of uranium over the incubation time, aiming to understand the evolving dynamics influenced by the microbial communities within the bentonite.

### 2. Materials and methods

#### 2.1. Experimental set up and elaboration of the microcosms

Spanish bentonite from “El Cortijo de Archidona” (Almería, Spain) was collected at approximately 90 cm deep in sterile containers using a soil auger under aseptic conditions. Once in the laboratory, the bentonite was stored at 4 °C until further use.

The microcosms were prepared according to the detailed protocol described in Povedano-Priego et al., (2023). Briefly, bentonite was previously dried at room temperature (approximately 25 °C) and homogenized inside a laminar flow hood. Each 250 mL sterile borosilicate bottle contained 40 g of ground bentonite saturated with 170 mL of equilibrium water, which was obtained by mixing 1 g of bentonite with 100 mL of distilled water for 24 h at 180 rpm. Then, the supernatant was collected after centrifuging at 10,000 x g for 5 min and sterilized by autoclave. The major elements composition of the equilibrium water was determined by Inductively Coupled Plasma-Mass Spectroscopy (ICP-MS) with a NexION 300D spectrometer. The data is provided in **Supplementary Table S1**. The pH ( $8.51 \pm 0.15$ ), oxidation-reduction potential ( $136.5 \pm 1.06$  eV) and conductivity ( $161.63 \pm 0.49$   $\mu\text{S}/\text{cm}$ ) were also measured in triplicate using a multi-parameter probe HQd Field Case HACH. The pH values of all the treatments were also analyzed in triplicate before (T. 0) and after 3, 6, and 9 months, and 3 years of incubation following the same methodology.

To accelerate the microbial processes, the microcosms were amended with electron donors such as sodium acetate (30 mM) and glycerol-2-phosphate (G2P, 10 mM), with each microcosm reaching a final volume of 230 mL. Furthermore, G2P was added as a carbon and organic phosphate source. Microcosms corresponding to uranium treatments (U) contained a final

concentration of 1.26 mM uranyl acetate ( $C_4H_6O_6U$ ) to study its effect on bentonite microbial diversity. This low concentration of uranium has been selected to simulate the initial stages of a progressive filtration of an uranium leak from the metal canister to the bentonite barrier. A stock solution of uranyl acetate (1 M) was prepared by dissolving the correct amount of the metal salt in  $NaClO_4$  solution at 0.1 M.  $NaClO_4$  was used to prepare the uranium stock solution due to its high solubility in water contributing to the solubility of uranyl acetate in comparison to other salts. In addition, it is relatively inert, which would prevent reactions and the formation of complexes with other compounds. The stock solution was sterilized by filtration through 0.22  $\mu m$  nitrocellulose filters since uranium solution cannot be autoclaved to avoid abiotic precipitation of this heavy metal at high temperatures. Subsequently the solution was stored at 4 °C until further use.

Moreover, some microcosms were inoculated with a bacterial consortium (BB) composed of 4 genera, previously identified in other studies to belong to the bacterial community of the Spanish bentonite (Lopez-Fernandez et al., 2018, 2014; Povedano-Priego et al., 2019, 2021). The strains *Bacillus* sp. BII-C3 and *Stenotrophomonas bentonitica* BII-R7 have been isolated from the Spanish bentonite, whilst *Pseudomonas putida* ATCC33015 and *Amycolatopsis ruanii* NCIMB14711 were purchased from the culture collection ATCC (American Type Culture Collection; <https://www.lgcstandardsatcc.org/>) and NCIMB (National Collection of Industrial Food and Marine Bacteria; <https://www.ncimb.com/>), respectively. *Bacillus* sp. BII-C3, *S. bentonitica* BII-R7 and *P. putida* were incubated in lysogeny broth (LB), whilst *A. ruanni* was grown in yeast-malt-glucose (YMG) medium. After the incubation time (48 h at 28 °C and 180 rpm), the cells were harvested (at 10,000 x g for 5 min) and washed twice with sodium chloride 0.9%, and one last time with the equilibrium water. The microcosms

## CHAPTER 4

were inoculated with each strain at a final optical density of 0.4 (measured at 600 nm) (Genesys 10 S UV-Vis; Thermo scientific, MA, USA).

Relevant conditions for the future DGRs were decided for the sample incubation: anoxia, darkness, and room temperature. The anoxic atmosphere was established using an inflow of N<sub>2</sub> for 20 min through butyl-rubber stopper. Three replicates of each treatment were elaborated (a total of 6 microcosms) (**Fig. 1**). Bentonite, interface, and supernatant samples were collected before (T<sub>0</sub>) and after 3-year incubation (T<sub>3</sub>). Natural bentonite (NB) from the field without any treatment has also been studied.

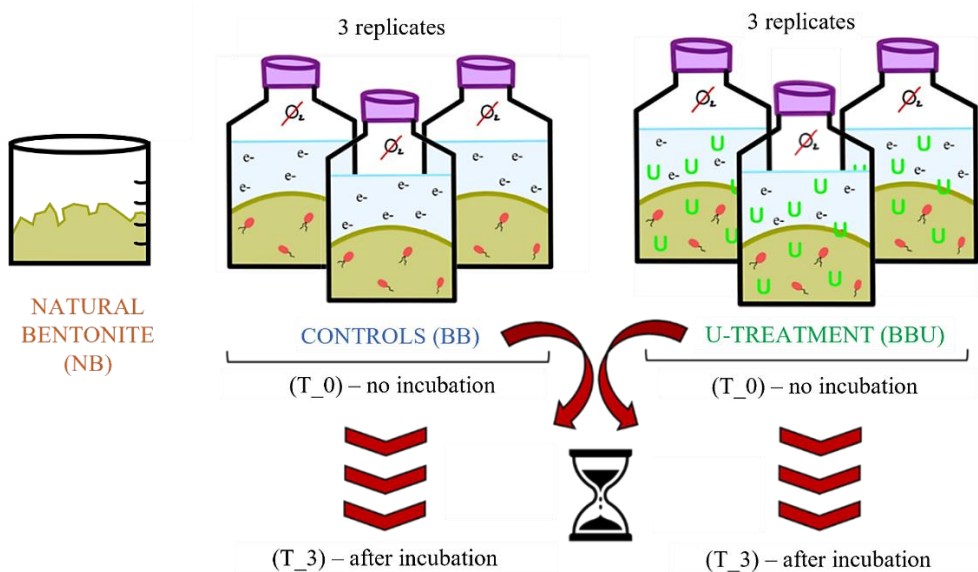


**Figure 1.** Schematic composition of the water-saturated microcosms under study (both controls and U-treated) incubated for 3 years under anaerobic conditions. NB: untreated bentonite as natural bentonite; BB: bacterial consortium; U: 1.26 mM uranyl acetate; e<sup>-</sup>: 30 mM sodium acetate and 10 mM glycerol-2-phosphate as electron donors.

## 2.2. Microbial diversity analyses

### 2.2.1. DNA extraction from bentonite samples

The microbial diversity of each treatment was studied by Next-Generation Sequencing (NGS). Firstly, DNA extractions of the bentonite microcosm

samples were performed according to the phenol-chloroform-based protocol described in detail by Povedano-Priego et al. (2021). The mechanical lysis was carried out by mixing sterile glass beads with approximately 400  $\mu\text{L}$  of bentonite slurry in 2 mL screw-tubes. 400  $\mu\text{L}$  of  $\text{NaH}_2\text{PO}_4$  solution (0.12 M, pH 8), 500  $\mu\text{L}$  of lysis buffer, and 24  $\mu\text{L}$  of freshly made lysozyme, as well as 2  $\mu\text{L}$  of proteinase K were added to perform the chemical lysis. The phenol-chloroform washing steps separate the DNA from the rest of the cellular debris. Subsequently, isopropanol and sodium acetate precipitate the DNA, which is then purified from impurities using 80% ethanol. The concentrations of the obtained DNA were measured by Qubit 3.0 Fluorometer (Life Technology, Invitrogen™).

### **2.2.2. Extracted DNA amplification and sequencing**

For the total community analysis, 16S rRNA gene libraries were constructed and sequenced by StabVida Company (Caparica, Portugal, <https://www.stabvida.com/es>). Specifically, V3-V4 variable regions of the bacterial 16S rRNA gene were amplified by PCR using the universal primers 341F (5'-CCTACGGGNGGCWGCAG-3') and 785R (5'-GACTACHVGGGTATCTAATCC-3') (Thijs et al., 2017).

Prior to amplifications, the samples were subjected to a quality control to guarantee good DNA integrity. The DNA was then purified using Sera-Mag Select kit (Cytiva) and the libraries were sequenced using MiSeq Reagent Kit v3 and 300bp paired end with the Illumina MiSeq platform.

### **2.2.3. Bioinformatics and statistical analysis**

Sequencing data were processed and analyzed using QIIME2 v2022.2 (Caporaso et al., 2010). The raw data were denoised using DADA2 plugin as

## CHAPTER 4

to remove low-quality regions, dereplicate the reads, and filter the chimeras (Callahan et al, 2016).

Alpha rarefaction curves were performed to check the quality of sequencing. After verification, the reads were grouped into OTUs and classified by taxon according to SILVA database (release 138 QIIME), with a clustering threshold of 99% similarity. Relative abundances of the taxa and alpha diversity indices were obtained using Explicet 2.10.5 (Robertson et al., 2013). A heatmap was created to represent differences between the bentonite treatments considering only genera with  $\geq 1\%$  relative abundance, by using the heatmap.2 function (gplots v. 3.0.1.1, “phyloseq”, and “RColorBrewer” package) of R v.4.2.1 software (McMurdie and Holmes, 2013; Warnes et al., 2022; Neuwirth, 2022; R Core Team, 2022). In addition, a principal coordinate analysis (PCoA) was performed using Past 4.04 (Hammer 2021) software based on the Bray-Curtis algorithm. Raw data were deposited in the Sequence Read Archive (SRA) at the National Center for Biotechnology Information (NCBI) under the Bio-Project ID number PRJNA1083466.

### **2.3. Survival of bacterial cells after incubation time**

#### **2.3.1. Heterotrophic aerobe survival and isolation of the selected strains**

After 3-years of incubation (T\_3), the heterotrophic aerobes were enumerated in triplicate using lysogeny broth (LB) agar medium at 10%. The number of viable cells was obtained as colony-forming units (CFU). For this purpose, 0.5 g of bentonite slurry with the bacterial consortium inoculated, with (T3\_BBU) and without U (T3\_BB), were re-suspended in 4.5 mL of sodium chloride 0.9% and the suspensions were stirred for 24 h at 128 rpm. Decimal dilutions were then prepared (to dilution  $10^{-5}$ ) and used to inoculate plates of 10% LB agar medium in triplicate, which were incubated for 72 h at 28 °C.

From the T3\_BBU treatment, those colonies with different morphologies and color were isolated and purified in LB 10% medium, since they may be interesting with regard to uranium tolerance. For microscopic observation, the isolates were Gram stained and examined in a LetizDialux 22 optic microscope. Genomic DNA was extracted from each colony by suspending a single pure colony in MilliQ water and heating for 10 min at 100 °C. The 16S rRNA gene of the extracted DNA was amplified using the universal bacterial primers 1492R (5'-TACGGYTACCTTGTTACGACTT-3') and 27F (5'-AAGAGTTTGATYMTGGCTCAG-3') and sequenced by bidirectional Sanger technology. The PCRs were performed using M.B.L. Recombinant Taq Polymerase kit (Material Blanco de Laboratorio, S.L., Spain) according to the manufacturer's instructions. PCR products were purified prior to sequencing using the Clean-Easy™ PCR Purification Kit (Canvax Biotech, Spain). The sequences were compiled and aligned using BioEdit. A comparative analysis was performed by matching these sequences with the ones in the GenBank database through the Basic Local Alignment Search Tool (BLAST).

### **2.3.2. Survival of SRB in Postgate medium**

The viability of SRB was also studied in the U amended sample (T3\_BBU). For this purpose, 1 g of bentonite slurry was added to 10 mL of Postgate medium (DSMZ\_Medium63, <https://www.dsmz.de>) under anaerobic conditions to promote the growth of this group of bacteria. Postgate cultures were incubated for 4 weeks at 28 °C in the dark. The presence of black precipitates after the incubation time would indicate the growth of bacteria involved in sulfate reduction. DNeasy PowerSoil Pro Kit (Qiagen, <https://www.qiagen.com/us>) was used to extract total DNA from the Postgate cultures. DNA concentration measurements were performed as mentioned before.

## CHAPTER 4

The amplification, sequencing and analysis of the extracted DNA were carried out as previously mentioned for the total community (sections: 2.2.2 and 2.2.3).

### **2.4. Microscopic and spectroscopic characterization of the uranium-treated microcosm**

High-resolution transmission electron microscope with high-angle annular dark-field (HAADF) imaging (Thermo Fisher Scientific TALOS F200X and FEI TITAN G2) coupled to energy dispersive X-ray spectroscopy (EDX) microanalysis was used to identify and characterize uranium accumulates after 3 months and 3 years of incubation. The acceleration voltage used to carry out the analysis was 200 kV. The intermediate layer formed between bentonite and supernatant was collected and prepared following the procedure used in Povedano-Priego et al. (2023). Selected area electron diffraction (SAED) and HRTEM combined with Fast Fourier Transform (FFT) were used to determine the crystalline nature of uranium precipitates.

Subsequently, the amended bentonite before ageing and the 3-year BBU microcosm were analyzed by X-ray photoelectron spectroscopy (XPS) to search for evidence of uranium phosphates. The interface between the bentonite and the supernatant of the BBU microcosm was sampled, dried, and pulverized. XPS measurements of this interface powder were conducted by Kratos AXIS Supra Photoelectron Spectrometer with a double anode X-ray source (Mg/Al) (Power 450 W). The source was monochromated Al K $\alpha$  (power 600W). High-resolution measurements of U 4f, P 2p, C 1s, O 1s, N 1s, Fe 2p and S 2p were performed, and deconvolution of the U 4f signal was performed (70% Gaussian / 30% Lorentzian line shape) to investigate potential element speciation. The software CasaXPS 2.3.22 (Fairley, N, 2021) was used for the correction of the peaks in XPS spectra.

X-ray diffraction (XRD) was used to characterize the U solid phases which could be precipitated as result of the microbial activity within bentonite microcosms amended with this heavy metal. Powder XRD patterns of non-incubated and incubated U-treated bentonites were recorded using a Bruker D8 Advanced diffractometer with Cu-K $\alpha$  radiation linked to a LINXEYE detector available at “Centro de Instrumentation Científica”, University of Granada. The obtained diffractograms were analysed using the software High Score+ and PDF2 database.

### 3. Results

#### 3.1. Microbial diversity analyses: richness and distribution of the bacterial communities

The total DNA was extracted and sequenced in triplicate for all the treatments, including natural raw bentonite (NB). Two replicates, namely T3\_BB3 and T3\_BBU2, were excluded from the analysis due to their remarkable differences to the other replicates. Up to 390,112 sequences of 16S rRNA gene were gathered in 538 OTUs. Values of Good’s coverage ( $> 0.99\%$  in all cases) indicated that the sequencing depth was enough to totally cover all the bacterial community (**Table 1**). The obtained OTUs were allocated in 30 phyla and 406 genera belonging to Bacteria and Archaea. Only Halobacterota (2.21% of OTUs) and Thermoplasmatota (0.03% of OTUs) represented the Archaea whilst the other 28 phyla were Bacteria. The most abundant bacterial phyla consisted of Proteobacteria (40.23%), Firmicutes (27.33%), Actinobacteriota (15.09%) and Chloroflexi (5.78%). The richness index (Sobs), diversity indices (ShannonH, and SimpsonD), and Shannon’s evenness showed higher values in NB. However, the same indexes were lower at T0\_BB and T0\_BBU, indicating lower diversity and uniformity. On the other hand, higher alpha diversity was observed after 3

years, which also indicated higher diversity and uniformity at this time. All these data are shown in **Table 1**.

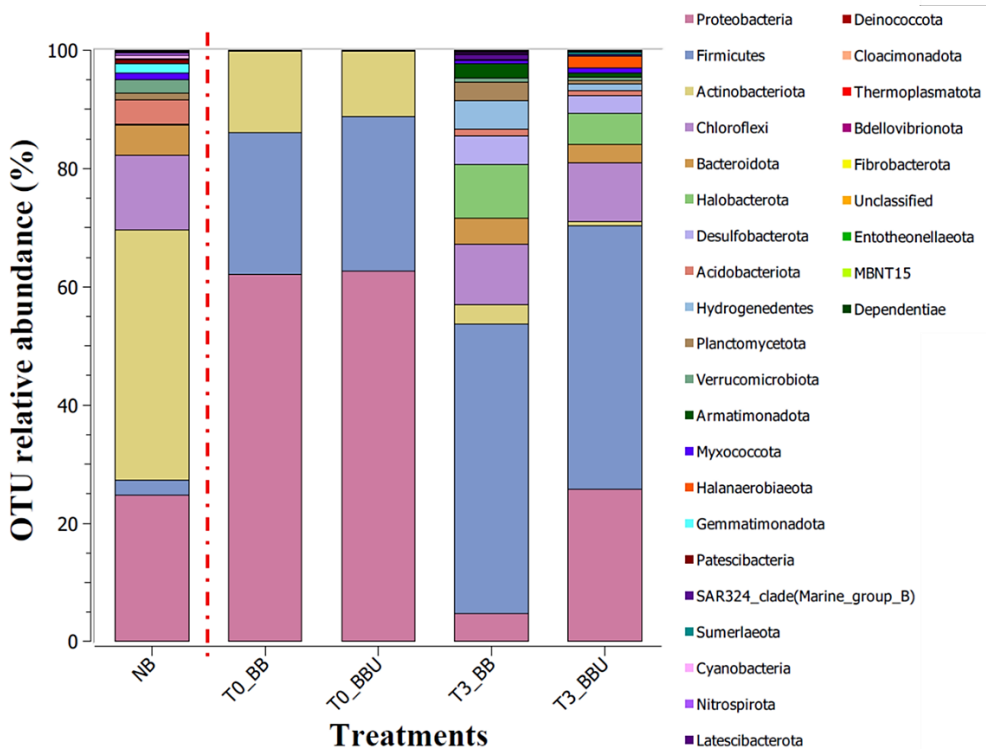
**Table 1.** Richness (Sobs), diversity (ShannonH and SimpsonD), and evenness (ShannonE) indices and Good's coverage values of the bacterial communities of the different treatments. NB: raw natural bentonite; BB: bentonite inoculated with bacterial consortium; U: uranyl acetate 1.26 mM; T0: time 0; T3: three years of incubation.

Sample	Sobs	ShannonH	ShannonE	SimpsonD	Good's coverage
NB	437.99	6.80	0.78	0.98	0.999
T0_BB	57.30	2.47	0.42	0.76	0.999
T0_BBU	48.50	2.65	0.47	0.76	0.999
T3_BB	112.00	4.65	0.68	0.92	1.000
T3_BBU	132.34	4.92	0.69	0.93	0.999

### 3.2. Effect of incubation time and uranium on the bentonite microbial diversity

At phylum level, the relative abundances changed depending upon the incubation time (**Fig. 2**). At time 0, in both treatments T0\_BB (62.16%) and T0\_BBU (62.64%), Proteobacteria was the most abundant phylum, mainly represented by two of the four bacterial consortium strains, *Pseudomonas* and *Stenotrophomonas* (**Fig. 3, Supplementary Table S2**). In the NB sample, Proteobacteria was also present at a relative abundance of 24.79%. The other two most abundant phyla, Firmicutes [T0\_BB (23.90%); T0\_BBU (26.17%)] and Actinobacteriota [T0\_BB (13.81%); T0\_BBU (11.10%)] also mainly corresponded to the genera of the consortium *Bacillus* and *Amycolatopsis*, respectively. After the 3-year incubation, the relative abundances of Firmicutes were higher in T3\_BB (48.94%), and T3\_BBU (44.64%) compared to time 0 samples [T0\_BB (23.90%), and T0\_BBU (26.17%)].

Many Firmicutes are spore-formers, which allow them to survive in extreme environments for prolonged periods of time. However, Actinobacteriota decreased during the incubation period as most of them are aerobic. The incubation period also revealed phyla of interest to DGR such as Desulfobacterota, which includes most of the bacteria involved in the reduction of sulfate to sulfide. In the NB sample, its relative abundance was only 0.24%, and < 0.001% at time 0. Its enrichment was probably enhanced by the anaerobic conditions resulting in higher values of relative abundances [T3\_BB (4.78%), T3\_BBU (2.99%)]. Similarly, the two exclusive phyla within the Archaea domain, Halobacterota (T3\_BB (9.15%), and T3\_BBU (5.25%)) and Thermoplasmatota (T3\_BB (0.11%), T3\_BBU (0.07%)) were slightly enriched in the 3-year incubated samples in comparison to T0 samples, where they were not detected.



## CHAPTER 4

**Figure 2.** Relative abundances of phyla belonging to Archaea and Bacteria in the raw natural bentonite and the treated water-saturated microcosms. Stacked bars represent the mean values of biological triplicates (except T3\_BB and T3\_BBU in duplicate). NB: raw natural bentonite; BB: bentonite inoculated with bacterial consortium; BBU: bentonite inoculated with bacterial consortium and treated with uranyl acetate; U: uranyl acetate 1.26 mM; T0: time 0; T3: three-year anoxic incubation.

The presence of uranium decreased the relative abundance of most phyla after the 3-year incubation, except for Firmicutes, Halanaerobiaeota, Sumerlaeota and Myxococcota, which increased to 20.93%, 2.09%, 0.32%, and 0.29%, respectively (**Fig. 2, Supplementary Table S2**). At genus level (**Fig. 3**), in the natural bentonite, as expected, the four strains of the consortium (*Pseudomonas*, *Stenotrophomonas*, *Amycolatopsis*, and *Bacillus*) were detected at very low relative abundances (0.16%, 0.01%, 1.35% and 1.15%, respectively). At time 0, these genera displaced the remaining microbial diversity in both treatments, T0\_BB and T0\_BBU, dominating the total community with relative abundances of 89.42% and 84.68%, respectively.

The abundances of these genera decreased over time, and the overall community became more heterogeneous, as indicated by the previously mentioned alpha diversity data (**Table 1**) and the relative abundances after 3-year incubation (**Supplementary Data S1**). This decrease in dominance by the bacterial consortium, along with the incubation conditions, allowed the detection of other genera such as *Pelosinus* (T3\_BB 22.91%, T3\_BBU 6%), *Clostridium\_sensu\_stricto\_13* (T3\_BB 7.91%, T3\_BBU 5.40%), *Methanosacina* (T3\_BB 7.36%, T3\_BBU 4.63%), *Fonticella* (T3\_BB 2.61%, T3\_BBU 5.73%), unclassified Anaerolineaceae (T3\_BB 5.31%, T3\_BBU 5.37%), Peptostreptococcaceae (T3\_BB 3.62%, T3\_BBU 5.04%), *Anaerolinea* (T3\_BB 4.43%, T3\_BBU 4.28%), and *Lentimicrobium* (T3\_BB 3.66%, T3\_BBU 2.92%), among others. Concerning the bacteria involved in

sulfate reduction (SRB), genera such as *Desulfovibrio* (T3\_BB 2.95%, T3\_BBU 0.97%), *Desulfosporosinus* (T3\_BB 0.81%, T3\_BBU 1.55%) and *Desulfobulbus* (T3\_BBU 1.65%) were also detected. Furthermore, apart from the previously mentioned *Methanosarcina*, other sequences affiliated with archaeal genera such as *Methanoculleus*, *Methanocella* and *Methanomassiliicoccus* were detected in low percentages of abundance (< 0.08%) (Supplementary Data S1).

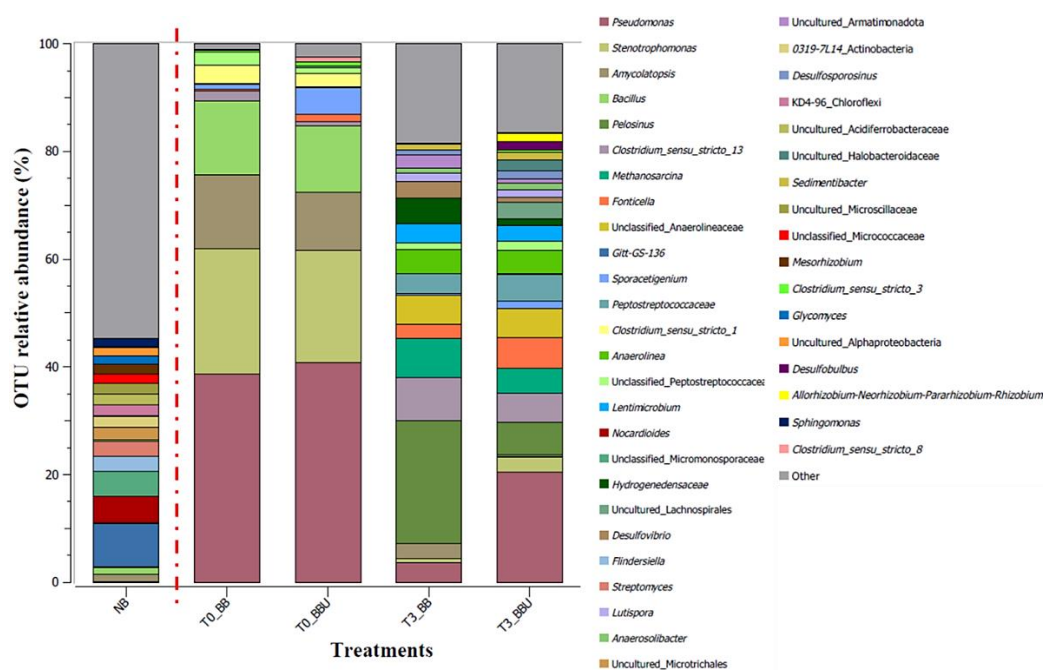


**Figure 3.** Relative abundances at genus level of the microbial communities in raw natural bentonite and the water-saturated microcosms. Cut off: 0.3% of relative abundance. Stacked bars represent the mean values of biological triplicates (except T3\_BB and T3\_BBU in duplicate). NB: raw natural bentonite; BB: bentonite inoculated with bacterial consortium; BBU: bentonite inoculated with bacterial consortium and treated with uranyl acetate; U: uranyl acetate 1.26 mM; T0: time 0; T3: three-year anoxic incubation.

The influence of U toxicity on the microbial community within the bentonite slurry microcosms was remarkable. The relative abundance of certain genera decreased in the presence of uranium. This was the case, mainly, for *Pelosinus* ( $\Delta$  -16.91%), *Hydrogenedensaceae* ( $\Delta$  -3.62%), the archaea

## CHAPTER 4

*Methanosarcina* ( $\Delta$  -3.06%), *Amycolatopsis* ( $\Delta$  -2.57%), and the sulfate-reducing bacterium *Desulfovibrio* ( $\Delta$  -1.98%). However, it is worth noting that another part of the community was enriched in the presence of this radionuclide. For instance, *Pseudomonas* ( $\Delta$  16.83%), *Fonticella* ( $\Delta$  3.12%), uncultured Lachnospirales ( $\Delta$  3.05%), *Stenotrophomonas* ( $\Delta$  2.03%), Peptostreptococcaceae ( $\Delta$  1.42%) and *Sporacetigenium* ( $\Delta$  0.91%) increased their relative abundance in the T3\_BBU treatment. The SRB *Desulfobulbus* ( $\Delta$  1.65%) and *Desulfosporosinus* ( $\Delta$  0.74%) also increased in the presence of U.

The differences between the treatments have also been studied by the principal coordinate analysis (PCoA), considering only the BB and BBU samples. Based on the Bray-Curtis distance, PCoA analysis of relative abundance at genus level grouped the microcosms into three different clusters (**Fig. 4**). All the samples corresponding to time 0 (T0\_BB and T0\_BBU) were clustered into a single group and there were no differences between U-treated and control samples. However, after a three-year anaerobic incubation, the uranium treatment was separated from the controls. These results agreed with those obtained by the heatmap (**Fig. 5**), establishing a clear difference between the bacterial diversity of Time 0 samples and Time 3 years, as well as between 3-year samples with and without uranium.

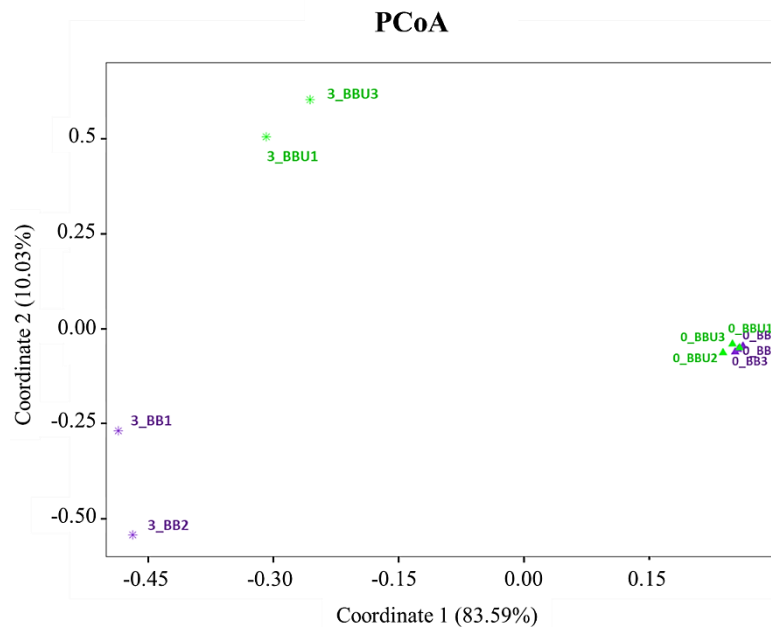


**Figure 4.** Principal coordinate analysis (PCoA) comparing the microbial community structure of the different microcosms in triplicate (except T3\_BB and T3\_BBU in duplicate). The distance is based on Bray-Curtis algorithm. Triangle (▲): Time 0; Star (\*): Time 3 years; purple color: controls without metal; green color: U-treatments. Samples studied in triplicates except T3\_BB and T3\_BBU in duplicate. BB: bentonite inoculated with bacterial consortium; BBU: bentonite inoculated with bacterial consortium and uranyl acetate; U: uranyl acetate 1.26 mM; 0: time 0; T3:3 -year incubation.

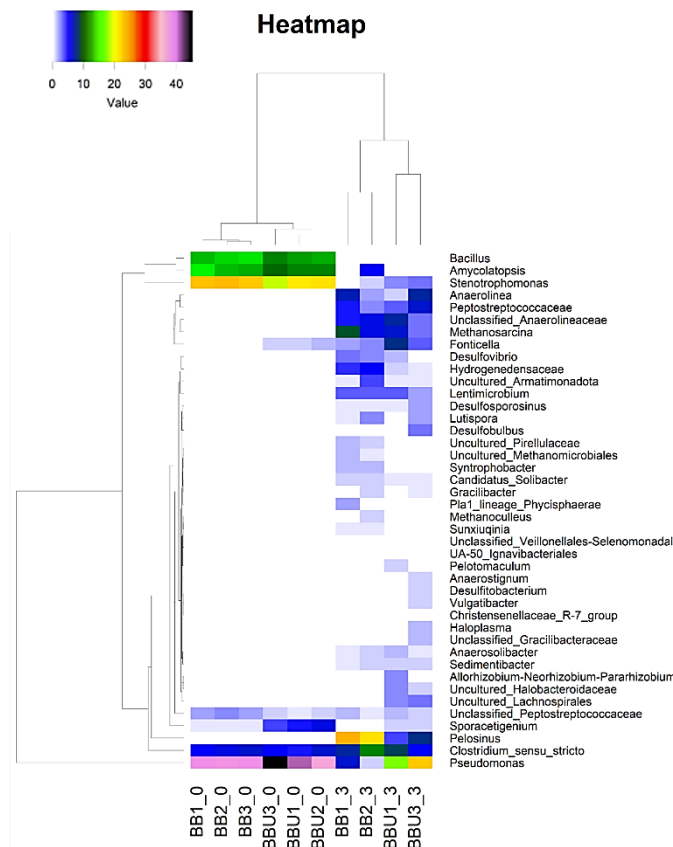


**Figure 5.** Heatmap of relative abundances and microbial distribution of the samples based on Manhattan distance. Cut off: 1%. Colors represent the varying levels of relative abundance for each genus. Samples studied in triplicates except T3\_BB and T3\_BBU in duplicate. BB: bentonite inoculated with bacterial consortium; BBU: bentonite inoculated with bacterial consortium and uranyl acetate; U: uranyl acetate 1.26 mM; 0: time 0; 3: 3-year incubation.

### 3.3. Survival of bacterial strains after 3-year of incubation

In this study, the long-term survival of aerobic heterotrophs was investigated by determining colony forming units (CFU) in 10% LB culture medium, which was used to promote an oligotrophic environment. After 72 h of aerobic incubation, growth was observed in both treatments (T3\_BB, T3\_BBU). The viable heterotrophs counted in T3\_BB were  $(3 \pm 0.56) \times 10^4$  CFU/g, lower than that of the U amended sample  $((2.37 \pm 0.64) \times 10^5$  CFU/g).

The U-amended bentonite was selected to isolate strains that initially would have tolerated the presence of the radionuclide. A total of 5 strains were isolated from the 3-year U-amended bentonite sample (**Table 2**). Three out of 5 strains belonged to the genus *Peribacillus* (*P. frigoritolerans* WS2-1 16S, *P. frigoritolerans* LZRD gt2, and *Peribacillus* sp. Sed8c), another to *Bacillus* (*B. korensis* IHBB 9908), and the last one to *Robertmurraya* (*Robertmurraya* sp. TRM82488).

**Table 2.** Affiliation of the 16S rRNA of T3\_BBU microbial isolates. BLAST revealed the closest phylogenetic relative strain, along with its similarity percentage and accession number.

Phylum	Isolate	Closest phylogenetic relative	Accession no., similarity (%)
Bacillota	BBU_1	<i>Peribacillus frigoritolerans</i> WS2-1 16S	MT605504.1, 98.39
Bacillota	BBU_2	<i>Peribacillus</i> sp. Sed8c	OR512255.1, 99.87
Bacillota	BBU_3	<i>Peribacillus frigoritolerans</i> LZRD gt2	OR079438.1, 100
Firmicutes	BBU_4	<i>Bacillus korensis</i> IHBB 9908	KR085887.1, 99.42
Firmicutes	BBU_5	<i>Robertmurraya</i> sp. TRM82488	OR434954.1, 100

As mentioned above, the study of the sulfate-reducing bacteria is of great interest for the DGR safety assessment as they could be involved in the

corrosion of the metal canisters where nuclear waste will be stored. SRB were enriched by the inoculation of U-amended bentonite sample (T3\_BBU) in the Postgate medium. After 30 days of anaerobic incubation at 28 °C, a black precipitate was observed which probably indicated the reduction of sulfate by SRB and formation of sulfides. Total DNA from this enrichment was extracted and the results showed that not only SRB were enriched (**Fig. 6; Supplementary Data S2**) since, a total of 116 OTUs were detected in this sample.

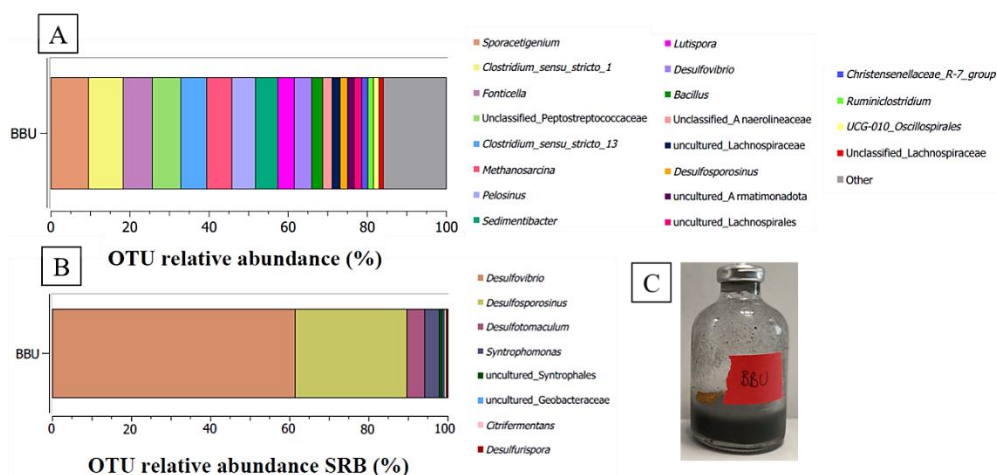


**Figure 6.** **A.** OTU relative abundances at genus level of the T3\_BBU microbial communities enriched in Postgate medium. Cut off: 1% of relative abundance. Stacked bars represent the mean values of biological triplicates. **B.** OTU relative abundances at genus level of the main SRB communities enriched in Postgate medium. **C.** Postgate medium inoculated with T3\_BBU bentonite after 30-day anaerobic incubation at 28 °C.

Genera such as *Sporacetigenium*, *Clostridium*, *Fonticella*, *unclassified\_Peptostreptococcaceae*, *Pelosinus* and *Sedimentibacter* were the most abundant in agreement with the results of microbial diversity studies detailed above. Most of the identified strains are strict anaerobes, spore formers and capable of consuming some components present in the Postgate medium such as phosphate or lactate (Detman et al., 2019; Bahl et al., 1982; Brockman & Wood, 1975; Mosher et al., 2012). On the other hand,

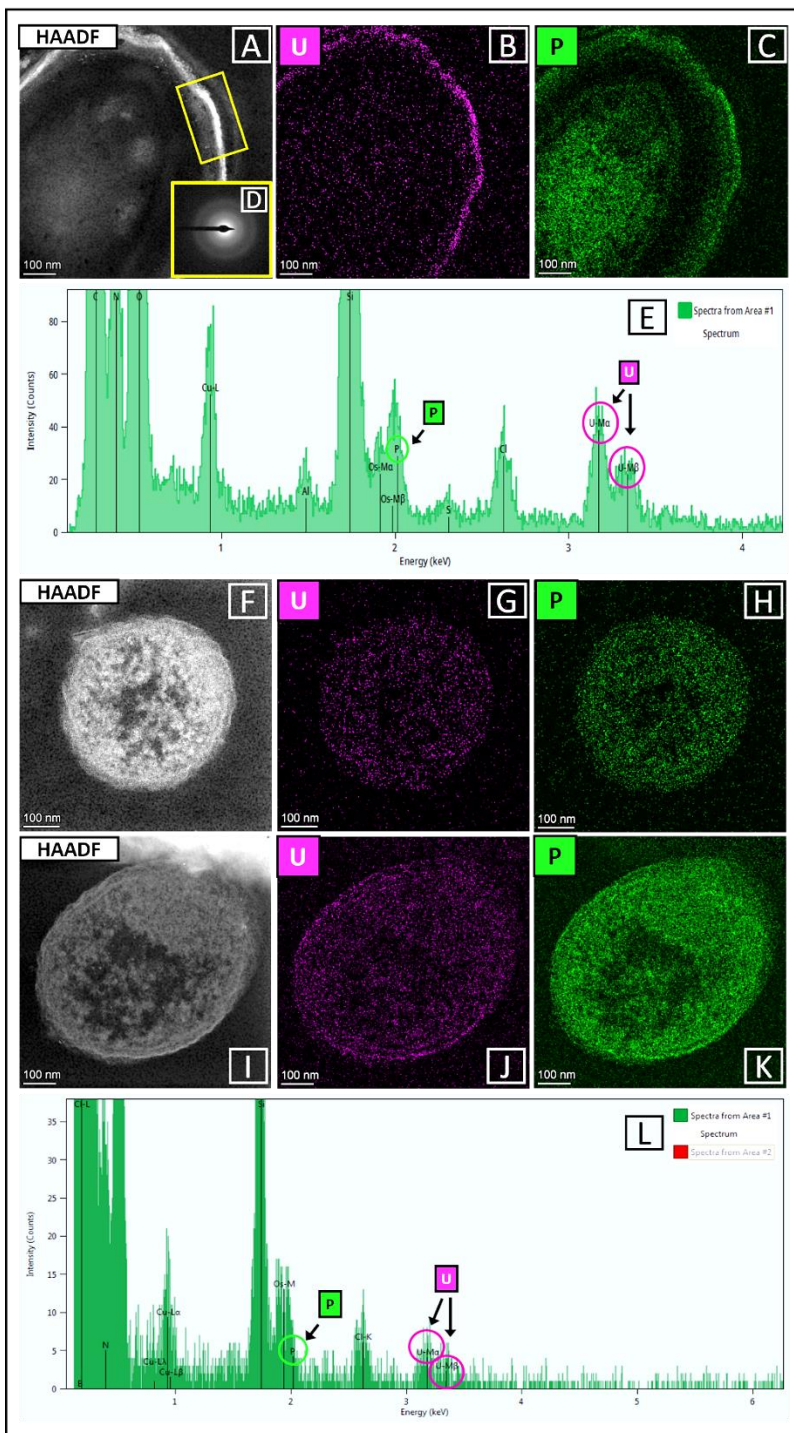
considering only the genera belonging to the SRB group, *Desulfovibrio*, and *Desulfosporosinus* were the most abundant with a relative abundance of 4.29% and 1.97%, respectively. Other genera such as *Desulfotomaculum*, *Syntrophomonas*, and *Desulfurispora* were also detected in low relative abundances (< 0.33%). All these SRB would be responsible for using the sulfate in the medium and precipitating visible black sulfides (**Fig. 6 C**).

### **3.4. Microscopic (STEM-HAADF) cellular localization of the uranium accumulates over incubation time**

After 3 months and 3 years of incubation, high-resolution transmission electron microscopy, coupled with energy dispersive X-ray spectroscopy (EDX), was used to study the cellular location of U accumulates and their chemical properties in the BBU sample. At both incubation times, the bentonite of the microcosm corresponding to the BBU treatment presented a grayish color compared to time 0 (**Supplementary Fig. S1**). The intermediate layer formed between bentonite and supernatant was collected and microscopically analyzed.

After 3 months of incubation, STEM-HAADF micrographs showed electron-dense accumulates at the cell wall level (**Fig. 7 A**). The EDX spectra and maps analyses revealed U and P as elemental composition of U accumulates (**Fig. 7 B, C, E**). Selected area electron diffraction (SAED) and HRTEM combined with Fast Fourier Transform (FFT) were used to determine the crystalline nature of these precipitates. These parameters showed no signal, which implies an amorphous nature (**Fig. 7 D**). Moreover, the cytoplasm of certain cells exhibited the presence of U signal. (**Fig. 7 G, J, L**). The identified uranium also aligned with the P signal as shown in **Figure 7 H, K, L**.

3 MONTHS



## CHAPTER 4

**Figure 7.** Scanning transmission electron microscopy-high-angle annular dark-field imaging (STEM-HAADF) image of BBU microcosm after 3-month incubation (A, F, I). The EDX maps with the elemental distribution of U in pink color, and P in green color (B, C, G, H, J, K) and their corresponding EDX spectra (E, L). The SAED pattern of selected area in A corresponds to the amorphous form of U-phosphates (D).

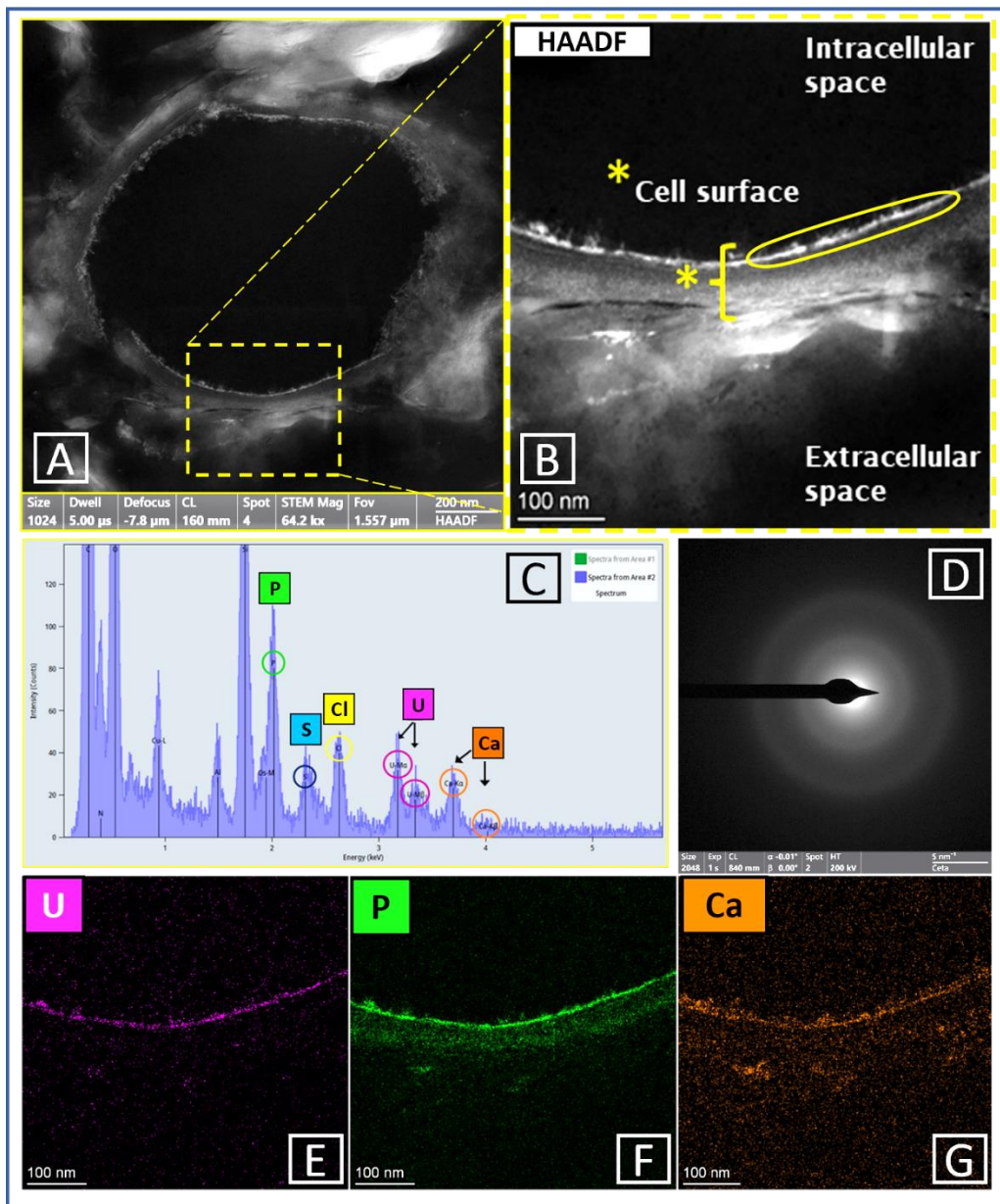
On the other hand, after 3 years of anoxic incubation, the U signal was not found in the extracellular space either. It was noteworthy that the abundance of bacterial cells was minimal, and the predominant ones displayed a morphology characteristic of bacterial spores (**Supplementary Fig. S2**). Additionally, most of the cells exhibited damaged cell walls (**Fig. 8**). At 3-year incubation time, U was only localized in the inner part of the cell wall area (**Fig. 8 A, B**). The EDX analyses confirmed the presence of both U and P signals, which is consistent with the observations made on the 3-month sample but with Ca also present (**Fig. 8 C, E, F, G**). These electron-dense zones were analyzed with SAED and FFT indicating amorphous nature of the accumulates (**Fig 8 D**).

### **3.5. X-ray photoelectron spectroscopy and X-ray diffraction: Characterization of uranium species in U-bentonite microcosm**

XPS analysis was undertaken to assess the presence of U in the samples before and after the 3-year incubation time. XPS peaks corresponding to U 4f were weak and with a high signal-to-noise ratio given the low concentration expected in the bentonite samples; however, their presence was still evident. A peak around 378.5 eV was attributed to the presence of potassium from the natural bentonite (K 2s), which makes the deconvolution and analysis of U 4f peaks more difficult. At T\_0, the high resolution XPS spectra showed a U 4f<sub>7/2</sub> at 385.4 eV, which has previously been assigned as U(VI) sorbed on montmorillonite (Drot et. al, 2007). After the 3-year incubation, an additional peak was observed at 381.6 eV, which has previously been reported as U(VO<sub>2</sub>)·(PO<sub>4</sub>)<sub>2</sub> (Dacheux et. al, 1996). The peak assigned to U(VO<sub>2</sub>)·(PO<sub>4</sub>)<sub>2</sub>

in the aged sample (T3\_BBU treatment) was absent in the T\_0 (see **Figure 9**).

### 3 YEARS



## CHAPTER 4

**Figure 8.** Scanning transmission microscopy-high-angle annular dark-field imaging (STEM-HAADF) image of BBU microcosm after 3-year incubation (A). Expanded image of A (B). The EDX maps with the elemental distribution of U in pink color, P in green color and Ca in orange color (E, F, G) and the corresponding EDX spectrum (C). The SAED pattern of selected area in B corresponds to the amorphous form of U-phosphates (D).

XPS signals usually attributed to U(IV) species as uraninite have been previously reported at 378.1 eV (Howng & Thorn, 1979). However, in the high-resolution scans shown in **Figure 9**, this signal also coincides with the peak of K 2s. Therefore, the confirmation of uraninite via XPS is less reliable. In order to validate the above observations, and given the difficulty of analyzing the U 4f peak due to its weak intensity and interference with the K 2s signal, the samples were also examined using X-ray diffractometry.

The XRD pattern of the untreated bentonite was similar to that of natural Spanish bentonite reported by Povedano-Priego et al. (2019). The bentonite consisted of at least 91% of smectite and accessory minerals in minor amounts (quartz, plagioclases, micas, cristobalite). No U mineral phases were detected. The XRD patterns obtained for the 3-year U-treated bentonite microcosms showed the main peaks characteristic of Spanish bentonite corresponding to major mineral phases like smectite and to minor phases (e.g. quartz), and calcite as well. In addition, the XRD diffractogram (**Supplementary Figure S3**) showed also the presence of a peak at  $9.88^\circ 2\theta$ , and small peaks at  $10.2$ - $9.60^\circ 2\theta$ , corresponding to uranium phosphate minerals of the autunite or meta-autunite group, including autunite (Ca), sodium autunite (Na) and saleeite (Mg). Other two small peaks at  $27.73$  (as a shoulder on the plagioclase peak at  $27.90$ ) and  $31.13^\circ 2\theta$  might correspond to uraninite ( $\text{UO}_2$ ).

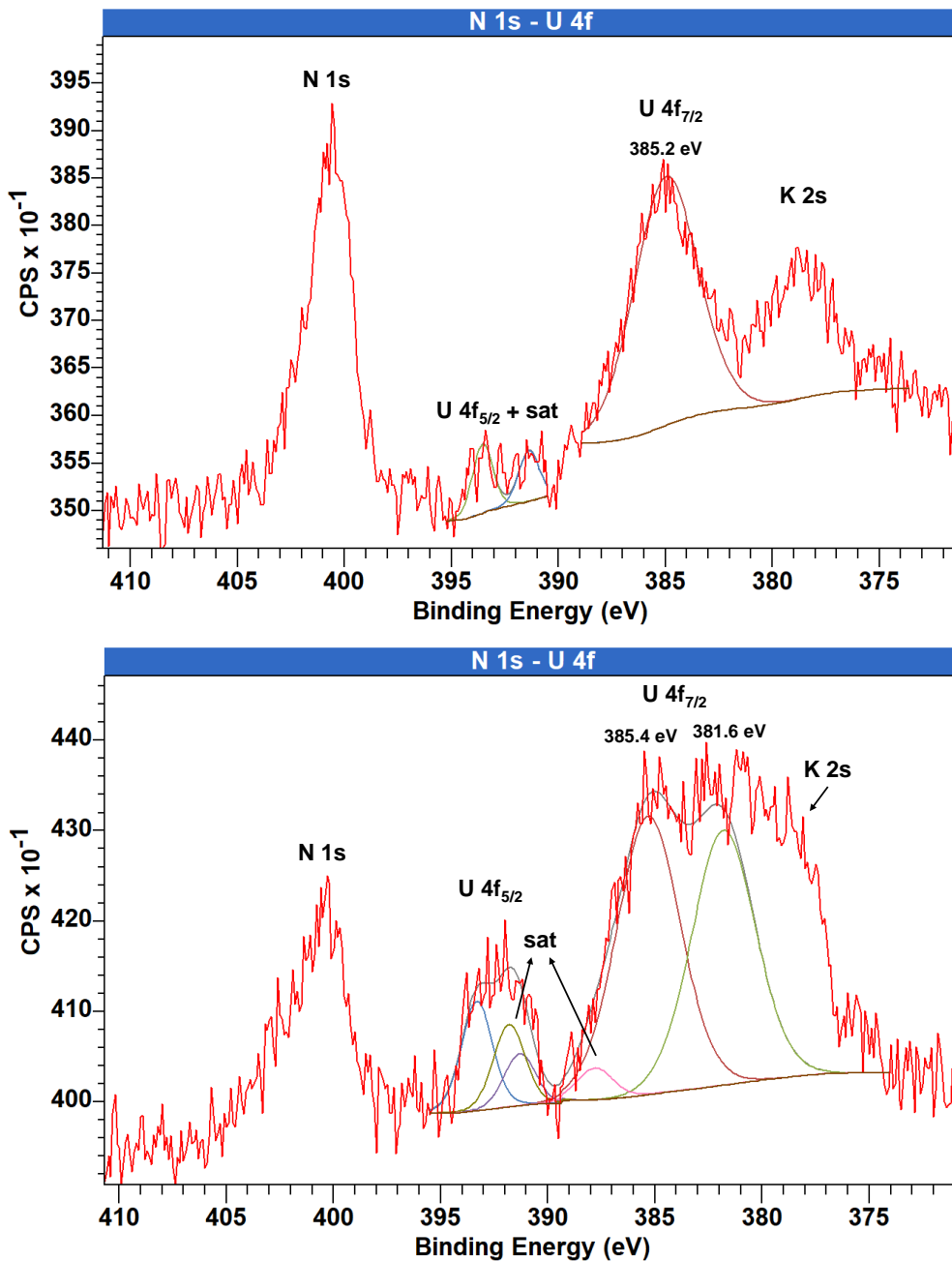


**Figure 9.** High resolution X-ray photoelectron spectra of the U 4f region for samples before (top) and after the 3-year incubation time (bottom).

### **3.6. pH analysis of microcosm supernatants over incubation time**

At time 0, 3, 6 and 9 months, and 3 years, supernatant samples were collected from the three replicates of each treatment (BB and BBU) to measure the pH. At the beginning of incubation, both microcosms had neutral pH values (around 7.4). During the first months of incubation (3, 6 and 9), the pH of both treatments increased until reaching basic values of 8.72 for BB and 8.86 for BBU (**Supplementary Table S3**). The pH evolution over time was similar in both cases, indicating that there were no notable differences between the treatment values. After the 3-year incubation, the pH value for each treatment was around 8.

## **4. Discussion**

### **4.1. Influence of incubation time and uranium on bentonite microbial diversity**

To accelerate the microbial processes that would occur in the bentonite barrier, the microcosms were amended with electron donors and inoculated with a bacterial consortium (BB) which is composed of 4 genera previously identified in bentonite (Lopez-Fernandez et al., 2018, 2014; Povedano-Priego et al., 2019, 2021). In addition, the experimental conditions of this study would simulate the scenario of filtration of groundwater loaded with organic compounds within the bentonite body during the disposal period (Marin, 2012).

Throughout the incubation time many changes were observed to occur between the time 0 (T0\_BB, T0\_BBU) and the 3-year (T3\_BB, T3\_BBU) microcosms. The bacterial diversity increased considerably after 3 years of incubation, compared to time 0 where the four strains of the consortium almost completely dominated the community. The long-term incubation of the samples allowed the community to shift completely, leading to the

enrichment of anaerobic and spore-forming bacteria. The microbial communities were dominated by representatives of the phylum Firmicutes, which includes most genera capable of forming endospores in adverse conditions (Filippidou et al., 2015). HRTEM microscopy images corroborated the presence of bacterial spores, as shown in **Supplementary Fig. S2**. Another phylum that stood out was Chloroflexi that includes most anaerobic genera (e.g. *Anaerolinea*) (Petriglieri et al., 2018), whilst the phylum Actinobacteriota, dominant in both NB and at time 0 microcosms (T0\_BB, T0\_BBU), decreased drastically, probably because the majority of bacteria belonging to this phylum are aerobic (Barka et al., 2016). The experimental anoxic conditions also favored the presence of anaerobic genera, such as the archaea *Methanosarcina* and the sulfate-reducing group of bacteria such as *Desulfovibrio*, *Desulfosporosinus* and *Desulfobulbus*. These findings align with the expected scenario in future DGRs, where upon the repository closure, oxic conditions will initially be contemplated. As time progresses a transition towards reducing conditions is foreseen, marked by the prevalence of anaerobic bacterial communities (Duro et al., 2014). The comparison of the microbial population incubated for 3 years showed that the presence of uranium seemed to differentially affect the relative abundance of some taxon in the bentonite. However, the most affected genera are playing a key role in the biogeochemical cycle of this radionuclide through different processes such as U phosphate biomineralization, enzymatic U(VI) reduction to uraninite ( $U(IV)O_2$ ), and biosorption, amongst others (Ruiz-Fresneda et al, 2023; Pinel-Cabello et al. 2021; Lopez-Fernandez et al, 2021; Povedano-Priego et al., 2019). These results could be supported by a combination of XPS, XRD, STEM and EDX data, indicating that the U speciation is likely to be governed by U(VI) and U(IV) as phosphate mineral phases of the autunite or meta-autunite groups and uraninite, respectively.

## CHAPTER 4

In our study, some strains of notable importance in interactions with uranium, such as *Pseudomonas* and *Stenotrophomonas*, were enriched in the treatment with this radionuclide (T3\_BBU). Several studies have demonstrated the ability of *Pseudomonas* to immobilize U through different processes including biosorption, biomineralization, and bioreduction (Zheng et al., 2022; Yu et al., 2022). Therefore, its presence and predominance under these conditions was not unexpected, since it is demonstrated to be a naturally occurring bacterium in uranium mines and it was also detected in uranium-treated bentonites incubated for six months under anoxic conditions (Choudhary & Sar, 2011; Chabalala & Chirwa, 2010; Povedano-Priego et al., 2022). Regarding *Stenotrophomonas*, this bacterium has also been previously studied for its ability to interact and resist U(VI) (Pinel-Cabello et al., 2021; Sanchez-Castro et al., 2020, 2021). Like *Pseudomonas*, this genus, specifically the species *S. bentonitica*, is one of the strains of the consortium added to the bentonite microcosms as it was previously isolated and characterized from Spanish bentonite samples (Sanchez-Castro et al., 2017). Two additional genera, namely *Fonticella* and *Sporacetigenium*, exhibited an increase in their relative abundance in the U-treatment. So far, no information exists explicitly linking these two strains to metal resistance, but the ability to withstand harsh environments may explain their presence under such DGR relevant conditions (Fraj et al., 2013; Gilmour et al., 2021; Engel et al., 2023).

On the other hand, the presence of uranium seemed to decrease the relative abundance of other microbes including *Pelosinus*, *Hydrogenedensaceae*, *Methanosarcina*, *Amycolatopsis* and *Desulfovibrio* that have the capacity to immobilize uranium (Newsome et al., 2015; Holmes et al., 2018; Povedano-Priego et al., 2019; Sani et al., 2006). However, despite of this decrease in relative abundance, the presence of these genera in the U amended samples

would affect the U biogeochemistry. For instance, even if the relative abundance of *Desulfovibrio* and *Methanosarcina* was decreased, they may still exhibit the ability to reduce U(VI) to U(IV), as reported by Sani et al., (2006) and Holmes et al., (2018), respectively. In our study, *Desulfovibrio* was dominating the enriched SRB population in the Postgate medium and *Methanosarcina* also appeared as viable archaea in this medium after 3 years in T3\_BBU. In addition, Thorgersen et al. (2017), demonstrated that surface layer proteins of *Pelosinus*, also viable in Postgate enrichment, were able to bind U through carboxyl and phosphate groups resulting in biosorption processes.

The presence of viable bacteria after 3 years of incubation was demonstrated in the present study. *Peribacillus*, *Bacillus* and *Robertmurraya* were isolated and identified in the T3\_BBU treatment. This was in accordance with Babich et al. (2021), who reported having isolated a strain aligning with the genus *Peribacillus* from sub-surface horizons of a uranium deposit in Russia. Kumari et al. (2015) also isolated *Bacillus korensis* from acidic copper mines, which implies its resistance in extreme environments. The last isolate was identified as *Robertmurraya* sp. This genus previously corresponded to *Bacillus*, and was reclassified in 2020 (Gupta et al., 2023). Therefore, there is no information on the relationship of this genus with uranium but the resistance of the *Bacillus* genus to this metal is very well documented (Panak et al., 2000; Pan et al., 2015; Banala et al., 2021).

As mentioned above, the enrichment in the Postgate medium of the uranium-treated bentonite (BBU) revealed the presence of viable SRB after 3 years of incubation. Several SRB are described for their capability to reduce U, being detected even in uranium mines (Zhu et al., 2023; Chang et al., 2001; Sani et al 2006). Reportedly, some SRB possess outstanding U(VI) reduction

capacity through processes involving c-type cytochromes, extracellular pili, electron shuttle, or thioredoxin reduction (You et al., 2021). The key role of these bacteria in the reduction of U(VI) to U(IV) could be supported by XRD data and the detection of uranium signal in the cell wall and inside the cytoplasm of different bacterial cells by STEM and EDX microscopy (see **Fig. 7, 8**).

### **4.2. Chemical speciation of U throughout the incubation time: Influence of bentonite microbial community**

The impact of microbial communities of the 3-year U amended bentonites in the chemical speciation of U was characterized by a combination of microscopic (STEM/HAADF/EDX) and spectroscopic (XPS and XRD) techniques. Both complementary methods showed the key role of biotic processes in affecting the U complexation. However, abiotic processes mediated by clay minerals can also be one of the main contributors to the fate of U in the studied samples. For example, Lee & Lee (2021) and Wazne et al., (2003) reported the adsorption capacity of minerals such as pyrite and other adsorbents (e.g. aluminum oxides and ferric oxyhydroxides) to uranium cations. Additionally, abiotic uranium reduction processes may have occurred. This involves the indirect reduction of U(VI) through Fe(II) produced by microbes utilizing Fe(III)-containing clays and oxides as terminal electron acceptors for anaerobic respiration (Latta, et al 2012; Wang, et al., 2019). Tsarev et al., (2016) reported that such electron transport systems can also be established by adsorbing Fe(II) ions on mineral surfaces, and reduced U(IV) species can subsequently be adsorbed on mineral surfaces or transformed into nanocrystalline uraninite, depending on pH values. Humic acids are also acknowledged to play a role in redox reactions, including the abiotic reduction of U(VI) (Wang et al., 2019). In addition, the

hydrogen sulfide, resulting from sulfate reduction by SRB, can abiotically reduce U(VI) to U(IV) or react with iron to form ferrous sulfide precipitates that may also reduce U(VI) (Boonchayaanant et al., 2010). The XPS data suggested two different U species which would correspond to U(VI) phosphate mineralization as  $U(VO_2) \cdot (PO_4)_2$  and U(VI) adsorption to clay minerals from the montmorillonite group. In addition, the XRD patterns obtained for the 3-year U-treated bentonite microcosms detected the presence of uranium phosphate minerals of the autunite or meta-autunite group and suggested the presence of uraninite. The formation of biogenic U(VI) phosphates was confirmed by electron microscopy and supported by microbial diversity data. STEM/HAADF/EDX analysis showed the presence of amorphous U phosphate accumulates in the inner part of the bacterial cell membranes indicating the key role of biotic processes in the U speciation in the studied ternary system. These U phosphates accumulates could correspond to meta-autunite mineral group, which was well described to be one the most U phosphate precipitated by bacteria (Beazley et al., 2007). It is well known that autunite phases are normally characterized by tetragonal morphology, including autunite and meta-autunite minerals such as chernikovite, meta-ankoleite, and sodium meta-autunite. It is possible that due to the high sensitivity of water retention to temperature, the loss of water during HRTEM could influence the interlayer configuration and hydrogen bonding, potentially causing a collapse in the crystal structure (Krivovichev et al., 2006). Hufton et al. (2021) have reported the ability of U(VI) to interact with the different components of the cell wall and cell membrane such as phospholipids and associated proteins of both gram-negative and gram-positive bacteria. They discussed that uranium ions could pass through the pores of the peptidoglycan due to their small size, facilitating the sorption process to the most inner compounds of the cell membrane and consequent U

## CHAPTER 4

complexation. U phosphate biomineralizing bacteria such as *Pseudomonas* and *Stenotrophomonas* were enriched in the U amended sample. Sanchez-Castro et al., (2021) have reported the biomineralization of U(VI) phosphates in the cell membrane of *Stenotrophomonas* sp. leading to the removal of about 98% of U from solution. This process was mediated by phosphatase activity located in the cell membrane, which cleaves organic phosphate substrate (G6P) releasing orthophosphates for the precipitation of this radionuclide. The U phosphate biomineralization by *Pseudomonas* has also been well documented (Choudhary and Sar, 2011). Additionally, two small peaks likely corresponding to uraninite ( $\text{UO}_2$ ) were observed by XRD. Thus, SRB from the genera *Desulfovibrio*, *Desulfosporosinus*, *Desulfotomaculum*, that prevail microbial diversity were reported to reduce U(VI) to U(IV) (Zhu et al., 2023; Chang et al., 2001; Sani et al 2006). No uraninite was detected by electron microscopy. Alessi et al. (2014) reported that uraninite usually lacks a crystalline structure, being less stable and easily re-oxidizable. In the same study, they demonstrated the ability of non-crystalline U(IV) coming from the reduction of U(VI) on the cell wall would tend to bind to free phosphate groups resulting in the formation of U(IV)-phosphate nanoparticles. This substantiates the hypotheses regarding uranium interactions, as evidenced by the detected peaks corresponding to uraninite ( $\text{UO}_2$ ), indicative of a likely bioreduction process (Howng et al.). The U(VI) binding by montmorillonite through a sorption process has also been reported (Dacheux et. Al, 1996; Drot et. al, 2007). Uraninite deposits have been previously reported in several studies in the cytoplasmic space of genera like *Pseudomonas* and *Desulfovibrio* (McLean and Beveridge, 2001; Sani et al., 2004). Merroun and Selenska-Pobell (2008) hypothesized the potential diffusion of reduced uranium nanoparticles from the periplasm to the

cytoplasm. However, the potential processes leading to intracellular uraninite precipitation remain unresolved.

Likewise, it is important to consider a potential abiotic reduction of U(VI). For example, the reduction by the hydrogen sulfide or Fe(II) resulting from sulfate reduction by SRB and Fe(III) reduction by IRB, respectively, in addition to the possible involvement of humic acids (Boonchayaanant et al., 2010, Latta, et al 2012; Wang, et al., 2019; Tsarev et al., 2016). Therefore, in the present study, U(VI) could be reduced not only directly by bacterial activity but also through various abiotic redox reactions.

The results presented and discussed in this work constitute a preliminary investigation into the potential effects of detrimental conditions, such as uranium leakage, groundwater infiltration, and bacterial activity on a heterogeneous and complex system like a future nuclear repository. Based on these initial findings, further studies could be conducted to elucidate at atomic and molecular scale the local coordination of U in the bentonite microcosms, obtaining more detailed understanding of the different biogeochemical processes that may occur. This could be achieved using spectroscopic techniques based on synchrotron radiation like EXAFS/XANES, micro-EXAFS, and X-ray microscopy.

## 5. Conclusions

Here, we provide clear experimental evidence that uranium and long-term incubation can shift microbial populations in bentonite microcosms amended with nutrients within the context of DGR. The 3-year incubation period entirely shaped the microbial diversity, favoring the prevalence of anaerobic and spore-forming microorganisms mainly from the phylum Firmicutes and Chloroflexi in addition to SRB. Viable SRB like *Desulfovibrio* and *Desulfosporosinus* were enriched from U amended bentonite microcosms

## CHAPTER 4

indicating their tolerance to this radionuclide. U amendment increased the relative abundance of microbial strains involved in the U biogeochemical cycle of U through U phosphate biomineralization (e.g. *Pseudomonas* and *Stenotrophomonas*) and U reduction as uraninite (e.g. *Desulfovibrio*). We demonstrated that the uranium speciation was significantly affected by the bentonite microbial populations in 3 years. A combination of XPS, XRD and STEM/HAADF analyses showed that U was present as U(VI) and U(IV) species. In the case of U(VI), biogenic U(VI) phosphates located in the inner part of the bacterial cell membranes in addition to U(VI)-adsorbed to clays such as montmorillonite were detected. XRD identified U-phosphate as autunine or meta- autunite group. Biogenic U(IV) species such as uraninite may be produced as a result of bacterial enzymatic reduction of U(VI). These results showed that bentonite microbes might be able to interact with U(VI) through U phosphate biomineralization and U(VI) reduction to U(IV) and the formation of uraninite. Abiotic processes would also govern the U fate through its sorption to bentonite clay or abiotic reduction. However, further research is required to elucidate which of the mentioned interaction processes would be conducted by viable bacteria to immobilize such toxic radionuclide in DGR relevant conditions. Nevertheless, these findings offer novel insights into the long-term behavior of bentonite microorganisms in the event of a potential release of one of the most critical waste elements in conjunction with simulated groundwater seepage.

### **Environmental Implications**

Ensuring future nuclear waste repository safety requires consideration of physicochemical and microbiological factors. This study provides novel insights into microbial behavior in bentonite barriers, addressing worst-case scenarios like waste leakage (e.g., uranium) and groundwater infiltration. We

present evidence of the enrichment of anaerobic and spore-forming microbes and viable sulfate-reducing bacteria (SRB) upon U-amended bentonite after a 3-year incubation. Furthermore, U speciation was affected by both biotic and abiotic processes, leading to its immobilization as U(VI) phosphates, uraninite, in addition to its sorption onto bentonite minerals. This implies that the U-immobilization within this barrier could positively enhance the safety performance of future DGRs.

### **Funding**

This study was supported by the grant RTI2018–101548-B-I00 “ERDF A way of making Europe” to MLM from the “Ministerio de Ciencia, Innovación y Universidades” (Spanish Government). The project leading to this application has received funding from the European Union's Horizon 2020 research and innovation program under grant agreement No 847593 to MLM and the grant FPU20/00583 to the first author from the “Ministerio de Universidades” (Spanish Government).

### **Declaration of Competing Interest**

The authors declare that they have no known competing financial interest or personal relationships that could have influenced the research reported in this paper.

### **Data availability**

The nucleotide sequences and metagenomics' raw data of this study were submitted to the sequence read archive (SRA) at NCBI: BioProject accession number PRJNA1083466.

### **Acknowledgements**

The authors acknowledge the assistance of Dr. F. Javier Huertas (IACT, Spain) for his guidance and help in collecting the bentonite from the deposit of Almería and Concepcion Hernandez-Castillo and Daniel García Muñoz Bautista Cerro for the preparation of samples for microscopic analyses. We also acknowledge the assistance of Dr. María del Mar Abad Ortega and other members of Centro de Instrumentación Científica (University of Granada, Spain) for the microscopy assistance. Funding for open access charge: Universidad de Granada / CBUA.

### **Credit authorship contribution statement**

Mar Morales-Hidalgo: Writing – review & editing, Writing – original draft, Visualization, Validation, Methodology, Investigation, Formal analysis, Conceptualization. Cristina Povedano-Priego: Writing – review & editing, Visualization, Validation, Methodology, Investigation, Formal analysis. Marcos F. Martinez-Moreno: Writing – review & editing, Investigation. Jesus J. Ojeda: Writing – review & editing, Visualization, Formal analysis. Fadwa Jroundi: Writing – review & editing, Validation, Methodology, Investigation, Formal analysis. Mohamed L. Merroun: Writing – review & editing, Writing – original draft, Validation, Supervision, Resources, Project administration, Methodology, Funding acquisition, Formal analysis, Conceptualization.

### **References**

- Alessi, D. S., Lezama-Pacheco, J. S., Stubbs, J. E., Janousch, M., Bargar, J. R., Persson, P., & Bernier-Latmani, R. (2014). The product of microbial uranium reduction includes multiple species with U(IV)–phosphate coordination. *Geochimica et Cosmochimica Acta*, 131, 115-127. <https://doi.org/10.1016/j.gca.2014.01.005>
- Babich, T. L., Semenova, E. M., Sokolova, D. S., Tourova, T. P., Bidzhieva, S. K., Loiko, N. G., Avdonin, G. I., Lutsenko, N. I. & Nazina, T. N. (2021). Phylogenetic diversity and potential activity of bacteria and fungi in the deep subsurface horizons of an

- uranium deposit. *Microbiology*, 90, 607-620.  
<http://dx.doi.org/10.1134/S0026261721040032>
- Bahl, H., Andersch, W., & Gottschalk, G. (1982). Continuous production of acetone and butanol by *Clostridium acetobutylicum* in a two-stage phosphate limited chemostat. *European journal of applied microbiology and biotechnology*, 15, 201-205. 0171-1741/82/0015/0201/\$ 01.00
- Banala, U. K., Das, N. P. I., & Toleti, S. R. (2021). Uranium sequestration abilities of *Bacillus bacterium* isolated from an alkaline mining region. *Journal of Hazardous Materials*, 411, 125053. <https://doi.org/10.1016/j.jhazmat.2021.125053>
- Barka, E. A., Vatsa, P., Sanchez, L., Gaveau-Vaillant, N., Jacquard, C., Klenk, H. P., Clément, C., Ouhdouch, Y. & van Wezel, G. P. (2016). Taxonomy, physiology, and natural products of Actinobacteria. *Microbiology and molecular biology reviews*, 80(1), 1-43. <https://doi.org/10.1128/mmbr.00019-15>
- Beazley, M. J., Martinez, R. J., Sobecky, P. A., Webb, S. M., & Taillefert, M. (2007). Uranium biomineralization as a result of bacterial phosphatase activity: insights from bacterial isolates from a contaminated subsurface. *Environmental science & technology*, 41(16), 5701-5707. <https://doi.org/10.1021/es070567g>
- Bengtsson, A. & Pedersen, K. (2017). Microbial sulphide-producing activity in water saturated Wyoming MX-80, Asha and Calcigel bentonites at wet densities from 1500 to 2000 kg·m<sup>-3</sup>. *Applied Clay Science*, 137, 203–212. <https://doi.org/10.1016/j.clay.2016.12.024>.
- Boonchayaanant, B., Gu, B., Wang, W., Ortiz, M. E., and Criddle, C. S. (2010). Can microbially-generated hydrogen sulfide account for the rates of U(VI) reduction by a sulfate-reducing bacterium? *Biodegradation*, 21, 81–95. <https://doi.org/10.1007/s10532-009-9283-x>
- Brockman, H. L., & Wood, W. A. (1975). D-Lactate dehydrogenase of *Peptostreptococcus elsdenii*. *Journal of bacteriology*, 124(3), 1454-1461. <https://doi.org/10.1128/jb.124.3.1454-1461.1975>
- Burzan, N., Murad Lima, R., Frutschi, M., Janowczyk, A., Reddy, B., Rance, A., Diomidis, N. & Bernier-Latmani, R. (2022). Growth and persistence of an aerobic microbial Community in Wyoming Bentonite MX-80 despite anoxic in situ conditions. *Frontiers in Microbiology*, 13, 858324. <https://doi.org/10.3389/fmicb.2022.858324>
- Callahan, B.J., McMurdie, P.J., Rosen, M.J., Han, A.W., Johnson, A.J., Holmes, S.P. 2016. DADA2: High-resolution sample inference from Illumina amplicon data. *Nature Methods*, 13(7), 581-3. <https://doi.org/10.1038/nmeth.3869>
- Caporaso, J.G., Kuczynski, J., Stombaugh, J., Bittinger, K., Bushman, F.D., Costello, E.K., Fierer, N., Peña, A.G., Goodrich, J.K., Gordon, J.I., Huttley, G.A., Kelley, S.T.,

## CHAPTER 4

- Knights, D., Koenig, J.E., Ley, R.E., Lozupone, C.A., McDonald, D., Muegge, B.D., Pirrung, M., Reeder, J., Sevinsky, J.R., Turnbaugh, P.J., Walters, W.A., Widmann, J., Yatsunencko, T., Zaneveld, J., Knight, R. (2010). QIIME allows analysis of high-throughput community sequencing data. *Nature Methods*, 7(5), 335-6. <https://doi.org/10.1038/nmeth.f.303>
- Chabalala, S., & Chirwa, E. M. (2010). Uranium(VI) reduction and removal by high performing purified anaerobic cultures from mine soil. *Chemosphere*, 78(1), 52-55. <https://doi.org/10.1016/j.chemosphere.2009.10.026>
- Chang, Y. J., Peacock, A. D., Long, P. E., Stephen, J. R., McKinley, J. P., Macnaughton, S. J., Anwar Hussain, A. K. M., Saxton, A. M. & White, D. C. (2001). Diversity and characterization of sulfate-reducing bacteria in groundwater at a uranium mill tailings site. *Applied and environmental microbiology*, 67(7), 3149-3160. <https://doi.org/10.1128/AEM.67.7.3149-3160.2001>
- Choudhary, S., & Sar, P. (2011). Uranium biomineralization by a metal resistant *Pseudomonas aeruginosa* strain isolated from contaminated mine waste. *Journal of hazardous materials*, 186(1), 336-343. <https://doi.org/10.1016/j.jhazmat.2010.11.004>
- Dacheux, N., Brandel, V., Genet, M., Bak, K., & Berthier, C. (1996). Solid solutions of uranium and thorium phosphates: synthesis, characterization and X-ray photoelectron spectroscopy. *New Journal of Chemistry*, 20(3), 301-310.
- Detman, A., Mielecki, D., Chojnacka, A., Salamon, A., Błaszczuk, M. K., & Sikora, A. (2019). Cell factories converting lactate and acetate to butyrate: *Clostridium butyricum* and microbial communities from dark fermentation bioreactors. *Microbial cell factories*, 18(1), 1-12. <https://doi.org/10.1186/s12934-019-1085-1>
- Drot, R., Roques, J., & Simoni, E. (2007). Molecular approach of the uranyl/mineral interfacial phenomena. *Comptes Rendus Chimie*, 10(10-11), 1078-1091. <https://doi.org/10.1016/j.crci.2007.01.014>
- Duro, L., Domènech, C., Grivé, M., Roman-Ross, G., Bruno, J., & Källström, K. (2014). Assessment of the evolution of the redox conditions in a low and intermediate level nuclear waste repository (SFR1, Sweden). *Applied Geochemistry*, 49, 192-205. <https://doi.org/10.1016/j.apgeochem.2014.04.015>
- Engel, K., Ford, S. E., Binns, W. J., Diomidis, N., Slater, G. F., & Neufeld, J. D. (2023). Stable microbial community in compacted bentonite after 5 years of exposure to natural granitic groundwater. *Msphere*, 8(5), e00048-23. <https://doi.org/10.1128/msphere.00048-23>
- Fairley, N., Fernandez, V., Richard-Plouet, M., Guillot-Deudon, C., Walton, J., Smith, E., ... & Baltrusaitis, J. (2021). Systematic and collaborative approach to problem solving using X-ray photoelectron spectroscopy. *Applied Surface Science Advances*, 5, 100112. <https://doi.org/10.1016/j.apsadv.2021.100112>

- Filippidou, S., Junier, T., Wunderlin, T., Lo, C. C., Li, P. E., Chain, P. S. & Junier, P. (2015). Under-detection of endospore-forming Firmicutes in metagenomic data. *Computational and structural biotechnology journal*, 13, 299-306. <https://doi.org/10.1016/j.csbj.2015.04.002>
- Fraj, B., Ben Hania, W., Postec, A., Hamdi, M., Ollivier, B., & Fardeau, M. L. (2013). *Fonticella tunisiensis* gen. nov., sp. nov., isolated from a hot spring. *International journal of systematic and evolutionary microbiology*, 63(Pt\_6), 1947-1950. <https://doi.org/10.1099/ij.s.0.041947-0>
- Gilmour, K. A., Davie, C. T., & Gray, N. (2021). An indigenous iron-reducing microbial community from MX80 bentonite—a study in the framework of nuclear waste disposal. *Applied Clay Science*, 205, 106039. <https://doi.org/10.1016/j.clay.2021.106039>
- Gilmour, K. A., Davie, C. T., & Gray, N. (2022). Survival and activity of an indigenous iron-reducing microbial community from MX80 bentonite in high temperature/low water environments with relevance to a proposed method of nuclear waste disposal. *Science of the Total Environment*, 814, 152660. <https://doi.org/10.1016/j.scitotenv.2021.152660>
- Gupta, R. S., Patel, S., Saini, N., & Chen, S. (2020). Robust demarcation of 17 distinct *Bacillus* species clades, proposed as novel Bacillaceae genera, by phylogenomics and comparative genomic analyses: description of *Robertmurraya kyonggiensis* sp. nov. and proposal for an emended genus *Bacillus* limiting it only to the members of the Subtilis and Cereus clades of species. *International journal of systematic and evolutionary microbiology*, 70(11), 5753-5798. <https://doi.org/10.1099/ijsem.0.004475>
- Gupta, R. S. (2023). Update on the genus *Robertmurraya*: a bacterial genus honoring Dr. Robert GE Murray (with some personal reminiscences). *Canadian Journal of Microbiology*, 69(10), 387-392. <https://doi.org/10.1139/cjm-2023-0070>
- Hall, D. S., Behazin, M., Binns, W. J., & Keech, P. G. (2021). An evaluation of corrosion processes affecting copper-coated nuclear waste containers in a deep geological repository. *Progress in Materials Science*, 118, 100766. <https://doi.org/10.1016/j.pmatsci.2020.100766>
- Hammer, O. 2001. PAST: paleontological statistics software package for education and data analysis. *Palaeontologia Electronica*. <http://palaeo-electronica.org>
- Holmes, D. E., Orelana, R., Giloteaux, L., Wang, L. Y., Shrestha, P., Williams, K., Lovley, D. R. & Rotaru, A. E. (2018). Potential for *Methanosarcina* to contribute to uranium reduction during acetate-promoted groundwater bioremediation. *Microbial ecology*, 76, 660-667. <https://doi.org/10.1007/s00248-018-1165-5>

## CHAPTER 4

- Howng, W. Y., & Thorn, R. J. (1979). X-ray photoelectron spectrum of U (4f) in condensates from UF<sub>4</sub> and ion bombarded Uf<sub>4</sub>; spectrum of UF<sub>3</sub>. *Chemical Physics Letters*, 62(1), 57-60. [https://doi.org/10.1016/0009-2614\(79\)80412-1](https://doi.org/10.1016/0009-2614(79)80412-1)
- Hufton, J., Harding, J., Smith, T., & Romero-González, M. E. (2021). The importance of the bacterial cell wall in uranium(VI) biosorption. *Physical Chemistry Chemical Physics*, 23(2), 1566-1576. <https://doi.org/10.1039/D0CP04067C>
- Krivovichev, S. V., Burns, P. C., & Tananaev, I. G. (2006). Crystal chemistry of actinide phosphates and arsenates. *Structural Chemistry of Inorganic Actinide Compounds*, 217.
- Kuleshova, M. L., Danchenko, N. N., Sergeev, V. I., Shimko, T. G., & Malashenko, Z. P. (2014). The properties of bentonites as a material for sorptive barriers. *Moscow University Geology Bulletin*, 69, 356-364. <https://doi.org/10.3103/S0145875214050044>
- Kumari, D., Pan, X., Achal, V., Zhang, D., Al-Misned, F. A., & Golam Mortuza, M. (2015). Multiple metal-resistant bacteria and fungi from acidic copper mine tailings of Xinjiang, China. *Environmental Earth Sciences*, 74, 3113-3121. <https://doi.org/10.1007/s12665-015-4349-z>
- Lakaniemi, A.-M., Douglas, G.B. & Kaksonen, A.H. (2019). Engineering and kinetic aspects of bacterial uranium reduction for the remediation of uranium contaminated environments. *Journal of Hazardous Materials*, 371, 198-212. <https://doi.org/10.1016/j.jhazmat.2019.02.074>
- Latta, D. E., Boyanov, M. I., Kemner, K. M., O'Loughlin, E. J., & Scherer, M. M. (2012). Abiotic reduction of uranium by Fe(II) in soil. *Applied geochemistry*, 27(8), 1512-1524. <https://doi.org/10.1016/j.apgeochem.2012.03.003>
- Lee, G., & Lee, W. (2021). Adsorption of uranium from groundwater using heated aluminum oxide particles. *Journal of Water Process Engineering*, 40, 101790. <https://doi.org/10.1016/j.jwpe.2020.101790>
- Lopez-Fernandez, M., Jroundi, F., Ruiz-Fresneda, M. A., & Merroun, M. L. (2021). Microbial interaction with and tolerance of radionuclides: underlying mechanisms and biotechnological applications. *Microbial Biotechnology*, 14(3), 810-828. <https://doi.org/10.1111/1751-7915.13718>
- Lopez-Fernandez, M., Matschiavelli, N., & Merroun, M. L. (2021). Bentonite geomicrobiology. *The Microbiology of Nuclear Waste Disposal*, 137-155. <https://doi.org/10.1016/B978-0-12-818695-4.00007-1>
- Lopez-Fernandez, M., Romero-González, M., Günther, A., Solari, P. L., & Merroun, M. L. (2018). Effect of U(VI) aqueous speciation on the binding of uranium by the cell surface of *Rhodotorula mucilaginosa*, a natural yeast isolate from bentonites. *Chemosphere*, 199, 351-360. <https://doi.org/10.1016/j.chemosphere.2018.02.055>

- Lopez-Fernandez, M., Cherkouk, A., Vílchez-Vargas, R., Jauregui, R., Pieper, D., Boon, N., Sanchez-Castro, I. & Merroun, M. L. (2015). Bacterial diversity in bentonites, engineered barrier for deep geological disposal of radioactive wastes. *Microbial ecology*, 70, 922-935. <https://doi.org/10.1007/s00248-015-0630-7>
- Lopez-Fernandez, M., Fernández-Sanfrancisco, O., Moreno-García, A., Martín-Sánchez, I., Sánchez-Castro, I., & Merroun, M. L. (2014). Microbial communities in bentonite formations and their interactions with uranium. *Applied geochemistry*, 49, 77-86. <https://doi.org/10.1016/j.apgeochem.2014.06.022>
- Marin, C. (2012). Particulate Phases Possibly Conveyed from Nuclear Waste Repositories by Groundwater. INTECH Open Access Publisher.
- Martinez-Moreno, M. F., Povedano-Priego, C., Morales-Hidalgo, M., Mumford, A. D., Ojeda, J. J., Jroundi, F., & Merroun, M. L. (2023). Impact of compacted bentonite microbial community on the clay mineralogy and copper canister corrosion: a multidisciplinary approach in view of a safe Deep Geological Repository of nuclear wastes. *Journal of Hazardous Materials*, 131940. <https://doi.org/10.1016/j.jhazmat.2023.131940>
- Martínez-Rodríguez, P., Sánchez-Castro, I., Ojeda, J. J., Abad, M. M., Descostes, M., & Merroun, M. L. (2023). Effect of different phosphate sources on uranium biomineralization by the *Microbacterium* sp. Be9 strain: A multidisciplinary approach study. *Frontiers in Microbiology*, 13, 1092184. <https://doi.org/10.3389/fmicb.2022.1092184>
- Masurat, P., Eriksson, S., & Pedersen, K. (2010). Evidence of indigenous sulphate-reducing bacteria in commercial Wyoming bentonite MX-80. *Applied Clay Science*, 47(1-2), 51-57. <https://doi.org/10.1016/j.clay.2008.07.002>
- McLean, J., & Beveridge, T. J. (2001). Chromate reduction by a pseudomonad isolated from a site contaminated with chromated copper arsenate. *Applied and Environmental Microbiology*, 67(3), 1076-1084. <https://doi.org/10.1128/AEM.67.3.1076-1084.2001>
- McMurdie, P.J., Holmes, S. (2013). Phyloseq: a R package for reproducible interactive analysis and graphics of microbiome census data. *PLoS One*, 8, e61217. <https://doi.org/10.1371/journal.pone.0061217>
- Merroun, M., Nedelkova, M., Rossberg, A., Hennig, C., & Selenska-Pobell, S. (2006). Interaction mechanisms of bacterial strains isolated from extreme habitats with uranium. *Radiochimica Acta*, 94(9-11), 723-729. <https://doi.org/10.1524/ract.2006.94.9-11.723>
- Merroun, M. L., & Selenska-Pobell, S. (2008). Bacterial interactions with uranium: an environmental perspective. *Journal of Contaminant Hydrology*, 102(3-4), 285-295. <https://doi.org/10.1016/j.jconhyd.2008.09.019>

## CHAPTER 4

- Mosher, J. J., Phelps, T. J., Podar, M., Hurt Jr, R. A., Campbell, J. H., Drake, M. M., Moberly, J. G. & Elias, D. A. (2012). Microbial community succession during lactate amendment and electron acceptor limitation reveals a predominance of metal-reducing *Pelosinus* spp. *Applied and Environmental Microbiology*, 78(7), 2082-2091. <https://doi.org/10.1128/AEM.07165-11>
- Neuwirth E. (2022). RColorBrewer: ColorBrewer Palettes. R package version 1.1–3, < <https://CRAN.R-project.org/package=RColorBrewer> >.
- Newsome, L., Morris, K., Trivedi, D., Bewsher, A., & Lloyd, J. R. (2015). Biostimulation by glycerol phosphate to precipitate recalcitrant uranium(IV) phosphate. *Environmental Science & Technology*, 49(18), 11070-11078. <https://doi.org/10.1021/acs.est.5b02042>
- Othman, S. A. (2023). Nuclear Energy From Current Perspective: A Short Review. *Enhanced Knowledge in Sciences and Technology*, 3(1), 011-015. Retrieved from <https://penerbit.uthm.edu.my/periodicals/index.php/ekst/article/view/5578>
- Pan, X., Chen, Z., Chen, F., Cheng, Y., Lin, Z., & Guan, X. (2015). The mechanism of uranium transformation from U(VI) into nano-uranophite by two indigenous *Bacillus thuringiensis* strains. *Journal of Hazardous Materials*, 297, 313-319. <https://doi.org/10.1016/j.jhazmat.2015.05.019>
- Panak, P., Raff, J., Selenska-Pobell, S., Geipel, G., Bernhard, G., & Nitsche, H. (2000). Complex formation of U(VI) with *Bacillus*-isolates from a uranium mining waste pile. *Radiochimica Acta*, 88(2), 71-76. <https://doi.org/10.1524/ract.2000.88.2.071>
- Petriglieri, F., Nierychlo, M., Nielsen, P. H., & McIlroy, S. J. (2018). In situ visualisation of the abundant *Chloroflexi* populations in full-scale anaerobic digesters and the fate of immigrating species. *PLoS One*, 13(11), e0206255. <https://doi.org/10.1371/journal.pone.0206255>
- Pinel-Cabello, M., Jroundi, F., López-Fernández, M., Geffers, R., Jarek, M., Jauregui, R., Vílchez-Vargas, R. & Merroun, M. L. (2021). Multisystem combined uranium resistance mechanisms and bioremediation potential of *Stenotrophomonas bentonitica* BII-R7: transcriptomics and microscopic study. *Journal of Hazardous Materials*, 403, 123858. <https://doi.org/10.1016/j.jhazmat.2020.123858>
- Povedano-Priego, C., Jroundi, F., Solari, P. L., Guerra-Tschuschke, I., del Mar Abad-Ortega, M., Link, A., Vilchez-Vargas, R. & Merroun, M. L. (2023). Unlocking the bentonite microbial diversity and its implications in selenium bioreduction and biotransformation: Advances in deep geological repositories. *Journal of Hazardous Materials*, 445, 130557. <https://doi.org/10.1016/j.jhazmat.2022.130557>
- Povedano-Priego, C., Jroundi, F., Lopez-Fernandez, M., Morales-Hidalgo, M., Martin-Sánchez, I., Huertas, F. J., Dopson, M. & Merroun, M. L. (2022). Impact of

- anoxic conditions, uranium(VI) and organic phosphate substrate on the biogeochemical potential of the indigenous bacterial community of bentonite. *Applied Clay Science*, 216, 106331. <https://doi.org/10.1016/j.clay.2021.106331>
- Povedano-Priego, C., Jroundi, F., Lopez-Fernandez, M., Shrestha, R., Spanek, R., Martín-Sánchez, I., Villar, M. V., Ševců, A., Dopson, M. & Merroun, M. L. (2021). Deciphering indigenous bacteria in compacted bentonite through a novel and efficient DNA extraction method: Insights into biogeochemical processes within the Deep Geological Disposal of nuclear waste concept. *Journal of Hazardous Materials*, 408, 124600. <https://doi.org/10.1016/j.jhazmat.2020.124600>
- Povedano-Priego, C., Jroundi, F., Lopez-Fernandez, M., Sánchez-Castro, I., Martín-Sánchez, I., Huertas, F. J., & Merroun, M. L. (2019). Shifts in bentonite bacterial community and mineralogy in response to uranium and glycerol-2-phosphate exposure. *Science of The Total Environment*, 692, 219-232. <https://doi.org/10.1016/j.scitotenv.2019.07.228>
- R Core Team. (2022). R: A language and environment for statistical computing. R Foundation for Statistical Computing, Vienna, Austria. <https://www.Rproject.org/>.
- Robertson, C. E., Harris, J. K., Wagner, B. D., Granger, D., Browne, K., Tatem, B., Feazel, M. L., Park, K., Pace, N. R. & Frank, D. N. (2013). Explicet: graphical user interface software for metadata-driven management, analysis and visualization of microbiome data. *Bioinformatics*, 29(23), 3100-3101. <https://doi.org/10.1093/bioinformatics/btt526>
- Ruiz-Fresneda, M. A., Martínez-Moreno, M. F., Povedano-Priego, C., Morales-Hidalgo, M., Jroundi, F., & Merroun, M. L. (2023). Impact of microbial processes on the safety of deep geological repositories for radioactive waste. *Frontiers in Microbiology*, 14, 1134078. <https://doi.org/10.3389/fmicb.2023.1134078>
- Ruiz-Fresneda, M. A., Eswayah, A. S., Romero-González, M., Gardiner, P. H., Solari, P. L., & Merroun, M. L. (2020). Chemical and structural characterization of Se(IV) biotransformations by *Stenotrophomonas bentonitica* into Se 0 nanostructures and volatile Se species. *Environmental Science: Nano*, 7(7), 2140-2155. <https://doi.org/10.1039/D0EN00507J>
- Sanchez-Castro, I., Martínez-Rodríguez, P., Abad, M. M., Descostes, M., & Merroun, M. L. (2021). Uranium removal from complex mining waters by alginate beads doped with cells of *Stenotrophomonas* sp. Br8: novel perspectives for metal bioremediation. *Journal of Environmental Management*, 296, 113411. <https://doi.org/10.1016/j.jenvman.2021.113411>
- Sanchez-Castro, I., Martínez-Rodríguez, P., Jroundi, F., Solari, P. L., Descostes, M., & Merroun, M. L. (2020). High-efficient microbial immobilization of solved U(VI) by the *Stenotrophomonas* strain Br8. *Water Research*, 183, 116110. <https://doi.org/10.1016/j.watres.2020.116110>

## CHAPTER 4

- Sanchez-Castro, I., Ruiz-Fresneda, M. A., Bakkali, M., Kämpfer, P., Glaeser, S. P., Busse, H. J., López-Fernández, M., Martínez-Rodríguez, P. & Merroun, M. L. (2017). *Stenotrophomonas bentonitica* sp. nov., isolated from bentonite formations. *International journal of systematic and evolutionary microbiology*, 67(8), 2779. <https://doi.org/10.1099%2Fijs.0.002016>
- Sani, R. K., Peyton, B. M., & Dohnalkova, A. (2004). Effect of uranium(VI) on *Desulfovibrio desulfuricans* G20: influence of soil minerals. *104th General Meeting of the Asm* (Abstract).
- Sani, R. K., Peyton, B. M., & Dohnalkova, A. (2006). Toxic effects of uranium on *Desulfovibrio desulfuricans* G20. *Environmental Toxicology and Chemistry: An International Journal*, 25(5), 1231-1238. <https://doi.org/10.1897/05-401R.1>
- Thijs, S., Op De Beeck, M., Beckers, B., Truyens, S., Stevens, V., Van Hamme, J. D., Weyens, N. & Vangronsveld, J. (2017). Comparative evaluation of four bacteria-specific primer pairs for 16S rRNA gene surveys. *Frontiers in microbiology*, 8, 494. <https://doi.org/10.3389/fmicb.2017.00494>
- Thorgersen, M. P., Lancaster, W. A., Rajeev, L., Ge, X., Vaccaro, B. J., Poole, F. L., Arkin, A. P., Mukhopadhyay, A. & Adams, M. W. (2017). A highly expressed high-molecular-weight S-layer complex of *Pelosinus* sp. strain UFO1 binds uranium. *Applied and environmental microbiology*, 83(4), e03044-16. <https://doi.org/10.1128/AEM.03044-16>
- Tondel, M. & Lindahl, L. (2019): Intergenerational Ethical Issues and Communication Related to High-Level Nuclear Waste Repositories. *Current Environmental Health Reports*, 6(4), 338-343. <https://doi.org/10.1007/s40572-019-00257-1>
- Tsarev, S., Waite, T. D., & Collins, R. N. (2016). Uranium reduction by Fe(II) in the presence of montmorillonite and nontronite. *Environmental Science & Technology*, 50(15), 8223-8230. <https://doi.org/10.1021/acs.est.6b02000>
- Villar, M. V., Pérez del Villar, L., Martín, P. L., Pelayo, M., Fernández, A. M., Garralón, A., Cuevas, J., Leguey, S., Caballero, E., Huertas, F. J., Jiménez de Cisneros, C., Linares, J., Reyes, E., Delgado, A., Fernández-Soler, J. M., & Astudillo, J. (2006). The study of Spanish clays for their use as sealing materials in nuclear waste repositories: 20 years of progress. *Journal of Iberian Geology*, 32, 15–36.
- Wang, Q., Zhu, C., Huang, X., & Yang, G. (2019). Abiotic reduction of uranium(VI) with humic acid at mineral surfaces: Competing mechanisms, ligand and substituent effects, and electronic structure and vibrational properties. *Environmental pollution*, 254, 113110. <https://doi.org/10.1016/j.envpol.2019.113110>
- Warnes G., Bolker B., Bonebakker L., Gentleman R., Huber W., Liaw A., Lumley T., Maechler M., Magnusson A., Moeller S., Schwartz M., Venables, B. (2022). *gplots: Various R Programming Tools for Plotting Data*. R package version 3.1.3. <https://CRAN.R-project.org/package=gplots>

- Wazne, M., Korfiatis, G. P., & Meng, X. (2003). Carbonate effects on hexavalent uranium adsorption by iron oxyhydroxide. *Environmental science & technology*, 37(16), 3619-3624. <https://doi.org/10.1021/es034166m>
- WNA. World Nuclear Association. (2021). Storage and disposal of radioactive waste. <https://www.world-nuclear.org/>
- Yang, S., Li, S., Jia, X. (2019). Production of medium chain length polyhydroxyalkanoate from acetate by engineered *Pseudomonas putida* KT2440. *Journal of Industrial Microbiology and Biotechnology*, 46(6), 793-800. <https://doi.org/10.1007/s10295-019-02159-5>
- You, W., Peng, W., Tian, Z., & Zheng, M. (2021). Uranium bioremediation with U(VI)-reducing bacteria. *Science of the Total Environment*, 798, 149107. <https://doi.org/10.1016/j.scitotenv.2021.149107>
- Yu, Q., Yuan, Y., Feng, L., Sun, W., Lin, K., Zhang, J., Zhang, Y., Wang, H., Wang, N. & Peng, Q. (2022). Highly efficient immobilization of environmental uranium contamination with *Pseudomonas stutzeri* by biosorption, biomineralization, and bioreduction. *Journal of Hazardous Materials*, 424, 127758. <https://doi.org/10.1016/j.jhazmat.2021.127758>
- Zheng, X., Hu, P., Yao, R., Cheng, J., Chang, Y., Mei, H., Shuxiang, S., Shujing, C. & Wen, H. (2022). Biosorption behavior and biomineralization mechanism of low concentration uranium(VI) by *Pseudomonas fluorescens*. *Journal of Radioanalytical and Nuclear Chemistry*, 331(11), 4675-4684. <https://doi.org/10.1007/s10967-022-08551-3>
- Zhu, F., Zhao, B., Min, W., & Li, J. (2023). Characteristics of groundwater microbial communities and the correlation with the environmental factors in a decommissioned acid in-situ uranium mine. *Frontiers in Microbiology*, 13, 1078393. <https://doi.org/10.3389/fmicb.2022.1078393>

## CHAPTER 4

Supplementary material for:

**Long-term tracking of the microbiology of uranium-amended water-saturated bentonite microcosms: A mechanistic characterization of U speciation**

**Mar Morales-Hidalgo**<sup>1,\*</sup>, Cristina Povedano-Priego<sup>1</sup>, Marcos F. Martinez-Moreno<sup>1</sup>, Jesus J. Ojeda<sup>2</sup>, Fadwa Jroundi<sup>1</sup>, Mohamed L. Merroun<sup>1</sup>

<sup>1</sup>*Faculty of Sciences, Department of Microbiology, University of Granada, Granada, Spain.*

<sup>2</sup>*Department of Chemical Engineering, Faculty of Science and Engineering, Swansea University, Swansea, United Kingdom*

## CHAPTER 4

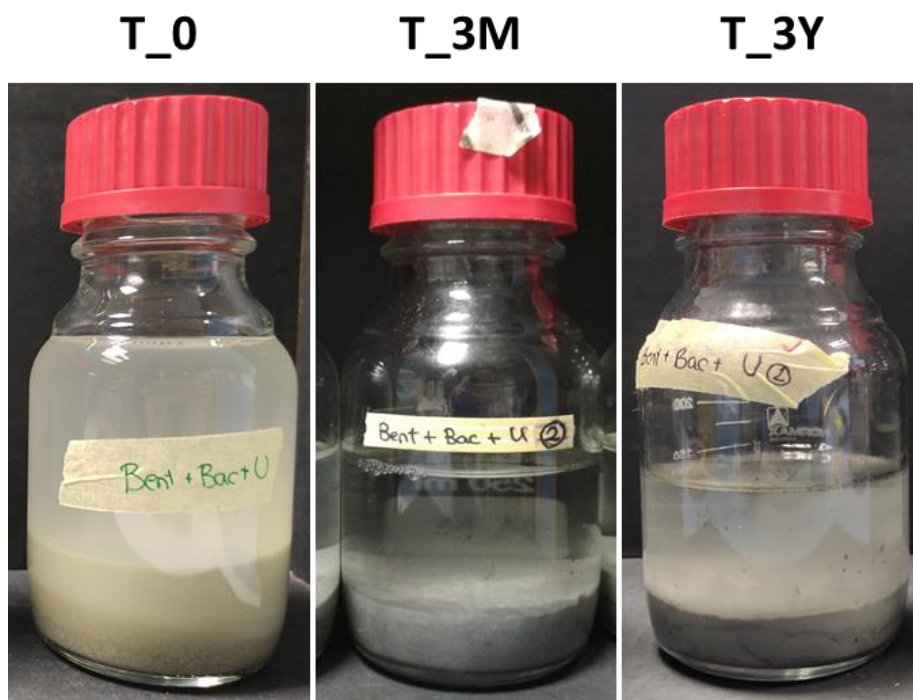
**Supplementary Table S1.** ICP-MS analysis of the major element's composition of the equilibrium water.

Element	PPB	Element	PPB	Element	PPB	Element	PPB	Element	PPB	Element	PPB
<b>Li</b>	1.10	<b>Be</b>	0.02	<b>Ni</b>	0.50	<b>Nb</b>	0.37	<b>La</b>	0.20	<b>As</b>	1.97
<b>Rb</b>	2.09	<b>Sc</b>	3.01	<b>Cu</b>	2.64	<b>Sn</b>	0.52	<b>Ce</b>	0.48	<b>Cd</b>	0.05
<b>Cs</b>	0.24	<b>V</b>	1.21	<b>Zn</b>	7.99	<b>Zr</b>	0.43	<b>Pr</b>	0.05	<b>Sb</b>	2.21
<b>Be</b>	0.16	<b>Cr</b>	0.73	<b>Ga</b>	0.17	<b>Pb</b>	16.07	<b>Nd</b>	0.17	<b>Er</b>	0.02
<b>Sr</b>	2.35	<b>Y</b>	0.23	<b>Mo</b>	1.13	<b>U</b>	4.91	<b>Sm</b>	0.05		

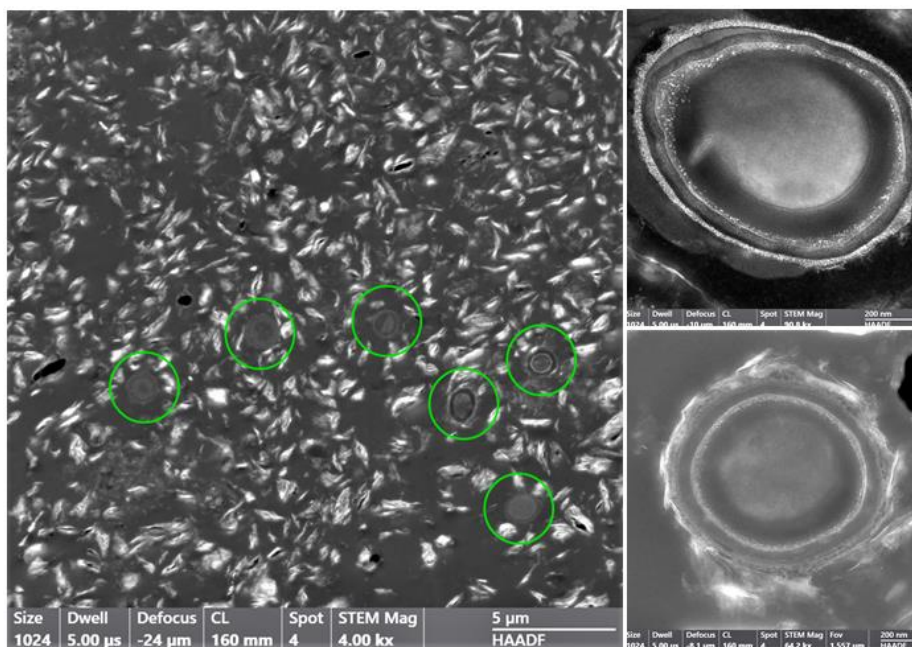
**Supplementary Table S2.** Phyla relative abundances of Archaea and Bacteria in the raw natural bentonite and the water-saturated microcosms under study in triplicates (except T3\_BB and T3\_BBU in duplicate). NB: raw natural bentonite; BB: bentonite inoculated with bacterial consortium; U: uranyl acetate 1.26 mM; T0: time 0; T3: three-year incubation.

Phyla	Relative abundances (%)				
	NB	T0_BB	T0_BBU	T3_BB	T3_BBU
Proteobacteria	24.79	62.16	62.64	4.79	25.72
Firmicutes	2.48	23.90	26.17	48.94	44.64
Actinobacteriota	42.35	13.81	11.10	3.24	0.72
Chloroflexi	12.58	0.02	0.03	10.27	9.89
Bacteroidota	5.11	0.02	0.02	4.33	3.19
Halobacterota	0.00	0.00	0.00	9.15	5.25
Desulfobacterota	0.24	0.00	0.00	4.78	2.99
Acidobacteriota	4.01	0.00	0.00	1.21	0.73
Hydrogenedentes	0.01	0.00	0.00	4.80	1.18
Planctomycetota	1.26	0.01	0.00	3.16	0.64
Verrucomicrobiota	2.16	0.02	0.00	0.67	0.50
Armatimonadota	0.08	0.00	0.00	2.46	0.72
Myxococcota	1.09	0.00	0.00	0.53	0.82
Halanaerobiaeota	0.01	0.00	0.00	0.00	2.09
Gemmatimonadota	1.62	0.00	0.00	0.00	0.00
Patescibacteria	0.70	0.05	0.03	0.12	0.00
SAR324_clade (Marine_group_B)	0.00	0.00	0.00	0.91	0.15
Sumerlaeota	0.08	0.00	0.00	0.13	0.45
Cyanobacteria	0.56	0.00	0.00	0.00	0.04
Nitrospirota	0.44	0.00	0.00	0.00	0.00

Latescibacterota	0.00	0.00	0.00	0.30	0.07
Deinococcota	0.22	0.00	0.00	0.00	0.00
Cloacimonadota	0.00	0.00	0.00	0.00	0.14
Thermoplasmata	0.01	0.00	0.00	0.11	0.07
Bdellovibrionota	0.10	0.00	0.00	0.00	0.00
Fibrobacterota	0.01	0.00	0.00	0.11	0.00
Unclassified	0.03	0.00	0.00	0.00	0.00
Entotheonellaeota	0.03	0.00	0.00	0.00	0.00
MBNT15	0.03	0.00	0.00	0.00	0.00
Dependentiae	0.01	0.00	0.00	0.00	0.00



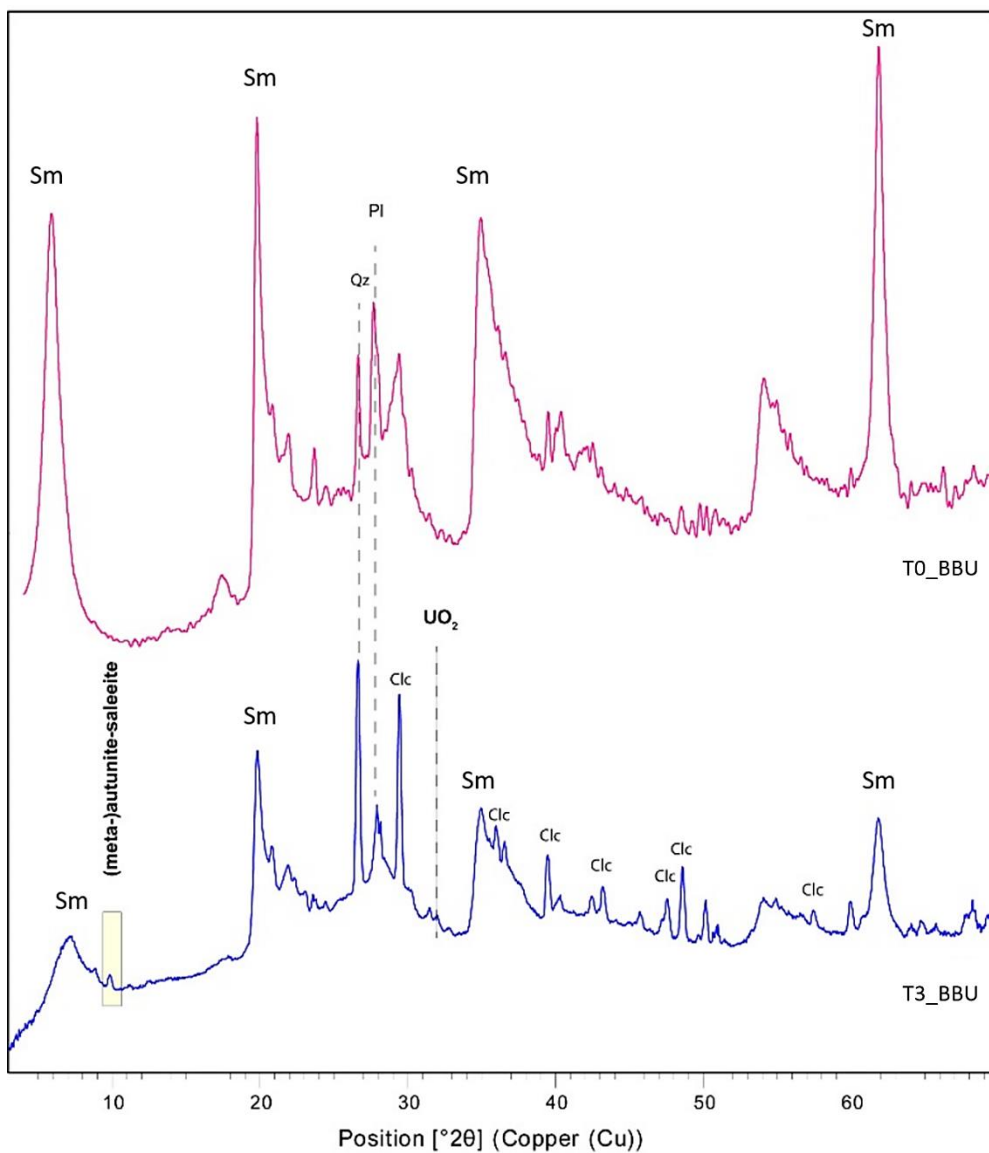
**Supplementary Figure S1.** Water-saturated bentonite microcosms treated with uranyl acetate at time 0, and after 3 months, and 3-year anoxic incubation at 28 °C. BBU: bentonite inoculated with bacterial consortium and treated with uranyl acetate 1.26 mM.



**Supplementary Figure S2.** Scanning transmission electron microscopy-high-angle annular dark-field imaging (STEM-HAADF) images of the spore cells found in BBU microcosm after 3-year incubation. Green circle: highlights the bacterial spores among the bentonite.

**Supplementary Table S3.** pH values of the supernatant from BB and BBU microcosms. Each measurement corresponds to the average between the values of the 3 replicates.

Treatments	Months				
	0	3	6	9	36 (3Y)
<b>BB</b>	7.41 ± 0.02	8.60 ± 0.16	8.66 ± 0.06	8.72 ± 0.01	7.68 ± 0.05
<b>BBU</b>	7.39 ± 0.06	8.76 ± 0.06	8.78 ± 0.10	8.86 ± 0.03	8.09 ± 0.13



**Supplementary Figure S3.** X-ray diffraction (XRD) patterns of T0\_BBU and T3\_BBU bentonite microcosm. BBU: bentonite inoculated with bacterial consortium and uranyl acetate; U: uranyl acetate 1.26 mM; T0: time 0. T3: 3-year incubation. Clc: calcite, Qz: quartz, Pl: plagioclase. Sm: smectite.

## CHAPTER 4

**Supplementary Data S1.** OTU relative abundances at genus level of the microbial communities in raw natural bentonite and the water-saturated microcosms under study in triplicates (except T3\_BB and T3\_BBU in duplicate). Cut off:  $\geq 0.1$ . NB: raw natural bentonite; BB: bentonite inoculated with bacterial consortium; U: uranyl acetate 1.26 mM; T0: time 0; T3: three-year incubation.

Genera	Relative abundances (%)				
	NB	T0_BB	T0_BBU	T3_BB	T3_BBU
<i>Pseudomonas</i>	0.16	38.62	40.87	3.64	20.47
<i>Stenotrophomonas</i>	0.01	23.30	20.75	0.76	2.79
<i>Amycolatopsis</i>	1.35	13.68	10.87	2.72	0.15
<i>Bacillus</i>	1.15	13.82	12.19	0.01	0.31
<i>Pelosinus</i>	0.00	0.00	0.00	22.91	6.00
<i>Clostridium_sensu_stricto_13</i>	0.15	1.74	0.81	7.91	5.40
<i>Methanosarcina</i>	0.00	0.00	0.00	7.36	4.63
<i>Fonticella</i>	0.04	0.33	1.42	2.61	5.73
Unclassified_Anaerolineaceae	0.00	0.00	0.00	5.31	5.37
<i>Gitt-GS-136</i>	8.03	0.02	0.03	0.00	0.00
<i>Sporacetigenium</i>	0.06	0.97	4.94	0.41	1.32
<i>Peptostreptococcaceae</i>	0.06	0.07	0.11	3.62	5.04
<i>Clostridium_sensu_stricto_1</i>	0.06	3.41	2.53	0.00	0.16
<i>Anaerolinea</i>	0.04	0.00	0.00	4.43	4.28
Unclassified_Peptostreptococcaceae	0.02	2.46	1.07	1.24	1.65
<i>Lentimicrobium</i>	0.00	0.00	0.00	3.66	2.92
<i>Nocardioides</i>	4.79	0.00	0.01	0.00	0.04
Unclassified_Micromonosporaceae	4.68	0.00	0.00	0.00	0.00
<i>Hydrogenedensaceae</i>	0.01	0.00	0.00	4.80	1.18

Uncultured_Lachnospirales	0.00	0.00	0.00	0.01	3.06
<i>Desulfovibrio</i>	0.01	0.00	0.00	2.95	0.97
<i>Flindersiella</i>	2.85	0.00	0.00	0.00	0.00
<i>Streptomyces</i>	2.71	0.00	0.00	0.00	0.00
<i>Lutispora</i>	0.02	0.00	0.00	1.56	1.38
<i>Anaerosolibacter</i>	0.22	0.06	0.21	1.03	1.26
Uncultured_Microtrichales	2.30	0.00	0.00	0.00	0.00
Uncultured_Armatimonadota	0.00	0.00	0.00	2.46	0.72
0319-7L14_Actinobacteria	2.11	0.00	0.00	0.00	0.00
<i>Desulfosporosinus</i>	0.05	0.00	0.00	0.81	1.55
<i>KD4-96_Chloroflexi</i>	2.05	0.00	0.00	0.00	0.00
Uncultured_Acidiferrobacteraceae	2.06	0.00	0.00	0.00	0.00
Uncultured_Microscillaceae	1.99	0.00	0.00	0.00	0.00
<i>Sedimentibacter</i>	0.00	0.00	0.01	1.07	1.35
Uncultured_Halobacteroidaceae	0.01	0.00	0.00	0.00	2.09
Unclassified_Micrococcaceae	1.70	0.01	0.08	0.00	0.00
<i>Mesorhizobium</i>	1.75	0.00	0.00	0.00	0.00
<i>Clostridium_sensu_stricto_3</i>	0.00	0.24	0.80	0.19	0.41
<i>Glycomyces</i>	1.61	0.00	0.00	0.00	0.00
<i>Desulfobulbus</i>	0.00	0.00	0.00	0.00	1.65
Uncultured_Alphaproteobacteria	1.62	0.00	0.00	0.00	0.00
<i>Clostridium_sensu_stricto_8</i>	0.11	0.21	0.86	0.06	0.20
<i>Allorhizobium-Neorhizobium-Pararhizobium-Rhizobium</i>	0.07	0.00	0.00	0.00	1.48
<i>Sphingomonas</i>	1.49	0.00	0.00	0.00	0.00

## CHAPTER 4

<i>Candidatus_Solibacter</i>	0.00	0.00	0.00	1.11	0.72
Uncultured_Vicinamibacterales	1.35	0.00	0.00	0.02	0.00
Unclassified_Nocardioidaceae	1.31	0.00	0.00	0.00	0.01
Uncultured_Pirellulaceae	0.01	0.00	0.00	1.49	0.30
<i>Vicinamibacteraceae</i>	1.23	0.00	0.00	0.00	0.00
Uncultured_Euzebyaceae	1.24	0.00	0.00	0.00	0.00
<i>Promicromonospora</i>	1.24	0.00	0.00	0.00	0.00
<i>Altererythrobacter</i>	1.25	0.00	0.01	0.00	0.00
<i>Pedosphaeraceae</i>	0.76	0.00	0.00	0.26	0.32
<i>Syntrophobacter</i>	0.00	0.00	0.00	1.66	0.13
<i>Haloplasma</i>	0.00	0.01	0.00	0.10	1.16
Uncultured_Methanomicrobiales	0.00	0.00	0.00	1.27	0.32
<i>Clostridium_sensu_stricto_10</i>	0.00	0.07	0.38	0.01	0.72
<i>Pla1_lineage</i>	0.00	0.00	0.00	1.42	0.22
Uncultured_Acidimicrobiia	1.10	0.00	0.00	0.00	0.00
<i>Gaiella</i>	1.11	0.00	0.00	0.00	0.00
Unclassified_Gracilibacteraceae	0.00	0.00	0.00	0.03	1.15
<i>Iamia</i>	0.90	0.05	0.07	0.00	0.00
<i>Gracilibacter</i>	0.00	0.00	0.00	0.80	0.54
<i>Steroidobacter</i>	1.04	0.00	0.00	0.00	0.00
<i>Desulfitobacterium</i>	0.00	0.00	0.00	0.33	0.74
<i>Longimicrobiaceae</i>	0.95	0.00	0.00	0.00	0.00
Unclassified	0.94	0.00	0.00	0.00	0.00
67-14	0.86	0.00	0.00	0.00	0.00

<i>Ohtaekwangia</i>	0.86	0.00	0.00	0.00	0.00
<i>Unclassified</i>	0.00	0.09	0.18	0.64	0.14
<i>Longispora</i>	0.79	0.00	0.00	0.00	0.00
<i>Unclassified</i>	0.01	0.00	0.79	0.00	0.00
<i>SAR324_clade(Marine_group_B)</i>	0.00	0.00	0.00	0.91	0.15
<i>Actinophytocola</i>	0.68	0.00	0.00	0.00	0.00
<i>Anaerostignum</i>	0.00	0.00	0.00	0.00	0.70
<i>Pelotomaculum</i>	0.00	0.00	0.00	0.00	0.73
<i>Vulgatibacter</i>	0.00	0.00	0.00	0.27	0.57
<i>Marmoricola</i>	0.66	0.00	0.00	0.00	0.00
<i>JG30-KF-CM45</i>	0.64	0.00	0.00	0.00	0.00
<i>Clostridium_sensu_stricto_12</i>	0.01	0.00	0.00	0.89	0.06
<i>Pelagibius</i>	0.66	0.00	0.00	0.00	0.00
<i>Anaerocolumna</i>	0.02	0.21	0.28	0.00	0.00
<i>Lysobacter</i>	0.58	0.00	0.00	0.00	0.00
<i>Sumerlaea</i>	0.08	0.00	0.00	0.13	0.45
uncultured	0.56	0.00	0.00	0.00	0.00
uncultured	0.57	0.00	0.00	0.00	0.00
<i>SRB2</i>	0.00	0.00	0.00	0.10	0.50
<i>Saccharimonadales</i>	0.52	0.01	0.01	0.00	0.00
<i>Unclassified</i>	0.55	0.00	0.00	0.00	0.00
<i>Shewanella</i>	0.00	0.00	0.00	0.01	0.56
<i>Bryobacter</i>	0.47	0.00	0.00	0.05	0.01
<i>Luteitalea</i>	0.49	0.00	0.00	0.00	0.00

## CHAPTER 4

<i>Ilumatobacter</i>	0.48	0.00	0.00	0.00	0.00
<i>Arthrobacter</i>	0.47	0.00	0.00	0.00	0.01
<i>OPB41</i>	0.00	0.00	0.00	0.21	0.37
<i>Solirubrobacter</i>	0.49	0.00	0.00	0.00	0.00
<i>Christensenellaceae_R-7_group</i>	0.00	0.00	0.00	0.32	0.32
<i>Ruminiclostridium</i>	0.01	0.00	0.00	0.18	0.37
uncultured	0.00	0.00	0.00	0.11	0.46
<i>Desulfotomaculum</i>	0.04	0.00	0.00	0.17	0.34
<i>Syntrophomonas</i>	0.00	0.00	0.00	0.28	0.34
<i>Woeseia</i>	0.49	0.00	0.00	0.00	0.00

---

**Supplementary Data S2.** OTU relative abundances at genus level of the growth of the microbial communities in T3\_BBU Postgate culture medium enrichment. Cut off:  $\geq 0.04\%$ .

Genera	Relative abundances (%)
	T3_BBU
<i>Sporacetigenium</i>	9.61
<i>Clostridium_sensu_stricto_1</i>	8.65
<i>Fonticella</i>	7.36
unclassified_Peptostreptococcaceae	7.22
<i>Clostridium_sensu_stricto_13</i>	6.59
<i>Methanosarcina</i>	6.38
<i>Pelosinus</i>	5.90
<i>Sedimentibacter</i>	5.56
<i>Lutispora</i>	4.35
<i>Desulfovibrio</i>	4.29
<i>Bacillus</i>	2.86
unclassified_Anaerolineaceae	2.23
uncultured_Lachnospiraceae	2.04
<i>Desulfosporosinus</i>	1.97
uncultured_Armatimonadota	1.75
uncultured_Lachnospirales	1.73
<i>Christensenellaceae_R-7_group</i>	1.58
<i>Ruminiclostridium</i>	1.46
<i>UCG-010_Oscillospirales</i>	1.37
unclassified_Lachnospiraceae	1.15
<i>Sunxiuqinia</i>	0.87
<i>Anaerostignum</i>	0.81
<i>Hydrogenedensaceae</i>	0.81
<i>Romboutsia</i>	0.72
<i>SRB2_Thermoanaerobacterales</i>	0.66
uncultured_Methanomicrobiales	0.60
<i>OPB41_Coriobacteriia</i>	0.57
<i>Anaerolinea</i>	0.51
<i>Pelotomaculum</i>	0.51
<i>Gracilibacter</i>	0.49
<i>Hydrogenoanaerobacterium</i>	0.46
<i>Oxobacter</i>	0.39
<i>Colidextribacter</i>	0.37
<i>Clostridium_sensu_stricto_10</i>	0.36

## CHAPTER 4

uncultured_Halobacteroidaceae	0.34
unclassified_Gracilibacteraceae	0.32
<i>Peptostreptococcaceae</i>	0.32
<i>Desulfotomaculum</i>	0.32
<i>Haloplasma</i>	0.31
<i>Methanocella</i>	0.30
<i>Desulfitobacterium</i>	0.30
<i>Lentimicrobium</i>	0.29
<i>Anaerosolibacter</i>	0.29
<i>Limnochordaceae</i>	0.26
<i>Syntrophomonas</i>	0.26
<i>Candidatus_Latescibacter</i>	0.25
uncultured_Christensenellaceae	0.23
<i>Allorhizobium-Neorhizobium-Pararhizobium-Rhizobium</i>	0.22
<i>Clostridium_sensu_stricto_12</i>	0.21
uncultured_Oscillospirales	0.18
<i>Clostridium_sensu_stricto_3</i>	0.17
uncultured_Anaerovoracaceae	0.16
<i>Methylocystis</i>	0.16
<i>Clostridium_sensu_stricto_8</i>	0.14
<i>Methanomassiliicoccus</i>	0.13
<i>Clostridium_sensu_stricto_7</i>	0.13
<i>SJA-15_Anaerolineae</i>	0.12
<i>Sporomusa</i>	0.12
uncultured_Gaiellales	0.11
<i>Brassicibacter</i>	0.11
<i>Sumerlaea</i>	0.11
uncultured_Pirellulaceae	0.09
<i>Gastranaerophilales</i>	0.08
uncultured_Veillonellales-Selenomonadales	0.08
<i>4572-13_Phycisphaerae</i>	0.08
<i>Actinotalea</i>	0.07
unclassified_Christensenellaceae	0.07
<i>ADurb.Bin063-1_Pedosphaeraceae</i>	0.07
<i>Nocardioides</i>	0.06
uncultured_Syntrophales	0.06
<i>Dehalobacter</i>	0.06
<i>SG8-4_Phycisphaerae</i>	0.06
<i>Pla1_lineage</i>	0.06

<i>Anaerocolumnna</i>	0.05
<i>Lachnoclostridium</i>	0.05
<i>NK4A214_group</i>	0.05
unclassified_Clostridia	0.05
uncultured_Firmicutes	0.05
<i>SAR324_clade (Marine_group_B)</i>	0.05
<i>Tuzzerella</i>	0.04
<i>Monoglobus</i>	0.04
uncultured_Peptococcaceae	0.04
<i>Anaerovorax</i>	0.04
uncultured_Syntrophomonadaceae	0.04

---

**Image from Posiva  
(Finland)**





*General discussion*

## GENERAL DISCUSSION

## GENERAL DISCUSSION

The deep geological repository (DGR) concept is designed with multiple barriers for managing high-level waste (HLW) and ensuring long-term security and integrity of this type of disposal (Tondel & Lindahl, 2019). The first barrier consists of metal canisters highly resistant to corrosion that will encapsulate the radioactive waste (IAEA, 2018). Each country selects a metal for the canister design, usually carbon steel, stainless steel, or copper, with ongoing research on using novel materials like titanium and nickel alloys (WNA, 2023; Morales-Hidalgo et al., 2024a). This Ph.D. thesis has focused on a DGR model based on copper canisters to evaluate their corrosion resistance under various biogeochemical conditions. The second artificial barrier would act as a backfilling and sealing material to contain, absorb, confine, and retain potential nuclear waste leaks, and to retard groundwater seepage (García-Romero et al., 2019; King et al., 2024). The barrier will be composed of highly compacted bentonite blocks, which will ensure the thorough integration of clay within the multisystem (King et al., 2024). The whole DGR structure will be emplaced in a host rock within a geologically stable formation, which would operate as a natural barrier.

Upon closure, the DGR environmental conditions will not remain constant but will fluctuate over the time. Initially, oxic conditions would occur, with no water saturation, intact bentonite compaction density, high temperatures, and high radiation doses. Over the time, a transition to a reducing atmosphere will follow, where an increase in the water activity, as a consequence of groundwater infiltration, loss of bentonite dry density, decrease of temperature, and radiation levels would prevail (King et al., 2017). Despite the harsh conditions within the DGR that may affect the survival and viability of microorganisms, some native microbes from bentonite, as well as those accidentally introduced through human activity, may inhabit this multisystem repository (Morales-Hidalgo et al., 2024a; Ruiz-Fresneda et al., 2023).

## GENERAL DISCUSSION

Therefore, understanding the interactions between these microorganisms and the different DGR barriers is crucial to guarantee the long-term safety performance of the repositories, as these microbes by their metabolic activity have the potential to significantly impact the surrounding environment.

Based on that, the main objective of this Ph.D. thesis was to evaluate the influence of various physicochemical and microbiological parameters on the stability and performance of different barriers (bentonite and copper metal canisters) in future DGRs for HLW (**Fig. 1**). Additionally, it is crucial to understand how conditions relevant to these repositories influence microbial activity, as this knowledge is essential for assessing their impact on both the stability of bentonite and the integrity of copper-based metal canisters. In order to evaluate all this, a multidisciplinary approach, integrating traditional microbiological techniques and state-of-the-art techniques in microscopy, molecular biology, spectroscopy, and analytical chemistry has been employed.

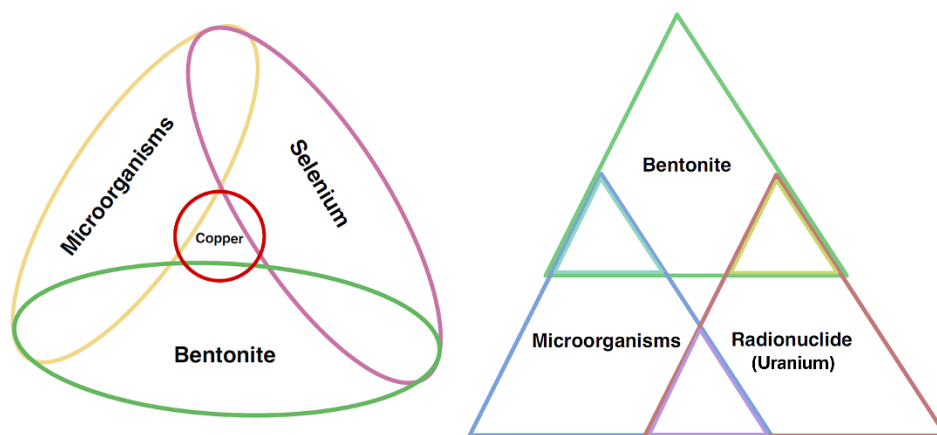


**Figure 1.** Ternary and quaternary systems studied in this Ph.D. thesis.

First of all, a more realistic scenario was studied. The first chapter investigated the **combined effects of radiation and compaction** on the microbiology and mineralogy of FEBEX bentonite, as well as on the corrosion of copper canisters. Specifically, the

focus was placed on the sulfate-reducing bacteria (SRB) group due to its significant role in copper corrosion. In this chapter, early post-closure conditions of a DGR were simulated, where bentonite experiences high compaction and elevated radiation doses. FEBEX bentonite was compacted to a density of  $1.6 \text{ g/cm}^3$  with a pure copper disk located in the core. Bentonite blocks were then subjected to gamma radiation at cumulative doses of 14 or 28 kGy over different incubation periods (6 months or 1 year). Additionally, some treatments included a bacterial consortium predominantly composed of SRB to enhance and accelerate their metabolic activity, facilitating a comprehensive assessment of their impact on copper corrosion.

The impact of **compaction** on the viability of aerobic heterotrophic bacterial cells was examined, revealing that bentonite native microorganisms are able to adapt to high-compaction conditions. Certain microorganisms, such as spore-formers, have managed to thrive in high-pressure environments, enabling them to endure conditions of high compaction density (Engel et al., 2023; Burzan et al., 2022; Pedersen et al., 2000). While high compaction condition is expected to suppress the activity of indigenous bentonite communities, these microorganisms can persist in a dormant state. The bacterial isolates from the compacted samples showed a high degree of phylogenetic similarity to the genus *Bacillus*, including the genera *Paenibacillus*, *Peribacillus*, *Neobacillus*, *Lysinibacillus*, and *Bacillus* itself. Most genera within the family Bacillaceae are well-known for their ability to survive harsh environmental conditions, such as drought or nutrient scarcity, by forming endospores (Mandic-Mulec et al., 2016). In addition, the viability of SRB was also studied, and the results showed a decrease in the SRB MPN  $\text{g}^{-1}$  of bentonite in the compacted samples after one year of incubation. Martinez-Moreno et al. (2023) reported a similar finding, noting a decrease in the viability of SRB in bentonite blocks compacted at a density of  $1.7 \text{ g/cm}^3$  after one year of incubation. Nevertheless, this reduction in viability could not be ascribed to a single factor, such as compaction. The depletion of electron

## GENERAL DISCUSSION

donors, such as acetate, which was initially added, could have also contributed to the decrease in the number of cells of this bacterial group.

One of the most detrimental effects in a repository environment is the influence of **radiation**. In our study, gamma radiation exposure negatively affected bacterial viability. In almost all cases, where the total cumulative dose was 14 or 28 kGy, no cell viability was observed. The treatment irradiated 6 months prior to 14 kGy dose stood out as the only exception. An incubation period before irradiation may have facilitated a better recovery and survival of the bacterial community from the radiation exposure. Therefore, these results indicated that gamma irradiation would affect cell viability differently depending on the developmental stage of the bacterial community at the time of irradiation. These results agreed with Pitonzo et al. (1999) who observed that irradiated bacteria, exposed to a total dose of up to 9.34 kGy, could potentially return to a fully cultivable state over time under more favorable environmental conditions. Regarding the viability of SRB, no growth was observed in any irradiated treatment, except for the SRB-consortium amended treatment irradiated initially with 14 kGy and subsequently incubated for six months. The 16S rRNA gene sequencing of the positive bottles of that early irradiated treatment, revealed the presence of *Desulfosporosinus* and *Bacillus*, indicating their survival and viability after irradiation. This finding was consistent with Haynes et al. (2018), who detected the same strains in FEBEX bentonite subjected to a 1 kGy gamma dose. However, the main outcome is that gamma irradiation at total cumulative doses of 14 kGy or 28 kGy adversely impacted the survival of SRBs, as most irradiated treatments showed no cell viability. The impact of gamma radiation was also assessed by studying the bentonite microbial communities in the 1-year incubation treatments. In general, the profile of the communities occurring in the different treatments included genera characteristic of soils (e.g., bentonite), many of which are known for their ability to thrive in adverse environments with limited water and nutrients, and even exposure to radiation. The most abundant genera in the samples, both with and without irradiation,

were *Saccharopolyspora*, *Streptomyces*, *Massilia*, *Acinetobacter*, and *Pseudomonas* (Saygin et al. (2021); Moussa et al. (2005); Ren et al., 2018; Gallego, 2016; Campos et al., 2010). Some of these genera could have formed spores as a resistance mechanism to these adverse conditions, as it is estimated that these resistant cells can withstand radiation up to five times more than normal vegetative cells (van Gerwen et al., 1999). Bacterial content, quantified by qPCR with the 16S rRNA gene, in samples irradiated after 6 months of incubation (14 kGy) was similar to that of unirradiated samples, but lower in those irradiated twice, with a cumulative dose of 28 kGy. These results agreed with those previously mentioned for viability studies. The initial 6-month incubation period, followed by an additional 6 months, likely facilitated adaptation of the bacterial community to the harsh conditions. This adaptation would have increased the relative abundance of bacterial genera less affected by experimental conditions. The subsequent post-radiation incubation period would have allowed cells to recover from the gamma radiation exposure.

On the other hand, concerning the mineralogical stability of bentonite, none of the studied parameters in Chapter 1 (compaction, radiation, or microorganisms) affected the properties of smectite, the predominant mineral group in bentonite. In all cases, X-ray diffraction (XRD) patterns indicated that the main character of a dioctahedral two-layer hydrated Ca-Mg-montmorillonite was maintained. Additionally, the smectites preserved their expansive properties, indicating that no illitization process had occurred. There is a debate in the published literature regarding the effect of gamma radiation on bentonite stability (Allard et al., 2009). Most studies suggested that significant alterations in bentonite properties would only occur with extremely high radiation doses. However, these conditions are unlikely to be encountered in future repositories. Furthermore, the surface of the copper disks was also studied using environmental scanning electron microscopy (ESEM) coupled with energy dispersive X-ray (EDX) and X-ray photoelectron spectroscopy (XPS). Based on the presence of corrosion products, the most altered disks were those from the non-irradiated

## GENERAL DISCUSSION

treatments, with copper oxides being the main corrosion products, as confirmed by XPS. In the future nuclear waste repository, oxygen will be present only during the initial years, gradually decreasing due to bacterial activity and mineral oxidation (King et al., 2017). In the present study, potential sources of oxygen included the assembly of the blocks under oxic conditions, the presence of oxygen molecules trapped in the bentonite (Burzan et al., 2022), and the pore water (Huttunen-Saarivirta et al., 2016). Copper disks from irradiated treatments showed less evidence of corrosion. Gamma radiation would indirectly retard the biotic corrosion of copper by negatively affecting the bentonite microbial activity. Copper sulfides were only detected in the treatments with the inoculated SRB consortium and were found exclusively within the bentonite, not on the copper surface. Hall et al. (2021) reported that microbial activity would primarily occur within the bentonite where biogenic corrosion would take place. More specifically, by SRB group, since these bacteria are frequently responsible for microbiologically influenced corrosion (MIC) damage through the production of  $\text{HS}^-$ , which combined with  $\text{H}^+$ , would result in  $\text{H}_2\text{S}$  (Little et al., 2020; Thauer et al., 2007). In addition, in the irradiated treatments, larger precipitates than copper sulfides with a sulfur signal were detected directly on copper surface. Analyses to confirm their exact nature are still pending, but it was hypothesized that they may be copper sulfates, whose precipitation could have been favored by the radiation. Li et al. (2021) reported that  $\gamma$ -radiation induces redox reactions leading to the precipitation of less soluble products such as salts.

Another key parameter in a DGR environment is the **temperature**. Therefore, this Ph.D. thesis included a study to evaluate the influence of high temperatures on bentonite microbiology, copper corrosion, and the mineralogical and chemical stability of bentonite (Chapter 2 and 3). The impact of temperature was investigated under conditions mimicking system failure, including waste leakage (e.g., selenium), groundwater seepage leading to loss of bentonite compaction properties (bentonite slurry), presence of electron donors and acceptors (acetate, lactate, and sulfate), and

high bacterial activity (inoculating a bacterial consortium composed of four genera naturally present in bentonite). These conditions would promote the development of bacterial activity. Spanish bentonite microcosms were prepared according to the specified treatments and incubated for 2 months at 60 °C. Additionally, a treatment with tyndallized bentonite was included as a heat shock reference, expected to exhibit lower bacterial activity, for comparison purpose. The incubation of the microcosms at high temperature favored thermophilic bacterial communities that are native to the bentonite. Among these genera were *Pseudomonas*, *Clostridium*, *Bacillus*, and *Tepidimicrobium* showing higher abundances, as well as others with lower relative abundance but of interest, such as *Caloribacterium*, *Thermaerobacter*, *Thermobacillus*, and *Thermacetogenium* (Slobodkina et al., 2012; Takai et al., 1999; Hattori et al., 2000). Thermophilic bacteria found in bentonites should be considered in the assessment of DGR safety, as these microorganisms can survive the high temperatures anticipated during the initial repository stages through mechanisms like heat-resistant proteins, rapid repair of sensitive molecules, and spore formation (King et al., 2017; Haynes et al., 2018; Den Besten et al., 2018). These findings are derived from molecular DNA sequencing studies, indicating that the presence of these sequences does not guarantee the viability or activity of these genera. Nonetheless, this data is of interest for understanding the changes occurring within the microbial communities across different treatments. The viability of the SRBs bacterial group relevant to copper corrosion, was also investigated. All treatments showed the presence of SRBs, indicating that they maintained cell viability under the 60°C incubation conditions. However, the heat-shocked bentonite treatment seemed to negatively impact the number of viable SRBs. Overall, these results underscore the resilience of this bacterial group to survive temperatures as high as 60 °C and maintain viability when favorable conditions (such as nutrient availability and a temperature of 28 °C) are present. Martinez-Moreno et al. (2024a) also discussed comparable findings, indicating the viability of SRBs in compacted bentonite blocks incubated at

## GENERAL DISCUSSION

60 °C. Once more, the mineralogical and chemical stability of Spanish bentonite was assessed and confirmed under these experimental conditions using XRD and X-ray fluorescence (XRF) analyses. No relevant changes due to temperature were observed either among treatments or when compared to untreated and unincubated raw bentonite. The results obtained from quantifying and identifying mineral phases align with previous studies by Lopez-Fernandez et al. (2015), Povedano-Priego et al. (2022) and Martinez-Moreno et al. (2024a). Microorganisms could affect the stability of the bentonite buffer by interacting with minerals (Meleshyn, 2014). A significant concern is the bioreduction of Fe(III), mediated by SRB and iron-reducing bacteria (IRB), which can promote the illitization of smectite (Pedersen et al., 2017). However, in the current study, despite some evidences of bacterial activity and the viability of SRB, there was no indication of smectite illitization or destabilization. Under experimental conditions, copper corrosion occurred during the high-temperature incubation. The surfaces of the copper plates that exhibited the most corrosion signs were those corresponding to treatments with the amended bacterial consortium. The high activity of this amended bacterial group, along with native bentonite bacteria, negatively impacted the copper, leading to increased corrosion products, including precipitates of copper oxides and possibly copper sulfides. Raman spectroscopy identified some of the copper oxide precipitates as copper(I) oxide. The formation of copper oxides is expected during the initial years after repository closure due to the presence of oxygen (Hall et al., 2021). The main cause of copper sulfide production is attributed to SRBs, whose viability was detected in all treatments. This suggests that they may have been active and facilitated the formation of  $\text{Cu}_x\text{S}$  through the reduction of sulfates to sulfides, promoted by lactate consumption (Dou et al., 2020; Matschiavelli et al. (2019); Martinez-Moreno et al., 2024b). In addition, Salehi Alaei et al. (2023) reported that the previously oxidized copper could react with  $\text{HS}^-$ , leading to the formation of  $\text{Cu}_2\text{S}$ .

Another failure scenario considered in relation to the DGR is nuclear waste leakage. This Ph.D. thesis specifically focused on the simulation of two types of radionuclides leaks: one involving selenium (Se) (Chapters 2 and 3) and the other involving uranium (U) (Chapter 4). These studies were conducted from a chemical, rather than a radiological, perspective. Starting with the **effect of selenium**, this metalloid was studied under the influence of incubation at 60 °C and the conditions mentioned in the previous section. Sodium selenite at a concentration of 2 mM was studied as an inactive analog of the radioactive isotope  $^{79}\text{Se}$ . In the HLW, the presence of this radioisotope  $^{79}\text{Se}$  is expected as one of the most critical metalloids, for its long half-life ranging from  $6.5 \times 10^4$  to  $1.13 \times 10^6$  years (Atwood, 2010). After only 4 days of incubation, microcosms inoculated with a bacterial consortium (comprising 4 bacterial genera previously isolated or identified in Spanish bentonite) were the first to exhibit orange color changes. The reddish-orange color indicated the presence of Se(0), suggesting that reduction of Se(IV) to Se(0) had occurred in these treatments (Ruiz-Fresneda et al., 2018; Povedano-Priego et al., 2023). The bacterial consortium accelerated the reduction of Se(IV), facilitated by three of the four strains, *Stenotrophomonas*, *Pseudomonas*, and *Bacillus*, which are known for their ability to reduce this metalloid (Ruiz-Fresneda et al., 2020; Tendenedzai et al., 2021; Borah et al., 2021). On the other hand, the treatments involving the consortium but not treated with Se, also underwent color changes during the two months of incubation, turning blackish in hue. The black color change observed in these treatments is likely due to hydrogen sulfide ( $\text{H}_2\text{S}$ ) production by bacterial activity. This  $\text{H}_2\text{S}$  can react with iron in bentonite, forming black precipitates of reduced iron (Fe) compounds (Miettinen et al., 2022; Matschiavelli et al., 2019). The findings from microscopic techniques such as scanning transmission electron microscopy (STEM), high-resolution transmission electron microscopy (HRTEM), selective area electron dispersion (SAED) and EDX, illustrated the influence of bentonite microorganisms on the chemical transformation of selenium. As mentioned above, the amended bacterial consortium accelerated the

## GENERAL DISCUSSION

reduction of Se(IV), resulting in the formation of intracellular amorphous or slightly monoclinic crystalline (*m*-Se) Se(0) nanospheres in the initial stages, and nanoaggregates of *m*-Se or Se+Fe after 2 months of incubation at 60 °C. This Se reduction process appeared to proceed more slowly in microcosms without the consortium, suggesting the involvement of native bentonite microbial communities. Regarding Se+Fe nanoaggregates, they likely corresponded to the mineral ferroselite (FeSe<sub>2</sub>). In the reducing environment of the incubation, ferroselite formation likely occurred through a series of bacterial-mediated processes. Initially, bacteria reduced Se(IV) to Se(0). Subsequently, certain bacteria, such as *Pseudomonas* and *Stenotrophomonas*, are known to reduce Fe(III) in bentonite smectites to Fe(II) (Naganuma et al., 2015; Pinel-Cabello et al., 2021). These Fe(II) ions could then react with Se(0) and 2e<sup>-</sup>, resulting in the formation of iron selenide, mineral known as ferroselite (Howard, 1977). In conclusion, the reduction of Se(IV) as insoluble precipitates and the formation of minerals like FeSe<sub>2</sub> suggested that bentonite microbial communities played a key role in the biogeochemical cycle of Se by immobilizing this important radionuclide, thereby reducing its mobility within DGR barriers. Regarding the influence of Se on bentonite microbial communities, in addition to the previously mentioned consortium genera, other native bacteria in bentonite also showed prominence in the presence of this metalloid. Examples include genera like *Aeribacillus* and *Symbiobacterium* which, along with others such as *Pseudomonas* and *Bacillus*, also naturally present in bentonite, likely contributed to the reduction of Se(IV) in treatments without the consortium, although at a slower rate (Povedano-Priego et al., 2023; Aoyagi et al., 2021; Avendaño et al., 2016; Yu et al., 2018). Conversely, other genera such as uncultured\_Bacillaceae, *Thermaerobacter*, and *Sporacetigenium* were adversely affected by Se. Nevertheless, bacteria that are more tolerant to Se can decrease the bioavailability of this toxic form in the environment, thereby reducing exposure for more sensitive bacteria. Moreover, the addition of Se appeared to have attenuated the influence of microbial activity on

copper corrosion. This phenomenon is likely due to the competition between Se(IV) and Cu for sulfide, generated by SRB, as a terminal electron acceptor (Hockin and Gadd, 2003). The interaction of Se(IV) with HS<sup>-</sup> could result in the depletion of free sulfide molecules, thereby diminishing the probability of sulfide reacting with copper. Despite Se(IV) appearing to negatively affect the viability of SRB determined by MPN, all Se treated samples exhibited positive results for the viability of this bacterial group, indicating that their activity likely influenced all these biochemical processes.

Finally, the effect of a **simulated uranium leak** was studied in Chapter 4. The impact of long-term incubation (3 years) in bentonite slurries has been studied for the first time. The main objectives were 1) to investigate alterations in the microbiology of bentonite after 3 years of exposure to uranium, focusing specifically on the viability of heterotrophic microorganisms and SRB, and 2) to examine changes in the chemical speciation of uranium over the long-term incubation period, with the aim of understanding the dynamics influenced by the microbial communities within bentonite. This experiment was also conducted under simulated conditions of system failure and high bacterial activity, including the use of an autochthonous bentonite bacterial consortium, water saturation, 1.26 mM uranyl acetate, and electron donors. Long-term incubation of the samples allowed the communities to change completely, leading to the enrichment of anaerobic and spore-forming bacteria. The microbial communities were dominated by representatives of the phylum Firmicutes, which includes most genera capable of forming endospores under adverse conditions (Filippidou et al., 2015). The experimental anoxic conditions also favored the presence of other anaerobic genera, such as the archaea *Methanosarcina* and the SRBs *Desulfovibrio*, *Desulfosporosinus*, and *Desulfobulbus*. These findings aligned with the expected scenario in future DGRs, where aerobic conditions are initially anticipated upon repository closure (King et al., 2017). Over time, a transition to reducing conditions is expected, characterized by the prevalence of anaerobic bacterial communities (Duro et al., 2014). Highly U-tolerant and viable bacterial

## GENERAL DISCUSSION

isolates of the genera *Peribacillus*, *Bacillus* and some SRBs such as *Desulfovibrio* and *Desulfosporosinus* were enriched from U-amended bentonite. The key role of U-tolerant bacteria in the reduction of U(VI) to U(IV) could be supported by XRD data and the detection of uranium signals in the cell walls and within the cytoplasm of various bacterial cells using STEM and EDX microscopy. The results obtained from XPS and XRD analyses revealed the presence of uranium in both U(VI) and U(IV) forms. Biogenic U(VI) phosphates, specifically  $U(UO_2)(PO_4)_2$ , were identified on the inner side of bacterial cell membranes, along with U(VI) adsorbed onto clays like montmorillonite. Uranium phosphate biomineralizing bacteria, such as *Pseudomonas* and *Stenotrophomonas*, were enriched in the U-amended sample. Sanchez Castro et al. (2021) reported the biomineralization of U(VI) phosphates in the cell membranes of *Stenotrophomonas* sp., resulting in the removal of approximately 98% of U from the solution. Additionally, biogenic U(IV) species, such as uraninite, can form through bacterial enzymatic reduction of U(VI). SRBs such as those from the genera *Desulfovibrio*, *Desulfosporosinus*, and *Desulfotomaculum*, which dominate microbial diversity, have been documented to reduce U(VI) to U(IV) (Zhu et al., 2023; Chang et al., 2001; Sani et al., 2006). It is also crucial to consider the potential for abiotic reduction of U(VI). For instance, U(VI) can be reduced by hydrogen sulfide or Fe(II), which are produced through sulfate reduction by SRBs and Fe(III) reduction by IRBs, respectively (Boonchayaanant et al., 2010; Latta et al., 2012; Tsarev et al., 2016). This research provided new insights into the long-term behavior of bentonite microorganisms in the event of a potential release of one of the most hazardous waste elements, leading to their immobilization into insoluble and more stable forms.

All in all, the findings of this Ph.D. thesis have demonstrated the influence of bentonite microorganisms, whether beneficial, detrimental, or neutral, on the biogeochemical processes that may occur in a deep geological repository environment for radioactive waste. Nevertheless, further investigation into the microbiology of

these repositories is essential to guarantee their optimal performance for at least 100,000 years.

## References

- Allard, T., and Calas, G. (2009). Radiation effects on clay mineral properties. *Applied Clay Science*, 43(2), 143-149. <https://doi.org/10.1016/j.clay.2008.07.032>
- Aoyagi, T., Mori, Y., Nanao, M., Matsuyama, Y., Sato, Y., Inaba, T., ... & Hori, T. (2021). Effective Se reduction by lactate-stimulated indigenous microbial communities in excavated waste rocks. *Journal of Hazardous Materials*, 403, 123908. <https://doi.org/10.1016/j.jhazmat.2020.123908>
- Atwood, D. A. (Ed.). (2010). *Radionuclides in the Environment*. Chichester, Reino Unido: John Wiley & Sons.
- Avendaño, R., Chaves, N., Fuentes, P., Sánchez, E., Jiménez, J. I., & Chavarría, M. (2016). Production of selenium nanoparticles in *Pseudomonas putida* KT2440. *Scientific Reports*, 6, 37155. <https://doi.org/10.1038/srep37155>
- Boonchayaanant, B., Gu, B., Wang, W., Ortiz, M. E., and Criddle, C. S. (2010). Can microbially-generated hydrogen sulfide account for the rates of U(VI) reduction by a sulfate-reducing bacterium? *Biodegradation*, 21, 81–95. <https://doi.org/10.1007/s10532-009-9283-x>
- Borah, S. N., Goswami, L., Sen, S., Sachan, D., Sarma, H., Montes, M., Peralta-Videa, J. R., Pakshirajan, K. & Narayan, M. (2021). Selenite bioreduction and biosynthesis of selenium nanoparticles by *Bacillus paramycooides* SP3 isolated from coal mine overburden leachate. *Environmental Pollution*, 285, 117519. <https://doi.org/10.1016/j.envpol.2021.117519>
- Burzan, N., Murad Lima, R., Frutschi, M., Janowczyk, A., Reddy, B., Rance, A., Diomidis, N., Bernier-Latmani, R. (2022). Growth and Persistence of an Aerobic Microbial Community in Wyoming Bentonite MX-80 Despite Anoxic in situ Conditions. *Frontiers in Microbiology*, 13. <https://doi.org/10.3389/fmicb.2022.858324>
- Campos, V. L., Valenzuela, C., Yarza, P., Kämpfer, P., Vidal, R., Zaror, C., ... & Rosselló-Móra, R. (2010). *Pseudomonas arsenicoxydans* sp nov., an arsenite-oxidizing strain isolated from the Atacama Desert. *Systematic and Applied Microbiology*, 33(4), 193-197. <https://doi.org/10.1016/j.syapm.2010.02.007>
- Chang, Y. J., Peacock, A. D., Long, P. E., Stephen, J. R., McKinley, J. P., Macnaughton, S. J., Anwar Hussain, A. K. M., Saxton, A. M. & White, D. C. (2001). Diversity and characterization of sulfate-reducing bacteria in groundwater at a uranium mill tailings site. *Applied and environmental microbiology*, 67(7), 3149-3160. <https://doi.org/10.1128/AEM.67.7.3149-3160.2001>

## GENERAL DISCUSSION

- Den Besten, H. M., Wells-Bennik, M. H., & Zwietering, M. H. (2018). Natural diversity in heat resistance of bacteria and bacterial spores: impact on food safety and quality. *Annual Review of Food Science and Technology*, 9, 383-410. <https://doi.org/10.1146/annurev-food-030117-012808>
- Dou, W., Pu, Y., Han, X., Song, Y., Chen, S., & Gu, T. (2020). Corrosion of Cu by a sulfate reducing bacterium in anaerobic vials with different headspace volumes. *Bioelectrochemistry*, 133, 107478. <https://doi.org/10.1016/j.bioelechem.2020.107478>
- Duro, L., Domènech, C., Grivé, M., Roman-Ross, G., Bruno, J., & Källström, K. (2014). Assessment of the evolution of the redox conditions in a low and intermediate level nuclear waste repository (SFR1, Sweden). *Applied Geochemistry*, 49, 192-205. <https://doi.org/10.1016/j.apgeochem.2014.04.015>
- Engel, K., Ford, S.E., Binns, W.J., Diomidis, N., Slater, G.F., Neufeld, J.D., (2023). Stable microbial community in compacted bentonite after 5 years of exposure to natural granitic groundwater. *mSphere*, 8, e00048-23. <https://doi.org/10.1128/msphere.00048-23>
- Filippidou, S., Junier, T., Wunderlin, T., Lo, C. C., Li, P. E., Chain, P. S. & Junier, P. (2015). Under-detection of endospore-forming Firmicutes in metagenomic data. *Computational and structural biotechnology journal*, 13, 299-306. <https://doi.org/10.1016/j.csbj.2015.04.002>
- Gallego, L. (2016). *Acinetobacter baumannii*: Factors involved in its high adaptability to adverse environmental conditions. *Journal of Microbiology & Experimentation*, 3(2), 00085. <http://dx.doi.org/10.15406/jmen.2016.03.00085>
- García-Romero, E., María Manchado, E., Suárez, M., & García-Rivas, J. (2019). Spanish Bentonites: A review and new data on their geology, mineralogy, and crystal chemistry. *Minerals*, 9(11), 696. <https://doi.org/10.3390/min9110696>
- Hall, D. S., Behazin, M., Binns, W. J., & Keech, P. G. (2021). An evaluation of corrosion processes affecting copper-coated nuclear waste containers in a deep geological repository. *Progress in Materials Science*, 118, 100766. <https://doi.org/10.1016/j.pmatsci.2020.100766>
- Hattori, S., Kamagata, Y., Hanada, S., & Shoun, H. (2000). *Thermacetogenium phaeum* gen. nov., sp. nov., a strictly anaerobic, thermophilic, syntrophic acetate-oxidizing bacterium. *International Journal of Systematic and Evolutionary Microbiology*, 50(4), 1601-1609. <https://doi.org/10.1099/00207713-50-4-1601>
- Haynes, H. M., Pearce, C. I., Boothman, C., & Lloyd, J. R. (2018). Response of bentonite microbial communities to stresses relevant to geodisposal of radioactive waste. *Chemical Geology*, 501, 58-67. <https://doi.org/10.1016/j.chemgeo.2018.10.004>
- Hockin, S. L., & Gadd, G. M. (2003). Linked redox precipitation of sulfur and selenium under anaerobic conditions by sulfate-reducing bacterial biofilms. *Applied and Environmental Microbiology*, 69(12), 7063-7072. <https://doi.org/10.1128/AEM.69.12.7063-7072.2003>

- Howard III, J. H. (1977). Geochemistry of selenium: formation of ferroselite and selenium behavior in the vicinity of oxidizing sulfide and uranium deposits. *Geochimica et Cosmochimica Acta*, 41(11), 1665-1678. [https://doi.org/10.1016/0016-7037\(77\)90176-4](https://doi.org/10.1016/0016-7037(77)90176-4)
- Huttunen-Saarivirta, E., Rajala, P., & Carpén, L. (2016). Corrosion behaviour of copper under biotic and abiotic conditions in anoxic ground water: electrochemical study. *Electrochimica Acta*, 203, 350-365. <https://doi.org/10.1016/j.electacta.2016.01.098>
- IAEA. (2018). Status and trends in spent fuel and radioactive waste management. Vienna, International Atomic Energy Agency. Nuclear Energy Series No. NW-T-1.14, 74. Available at: [https://www-pub.iaea.org/MTCD/Publications/PDF/PUB1963\\_web.pdf](https://www-pub.iaea.org/MTCD/Publications/PDF/PUB1963_web.pdf)
- King, F., Hall, D. S., & Keech, P. G. (2017). Nature of the near-field environment in a deep geological repository and the implications for the corrosion behaviour of the container. *Corrosion Engineering, Science and Technology*, 52(sup1), 25-30. <https://doi.org/10.1080/1478422X.2017.1330736>
- King, F., Kolář, M., Briggs, S., Behazin, M., Keech, P., & Diomidis, N. (2024). Review of the Modelling of Corrosion Processes and Lifetime Prediction for HLW/SF Containers—Part 2: Performance Assessment Models. *Corrosion and Materials Degradation*, 5(2), 289-339. <https://doi.org/10.3390/cmd5020013>
- Latta, D. E., Boyanov, M. I., Kemner, K. M., O'Loughlin, E. J., & Scherer, M. M. (2012). Abiotic reduction of uranium by Fe(II) in soil. *Applied geochemistry*, 27(8), 1512-1524. <https://doi.org/10.1016/j.apgeochem.2012.03.003>
- Li, Z., Yang, Y., Relefors, A., Kong, X., Siso, G. M., Wickman, B., ... & Soroka, I. L. (2021). Tuning morphology, composition and oxygen reduction reaction (ORR) catalytic performance of manganese oxide particles fabricated by  $\gamma$ -radiation induced synthesis. *Journal of Colloid and Interface Science*, 583, 71-79. <https://doi.org/10.1016/j.jcis.2020.09.011>
- Little, B. J., Hinks, J., & Blackwood, D. J. (2020). Microbially influenced corrosion: Towards an interdisciplinary perspective on mechanisms. *International Biodeterioration & Biodegradation*, 154, 105062. <https://doi.org/10.1016/j.ibiod.2020.105062>
- Lopez-Fernandez, M., Cherkouk, A., Vílchez-Vargas, R., Jauregui, R., Pieper, D., Boon, N., ... & Merroun, M. L. (2015). Bacterial diversity in bentonites, engineered barrier for deep geological disposal of radioactive wastes. *Microbial ecology*, 70, 922-935. <https://doi.org/10.1007/s00248-015-0630-7>
- Mandic-Mulec, I., Stefanic, P., & van Elsas, J. D. (2016). Ecology of bacillaceae. *The bacterial spore: From molecules to systems*, 59-85. <https://doi.org/10.1128/9781555819323.ch3>
- Martinez-Moreno, M. F., Povedano-Priego, C., Morales-Hidalgo, M., Mumford, A. D., Ojeda, J. J., Jroundi, F., & Merroun, M. L. (2023). Impact of compacted bentonite microbial community on the clay mineralogy and copper canister corrosion: a multidisciplinary approach in view of a safe Deep Geological Repository of nuclear wastes. *Journal of Hazardous Materials*, 131940. <https://doi.org/10.1016/j.jhazmat.2023.131940>

## GENERAL DISCUSSION

- Martinez-Moreno, M.F., Povedano-Priego, C., Mumford, A.D., Morales-Hidalgo, M., Mijndonckx, K., Jroundi, F., Ojeda, J.J., Merroun, M.L., (2024a). Microbial responses to elevated temperature: Evaluating bentonite mineralogy and copper canister corrosion within the long-term stability of deep geological repositories of nuclear waste. *Science of The Total Environment*, 915, 170149. <https://doi.org/10.1016/j.scitotenv.2024.170149>
- Martinez-Moreno, M. F., Povedano-Priego, C., Morales-Hidalgo, M., Mumford, A. D., Aranda, E., Vilchez-Vargas, R., ... & Merroun, M. L. (2024b). Microbial influence in Spanish bentonite slurry microcosms: unveiling a-year long geochemical evolution and early-stage copper corrosion related to nuclear waste repositories. *Environmental Pollution*, 124491. <https://doi.org/10.1016/j.envpol.2024.124491>
- Matschiavelli, N., Kluge, S., Podlech, C., Standhaft, D., Grathoff, G., Ikeda-Ohno, A., ... & Cherkouk, A. (2019). The year-long development of microorganisms in uncompacted bavarian bentonite slurries at 30 and 60 °C. *Environmental science & technology*, 53(17), 10514-10524. <https://doi.org/10.1021/acs.est.9b02670>
- Meleshyn, A. (2014). Microbial processes relevant for the long-term performance of high-level radioactive waste repositories in clays. *Geological Society, London, Special Publications*, 400(1), 179-194. <https://doi.org/10.1144/SP400.6>
- Miettinen, H., Bomberg, M., Bes, R., Tiljander, M., & Vikman, M. (2022). Transformation of inherent microorganisms in Wyoming-type bentonite and their effects on structural iron. *Applied Clay Sciences*, 221, 106465. <https://doi.org/10.1016/j.clay.2022.106465>
- Morales-Hidalgo, M., Povedano-Priego, C., Martinez-Moreno, M. F., Ruiz-Fresneda, M. A., Lopez-Fernandez, M., Jroundi, F., & Merroun, M. L. (2024a). Insights into the Impact of Physicochemical and Microbiological Parameters on the Safety Performance of Deep Geological Repositories. *Microorganisms*, 12(5), 1025. <https://doi.org/10.3390/microorganisms12051025>
- Moussa, L. A. A., Mansour, F. A., Serag, M. S., & Abou El-Nour, S. A. M. (2005). Effect of gamma radiation on the physiological properties and genetic materials of *Streptomyces albaduncus* and *S. erythrogresius*. *International Journal of Agriculture and Biology*, 7(2), 197-202.
- Naganuma, T., Sato, M., Hoshii, D., Amano-Murakami, Y., Iwatsuki, T., & Mandernack, K. W. (2006). Isolation and characterization of *Pseudomonas* strains capable of Fe(III) reduction with reference to redox response regulator genes. *Geomicrobiology Journal*, 23(3-4), 145-155. <https://doi.org/10.1080/01490450600596565>
- Pedersen, K., Bengtsson, A., Blom, A., Johansson, L., & Taborowski, T. (2017). Mobility and reactivity of sulphide in bentonite clays—implications for engineered bentonite barriers in geological repositories for radioactive wastes. *Applied Clay Science*, 146, 495-502. <https://doi.org/10.1016/j.clay.2017.07.003>
- Pedersen, K., Motamedi, M., Karnland, O., Sandén, T., (2000). Mixing and sulphate-reducing activity of bacteria in swelling, compacted bentonite clay under high-level radioactive waste

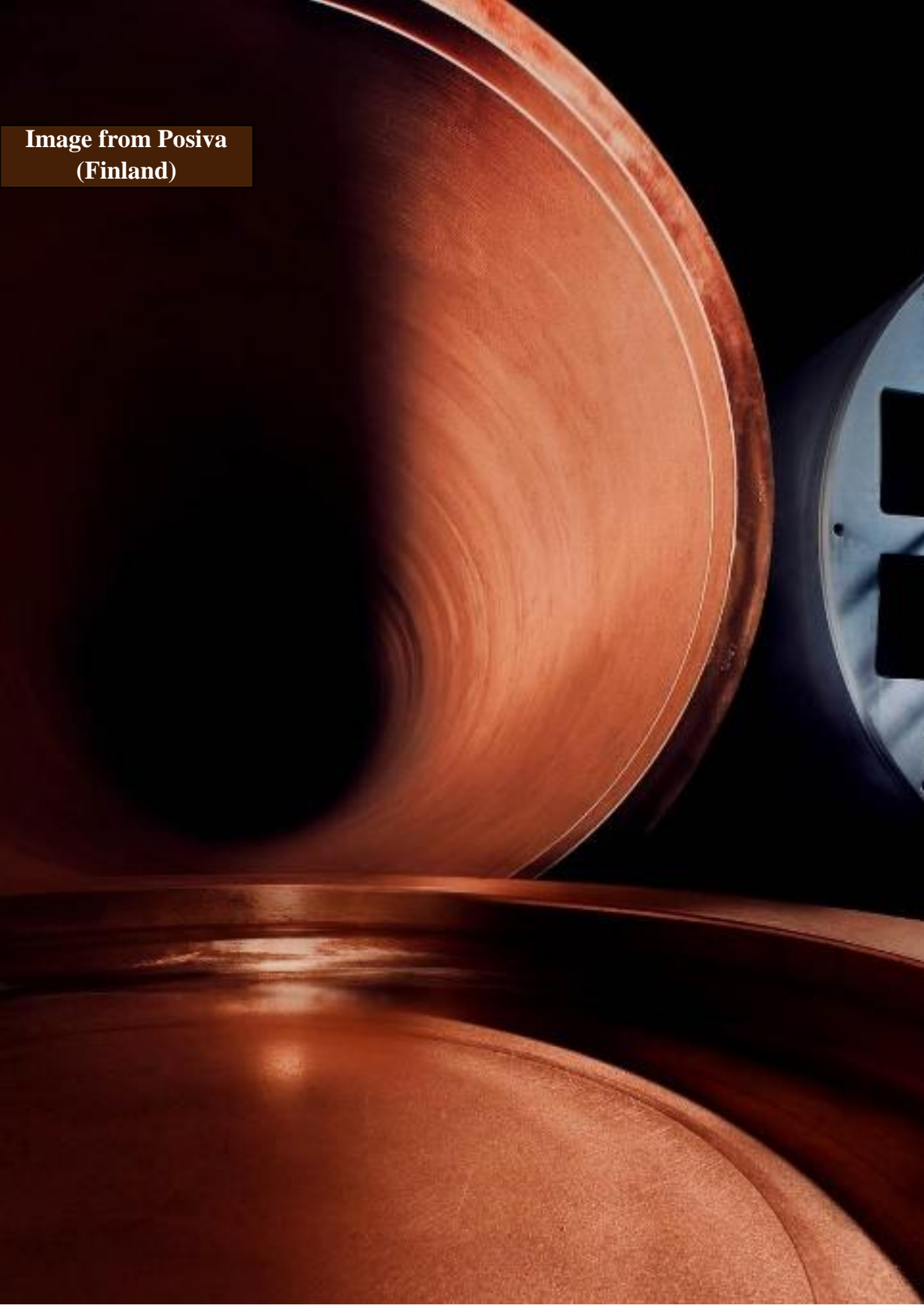
- repository conditions. *Journal of Applied Microbiology*, 89, 1038–1047. <https://doi.org/10.1046/j.1365-2672.2000.01212.x>
- Pinel-Cabello, M., Jroundi, F., López-Fernández, M., Geffers, R., Jarek, M., Jauregui, R., ... & Merroun, M. L. (2021). Multisystem combined uranium resistance mechanisms and bioremediation potential of *Stenotrophomonas bentonitica* BII-R7: transcriptomics and microscopic study. *Journal of Hazardous Materials*, 403, 123858. <https://doi.org/10.1016/j.jhazmat.2020.123858>
- Pitonzo, B. J., Amy, P. S., & Rudin, M. (1999). Effect of gamma radiation on native endolithic microorganisms from a radioactive waste deposit site. *Radiation Research*, 152(1), 64-70. <https://doi.org/10.2307/3580050>
- Povedano-Priego, C.; Jroundi, F.; Solari, P.L.; Guerra-Tschuschke, I.; Abad-Ortega, M.D.M.; Link, A.; Vilchez-Vargas, R.; and Merroun, M.L. (2023). Unlocking the bentonite microbial diversity and its implications in selenium bioreduction and biotransformation: Advances in deep geological repositories. *Journal Hazardous Material*, 445, 130557. <https://doi.org/10.1016/j.jhazmat.2022.130557>
- Povedano-Priego, C., Jroundi, F., Lopez-Fernandez, M., Sánchez-Castro, I., Martín-Sánchez, I., Huertas, F. J., & Merroun, M. L. (2019). Shifts in bentonite bacterial community and mineralogy in response to uranium and glycerol-2-phosphate exposure. *Science of the total environment*, 692, 219-232. <https://doi.org/10.1016/j.scitotenv.2019.07.228>
- Ren, M., Li, X., Zhang, Y., Jin, Y., Li, S., & Huang, H. (2018). *Massilia armeniaca* sp. nov., isolated from desert soil. *International Journal of Systematic and Evolutionary Microbiology*, 68(7), 2319-2324. <https://doi.org/10.1099/ijsem.0.002836>
- Ruiz-Fresneda, M. A., Martínez-Moreno, M. F., Povedano-Priego, C., Morales-Hidalgo, M., Jroundi, F., & Merroun, M. L. (2023). Impact of microbial processes on the safety of deep geological repositories for radioactive waste. *Frontiers in Microbiology*, 14, 1134078. <https://doi.org/10.3389/fmicb.2023.1134078>
- Ruiz-Fresneda, M. A., Eswayah, A. S., Romero-Gonzalez, M., Gardiner, P. H., Solari, P. L., & Merroun, M. L. (2020). Chemical and structural characterization of SeIV biotransformations by *Stenotrophomonas bentonitica* into Se0 nanostructures and volatiles Se species. *Environmental Science: Nano*, 5, 2103–2116. <https://doi.org/10.1039/D0EN00507J>
- Ruiz-Fresneda, M. A., Martín, J. D., Bolívar, J. G., Cantos, M. V. F., Bosch-Estévez, G., Moreno, M. F. M., & Merroun, M. L. (2018). Green synthesis and biotransformation of amorphous Se nanospheres to trigonal 1D Se nanostructures: impact on Se mobility within the concept of radioactive waste disposal. *Environmental Science: Nano*, 5(9), 2103-2116. <https://doi.org/10.1039/C8EN00221E>
- Salehi Alaei, E., Guo, M., Chen, J., Behazin, M., Bergendal, E., Lilja, C., ... & Noël, J. J. (2023). The transition from used fuel container corrosion under oxic conditions to corrosion in an anoxic

## GENERAL DISCUSSION

- environment. *Materials and Corrosion*, 74(11-12), 1690-1706.  
<https://doi.org/10.1002/maco.202313757>
- Sanchez-Castro, I., Martínez-Rodríguez, P., Abad, M. M., Descostes, M., & Merroun, M. L. (2021). Uranium removal from complex mining waters by alginate beads doped with cells of *Stenotrophomonas* sp. Br8: novel perspectives for metal bioremediation. *Journal of Environmental Management*, 296, 113411. <https://doi.org/10.1016/j.jenvman.2021.113411>
- Sani, R. K., Peyton, B. M., & Dohnalkova, A. (2006). Toxic effects of uranium on *Desulfovibrio desulfuricans* G20. *Environmental Toxicology and Chemistry: An International Journal*, 25(5), 1231-1238. <https://doi.org/10.1897/05-401R.1>
- Saygin, H., Ay, H., Guven, K., Inan-Bektas, K., Cetin, D., & Sahin, N. (2021). *Saccharopolyspora karakumensis* sp. nov., *Saccharopolyspora elongata* sp. nov., *Saccharopolyspora aridisoli* sp. nov., *Saccharopolyspora terrae* sp. nov. and their biotechnological potential revealed by genome analysis. *Systematic and applied microbiology*, 44(6), 126270. <https://doi.org/10.1016/j.syapm.2021.126270>
- Slobodkina, G. B., Kolganova, T. V., Kostrikina, N. A., Bonch-Osmolovskaya, E. A., & Slobodkin, A. I. (2012). *Caloribacterium cisternae* gen. nov., sp. nov., an anaerobic thermophilic bacterium from an underground gas storage reservoir. *International journal of systematic and evolutionary microbiology*, 62(Pt\_7), 1543-1547. <https://doi.org/10.1099/ijs.0.033076-0>
- Takai, K., Inoue, A., & Horikoshi, K. (1999). *Thermaerobacter marianensis* gen. nov., sp. nov., an aerobic extremely thermophilic marine bacterium from the 11000 m deep Mariana Trench. *International Journal of Systematic and Evolutionary Microbiology*, 49(2), 619-628. <https://doi.org/10.1099/00207713-49-2-619>
- Tenededzai, J. T., Brink, H. G., & Chirwa, E. M. (2021). Formation of Elemental Selenium Nanoparticles (SeNPs) from the Reduction of Selenite (SeO<sub>3</sub><sup>2-</sup>) by a Pure Culture of *Pseudomonas Stutzeri* NT-i. *Chemical Engineering Transactions*, 86, 193-198. <https://doi.org/10.3303/CET2186033>
- Thauer, R.K., Stackebrandt, E., Hamilton, W.A. (2007). Energy metabolism and phylogenetic diversity of sulphate-reducing bacteria. *Sulphate-reducing bacteria*, 1-38. <https://doi:10.1017/cbo9780511541490.002>
- Tondel, M. & Lindahl, L. (2019): Intergenerational Ethical Issues and Communication Related to High-Level Nuclear Waste Repositories. *Current Environmental Health Reports*, 6(4), 338-343. <https://doi.org/10.1007/s40572-019-00257-1>
- Tsarev, S., Waite, T. D., & Collins, R. N. (2016). Uranium reduction by Fe(II) in the presence of montmorillonite and nontronite. *Environmental Science & Technology*, 50(15), 8223-8230. <https://doi.org/10.1021/acs.est.6b02000>

- Van Gerwen, S. J., Rombouts, F. M., Van't Riet, K., & Zwietering, M. H. (1999). A data analysis of the irradiation parameter D10 for bacteria and spores under various conditions. *Journal of food Protection*, 62(9), 1024-1032. <https://doi.org/10.4315/0362-028X-62.9.1024>
- WNA. World Nuclear Association. (2023). Storage and disposal of radioactive waste. <https://www.world-nuclear.org/>
- Yu, Q., Boyanov, M. I., Liu, J., Kemner, K. M., & Fein, J. B. (2018). Adsorption of selenite onto *Bacillus subtilis*: The overlooked role of cell envelope sulfhydryl sites in the microbial conversion of Se(IV). *Environmental Science & Technology*, 52(18), 10400-10407. <https://doi.org/10.1021/acs.est.8b02280>
- Zhu, F., Zhao, B., Min, W., & Li, J. (2023). Characteristics of groundwater microbial communities and the correlation with the environmental factors in a decommissioned acid in-situ uranium mine. *Frontiers in Microbiology*, 13, 1078393. <https://doi.org/10.3389/fmicb.2022.1078393>

**Image from Posiva  
(Finland)**





# *Conclusions*

## CONCLUSIONS

## CONCLUSIONS

1. Bentonite compaction at  $1.6 \text{ g/cm}^3$ , combined with anoxic conditions and low nutrient availability, favors the survival of spore-forming bacteria that are resistant to extreme environments, such as desiccation and oligotrophy.
2. Gamma radiation at doses of 14 kGy and 28 kGy negatively impacted aerobic-heterotrophic microorganisms and sulfate-reducing bacteria (SRB). However, a 6-month incubation period of the bentonite blocks before radiation exposure enhanced their survival.
3. Gamma radiation indirectly delayed the biotic corrosion of copper by negatively affecting the microbiology of bentonite. The main copper corrosion products were copper oxides, while biogenic copper sulfides, produced by SRB, were also detected but only within the bentonite.
4. High temperatures (60 °C incubation or 110 °C as tyndallization treatment) promoted the survival of native bentonite microorganisms, which are well-adapted to these conditions. The presence of thermophilic bacteria in bentonites would be crucial for assessing the safety of future deep geological repositories (DGR), as these resilient microorganisms are likely to persist during the early stages of the repository.
5. Indigenous bacterial genera from Spanish bentonite could interact with selenium (Se) at elevated temperatures, leading to its reduction and resulting in the formation of Se(0) nanoparticles and/or minerals like ferroselite. This microbial activity enhanced the immobilization of Se, reducing its mobility, and ensuring the long-term DGR stability in case of metal canister failure.
6. SRB, particularly genera like *Desulfosporosinus*, *Desulfotomaculum*, and *Desulfohalotomaculum*, were key contributors to copper corrosion under

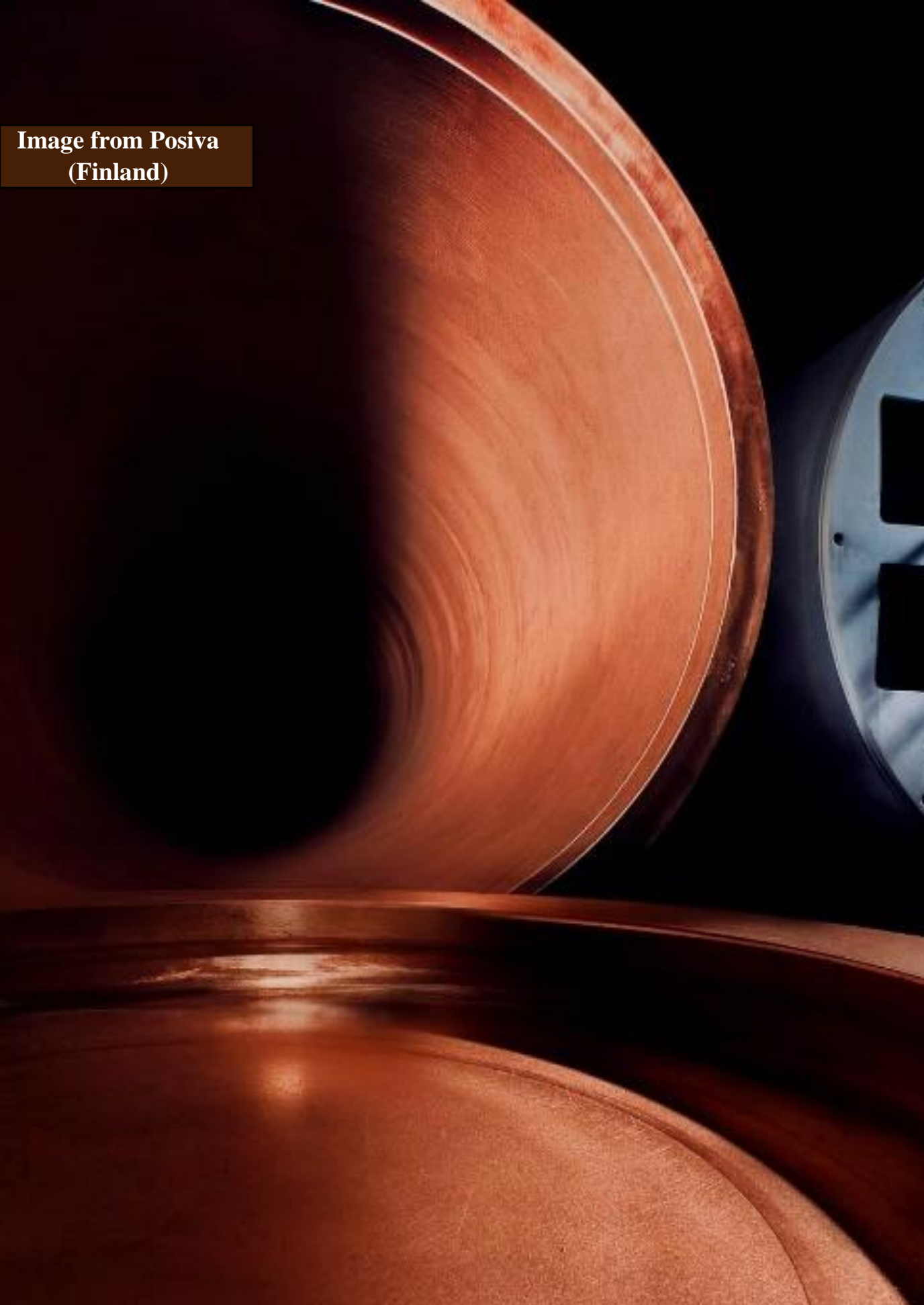
## CONCLUSIONS

DGR relevant conditions. They reduce sulfate to sulfide, which can induce copper corrosion.

7. The presence of selenite [Se(IV)] reduced copper corrosion by competing with this metal for hydrogen sulfide, limiting the formation of copper sulfides.
8. Long-term incubation (3 years) and the presence of uranium (U) shifted bentonite microbial populations, favoring anaerobic and spore-forming microorganisms alongside SRB.
9. Bentonite microbial communities played a crucial role in influencing uranium speciation and could affect its biogeochemical cycle through processes like U phosphate biomineralization and/or U reduction.
10. Spanish bentonite remained mineralogically and chemically stable under the harsh experimental conditions (gamma radiation, high temperature, presence of selenium and uranium, bentonite compaction, microbial activity, etc.), showing no relevant changes in elemental composition or swelling capacity.

## CONCLUSIONS

**Image from Posiva  
(Finland)**





# *Conclusiones*

## CONCLUSIONES

## CONCLUSIONES

1. La compactación de la bentonita a  $1,6 \text{ g/cm}^3$ , en combinación con condiciones anóxicas y baja disponibilidad de nutrientes, favoreció la supervivencia de bacterias formadoras de esporas que presentan resistencia a ambientes extremos, tales como la desecación y la escasez de nutrientes.
2. La exposición a radiación gamma a dosis de 14 kGy y 28 kGy afectó negativamente a los microorganismos aerobios heterotróficos y a las bacterias reductoras de sulfato (SRB). No obstante, un periodo de incubación de 6 meses de los bloques de bentonita previo a la exposición a la radiación incrementó su supervivencia.
3. La radiación gamma inhibió de manera indirecta la corrosión biótica del cobre al afectar negativamente la microbiota de la bentonita. Los principales productos de corrosión del cobre fueron óxidos de cobre, junto con sulfuros de cobre biogénicos, producidos por las SRB, detectados exclusivamente en la bentonita.
4. Las temperaturas elevadas ( $60 \text{ }^\circ\text{C}$  o el tratamiento de tinalización a  $110 \text{ }^\circ\text{C}$ ) favorecieron la supervivencia de microorganismos nativos de la bentonita adaptados a estas condiciones. La presencia de bacterias termófilas en la bentonita es crucial para la evaluación de la seguridad de los futuros almacenamientos geológicos profundos (AGP), ya que es probable que estos microorganismos persistan durante las fases iniciales del depósito.
5. Los géneros bacterianos autóctonos de la bentonita española podrían interactuar con el selenio (Se) a altas temperaturas, promoviendo su reducción y la subsecuente formación de nanopartículas de  $\text{Se}(0)$  y/o minerales como la ferroselita. Esta actividad microbiana favoreció la inmovilización del Se, disminuyendo su movilidad y asegurando la

## CONCLUSIONES

estabilidad a largo plazo de los AGP en caso de fallo del contenedor metálico.

6. Las SRB, en particular géneros como *Desulfosporosinus*, *Desulfotomaculum* y *Desulfohalotomaculum*, desempeñaron un papel fundamental en la corrosión del cobre bajo condiciones de AGP. Estas bacterias reducen el sulfato a sulfuro, que puede inducir la corrosión del cobre.
7. La presencia de selenito disminuyó la corrosión del cobre al competir con este metal por el sulfuro de hidrógeno, lo que limita la formación de sulfuros de cobre.
8. La incubación a largo plazo (3 años) y la presencia de uranio (U) modificaron la estructura de las comunidades microbianas de la bentonita, favoreciendo a los microorganismos anaerobios y formadores de esporas, junto con SRB.
9. Las comunidades microbianas presentes en la bentonita desempeñaron un papel crucial en la especiación del U y pudieron contribuir a su ciclo biogeoquímico a través de procesos como la biomineralización en fosfato de U y/o la reducción de U.
10. La bentonita española permaneció mineralógica y químicamente estable bajo todas las extremas condiciones experimentales (radiación gamma, alta temperatura, presencia de selenio y uranio, compactación de bentonita, actividad microbiana, etc.), sin presentar cambios relevantes en su composición elemental ni en su capacidad de hinchamiento.



# UNIVERSIDAD DE GRANADA